U. Morali / Hacettepe J. Biol. & Chem., 2020, 48 (3), 203-210

Research Article

Hacettepe Journal of Biology and Chemistry

journal homepage: www.hjbc.hacettepe.edu.tr

Influence of Charge Conditions on Battery Dynamics of A Commercial Lithium-Ion Cell

Ticari Bir Lityum-İyon Pilinin Batarya Dinamikleri Üzerinde Şarj Koşullarının Etkisi

Ugur Morali

Department of Chemical Engineering, Eskisehir Osmangazi University, Eskisehir, Turkey.

ABSTRACT

Electrochemical impedance spectroscopy measurements were performed to determine the effect of the state-of-charge, charge current, and current-drop time on battery dynamics of a commercial 2032 lithium-ion coin cell. The impedance response was systematically investigated and discussed by using the Taguchi design. The results showed that the state-of-charge had a statistically significant effect on both the resistance for solid electrolyte interphase formation and cathodic charge transfer resistance. It was showed that the Taguchi design is a valuable tool for analyzing battery dynamics obtained through the equivalent circuit model. The Taguchi design opened the door for a robust design of lithium-ion batteries in real life.

Key Words

Impedance spectroscopy, lithium-ion batteries, battery dynamics, Taguchi design.

ÖZ

Ticari bir 2032 lityum-iyon para pilinin batarya dinamikleri üzerinde şarj durumu, şarj akımı ve akım düşüş zamanının etkilerini belirlemek üzere elektrokimyasal empedans spektroskopisi ölçümleri gerçekleştirildi. Empedans cevabı Taguchi tasarımı kullanılarak sistematik bir şekilde araştırıldı ve tartışıldı. Sonuçlar şarj durumunun katı elektrolit ara fazı oluşum direnci ve katodik şarj aktarım direnci üzerinde istatistiksel olarak anlamlı bir etkiye sahip olduğunu gösterdi. Taguchi tasarımının eşdeğer devre modeli ile elde edilen batarya dinamiklerinin analiz edilmesinde önemli bir araç olduğu gösterildi. Taguchi tasarımı gerçek yaşamda lityum-iyon bataryalarının gürbüz bir tasarımı için bir olanak sağlamıştır.

Anahtar Kelimeler

Empedans spektroskopisi, lityum-iyon bataryalar, batarya dinamikleri, Taguchi tasarımı.

Article History: Received: Jan xx, 2020; Revised: Mar xx 2020; Accepted: Mar 15, 2020; Available Online: Apr 1, 2020.

DOI: https://doi.org/10.15671/hjbc.677841

Correspondence to: U. Morali, Department of Chemical Engineering, Eskisehir Osmangazi University, Eskisehir, Turkey.

E-Mail: umorali@ogu.edu.tr

INTRODUCTION

There is a growing interest in the use of lithium-ion batteries (LIBs) in the fields of electronic, transportation and energy storage [1, 2]. The LIBs are assumed to have a predominant role among the various electrochemical energy storage systems. Additionally, electric vehicles with the LIBs have numerous advantageous such as better performance and zero-emission since the high energy density of the LIBs [3]. It is usually recognized that the power and energy density of LIBs depend on the electrochemical characteristics of battery components [4]. These components include anode, cathode, electrolyte, and current collectors [2]. A deep understanding of electrochemical processes in the LIBs is a critical point to optimize operation mode, safety, and cycle life to improve the reliability of the rechargeable energy storage systems. The electrochemical characteristics of LIBs can be exhibited through electrochemical impedance spectroscopy (EIS) [5]. The EIS has been demonstrated to exhibit superior characterization of battery dynamics [6]. The advantage of the EIS method is due to its non-destructive measurements, compared to other methods. The LIBs are used in the energy-required systems under different operation conditions. The parameters such as charging rate and state of charge (SOC) can influence battery performance of the LIBs. For instance, fast charging rate and high states of charge lead to the formation of Li-plating at the surface of the anode [2]. These parameters can also lead to the formation of solid electrolyte interphase (SEI) on the anode [7]. The SEI layer can be considered as a further layer between the electrolyte and the anode. In other words, these formations in the LIBs provoke the battery degradation and power fade. Therefore, the determination of the influence of both the charging current and SOC on battery dynamics is of great importance.

Recently, tremendous efforts have been made to clarify the electrochemical properties of LIBs under different process conditions [8, 9]. However, statistical evaluation of battery dynamics has not been studied in the literature. On the other hand, the identification of the significance of charging current at states of charge improves the high rate capability for charging operation. The dependence of battery dynamics on SOC and charging current is examined due to its importance in deciding the operating strategy. Accordingly, the influence of both charge current and SOC on dynamics of 2032 button cell, which has the cathode of $LiNiMnO_2$ and the anode of graphitic carbon, has been quantified by using EIS method combined with the Taguchi design.

MATERIALS and METHODS

Commercially available and rechargeable 2032 button lithium-ion (Li-ion) cells were purchased from Sony Energy Devices Corp. The 2032 notation shows that the cell was 20 mm in diameter and 3.2 mm in height. The cathode was a lithium metal oxide such as $LiNiMnCoO_2$, and the anode was graphitic carbon. First the open circuit potential (OCP) was measured over 120 seconds with a sample period of 0.5 seconds. The cells as received had an OCP of 3.715±0,001 V. Then, the cells were charged at a current of 200 mA to 4.20 V. The discharge profile of the cells was obtained at a current of 177 mA down to and including 3.20 V. The resulting discharge profile was used to obtain a correlation between cell potential and state-of-charge. Charge-discharge measurements and EIS analyses were performed by using Gamry Reference 3000 Potentiostat/Galvonastat/ZRA. Gamry Instruments coin cell battery holder was used to protect the electrochemical measurements from the noises of cable connections. Gamry Faraday cage was also used to provide prevention due to the outer

Table 1. Experimental runs based on the L9 orthogonal array.

Run	SOC, %	Charge current, mA	Current drop time, second
1	35	30	30
2	35	15	20
3	35	5	10
4	70	30	20
5	70	15	10
6	70	5	30
7	100	30	10
8	100	15	30
9	100	5	20

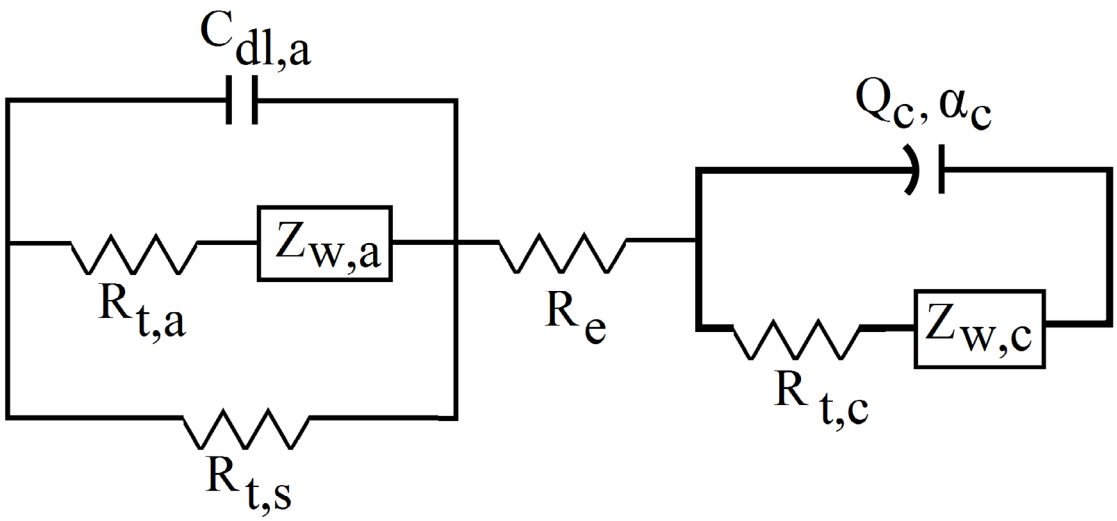

Figure 1. Equivalent circuit representation of the mathematical model used for the 2032 LIB.

electric field. The charging process was executed by the constant-current and constant-potential procedure. The 2032 button cells were charged from 3.20 V to the different SOCs by applying different charging currents. When the SOC reached the specified potential (35% SOC, 70% SOC and 100% SOC), the charging current (30 mA, 15 mA and 5 mA) was allowed to decrease to 1 mA for a specific drop-time (30 min, 20 min and 10 min). The impedance measurements at open-circuit were performed over a range of frequency between 100 kHz and 0.01 Hz by applying 1 mV potential perturbation. After each measurement, the cells were discharged at 0.5 C down to potential of 3.20 V, and subjected to the next Taguchi run. The set of experimental runs based on the Taguchi design was created by using Minitab®17 (Table 1). The Taguchi method is summarized in our previous study for detailed information [10]. Impedance data for each measurement was obtained through at least three replicated runs to ensure that the results were both consistent and reproducible. All of the impedance data gathered was analyzed by using Gamry Echem Analyst software.

A quantitative analysis of the fit of an equivalent circuit model to the impedance data was performed to characterize the impedance spectra. The equivalent circuit model developed by Erol and Orazem was used in this study (Figure 1) [11]. The equivalent circuit model contains an electrolyte resistance R_e, a charge transfer resistance for anode $R_{t,a}$, a double layer capacitance for anode $C_{dl,a}$, the diffusion impedance for anode $Z_{w,a}$, the charge transfer resistance for solid electrolyte interphase $R_{t,s}$, the constant phase element for cathode CPE (Q_c and α_c), the charge transfer resistance for cathode Rt,c and the diffusion impedance for cathode $Z_{w,c}$. A full description of the mathematical model is provided in Ref. [11] and will therefore not be duplicated here.

RESULTS and DISCUSSION

The impedance response of the 2032 Li-ion coin cells is presented as functions of SOC, charge current, and current drop time. Then, the equivalent circuit model fitted to the EIS data. Finally, the influential factors were determined through the Taguchi design.

Analysis of impedance response

The impedance response of 2032 coin cells is presented in Nyquist format (Figure 2). Three regions can be identified in the Nyquist plots. The Nyquist plots consist of two capacitive loops in the high and medium frequency regions [12]. A straight line at low frequencies is also seen in the representation of the impedance data [1]. The semi-circle at the higher frequencies represented the electrochemical phenomena at the anode side of the cell. The high frequency semi-circles in the Nyquist plots were observed not to change so much through the entire conditions. The high frequency semi-circle is generally ascribed to the impedance associated with the behavior of Li-ions through the SEI layer on anode [11]. The magnitude of the semi-circles representing the impedance through the SEI layer showed that the movement of the Li-ions exhibited same behavior over the all runs. On the other hand, the impedance response at medium frequencies is not an exact semi-circle. Thus,

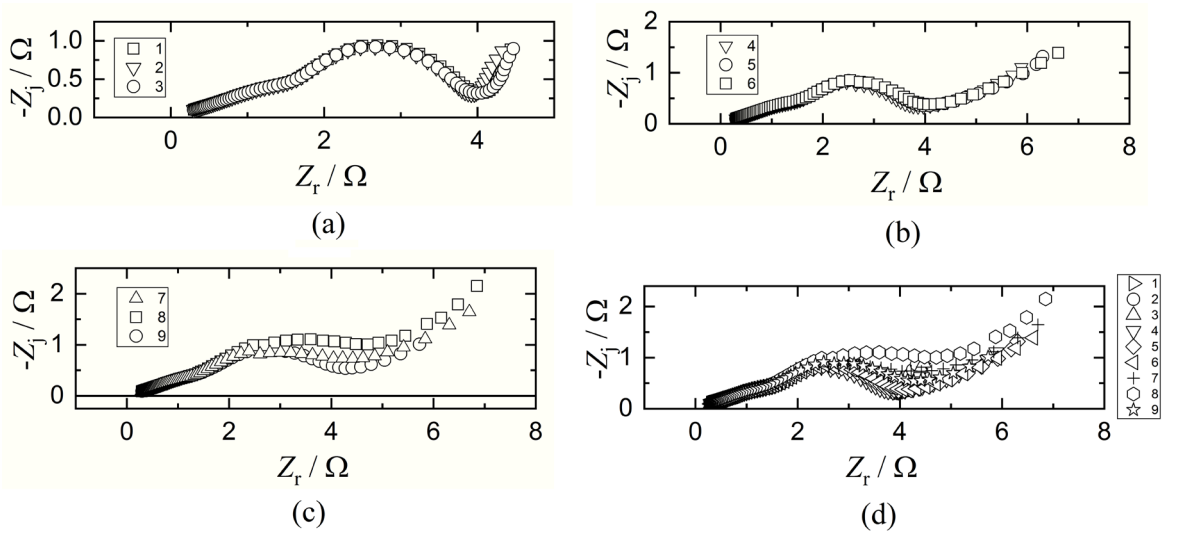

Figure 2. Impedance response in Nyquist format for a 2032 coin cell: a) as obtained from the runs 1-3; b) as obtained from the runs 4-6; c) as obtained from the runs 7-9; d) as obtained from all the runs in the L9 orthogonal array.

the loop in the medium frequency region of the Nyquist plots can be identified as a depressed semi-circle. The depressed semi-arc reflected the electrochemical reactions and other side reactions occurring at the cathode side of the battery [13]. The depressed semi-circle can be ascribed to the high charge transfer resistance associated with desolvation/solvation of Li-ions, and Li-ion intercalation/deintercalation into/from the cathode [14, 15]. The medium frequency representation of the impedance data showed that the size of the depressed semi-circle increased with the increasing SOC. The higher semi-arc at medium frequencies indicated that the Li-ion transportation over the cathode was difficult. The differences in the size and shape of the impedance response at medium frequencies showed that the applied conditions changed the charge transfer resistance for the cathode. Additionally, the impedance response of the 2032 Li-ion battery cells resemble the one resulted for lithium/graphite 2032 cell by Erol and Orazem [11]. The line in the low-frequency region corresponds to the behavior of lithium ions to diffuse from electrolyte to the electrode or vice versa [13]. The 2032 cells at the different conditions led to changes in the slope of the straight line in the Nyquist plot captured by the EIS measurements. The differences in the slope of straight line implied that the diffusion of Li-ions was influenced by the applied operation parameters.

Regression of battery dynamics

The mathematical representation of the equivalent circuit model (Figure 1) was used to fit the model to the impedance data. The resulting mathematical model can be presented as

$$Z = Z_{a||s} + R_e + Z_c \quad (1)$$

The impedance at negative electrode Za||s in Equation 1, given as

$$Z_{a||s}(\omega) = ((R_{t,a} + Z_{w,a})\,R_{t,s}) / (R_{t,a} + Z_{w,a} + j\omega\,(R_{t,a} + Z_{w,a})\,R_{t,s}C_{dl||s}) \quad (2)$$

The cathode impedance Zc in Equation 1 can be expressed as

$$Z_c = (R_{t,c} + Z_{w,c}) / (1 + j\omega^{\alpha c}(R_{t,c} + Z_{w,c})\,Q_c) \quad (3)$$

Zw,c is the Warburg impedance and can be defined as

$$Z_{w,c} = A_{w,c} / (j\omega)^{0.5} \quad (4)$$

where Aw,c is coefficient of Warburg impedance.

The regressed model parameters are listed with confidence intervals (Table 2). The resulting values of battery dynamics showed that the applied factors (SOC, charge current and current-drop time) influenced the dynamic behavior of the cells. The following results will focus on the four resistors R_e, $R_{t,s}$, $R_{t,a}$, and $R_{t,c}$ assigned in the equivalent circuit model. These four resistors are ge-

Table 2. Comparison of regression results with confidence intervals for model parameters.

Run	R_e $\Omega\ cm^2$	$R_{t,s}$ $\Omega\ cm^2$	$R_{t,a}$ $\Omega\ cm^2$	$Z_{w,a}$ $\Omega\ cm^2\ s^{-0.5}$	$C_{dl,a}$ $\mu F\ cm^{-2}$	Q_c $F\ cm^{-2}\ s^{\alpha c-1}$	α_c	$R_{t,c}$ $\Omega\ cm^2$	$Z_{w,c}$ $\Omega\ cm^2\ s^{-0.5}$
1	0.2228±0.0211	1.355±0.02646	0.1618±0.0153	14.19±0.777	8.257±2.323	0.0374±0.0027	0.841±0.0304	2.396±0.089	3.891±0.328
2	0.2205±0.0210	1.355±0.02629	0.1623±0.0152	14.3±0.778	8.217±2.299	0.03646±0.0026	0.855±0.0306	2.285±0.085	4.063±0.342
3	0.2209±0.0201	1.344±0.02577	0.1643±0.0150	14.41±0.776	8.49±2.263	0.03857±0.0027	0.831±0.0306	2.369±0.091	3.727±0.304
4	0.2286±0.0181	1.199±0.02427	0.1623±0.0157	14.79±0.850	9.657±2.436	0.05322±0.0051	0.706±0.0469	2.705±0.201	2.632±0.417
5	0.2314±0.018	1.203±0.02449	0.1633±0.0160	14.67±0.856	9.717±2.435	0.05360±0.0049	0.694±0.0418	2.871±0.192	2.639±0.433
6	0.2235±0.0224	1.148±0.02678	0.1488±0.0167	13.69±0.919	8.489±2.785	0.05279±0.0045	0.677±0.0371	2.970±0.175	1.370±0.0677
7	0.2322±0.0164	0.8522±0.02255	0.1277±0.0164	18.17±1.398	13.03±3.892	0.09259±0.0081	0.536±0.0295	5.296±0.486	1.023±0.0559
8	0.2367±0.018	0.982±0.02399	0.1341±0.0173	15.93±0.0011	11.52±0.0035	0.07472±0.0078	0.589±0.0404	5.159±0.569	1.280±0.346
9	0.2303±0.0191	1.006±0.02457	0.1444±0.0168	15.36±0.0010	10.3±3.085	0.06322±0.0059	0.607±0.0345	3.839±0.276	2.378±0.636

nerally identified as battery dynamics. The electrolyte resistance slightly increased with increasing SOC. The electrolyte resistance at 100% SOC was higher than that at 35% SOC. The increase in the electrolyte resistance could be attributed to the concentration of Li-ions in the electrolyte. The charge transfer resistance for the SEI formation was higher than the charge transfer resistance for the anode intercalation. The higher charge transfer resistance for the SEI formation reaction indicated that the impedance response at the anode side of the cells was largely due to the SEI layer formed on the anode. It can be seen the cathodic charge transfer resistance value as an increasing function of SOC for all charge currents; however, the increasing trend became more evident at 100% SOC. An additional layer on the cathode can be formed during the cell operations. The formed cathodic layer is generally attributed to the side-reaction products [9]. Furthermore, the side-reactions can consume the Li-ions in the cells. Thus, the increase in the charge transfer resistance for the cathode can be ascribed to both the consumption of Li-ions and the formation of the cathodic layer.

Taguchi design of battery dynamics

The Taguchi design provides appropriate data to get an efficient statistical analysis. The statistical approach provides to enable the evaluation of the influence of all levels of factors at the same time. The determination of the objective function is the first step of the Taguchi design. In this study, the objective function was minimization of battery dynamics of the 2032 coin cells. Battery dynamics were R_e, $R_{t,s}$, $R_{t,a}$ and $R_{t,c}$ representing the electrolyte resistance, the resistance for the SEI formation reaction, the resistance for the anodic charge transfer reaction and the cathodic charge transfer resistance, respectively. It is important to note that the resistances representing battery dynamics of the 2032 button cells should be as low as possible. Therefore, smaller-is-better quality characteristic was selected as signal-to-noise ratio (S/N) to determine the significance of the response variables (battery dynamics). The S/N ratios for all the levels of the factors (SOC, charge current and drop time) were calculated and represented in response table (Table 3). The applied L9 orthogonal array enabled to analyze the entire parameter space (Table 1).

The effect of SOC on battery dynamics was the highest based on the results of the response table. Rank 1 indicated the higher significance level of the SOC for all the resistances. In other words, small changes in the SOC substantially influence battery dynamics. It is important to emphasize that the SOC with the largest delta value was given rank 1 for all the resistances. On the other hand, rank 2 for the R_e indicated that the applied charge current was the second influential factor on the electrolyte resistance. The influence of the time allowed for the current drop on the electrolyte resistance was lower than the effects of SOC and charge current. The effect of the drop time on the R_e parameter was indicated by the difference between the highest and lowest S/N ratios of the drop time. The lowest difference in the S/N ratios of the drop time induced Rank 3 for the drop time. For battery dynamics except for the electrolyte resistance, the drop time with the second largest delta value was given rank 2. Thus, the charge current was given Rank 3. The response table also showed that the influence of drop time on the charge transfer resistance for the SEI formation reaction was higher than that of the

Table 3. Response table of battery dynamics for signal-to-noise ratios (S/N) - smaller is better.

R_e				$R_{t,s}$			
Level	SOC	charge current	drop time	Level	SOC	charge current	drop time
1	13.1	12.96	12.84	1	-2.6152	-1.2729	-0.928
2	12.85	12.79	12.9	2	-1.4602	-1.3612	-1.4224
3	12.65	12.85	12.86	3	0.4992	-0.942	-1.2257
Delta	0.45	0.17	0.06	Delta	3.1144	0.4192	0.4943
Rank	1	2	3	Rank	1	3	2
$R_{t,a}$				$R_{t,c}$			
Level	SOC	charge current	drop time	Level	SOC	charge current	drop time
1	15.77	16.35	16.43	1	-7.42	-9.544	-10.377
2	16.03	16.33	16.13	2	-9.086	-10.197	-9.168
3	17.38	16.5	16.61	3	-13.472	-10.237	-10.432
Delta	1.61	0.17	0.47	Delta	6.052	0.694	1.264
Rank	1	3	2	Rank	1	3	2

charge current. This order between the charge current and drop time was in force for both the anodic charge transfer resistance and cathodic charge transfer resistance.

To perform analysis of variance (ANOVA), a significance level of 0.05 was selected from the typical values for alpha. The significance level of 0.05 indicates a 5% risk of concluding that the coefficient is not 0 when it is. A calculated probability (P-value) was calculated to indicate the evidence against the null hypothesis. The ANOVA results (Table 4) showed that no significant effect of both the SOC, charge current, and drop time on the electrolyte resistance was observed since the P-values for the Re were higher than 0.05. The P-values of the SOC smaller than 0.05 indicated that there was a statistically significant association between the charge level and both $R_{t,s}$, and $R_{t,c}$. The results statistically indicated that there was no relationship between the charge current and battery dynamics was visible. In addition, the P-value bigger than 0.05 showed that the influence of drop time on battery dynamics was not statistically significant.

Conclusion

The impact of state-of-charge, charging current and drop time on battery dynamics of the commercial 2032 $LiNiMnCoO_2$|C battery was assessed by using the electrochemical impedance spectroscopy combined with the Taguchi design. The state-of-charge was a crucial factor greatly affecting battery dynamics. The statistically significant association was observed between the state-of-charge and the resistance for the solid electrolyte interphase formation reaction. In addition, the state-of-charge had a profound influence on the cathodic charge transfer resistance. The electrochemical impedance spectroscopy combined with the Taguchi design opened the door for a more detailed understanding of a commercial $LiNiMnCoO_2$|C coin cell that enables a robust design of lithium-ion batteries in real life.

Acknowledgments

This study was supported by Eskisehir Osmangazi University Scientific Research Foundation (grant number 2017-1911).

Table 4. Response table of battery dynamics for signal-to-noise ratios (S/N) - smaller is better.

			R_e			
Source	DF	Seq SS	Adj SS	Adj MS	F	P
SOC	2	0.0002049	0.0002049	0.0001024	10.73	0.085
Charge current	2	0.000033	0.000033	0.0000165	1.73	0.366
Drop time	2	0.0000046	0.0000046	0.0000023	0.24	0.806
Error	2	0.0000191	0.0000191	0.0000095		
Total	8	0.0002616				
			$R_{t,a}$			
Source	DF	Seq SS	Adj SS	Adj MS	F	P
SOC	2	0.0012893	0.0012893	0.0006447	7.74	0.114
Charge	2	0.0000111	0.0000111	0.0000055	0.07	0.938
current	2	0.0000989	0.0000989	0.0000495	0.59	0.627
Error	2	0.0001666	0.0001666	0.0000833		
Total	8	0.001566				
			$R_{t,s}$			
Source	DF	Seq SS	Adj SS	Adj MS	F	P
SOC	2	0.248033	0.248033	0.124016	30.22	0.032
Charge	2	0.00311	0.00311	0.001555	0.38	0.725
current	2	0.004315	0.004315	0.002158	0.53	0.655
Error	2	0.008208	0.008208	0.004104		
Total	8	0.263666				
			$R_{t,c}$			
Source	DF	Seq SS	Adj SS	Adj MS	F	P
SOC	2	9.7503	9.7503	4.8752	25.37	0.038
Charge	2	0.3095	0.3095	0.1547	0.81	0.554
current	2	0.6434	0.6434	0.3217	1.67	0.374
Error	2	0.3844	0.3844	0.1922		
Total	8	11.0876				

References

1. U. Moralı, S. Erol, 18650 lityum-iyon ve 6HR61 nikel-metal hidrit tekrar şarj edilebilir pillerinin elektrokimyasal empedans analizi, J. Fac. Eng. Archit. Gaz., 35 (2020) 297-310.
2. H. Wang, S. Frisco, E. Gottlieb, R. Yuan, J.F. Whitacre, Capacity degradation in commercial Li-ion cells: The effects of charge protocol and temperature, J. Power Sources, 426 (2019) 67-73.
3. R. Gopalakrishnan, Y. Li, J. Smekens, A. Barhoum, G. Van Assche, N. Omar, J. Van Mierlo, Electrochemical impedance spectroscopy characterization and parameterization of lithium nickel manganese cobalt oxide pouch cells: dependency analysis of temperature and state of charge, Ionics, 25 (2018) 111-123.
4. T. Amietszajew, E. McTurk, J. Fleming, R. Bhagat, Understanding the limits of rapid charging using instrumented commercial 18650 high-energy Li-ion cells, Electrochim. Acta, 263 (2018) 346-352.
5. S. Erol, M.E. Orazem, R.P. Muller, Influence of overcharge and over-discharge on the impedance response of LiCoO2|C batteries, J. Power Sources, 270 (2014) 92-100.
6. S. Buteau, D. Dahn, J. Dahn, Explicit conversion between different equivalent circuit models for electrochemical impedance analysis of lithium-ion cells, J. Electrochem. Soc., 165 (2018) A228-A234.
7. C. Yu, S. Ganapathy, E. Eck, H. Wang, S. Basak, Z. Li, M. Wagemaker, Accessing the bottleneck in all-solid state batteries, lithium-ion transport over the solid-electrolyte-electrode interface, Nat. Commun., 8 (2017) 1086.

8. J. Xu, X. Wang, N. Yuan, J. Ding, S. Qin, J.M. Razal, X. Wang, S. Ge, Y. Gogotsi, Extending the low temperature operational limit of Li-ion battery to− 80°C, Energy Stor. Mater., 23 (2019) 383-389.
9. A. Schmidt, A. Smith, H. Ehrenberg, Power capability and cyclic aging of commercial, high power lithium ion battery cells with respect to different cell designs, J. Power Sources, 425 (2019) 27-38.
10. U. Moralı, H. Demiral, S. Şensöz, Optimization of activated carbon production from sunflower seed extracted meal: Taguchi design of experiment approach and analysis of variance, J. Clean. Prod., 189 (2018) 602-611.
11. S. Erol, M.E. Orazem, The influence of anomalous diffusion on the impedance response of $LiCoO_2$|C batteries, J. Power Sources, 293 (2015) 57-64.
12. A. Barai, K. Uddin, M. Dubarry, L. Somerville, A. McGordon, P. Jennings, I. Bloom, A comparison of methodologies for the non-invasive characterisation of commercial Li-ion cells, Prog. Energ. Combust., 72 (2019) 1-31.
13. D. Juarez-Robles, C.F. Chen, Y. Barsukov, P.P. Mukherjee, Impedance evolution characteristics in lithium-ion batteries, J. Electrochem. Soc., 16 (2017) A837-A847.
14. R. Tatara, P. Karayaylali, Y. Yu, Y. Zhang, L. Giordano, F. Maglia, R. Jung, J.P. Schmidt, I. Lund, Y. Shao-Horn, The effect of electrode-electrolyte interface on the electrochemical impedance spectra for positive electrode in Li-ion battery, J. Electrochem. Soc., 166 (2019) A5090-A5098.
15. A. Yürüm, Sunflower Stalk Based Activated Carbon for Supercapacitors, Hacettepe J. Biol. Chem., 47 (2019) 235-247.

A. Ayna / Hacettepe J. Biol. & Chem., 2020, 48 (3), 211-218

Research Article

Hacettepe Journal of Biology and Chemistry

journal homepage: www.hjbc.hacettepe.edu.tr

Apoptotic Effects of Beta-Carotene, Alpha-Tocopherol and Ascorbic Acid on PC-3 Prostate Cancer Cells

Beta-Karoten, Alfa-Tokoferol ve Askorbik Asidin PC-3 Prostat Kanser Hücrelerine Apoptotik Etkileri

Adnan Ayna

Department of Chemistry, Faculty of Sciences and Arts, Bingöl University, Bingöl, Turkey.

ABSTRACT

Prostate cancer (PC) is one of the most commonly diagnosed cancer types being the second major reason of cancer-associated death in male particularly over the age of 50. Accumulating scientific evidences suggest the role oxidative stress and reactive oxygen species (ROS) in prostate cancer. A variety of factors including carcinogenic molecules, infectious diseases and toxic compounds can induce ROS production which turns into a strong contribution to the disturbed homeostasis and genetic mutation. Antioxidants can decrease the negative effects of ROS *in vitro*. Vitamin C (Ascorbic acid, Asc), vitamin A (beta carotenoids and retinoids, β-Crt) and vitamin E (alpha tocopherol, α-Toc) play an important role in inhibition of oxidative stress and diminishing of free radicals in the body. The aim of this study was to determine the anticancer effect of α-Toc, β-Crt and Asc on PC-3 prostate cancer cells *in vitro*. This was carried out by cell proliferation, ROS and Lipid Peroxidation assay, caspase-3 and propidium iodide staining experiments. The findings suggest that these agents behave as prooxidant by lowering cell viability and increasing the production of ROS and LPO in prostate cancer. These oxidants induce apoptosis as supported by caspase-3 (the enzyme playing key role in programmed cell death) staining by displaying a marked increase in the expression level of caspase-3 enzyme.

Key Words

Prostate cancer; reactive oxygen species; apoptosis; caspase-3.

ÖZ

Prostat kanseri (PC), özellikle 50 yaşın üzerindeki erkeklerde kansere bağlı ölümlerin ikinci büyük nedeni olan ve en yaygın olarak teşhis edilen kanser tiplerinden biridir. Bilimsel çalışmalar oksidatif stres ve Reaktif oksijen türlerinin (ROS) prostat kanseri üzerindeki rolünü göstermektedir. ROS, kanserojen moleküller, enfeksiyon, toksi bileşikler gibi homeostaza ve genetik mutasyona neden olabilecek bileşikler tarafından üretilir. Antioksidanlar, ROS'un olumsuz etkilerini *in vitro* olarak azaltabilir. C vitamini (Askorbik asit, Asc), A vitamini (beta karotenoidler ve retinoidler, β-Crt) ve E vitamini (alfa tokoferol, α-Toc) oksidasyonun önlenmesinde ve vücuttaki serbest radikallerin konsantrasyonunun azaltılmasında önemli rol oynar. Bu çalışmanın amacı, α-Toc, β-Crt ve Asc'nin PC-3 prostat kanseri hücreleri üzerindeki *in vitro* antikanser etkisini belirlemektir. Bu amaç, hücre çoğalması, ROS ve Lipid Peroksidasyon deneyi, kaspaz-3 ve propidium iyodür boyama deneyleri ile gerçekleştirildi. Bulgular, bu ajanların, prostat kanseri hücrelerinde hücre canlılığını azaltarak ve ROS ve LPO üretimini artırarak proksidan olarak davrandığını göstermektedir. Bu oksidanlar kaspaz-3 (programlı hücre ölümünde rol alan önemli bir enzim) boyamasıyla desteklendiği üzere apoptozu kaspaz-3 enziminin ekspresyonunu artırarak indüklemiştir.

Anahtar Kelimeler

Prostat kanseri; reaktif oksijen türleri; apoptoz; kaspaz-3.

Article History: Received: Jan 2, 2020; Revised: Mar 15 2020; Accepted: Mar 15, 2020; Available Online: Apr 1, 2020.

DOI: https://doi.org/10.15671/hjbc.519212

Correspondence to: Department of Chemistry, Faculty of Sciences and Arts, Bingöl University, Bingöl, Turkey.

E-Mail: aayna@bingol.edu.tr

INTRODUCTION

Prostate cancer is one of the most common cancer types of men in the World 10% of which results in death [1]. Many studies have focused the relation between oxidative stress and prostate cancer [2-4]. The generation of reactive oxygen species (ROS) and changes in redox status are common biochemical phenomena in cancer cells. ROS can attack polyunsaturated fatty acids of lipid membranes and induce lipid peroxidation (LPO). An excessive increase in the amount of ROS and LPO induced by different prooxidants leads to oxidative stress and apoptosis leading to overcleaning of the cellular antioxidant defense system [5-6]. Antioxidants have been widely used as dietary supplements and have been investigated for their effectiveness in prevention of many diseases including various types of cancer. The vitamins C (Ascorbic acid, Asc), A (beta carotenoids and retinoids, β-Crt) and E (alpha tocopherol, α-Toc) are known to act as antioxidants by delaying or inhibiting oxidation and reducing the concentration of free radicals in the body. In addition to their use in cancer prevention, supplemental antioxidants have usually been prescribed to cancer patients either by clinicians or patients themselves [7-8]. Vitamin E is reported as an efficient lipid soluble antioxidant that functions as a 'chain breaker' during lipid peroxidation process in cell membranes. It shows functionality by intercepting lipid peroxyl radicals ($LOO^{\cdot}$) and terminating the lipid peroxidation chain reactions resulting in stable tocopheroxyl radical which is insufficiently reactive to initiate lipid peroxidation itself in normal circumstances, showing an essential criterion of a good antioxidant [9- 12]. Additionally, some studies demonstrate that vitamin E shows its antioxidant properties through scavenging $LOO^{\cdot}$ in vivo as well as *in vitro* systems. Despite being good scavenger of lipid peroxyl, itis not an efficient scavenger of $^{\cdot}OH$ and alkoxyl radicals ($^{\cdot}OR$) in vivo [13].

Vitamin C or ascorbic acid, is a well-known water-soluble free radical scavenger. In addition to its role being a free radical scavenger, it has important function in regeneration of vitamin E in cell membranes within combination with reducing antioxidant glutathione [14-16, 9].

The precursors of vitamin A, β-Crt, are natural compounds with lipophilic properties. 500 different compounds of carotenoids have been reported until today. Most of the studied carotenoids have an extended system of conjugated double bonds, which is responsible for their antioxidant activity. Epidemiologic research in humans have demonstrated that β-Crt has an important role in cancer prevention. In addition to this, the carotenoids have also been demonstrated to have the ability of inhibiting free radical reactions. Among these carotenoids, β-Crt was shown to reduce tri chloromethylperoxyl radicals. β-Crt was also found to inhibit the oxidation of model compounds (tetralin and methyl linoleate) by peroxyl radicals [17].

The aim of this study was to determine the anticancer effect of α-Toc, β-Crt and Asc on PC-3 prostate cancer cells *in vitro* and elucidate underlying molecular mechanism of the antioxidants. In this context, the effects of these antioxidants on cell viability, production of ROS and LPO and their relationship with apoptosis were evaluated in this study.

MATERIALS and METHODS

Cell Culture

Human prostate cancer cells [PC-3 (ATCC® CRL1435™) were cultured in complete endothelial growth media containing 10 % fetal bovine serum, 1 % penicillin-streptomycin (10000 units/ml, 10 mg/ml streptomycin). The cells were cultured in humidified incubator with 5 % CO2 and checked every two or three days. Cells were checked for mycoplasma contamination by using EZ-PCR mycoplasma test kit (Biological Industries).

Cell Proliferation Assay

Water Soluble Tetrazolium-1 (WST-1) cell proliferation assay kit (Clontech Laboratories, USA) was used to investigate the effects of α-Toc, β-Crt and Asc on PC-3 cells. Experiments were carried out according to the procedure provided by the supplier. Initially 10.000 PC-3 cells were seeded in 96-well plate. After that the cells were treated with different doses of agents between 15 to 60 µg/ml. Subsequently, 5 µl of WST-1 was added into each well. After 4h incubation, absorbance of each well was recorded at 450 nm (reference: 630 nm) by SpectraMax Plus 384 Microplate Reader (Molecular Devices, USA).

Intracellular ROS Detection

The amount of ROS was measured by 2′,7′-dichlorodihydrofluorescin diacetate (DCFH-DA). The cells were treated with 60 µg/ml of α-Toc, β-Crt and Asc. 1x 106 cells were harvested and incubated in the presence of 2 µM

DCFH-DA at 37°C for 1h. Fluorescence measurements were recorded by a spectrofluorometer (Perkin-Elmer LS-55, USA) at wavelengths of 485 nm (excitation) and 525 nm (emission).

Lipid Peroxidation Assay

The antioxidant activity of -Toc, β-Crt and Asc was evaluated by LPO assay measuring malondialdehyde as a malondialdehyde-thiobarbituric acid adduct as explained by Smith [18]. Malondialdehyde bis was used for standard graph preparation [18].

Propidium Iodide Staining for Apoptosis

Cells were seeded and harvested in 96-well plate. Later, cells were treated with 60 μg/ml of α-Toc, β-Crt and Asc. Then, the cells were washed with PBS twice. Propidium iodide was added to each well and cells were imaged by inverted microscope with fluorescence attachment (Olympus, JAPAN).

Immunohistochemical Staining of Caspase-3

Immunohistochemical staining was performed as explained in [19]. The cells containing dark brown nuclei or cytoplasm identified as caspase-3 (+) cells.

RESULTS

Cell Viability

The viability of α-Toc, β-Crt and Asc on PC 3 cell line was determined by WST-1 assay. The results of representative experiments are shown (Figure 1). In general all antioxidants tested within this study decreased cell viability at concentrations of 60 μg/ml when compared to control.

Intracellular ROS and LPO Analysis

To determine whether these antioxidants could effect ROS production, a well-developed ROS assay was used. The results demonstrated that ROS production increased in comparison with non-treated prostate cancer cells (Figure 2a). Lipid peroxidation assay was used to assess oxidative stress by measuring the amount of malondialdehyde (MDA) in controls. The test results indicated a dose-dependent increase in MDA production. As shown in Figure 2b, the data revealed significant differences ($p<0.001$) in MDA production at 60 μg/ml of α-Toc, β-Crt and Asc compared to the control (0 μg/ml).

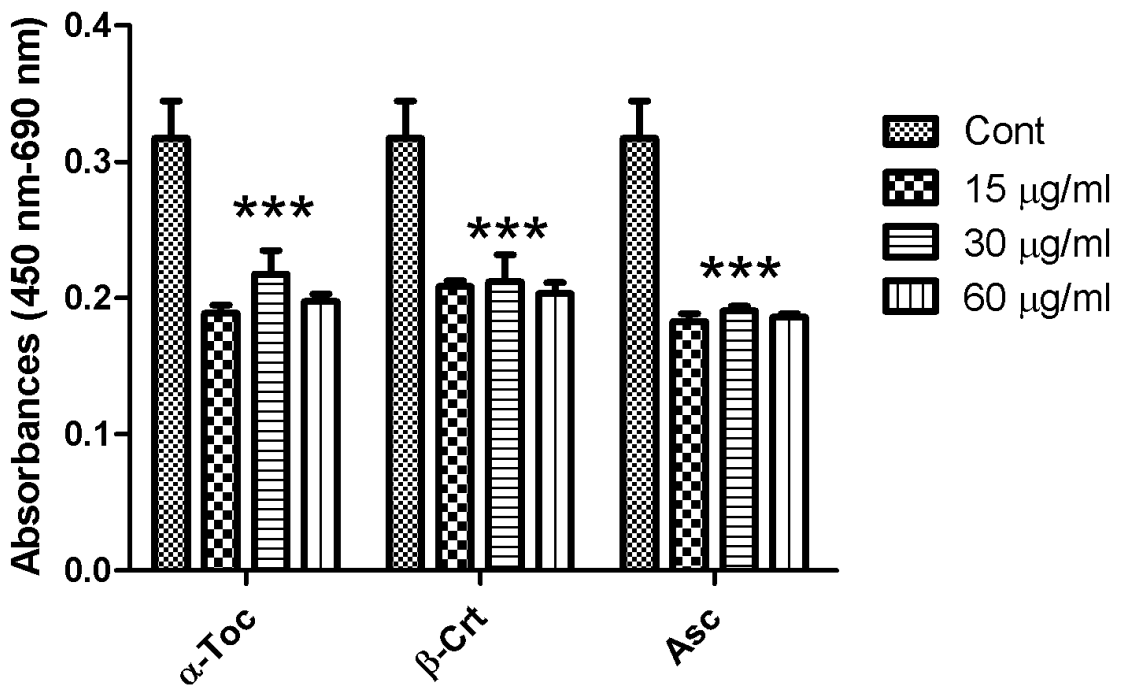

Figure 1. The effect of α-Toc, β-Crt and Asc in PC-3. Cell viability was examined by WST-1 assay. The data were expressed by mean ± SEM ($n \geq 3$). ***$p < 0.001$ Cont vs all antioxidants

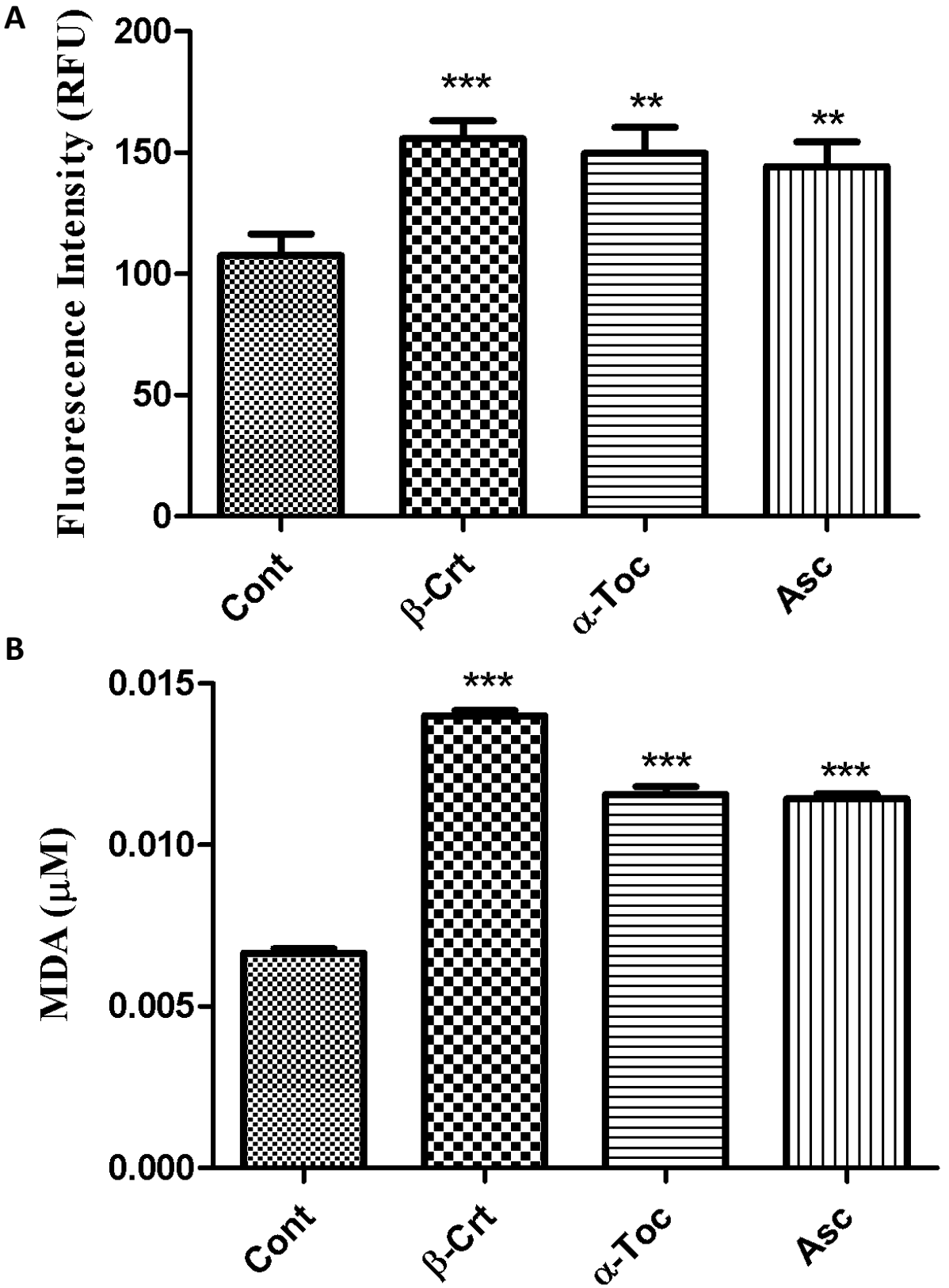

Figure 2. The effect of α-Toc, β-Crt and Asc on ROS (a) generation and LPO levels (b) in PC-3. Cells were exposed to antioxidants. Data were presented by mean ± SEM. (n = 3).

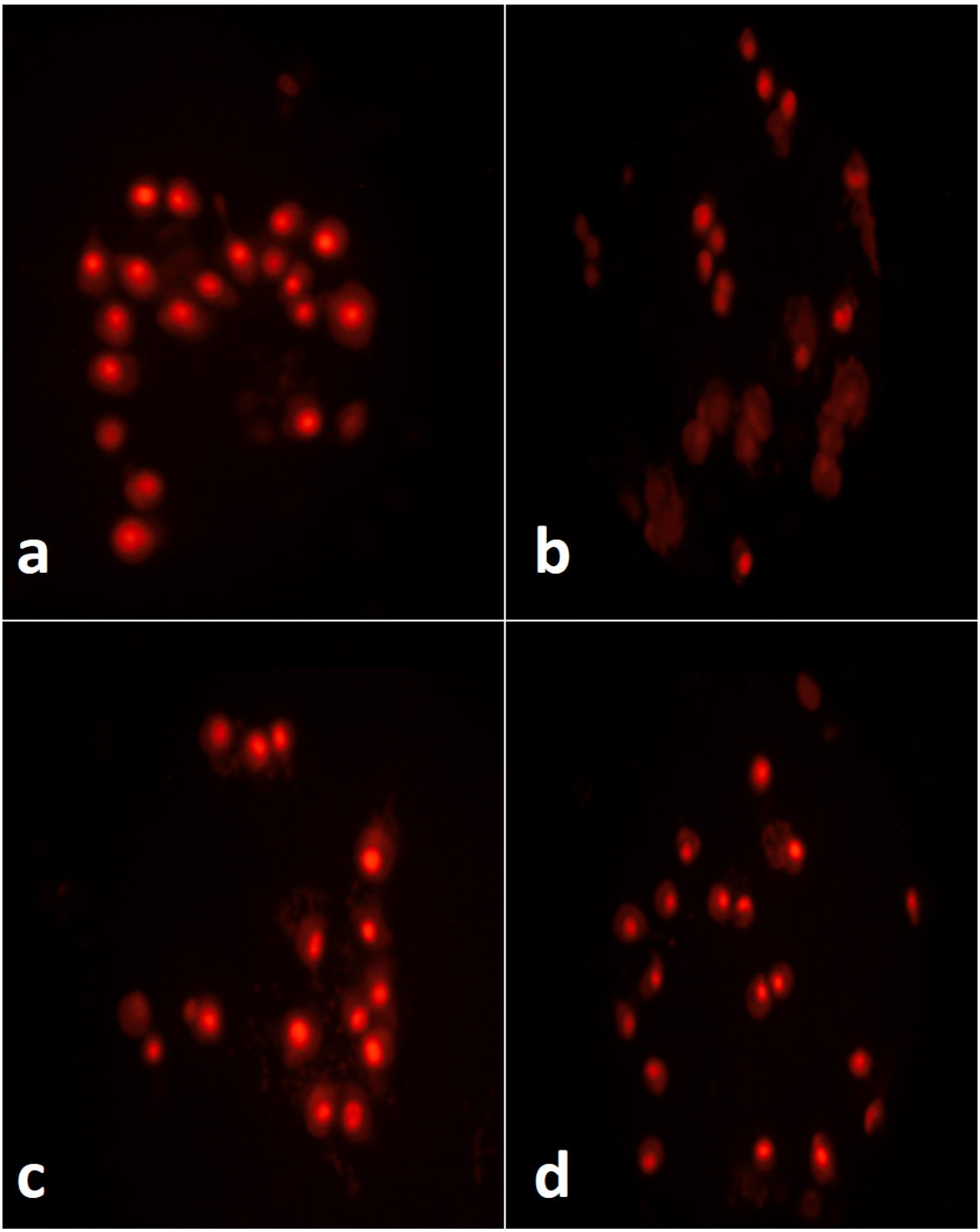

Figure 3. The effect of α-Toc (c), β-Crt (a) and Asc compared (d) to the control (0 µg/ml) (a) on apoptosis evidenced by propidium staining.

Propidium iodide Staining

Propidium iodide staining of cellular nuclei was used as a marker for cell death during the 24 h. Cells are characterized by the typical nuclear modifications. In apoptotic stages, the cells are characterized by a shrink in nucleus. Apoptotic cells were less colored as shown in (Figure 3)

Caspase-3 Staining

To further investigate that the cell death indicated by propidium iodide staining was arisen from apoptotic cascade, immunohistochemical staining of the cells was carried for the active form of caspase 3—a downstream effector of apoptosis—using mouse monoclonal caspase-3 p11 antibody (diluted at 1:500; Santa Cruz Biotechnology, USA). The results indicate the presence of caspase 3 positive represented by black dot shown by arrows (Figure 4). This further demonstrates that the effect of these antioxidants is through apoptotic pathway.

DISCUSSION

Cancer, is one of the major causes of mortality in the world. Recently, it was reported that cancerous cells are linked with high ROS levels, as a result of metabolic, genetic and microenvironment-dependent changes. ROS are generated through the metabolism of oxygen during mitochondrial aerobic respiration. High amount of ROS in cells damage or mutate the DNA of the cells [20].

Despite being studied widely, there has been no precise therapy for prostate cancer to date. Therefore, novel treatment strategies are needed. Regular consumption of natural flavonoids may be associated with a decreased risk of the cancers.

One of the most important antioxidant that fights against lipid peroxidation of cell membranes is Vitamin E. It can alter the oxidative stress biomarkers positively [21].

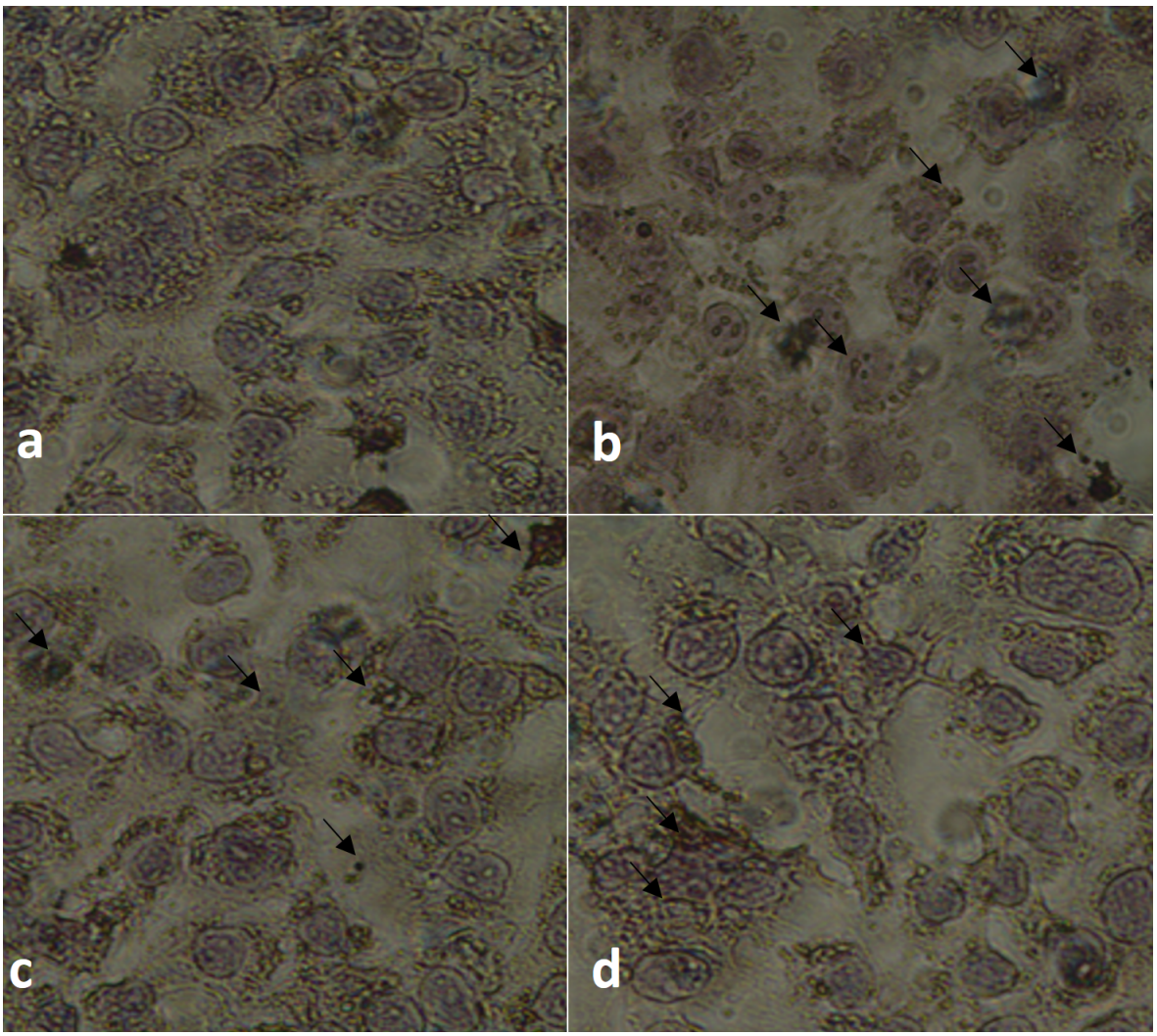

Figure 4. The effect of α-Toc (c), β-Crt (a) and Asc compared (d) to the control (0 μg/ml) (a) on apoptosis related active caspase-3 in PC-3. The cells were imaged under the inverted light microscope and caspase-3 expressing cells were clearly visible with their dark brown color.

Previous studies demonstrated that, β-CRT and retinol supplementation had no effect on the prostate cancer. İt was reported that daily supplementation with selenium (200 µg), vitamin E (400 IU) or both for decreased incidence of prostate cancer in men aged over 50 years. On the other hand, supplementation with 400 IU vitamin E every other day, 500 mg vitamin C every day or a combination of the two were reported to decrease the incidence of cancer in male US physicians aged 50 years or more [6, 22-24].

Recent studies reported that these antioxidants can be behaved as an antioxidant or prooxidant, depending on the redox potential of the biological environment in which it involves [25]. At low concentrations, the antioxidants are reported to act as an antioxidant, inhibiting free radical production, while at high concentrations, they presumably behave as a prooxidant, propagating free radical-induced reactions, consuming endogenous antioxidants and inducing DNA damage. Herein the focus of this study was causing oxidative stress and apoptosis of PC-3 by α-Toc, β-Crt and Asc. It was found that these antioxidants led to an increase in the LPO marker MDA and ROS production at high concentration of the agents tested suggesting it behaves as a prooxidant in this study. ROS have high chemical activity and they play important roles in the regulation of cell proliferation and apoptosis. The level of ROS and lipid peroxidation was highly increased in PC3 cells in response to antioxidants tested within this study in comparison with untreated control cells, as shown in Figure 2 ($p<0.001$). These results suggest that α-Toc, β-Crt and Asc induced mitochondrial dysfunction through the depolarization of the mitochondrial membrane potential and the generation of ROS, which resulted in lipid peroxidation in PC-3 cells. Apoptosis and necrosis are the two important types of cell death for which the molecular mechanisms have been widely studied [26]. Apoptosis, programmed cell death, is a normal developmental process that is characterized by nuclear condensation and cleavage of critical cellular proteins [27]. Apoptosis and necrosis represent two different mechanisms during cellular death. The dynamics of cellular lesions in these two processes are different. It was previously reported that plasma membrane damage, occurring as a primary event during necrosis represents, on the contrary, it is a delayed but massive phenomenon during apoptosis. One way to detect whether the antioxidants induced apoptosis or necrosis is to carry out caspase 3 staining. Therefore, in this research, in addition to investigation of cell viability and ROS and LPO production in PC-3 cell line, the expression of apoptotic caspase-3 enzyme (protease enzyme that play a key role in apoptosis) was studied by immunohistochemical staining. As shown in Figure 4, treatment of PC-3 cells with α-Toc, β-Crt and Asc displayed a marked increase in the expression level of caspase-3 suggesting the elevation in apoptotic enzyme by the antioxidants may account for the anti-apoptotic effect.

CONCLUSION

This study investigated *in vitro* anticancer effect of α-Toc, β-Crt and Asc on PC-3 prostate cancer cells by cell proliferation, ROS and Lipid Peroxidation assay, caspase-3 and propidium iodide staining experiments. The results confirmed that these molecules behaved as prooxidant by decreasing cell viability and increasing ROS and LPO levels in PC-3 cells. It was found that they induced apoptotic pathway as they increased expression level of apoptotic gene caspase-3.

References

1. K. Turkekul, R.D. Colpan, T. Baykul, M.D. Ozdemir, S. Erdogan, Esculetin inhibits the survival of human prostate cancer cells by inducing apoptosis and arresting the cell cycle, J. Cancer Prev., 23 (2018) 10-17.
2. A. Chomyn, G. Attardi, MtDNA mutations in aging and apoptosis, Biochem. Biophys. Res. Commun., 304(2003), 519-529.
3. G.D. Dakubo, R.L. Parr, L.C. Costello, R.B. Franklin, R.E. Thayer, Altered metabolism and mitochondrial genome in prostate cancer. J. Clin. Pathol., 59 (2006) 10-16.
4. N. Khurana, S. Sikka, Targeting crosstalk between Nrf-2, NF-κB and androgen receptor signaling in prostate cancer Cancers, 10 (2018) 352.
5. G. Barrera, Oxidative stress and lipid peroxidation products in cancer progression and therapy, ISRN Oncol., 2012 (2012), 1-21.
6. R.K. Khurana, A. Jain, A. Jain, T. Sharma, B. Singh, P. Kesharwani, Administration of antioxidants in cancer: debate of the decade, Drug Discov. Today, 23 (2018) 763-770
7. A.A. de Carvalho Melo-Cavalcante, L. da Rocha Sousa, M.V.O.B. Alencar, J.V. de Oliveira Santos, A.M. oliveira da Mata, M.F.C. Paz, J. C.R. Gonçalves, Retinol palmitate and ascorbic acid: Role in oncological prevention and therapy, Biomed. Pharmacother., 109 (2019) 1394-1405.
8. C. Sato, S. Kaneko, A. Sato, N. Virgona, K. Namiki, T. Yano, Combination Effect of δ-Tocotrienol and γ-Tocopherol on Prostate Cancer Cell Growth. J. Nutr. Sci. Vitaminol., 63 (2017) 349-354.

9. S.B. Nimse, D. Pal, Free radicals, natural antioxidants, and their reaction mechanisms. Rsc Adv., 5 (2015) 27986-28006.
10. P.K. Witting, J.M. Upston, R. Stocker, Role of α-tocopheroxyl radical in the initiation of lipid peroxidation in human low-density lipoprotein exposed to horse radish peroxidase, Biochem., 36 (1997) 1251-1258.
11. P. Morlière, L.K, Patterson, C.M. Santos, A.M. Silva, J.C. Mazière, P. Filipe, R. Santus, The dependence of α-tocopheroxyl radical reduction by hydroxy-2, 3-diarylxanthones on structure and micro-environment, Org. Biomol. Chem., 10 (2012) 2068-2076.
12. R. Stocker, V.W. Bowry, B. Frei, Ubiquinol-10 protects human low density lipoprotein more efficiently against lipid peroxidation than does alpha-tocopherol, Proc. Natl. Acad. Sci. U.S.A., 88 (1991) 1646-1650.
13. E. Niki, Role of vitamin E as a lipid-soluble peroxyl radical scavenger: *in vitro* and in vivo evidence, Free. Radic. Biol. Med., 66 (2014) 3-12.
14. E. Niki, Action of ascorbic acid as a scavenger of active and stable oxygen radicals, Am. J. Clin. Nutr., 54 (1991) 1119-1124.
15. K.L. Retsky, M.W. Freeman, B. Frei, Ascorbic acid oxidation product (s) protect human low density lipoprotein against atherogenic modification. Anti-rather than prooxidant activity of vitamin C in the presence of transition metal ions, J. Biol. Chem., 268 (1993) 1304-1309.
16. C.W. Oh, M. Li, E.H, Kim, J.S. Park, J.C. Lee, S.W. Ham, Antioxidant and radical scavenging activities of ascorbic acid derivatives conjugated with organogermanium, Bull. Korean Chem. Soc., 31 (2010) 3513-3514.
17. J.A. Satia, A. Littman, C.G. Slatore, J.A. Galanko, E. White, Long-term use of β-carotene, retinol, lycopene, and lutein supplements and lung cancer risk: Results from the vitamins and lifestyle (VITAL) study, Am. J. Epidemiol., 169 (2009) 815-828.
18. M.T. Smith, H. Thor, P. Hartzell, S. Orrenius, The measurement of lipid peroxidation in isolated hepatocytes, Biochem. Pharmacol., 1 (1982) 19-26.
19. M. Tartik, E. Darendelioglu, G. Aykutoglu, G. Baydas, Turkish propolis supresses MCF-7 cell death induced by homocysteine, Biomed. Pharmacother., 82 (2016) 704-712.
20. B. Poljsak, D. Šuput, I. Milisav, Achieving the balance between ROS and antioxidants: when to use the synthetic antioxidants, Oxid. Med. Cell. Longev., 2013 (2013).
21. F. Hecht, C.F. Pessoa, L.B. Gentile, D. Rosenthal, D.P. Carvalho, R.S. Fortunato, The role of oxidative stress on breast cancer development and therapy, Tumor Biol., 37 (2016) 4281-4291.
22. G.E. Goodman, M.D. Thornquist, J. Balmes, M.R. Cullen, F.L. Meyskens Jr, G.S. Omenn, J.H. Williams Jr, The Beta-Carotene and Retinol Efficacy Trial: incidence of lung cancer and cardiovascular disease mortality during 6-year follow-up after stopping β-carotene and retinol supplements, J. Natl. Cancer Inst., 96 (2004) 1743-1750.
23. W.G. Christen, J.M. Gaziano, C.H. Hennekens, PHYSICIANS, F. T. S. C. O., & STUDY II, H. E. A. L. T. H., Design of Physicians' Health Study II—a randomized trial of beta-carotene, vitamins E and C, and multivitamins, in prevention of cancer, cardiovascular disease, and eye disease, and review of results of completed trials, Ann. Epidemiol., 10 (2000) 125-134.
24. E.A. Klein, I.M. Thompson, C.M. Tangen, J.J. Crowley, M.S. Lucia, P.J. Goodman, D.D. Karp, Vitamin E and the risk of prostate cancer: the Selenium and Vitamin E Cancer Prevention Trial (SELECT), JAMA, 306 (2011) 1549-1556.
25. Y. Cui, Z. Lu, L. Bai, Z. Shi, W.E. Zhao, B. Zhao, β-Carotene induces apoptosis and up-regulates peroxisome proliferator-activated receptor γ expression and reactive oxygen species production in MCF-7 cancer cells, Eur. J. Cancer, 43 (2007) 2590-2601.
26. V. Nikoletopoulou, M. Markaki, K. Palikaras, N. Tavernarakis, Crosstalk between apoptosis, necrosis and autophagy, Biochim. Biophys. Acta- Mol. Cell Res., 1833 (2013) 3448-3459
27. J.J. Stevens, B. Graham, E. Dugo, B. Berhaneselassie-Sumner, K. Ndebele, P.B. Tchounwou, Arsenic trioxide induces apoptosis via specific signaling pathways in HT-29 colon cancer cells, J. Cancer Sci. Ther., 9 (2017) 298.

Ş.Kara and M.Akcan / Hacettepe J. Biol. & Chem., 2020, 48 (3), 219-229

Review Article

Hacettepe Journal of Biology and Chemistry

journal homepage: www.hjbc.hacettepe.edu.tr

Disulfide-Rich Peptides in Drug Development

İlaç Geliştirmede Disülfit-Zengin Peptidler

Şeyda Kara and Muharrem Akcan*

Department of Biochemistry, Faculty of Arts and Sciences, Kütahya Dumlupınar University, Kütahya, Turkey.

ABSTRACT

Peptides are important biomolecules in drug development with their high specificities to their targets. Many peptide-based drug candidates have been increasingly involved in clinical and preclinical studies. Unfortunately, peptides have some disadvantages such as poor metabolic stability, poor oral bioavailability and high production costs. These problems can be overcome by modifications that have been inspired from highly stable disulfide-rich peptides already found in nature. This review describes the structure and bioactivity of disulfide-rich peptides and their development with various modifications to become candidate molecules in drug design and development studies.

Key Words

Therapeutic peptides, drug development, cyclotides, peptide stability.

ÖZ

Peptidler, ilaç geliştirmede hedeflerine yüksek özgüllükleri olan önemli biyomoleküllerdir. Birçok peptid-bazlı ilaç adayı, klinik ve preklinik çalışmalarda giderek daha fazla yer almaktadır. Ne yazık ki, peptidlerin zayıf metabolik stabilite, zayıf oral biyoyararlanım ve yüksek üretim maliyetleri gibi bazı dezavantajları vardır. Bu problemler, hali hazırda doğada bulunan oldukça stabil disülfit bakımından zengin peptidlerden ilham alınarak yapılan modifikasyonlar ile çözülebilir. Bu derlemede disülfit-zengin peptidlerin yapı ve biyoaktiviteleri ve ilaç tasarım ve geliştirme çalışmalarında aday moleküller haline gelmek için çeşitli modifikasyonlarla geliştirilmeleri anlatılmaktadır.

Anahtar Kelimeler

Terapötik peptidler, ilaç geliştirme, siklotitler, peptid stabilitesi.

Article History: Received: Jan 20, 2020; Revised: Mar 12 2020; Accepted: Mar 15, 2020; Available Online: Apr 1, 2020.

DOI: https://doi.org/10.15671/hjbc.658764

Correspondence to: M. Akcan, Department of Biochemistry, Faculty of Arts and Sciences, Kütahya Dumlupınar University, Kütahya, Turkey.

E-Mail: muharrem.akcan@dpu.edu.tr

THERAPEUTIC PEPTIDES

Therapeutic molecules are divided into two main classes as molecules with less than 500 Da molecular weight and protein-structured biologicals with molecular weight greater than 5000 Da. Although small molecule therapeutics are known to be stable molecules as they do not degrade when taken into the body, they have low specificity to their targets and hence side effects, as they can create undesirable interactions with other regions outside the active site of the target molecule. On the other hand, because of their large molecular structures, biologicals bind to their targets with high specificity and thus produce less side effects. Therefore, the number of biologicals approved by drug authorities has increased in recent years [1-3]. However, biologicals are easily degraded by proteases because of their protein-based structures, resulting in reduced bioavailability and hence a more limited effect. In today's pharmaceutical research and development, many studies have been carried out to eliminate these disadvantages of small molecule therapeutics and biologicals. In recent years, peptides have become molecules of interest in such studies. Peptides ranging in molecular weight from 500 Da to 5000 Da have advantages such as high target specificity, less toxicity and less deposition in tissues as biologicals (Figure 1). They can also easily pass through the cell walls as small molecules and interact with their target molecules.

Peptides are biomolecules formed by binding of 40 and/or fewer amino acids to each other by peptide bonds. The therapeutic efficacy of the peptides has been extensively studied and is of great interest in the diagnosis and treatment of many diseases [4].

To date, peptides have been isolated from many organisms, particularly from microorganisms, animals and plants, and their therapeutic efficacy has been studied by many research groups [5-8]. These peptides are used in today's drug screening, design and development studies, and some have already been approved as drugs. For example, cyclosporin A, isolated from *Tolypocladium inflatumizole* fungus, is a peptide having 11 residues and has oral bioavailability [9-11]. Although its antifungal activity is known at first, it is currently used as an immunosuppressant in organ transplants [12]. Linaclotide, another peptide drug that can be taken orally, interacts

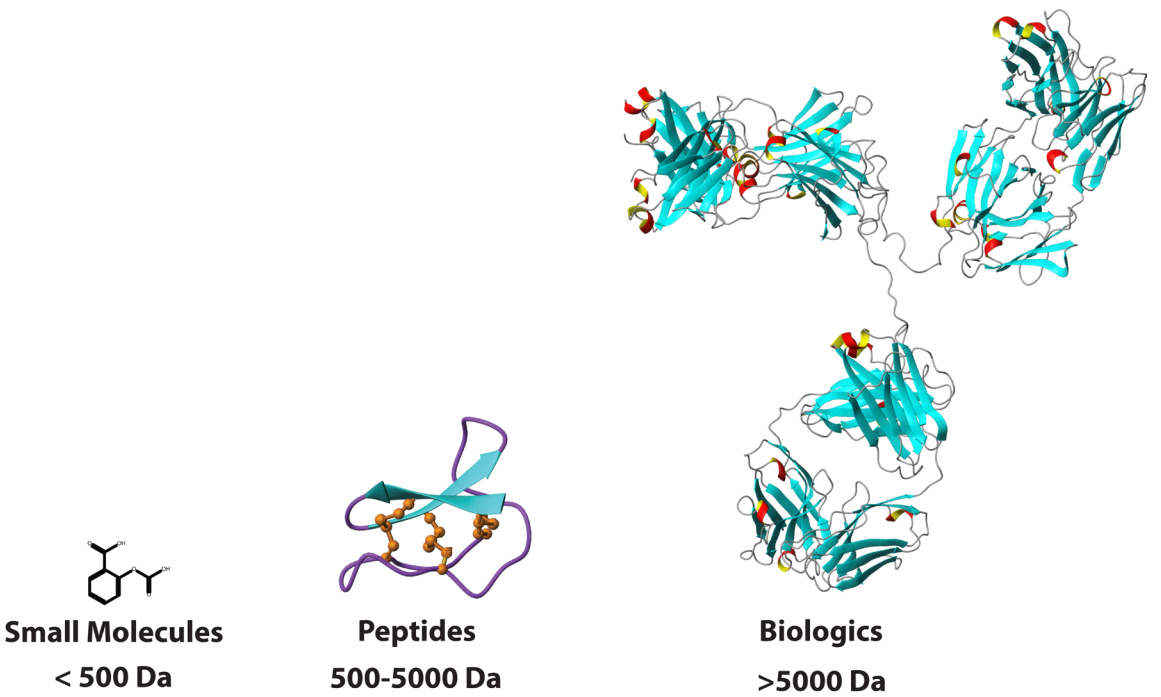

Figure 1. Illustration of therapeutic molecule structures by molecular weight. Peptides are therapeutic biomolecules between small molecules and biologicals based on their molecular weight and are used in today's pharmaceutical research and development. Aspirin, kalata B1 (PDB code: 1NB1) and IgG2a (PDB code: 1IGT) monoclonal antibody are given as examples for small molecules, peptides and biologicals, respectively. Kalata B1 and IgG2a molecular structures were prepared with MOLMOL [Figure was adapted from reference 6].

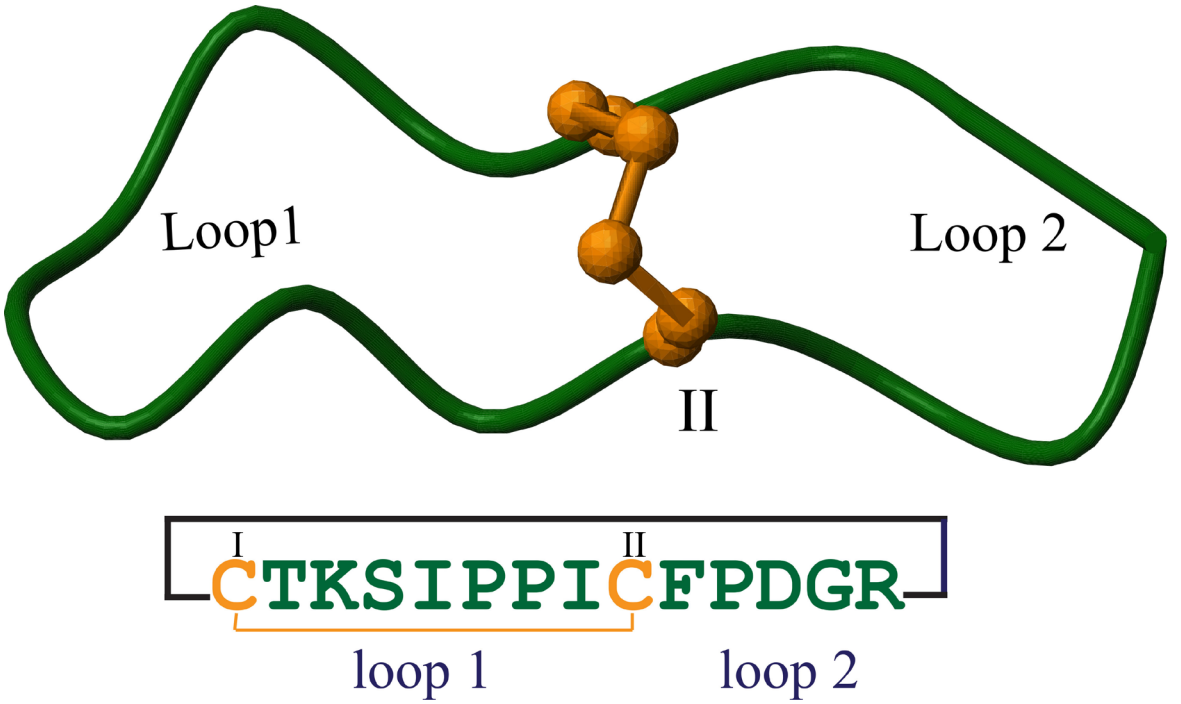

Figure 2. The three-dimensional structure and amino acid sequence of SFTI-1 peptide (PDB code: 1JBL). The peptide has 14 residues and a disulfide bridged cyclic backbone structure. The peptide backbone is shown in green, and the Cys amino acids forming the disulfide bridge are shown in orange. Molecular structure was prepared with MOLMOL [Figure was adapted from reference 6].

with guanylate cyclase C and is used in the treatment of irritable bowel syndrome. This peptide drug has 14 residues and three disulfide bridges. Colistin, a peptide drug isolated from *Paenibacillus polymyxa*, is used in infectious diseases caused by gram (-) bacteria. Another drug with antimicrobial activity is daptomycin which was approved in 2013 by the American Food and Drug Administration (FDA), is a lipopeptide isolated from *Streptomyces roseosporus*.

Peptides, particularly from venoms, saliva and skin secretions of animals, have an important place in the development of peptide-based drugs because of their high therapeutic potentials. Eptifibatide, isolated from snake venom has been used clinically since 1998 for its anticoagulant activity [13]. Captopril, another peptide drug isolated from snake venom, is used in the treatment of hypertension with angiotensin converting enzyme (ACE) inhibitor activity [14]. Tirofiban, Batroxobin, Hemocoagulase, Ximelagatran are other peptide drugs in the market derived from snake venoms [15-18]. Another therapeutic peptide of animal origin is Exenatide, which is isolated and developed from the saliva of the Gila monster lizard. This C-terminal amidated and 39 amino acid long peptide was approved by FDA in 2005 for the treatment of Type 2 diabetes [19].

Peptides derived from conus species of marine snails living in tropical oceans are called conotoxins [20,21]. Conotoxins are disulfide-rich linear biomolecules with 12-40 amino acids. Because of their high potency and selectivity on potassium, sodium, calcium and chloride ion channels and receptors, conotoxins are considered as important therapeutics [22,23]. The synthetic version of 25 amino acid-long MVIIA peptide derived from the venom of the *C. magus* cone snail is the first conotoxin-type peptide drug used for the treatment of chronic pain under the generic name of Ziconotide (Prialt®) [24,25]. Another promising conotoxin is Vc1.1 peptide from the venom of *C. victoria* and has 16 amino acids with two disulfide bonds. It can inhibit nicotinic acetylcholine receptors (nAChR) and its synthetically cyclized version has higher stability compared to lineer version [26].

Chlorotoxin is a 36 amino acids long scorpion venom peptide isolated from *Leiurus quinquestriatus* venom. Three-dimensional structure of chlorotoxin has been identified by Nuclear Magnetic Resonance (NMR) spectroscopy [27]. It has an α-helix and three β-sheets structure with four disulfide bonds. A synthetic iodine derivative of chlorotoxin, ^{131}I-TM-601, was reported as

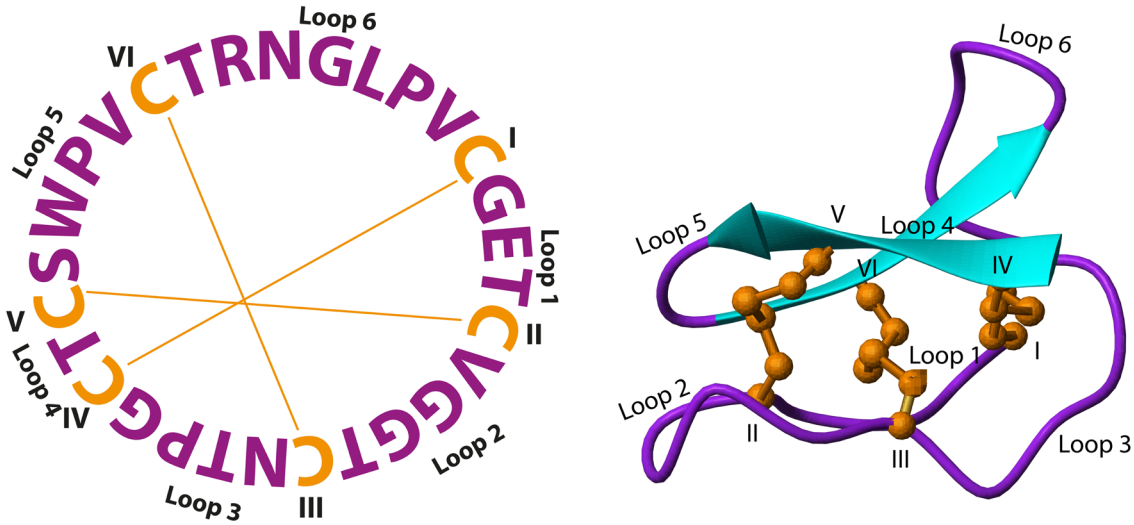

Figure 3. Amino acid sequence and three-dimensional structure of Kalata B1 peptide (PDB code: 1NB1). The peptide has a cyclic backbone structure and six Cys residues forming the three disulfide bridges. The peptide backbone is shown in purple, and the Cys amino acids and the disulfide bonds are shown in orange. The three-dimensional structure on the right was prepared with MOLMOL [Figure was adapted from reference 6].

it can bind to glioma, but not to normal tissues [28]. It has been reported that chlorotoxin can also bind Annexin 2 which is an extracellular matrix protein of cancer cells. This cancer cell selectivity of chlorotoxin has been utilized to develop a conjugated molecule of the peptide with a fluorescent dye. The conjugate is called "tumor paint" which can highlight brain tumor cells under fluorescent light during surgical resection [29,30] and help surgeons to distinguish cancer cells from normal cells more precisely. Tozuleristide (BLZ-100) is a version of tumor paint developed by conjugating chlorotoxin with the near-infrared fluorophore indocyanine green for imaging pediatric brain tumors and it is now in phase I clinical trials [31].

In addition to conotoxins and chlorotoxin and other venom peptides, macaque and baboon leukocytes, frog skin secretions, spider hemocytes and bee venoms are also other rich sources of bioactive peptides that have been under investigation for the development of peptide therapeutics for many decades [32-35].

Plants are other important sources of bioactive peptides that are frequently used in drug research and development studies due to their high stability and cell penetration abilities. They have also antimicrobial, anti-HIV and anticancer bioactivities [36]. For example, trypsin inhibitor SFTI-1 peptide isolated from sunflower plant is one of the most studied plant-derived peptides with high stability. It is a 14 amino acid long single disulfide-bridged cyclic peptide with a lysine residue which provide the trypsin inhibitor activity. In addition to the cyclic backbone and the single disulfide bridge, hydrogen bonds between the two antiparallel β-sheets also have a significant effect on the stability of SFTI-1 [37]. While having a homologous sequence to Bowman-Birk inhibitors that inhibit trypsin/chymotrypsin enzymes, it has also been reported to inhibit the matriptase enzyme that induces cancer cell metastasis [38,39]. In Figure 2, the three-dimensional solution structure and amino acid sequence of SFTI-1 are shown.

Because of their diverse and invaluable bioactivities, peptides have an important role in pharmaceutical research and development studies. However, the major challenges in the development of peptide-based drugs are their poor stability and consequently poor oral bioavailability. In order to overcome this problem, the drug development studies firstly discover the peptide or peptide epitope and aims to increase the stability and bioavailability of this epitope by various strategies. Strategies for increasing peptide stability has been initially inspired by the structure and bioactivity of plant derived disulfide-rich peptides (e.g. cyclotides) found in nature.

Disulfide Rich Peptides; Cyclotides

In the 1960s, Norwegian Doctor Lorents Gran observed that women living in the Democratic Republic of Congo in Africa boiled *Oldenlandia affinis* plant and drank its

tea to facilitate childbirth. It has been reported that the main active ingredient in this uterotonic plant extract is the kalata-kalata peptide, which does not denature despite boiling in water and is resistant to proteolytic enzymes when administered orally [40]. Approximately 25 years later, the peptide was renamed as kalata B1 and was reported to have a cyclic peptide backbone and a cystine knot motif arranged by its three disulfide bonds (Figure 3) [41,42].

Cyclotides are found in Rubiaceae, Violaceae, Cucurbitacea, Solanaceae and Fabaceae plant families [43]. In the following years, new cyclotides were isolated from *Panicum laxum*, a member of the single-core Poaceae plant family [44,45]. They are cyclic peptides with 28-37 residues, of which six are Cys residues. The peptide sequence between the two Cys amino acids is called "loop". In loop 1, the cyclotides generally contain a total of 3-4 amino acids with a Glu residue, 4-8 amino acids in loop 2, 3-7 amino acids in loop 3, only one amino acid (Ser, Thr or Ile) in loop 4, 4-5 amino acids in loop 5, and 5-8 amino acids in loop six [46-48]. The lists and activities of cyclotides are deposited in a database called Cybase (http://www.cybase.org.au/) [49].

The three disulfide bonds of cyclotides are arranged in themselves to form the cyclic cystine knot (CCK) structural motif. This CCK motif, which is the most characteristic feature of cyclotides, is the ring structure formed by Cys1-Cys4 and Cys2-Cys5 disulfide bridges together and the third disulfide bridge formed by Cys3-Cys6 embed this ring to form CCK motif (Figure 4). This motif is extremely important as it gives chemical, thermal and enzymatic resistance to the peptide structure [50]. Cyclotides have an important role in drug research and development due to the outstanding stability of CCK motif and the cyclic backbone, their tolerance to sequence modifications, and the ability of some cyclotides to cross the cell membrane.

Cyclotides are divided into three sub-classes as Möbius, bracelet and trypsin inhibitors. The Möbius and bracelet cyclotides are similar but are separated by the presence or absence of a cis-Trp-Pro bond in loop 5, respectively. Examples of the most commonly used cyclotides in drug design studies as Möbius and Trypsin inhibitors are kalata B1 and MCoTI-II peptides, respectively. Bracelet subfamily peptides are not preferred very much in the studies due to the lack of conformation in the natural form of the peptide after they are synthetically produced [51,52].

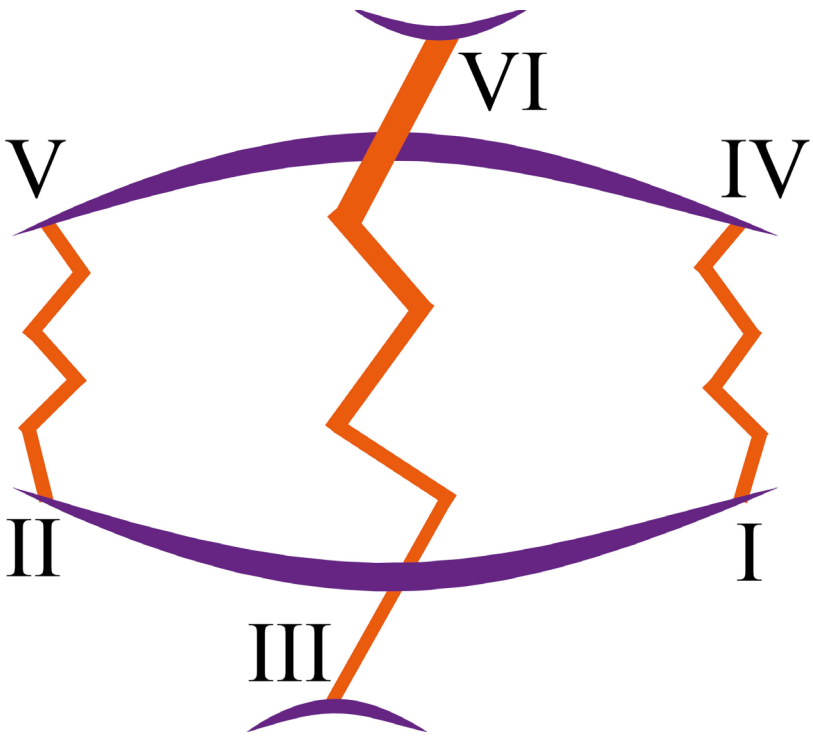

Figure 4. Cyclic cystine knot (CCK) motif. Three disulfide bonds are arranged in themselves in which two of them form a ring and the third one embeds this ring to form a knot motif. The CCK motif provides outstanding resistance to peptides against chemical, thermal and enzymatic effects. The peptide backbone is shown in purple and disulfide bridges in orange [Figure was adapted from reference Figure was adapted from reference].

In addition to the high stability of cyclotides, it has been shown that they also have many important bioactivities. The most important task of these peptides is to protect the plant against insects that was reported in a study in which cyclotides can inhibit the growth of *Helicoverpa larvae* (insecticide) [53]. Cyclotides have also been reported in many studies to have nematicide, molluscicide, anti-HIV and antimicrobial activities [54-57]. Because of these remarkable pharmacological properties, many research groups have been investigating cyclotides for a couple of decades.

The positive charge that gives the antimicrobial effect to cyclotides is extremely important for their membrane activities. The positively charged cyclotides can electrostatically interact with the negative charge on the membranes of tumor cells, bacteria and pathogens, break down the membranes of the cells and enter them. The bioactivities of Möbius and bracelet cyclotides change in relation to the presence or absence of phosphotylethanolamine (PE), one of the membrane phospholipids found in the membrane, and high affinities of these cyclotides against PE have been reported [58,59]. However, MCoTI-II, which does not have an affinity for PE, can enter the cell as a result of its interaction with phosphatidylinositol (PI) and phosphate acids (PA) in the membrane [60,61]. Furthermore, the first loop of cyclotides, particularly the Glu residue, is extremely important for membrane degrading activity [62]. The cytotoxic effects of cyclotides varv A and varv F belonging to the Möbius subfamily and cycloviolacin O2 from the bracelet subfamily were also examined and these cyclotides showed selective cytotoxic effects by interacting with cancer cells containing more negatively charged phosphatidylserine (PS) in their membranes compared to normal cells [63-65].

Strategies for Enhancing Peptide Stability

Although peptides have significant bioactivities, they degrade as proteins when taken orally due to the low pH of stomach content and their susceptibility to proteases such as trypsin, chymotrypsin, pepsin and carboxy peptidases. If the peptide medications that should be taken frequently for treatment would be taken by injection which is not preferred by the patients. Peptide drugs are given by parenteral injection due to their poor oral bioavailability. For example, the peptide hormone insulin is administered by injection to treat diabetes because of its susceptibility to various proteases in the body. Therefore, the stability of the peptide-based drug leads needs to be enhanced with various strategies to be resistant to proteases without affecting peptide bioactivity. Cyclization of peptide backbone, grafting and addition of unnatural amino acids to the peptide sequence or modifications of amino acids are important strategies for this purpose. In Figure 5 below, strategies that can be applied to increase peptide stability are given.

Cyclization of Peptide Backbone

Perhaps the most important strategy to improve the peptide stability is the cyclization of linear peptide backbone that has been inspired by the emergence of cyclic peptides with high stability (e.g. cyclotides) [66-70]. It has been possible to obtain peptide structures that are more resistant to proteolytic enzymes by using bridges formed between amino acids side chains or joining the peptide backbone N- and C-terminals using linker residues that has an appropriate length of the distance between the terminals of the peptide without disrupting the overall three-dimensional structures but to increase the peptide stability.

Conotoxins have limited stability to proteolytic enzymes due to their linear frameworks. The cyclization method has been one of the most preferred method for increasing the stability of these peptides. The most famous example is the cyclization of α-conotoxin Vc1.1 peptide backbone reported in 2010 [71]. In this study, considering the three-dimensional structure, the peptide was cyclized with six linker residues (GGAAGG) in accordance with the distance between the N- and C-terminals of Vc1.1. After cyclization, the three-dimensional structure of the peptide was preserved as native fold and the peptide stability was increased by 46% compared to linear Vc1.1. cVc1.1 has been also more stable in simulated gastric fluid and simulated intestinal fluid compared to linear Vc1.1 and orally active in rat model used in the study. Another example is the cyclization of an 18 amino acid long Gomesin peptide isolated from hemocytes of spider *Acanthoscurria gomesiana*. After cyclization, it's found that stability and cytotoxicity of this antimicrobial peptide to HeLa cells increased compared to its linear version [72].

Peptide backbone cyclization has been successfully applied on many other linear bioactive peptides, particularly on conotoxins, scorpion venom peptide chlorotoxin (CTX) and wasp venom mastoparan (MP-C) peptide [30,73-76].

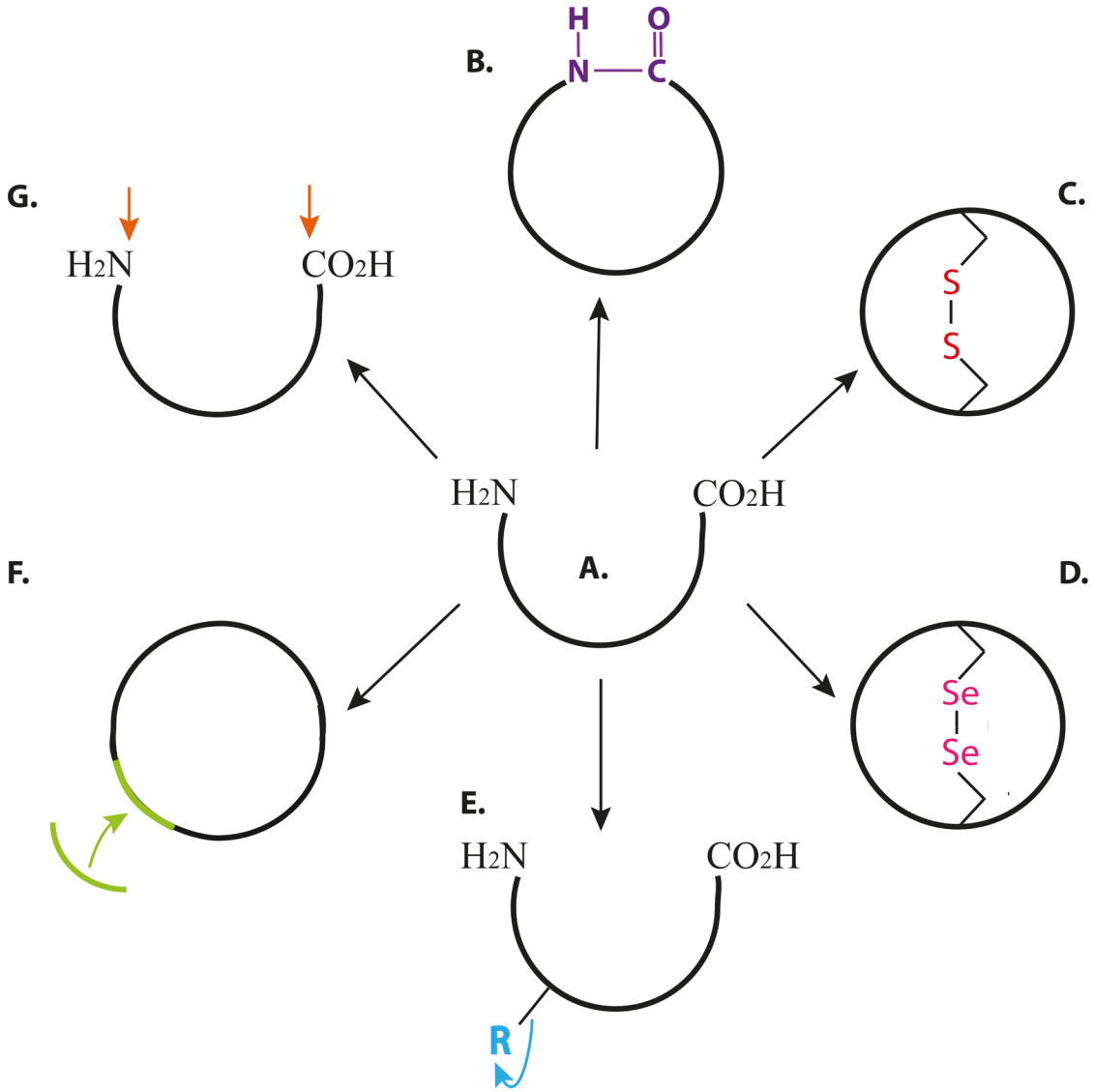

Figure 5. Strategies to increase peptide stability to make peptides resistant to proteases without affecting their bioactivities. **A.** linear peptide structure. **B.** head-to-tail peptide backbone cyclization. **C.** addition of disulfide bridges. **D.** addition of diselenide bridges. **E.** stereochemically inversion of amino acids (use of D-amino acids). **F.** grafting of an active peptide epitope and **G.** capping the N- and C-terminals [Figure was adapted from reference 6].

Grafting of Peptide Epitopes

Placing bioactive short linear peptide epitopes on the peptide scaffolds with proven stability is known as grafting. It has been reported in many studies that the stability of the bioactive linear epitope can be increased by grafting [77-80]. Since the plant-derived peptides kalata B1, MCoTI-II and SFTI-1 peptides are highly resistant to chemicals, heat and enzymes, they have been used more in many peptide-based drug development studies than other peptides to date. Since these prototypic peptides can also be synthesized by solid phase peptide synthesis (SPPS) methods and can easily be folded correctly as their native forms, peptide epitope grafting studies in the literature have generally been applied by utilizing these three peptides.

In the literature, grafting studies are mainly carried out on the sixth loop of cyclotides, which appears to be tolerant to sequence replacements. Because the first and fourth loops of cyclotides form the main center and contain a limited number of amino acids (e.g. loop 1 has 3-4 residues and loop 4 has only one residue). The second loop is important for peptide folding as it can form salt bridges. The structure and properties of the

peptide epitope are as important as the loop where the grafting will be performed. Abdul Ghani et al. studied the effect of structure and bioactivity by altering some mutual loops of kalata B1 and MCoTI-II and reported that the CCK motif is resistant to intact if covalent bond interactions do not occur, but bioactivity can vary greatly even with minor changes, including point mutations. Therefore, the previous literature data should be carefully examined before any grafting studies [67,68].

Thrombospondin-1 (TSP-1) is a fragment of a seven-amino acid peptide with an anti-antigenogenic effect. In order to increase the stability of this peptide, grafting of the seven-residue bioactive epitope (GVITRIR) of TSP-1 onto MCoTI-II and SFTI-1 was reported in 2015. For both synthesized grafted peptides, the stability of the peptide epitope was increased while maintaining its bioactivity inherent as in native TSP-1 [81].

In another study, the bradykinin B1 receptor antagonists DALK peptide with nine amino acid residues was grafted onto loop 6 of kalata B1 for inflammatory pain treatment and reported notable stable in human serum for more than six hours with almost 90% remained intact while DALK was degraded completely in this time period. In this study, it was also demonstrated that the grafted peptide was orally active [82]. In a following study, the peptide was also grafted separately on both loops of SFTI-1. The peptides were synthesized in both linear and cyclic forms [83]. The stability of each synthesized peptide was significantly increased, and the linear peptides exhibited less trypsin activity than bradykinin peptide epitope and cyclic grafted peptides.

Peptide Analogs

Peptide analogs harboring unnatural amino acids in the sequence are one of the strategies that can be used to enhance peptide stability against proteases. Polybia-CP, isolated from *Polybia paulista* wasp venom, is a 12 residue C-terminal amidated antimicrobial peptide. In 2017, Jia et al. synthesized its analog with D-amino acids in order to optimize the stability of this peptide and reported that the stability of the modified peptide was enhanced against trypsin and chymotrypsin enzymes. In the same study, the hemolytic effect of the peptide was significantly reduced compared to native Polybia-CP, although the antimicrobial effect was slightly reduced [84].

The plant-derived kalata B1 peptide achieves many important bioactivities by its electrostatic interaction with the cell membrane. In 2011, Sando and colleagues synthesized kalata B1 with D-amino acids and investigated its effects on cell membrane compared to kalata B1 in its native form. D-kalata B1 was reported to have lower hemolytic activity. In addition, although the membrane affinity of D-kalata B1 was less, its anti-HIV activity, cytotoxicity, and hemolytic effect continued even they have slightly decreased [85].

In addition to cyclization, grafting and the use of unnatural amino acids, replacement of disulfide bonds by diselenide bonds, covalent coupling of the peptide with polyethyleneglycol (PEG) or lipids and truncation or capping of the N- and C-terminals of the peptide have also been reported to increase the stability of the peptides [86-89].

In conclusion, disulfide-rich peptides found in plants and animals are promising drug scaffolds due to their high stabilities and diverse bioactivities including antimicrobial, anti-HIV, anticancer, analgesia, hypertension and more. Furthermore, although peptides have some drawbacks, they can be chemically modified to overcome the disadvantages such as stability and hemolytic activity and to contribute novel bioactivities.

References

1. P. Chames, M. Van Regenmortel, E. Weiss, D. Baty, Therapeutic antibodies: successes, limitations and hopes for the future, Br. J. Pharmacol., 157 (2009) 220-233.
2. N. Munoz-Durango, M.S. Pizarro-Ortega, E. Rey-Jurado, F.E. Diaz, S.M. Bueno, A.M. Kalergis, Patterns of antibody response during natural hRSV infection: insights for the development of new antibody-based therapies, Expert Opin. Investig. Drugs, 27 (2018) 721-731.
3. T.M. Pierpont, C.B. Limper, K.L. Richards, Past, present, and future of rituximab-the world's first oncology monoclonal antibody therapy, Front. Oncol., 8 (2018) 163.
4. J.L. Lau, M.K. Dunn, Therapeutic peptides: Historical perspectives, current development trends, and future directions, Bioorg. Med. Chem., (2017) 2700-2707.
5. R. Koradi, M. Billeter, K. Wuthrich, MOLMOL: A program for display and analysis of macromolecular structures, J. Mol. Graph., 14(1996) 51-55.
6. Ş. Kara, Tümör ile ilişkili peptidlerin sentezi ve kararlılıklarının incelenmesi-Synthesis and examination of stabilities of tumor-related peptides, M.Sc. Thesis, Number: 529178, Kütahya Dumlupınar University, Graduate School of Sciences, 2018.
7. L. Thorstholm, D.J. Craik, Discovery and applications of naturally occurring cyclic peptides, Drug Discov. Today Technol., 9 (2012) e1-e70.

8. J. Koehbach, D.J. Craik, The Vast Structural Diversity of Antimicrobial Peptides, Trend. Pharmaco. Sci., 40 (2019) 517-528.
9. J.F. Borel, C. Feurer, H.U. Gubler, H. Stahelin, Biological effects of cyclosporin A: a new antilymphocytic agent, Agents Actions, 6 (1976) 468-475.
10. C. Spitzfaden, H.P. Weber, W. Braun, J. Kallen, G. Wider, H. Widmer, M.D. Walkinshaw, K. Wuthrich, Cyclosporin A-cyclophilin complex formation. A model based on X-ray and NMR data, FEBS Lett., 300 (1992) 291-300.
11. X. Yang, P. Feng, Y. Yin, K. Bushley, J.W. Spatafora, C. Wang, Cyclosporine biosynthesis in *Tolypocladium inflatum* benefits fungal adaptation to the environment, mBio, 9 (2018) e01211-01218.
12. J. Klages, C. Neubauer, M. Coles, H. Kessler, B. Luy, Structure refinement of cyclosporin a in chloroform by using RDCs measured in a stretched PDMS-gel, Chembiochem., 6 (2005) 1672-1678.
13. J.C. O'Shea, J.E. Tcheng, Eptifibatide: a potent inhibitor of the platelet receptor integrin glycoprotein IIb/IIIa, Expert Opin. Pharmacother., 3 (2002) 1199-1210.
14. D.W. Cushman, M.A. Ondetti, History of the design of captopril and related inhibitors of angiotensin converting enzyme, Hypertension, 17 (1991) 589-592.
15. Lodha, M. Kamaluddeen, A. Akierman, H. Amin, Role of hemocoagulase in pulmonary hemorrhage in preterm infants: a systematic review, Indian J. Pediatrics., 78 (2011) 838-844.
16. S.J. Ho, T.A. Brighton, Ximelagatran: Direct thrombin inhibitor, Vasc. Health Risk Manag., 2 (2006) 49-58.
17. T.T. Vu, A.R. Stafford, B.A. Leslie, P.Y. Kim, J.C. Fredenburgh, J.I. Weitz, Batroxobin binds fibrin with higher affinity and promotes clot expansion to a greater extent than thrombin, J. Biol. Chem., 288 (2013) 16862-16871.
18. T.M. A. El-Aziz, A.G. Soares, J.D. Stockand, Snake venoms in drug discovery: valuable therapeutic tools for life saving, Toxins, 11 (2019) E564.
19. Barnett, Exenatide, Expert Opin. Pharmacother., 8 (2007) 2593-2608.
20. W.R. Gray, A. Luque, B.M. Olivera, J. Barrett, L.J. Cruz, Peptide toxins from Conus geographus venom, J. Biolog. Chem., 256 (1981) 4734-4740.
21. H. Terlau, B.M. Olivera, Conus venoms: a rich source of novel ion channel-targeted peptides, Physiolog. Rev., 84 (2004) 41-68.
22. B. Gao, C. Peng, J. Yang, Y. Yi, J. Zhang, Q. Shi, Cone snails: a big store of conotoxins for novel drug discovery, Toxins, 9 (2017) E397.
23. H.M. Duque, S.C. Dias, O.L. Franco, Structural and functional analyses of cone snail toxins, Mar. Drugs, 17 (2019) E370.
24. K.K. Jain, An evaluation of intrathecal ziconotide for the treatment of chronic pain, Expert Opin. Investig. Drugs, 9 (2000) 2403-2410.
25. G.P. Miljanich, Ziconotide: Neuronal calcium channel blocker for treating severe chronic pain, Curr. Med. Chem., 11 (2004) 3029-3040.
26. R.J. Clark, H. Fischer, S.T. Nevin, D.J. Adams, D.J. Craik, The synthesis, structural characterization, and receptor specificity of the alpha-conotoxin Vc1.1, J. Biol. Chem., 281 (2006) 23254-23263.
27. J.A. DeBin, J.E. Maggio, G.R. Strichartz, Purification and characterization of chlorotoxin, a chloride channel ligand from the venom of the scorpion, Amer. J. Physiol. Cell Physiol., 264 (1993) C361-369.
28. A.N. Mamelak, S. Rosenfeld, R. Bucholz, A. Raubitschek, L.B. Nabors, J.B. Fiveash, S. Shen, M.B. Khazaeli, D. Colcher, A. Liu, M. Osman, B. Guthrie, S. Schade-Bijur, D.M. Hablitz, V.L. Alvarez, M A. Gonda, Phase I single-dose study of intracavitary-administered iodine-131-TM-601 in adults with recurrent high-grade glioma, J. Clin. Oncol., 24, (2006) 3644-3650.
29. M. Veiseh, P. Gabikian, S.B. Bahrami, O. Veiseh, M. Zhang, R.C. Hackman, A.C. Ravanpay, M.R. Stroud, Y. Kusuma, S.J. Hansen, D. Kwok, N.M. Munoz, R.W. Sze, W.M. Grady, N.M. Greenberg, R.G. Ellenbogen, J.M. Olson, Tumor paint: a chlorotoxin: Cy5.5 bioconjugate for intraoperative visualization of cancer foci, Cancer Res., 67 (2007) 6882-6888.
30. M. Akcan, M.R. Stroud, S.J. Hansen, R.J. Clark, N.L. Daly, D.J. Craik, J.M. Olson, Chemical re-engineering of chlorotoxin improves bioconjugation properties for tumor imaging and targeted therapy, J. Med. Chem., 54 (2011) 782-787.
31. C.G. Patil, D.G. Walker, D.M. Miller, P. Butte, B. Morrison, D.S. Kittle, S.J. Hansen, K.L. Nufer, K.A. Bymes-Blake, M. Yamada, L.L. Lin, K. Pham, J. Perry, J. Parrish-Novak, L. Ishak, T. Prow, K. Black, A.N. Mamelak, Phase 1 Safety, Pharmacokinetics, and fluorescence imaging study of tozuleristide (BLZ-100) in adults with newly diagnosed or recurrent gliomas, Neurosurgery, (2019) E641-E649.
32. A.C. Conibear, K.J. Rosengren, P.J. Harvey, D.J. Craik, Structural characterization of the cyclic cystine ladder motif of theta-defensins, Biochemistry, 51 (2012) 9718-9726.
33. Demori, Z.E. Rashed, V. Corradino, A. Catalano, L. Rovegno, L. Queirolo, S. Salvidio, E. Biggi, M. Zanotti-Russo, L. Canesi, A. Catenazzi, E. Grasselli, Peptides for skin protection and healing in amphibians, Molecules, 347 (2019) E347.
34. P. Escoubas, F. Bosmans, Spider peptide toxins as leads for drug development, Expert Opin. on Drug Discov., 2 (2007) 823-835.
35. R. Wehbe, J. Frangieh, M. Rima, D.E. Obeid, J.M. Sabatier, Z. Fajloun, Bee venom: overview of main compounds and bioactivities for therapeutic interests, Molecules, 24 (2019) E2997.
36. S.T. Henriques, D.J. Craik, Cyclotides as templates in drug design, Drug Discov. Today, 15 (2010) 57-64.
37. B. Franke, J.S. Mylne, K.L. Rosengren, Buried treasure: biosynthesis, structures and applications of cyclic peptides hidden in seed storage albumins, Nat. Prod. Rep., 35 (2018) 137-146.
38. Y.Q. Long, S.L. Lee, C.Y. Lin, I.J. Enyedy, S. Wang, P. Li, R.B. Dickson, P.P. Roller, Synthesis and evaluation of the sunflower derived trypsin inhibitor as a potent inhibitor of the type II transmembrane serine protease, matriptase, Bioorg. Med. Chem. Lett., 11 (2001) 2515-2519.
39. M.L. Colgrave, M.J. Korsinczky, R.J. Clark, F. Foley, D.J. Craik, Sunflower trypsin inhibitor-1, proteolytic studies on a trypsin inhibitor peptide and its analogs, Biopolymers, 94 (2010) 665-672.
40. L. Gran, On the effect of a polypeptide isolated from "Kalata-Kalata" (*Oldenlandia affinis* DC) on the oestrogen dominated uterus, Acta Pharmacol. Toxicol., 33 (1973) 400-408.
41. P.K. Pallaghy, K.J. Nielsen, D.J. Craik, R.S. Norton, A common structural motif incorporating a cystine knot and a triple stranded beta sheet in toxic and inhibitory polypeptides, Protein Sci., 3 (1994) 1833-1839.
42. O. Saether, D.J. Craik, I.D. Campbell, K. Sletten, J. Juul, D.G. Norman, Elucidation of the primary and three-dimensional structure of the uterotonic polypeptide kalata B1, Biochemistry, 34 (1995) 4147-4158.

43. J. Weidmann, D.J. Craik, Discovery, structure, function, and applications of cyclotides: circular proteins from plants, J. Exp. Bot., 67 (2016) 4801-4812.
44. K.T.N. Giang, Y.L. Lian, E.W.H. Pang, Q.T.N. Phuong, T.D. Tran, J.P. Tam, Discovery of linear cyclotides in monocot plant Panicum laxum of poaceae family provides new insights into evolution and distribution of cyclotides in plants, J. Biolog. Chem., 288 (2013) 3370-3380.
45. S. Park, K. O. Yoo, T. Marcussen, A. Backlund, E. Jacobsson, K. J. Rosengren, I. Doo, U. Goransson, Cyclotide evolution: insights from the analyses of their precursor sequences, structures and distribution in violets (Viola), Front. Plant Sci., 8 (2017) 2058.
46. D.J. Craik, N.L. Daly, T. Bond, C. Waine, Plant cyclotides: a unique family of cyclic and knotted proteins that defines the cyclic cystine knot structural motif, J. Mol. Biol., 294 (1999) 1327-1336.
47. D.J. Craik, Joseph Rudinger memorial lecture: Discovery and applications of cyclotides (2013).
48. Y.H. Huang, Q. Du, D.J. Craik, Cyclotides: disulfide-rich peptide toxins in plants, Toxicon., 25 (2019) 33-44.
49. C.K. Wang, Q. Kaas, L. Chiche, D.J. Craik, CyBase: A database of cyclic protein sequences and structures, with applications in protein discovery and engineering, Nucleic Acids Res., 36 (2008) D206-210.
50. M.L. Colgrave, D.J. Craik, Thermal, chemical, and enzymatic stability of the cyclotide kalata B1: The importance of the cyclic cystine knot, Biochemistry, 43 (2004) 5965-5975.
51. S. Gunasekera, N.L. Daly, R.J. Clark, D.J. Craik, Dissecting the oxidative folding of circular cystine knot miniproteins, Antioxid. Red. Signal., 11 (2009) 971-980.
52. T.L. Aboye, R.J. Clark, R. Burman, M.B. Roig, D.J. Craik, U. Goransson, Interlocking disulfides in circular proteins: toward efficient oxidative folding of cyclotides, Antioxid. Redox Signal., 14 (2011) 77-86.
53. C.V. Jennings, K.J. Rosengren, N.L. Daly, M. Plan, J. Stevens, M.J. Scanlon, C. Waine, D.G. Norman, M.A. Anderson, D.J. Craik, Isolation, solution structure, and insecticidal activity of kalata B2, a circular protein with a twist: do Mobius strips exist in nature? Biochemistry, 44 (2005) 851-860.
54. C. Jennings, J. West, C. Waine, D. Craik, M. Anderson, Biosynthesis and insecticidal properties of plant cyclotides: the cyclic knotted proteins from *Oldenlandia affinis*, Proceedings of the National Academy of Sciences of the United States of America, 98 (2001) 10614-10619.
55. M.R. Plan, I. Saska, A.G. Cagauan, D.J. Craik, Backbone cyclised peptides from plants show molluscicidal activity against the rice pest *Pomacea canaliculata* (Golden Apple Snail) (2008) 5237-5241.
56. N.L. Daly, K.J. Rosengren, D.J. Craik, Discovery, structure and biological activities of cyclotides, Advan. Drug Deliver. Rev., 61 (2009) 918-930.
57. D.J. Craik, Host-defense activities of cyclotides, Toxins (Basel), 4 (2012) 139-156.
58. S.T. Henriques, Y.H. Huang, M. Castanho, L.A. Bagatolli, S. Sonza, G. Tachedjian, N.L. Daly, D.J. Craik, Phosphatidylethanolamine binding is a conserved feature of cyclotide-membrane interactions, J. Biologic. Chem., 287 (2012) 33629-33643.
59. S.T. Henriques, Y.H. Huang, S. Chaousis, M.A. Sani, A.G. Poth, F. Separovic, D.J. Craik, The prototypic cyclotide kalata B1 has a unique mechanism of entering cells, Chem. Biol., 22 (2015) 1087-1097.
60. L. Cascales, S. T. Henriques, M.C. Kerr, Y.H. Huang, M.J. Sweet, N.L. Daly, D.J. Craik, Identification and characterization of a new family of cell-penetrating peptides: cyclic cell-penetrating peptides, J. Biol. Chem., 286 (2011) 36932-36943.
61. S.J. De Veer, J. Weidmann, D.J. Craik, D.J. Cyclotides as tools in chemical biology, Acc. Chem. Res., 50 (2017) 1557-1565.
62. Hermann, E. Syangard, P. Claeson, J. Gullbo, L. Bohlin, U. Göransson, Key role of glutamic acid for the cytotoxic activity of the cyclotide cycloviolacin O_2, Cell. Mol. Life Sci., 63 (2006) 235-245.
63. P. Lindholm, U. Göransson, S. Johans, P. Claeson, J. Gullbo, R. Larsson, L. Bohlin, A. Backlund, Cyclotides: a novel type of cytotoxic agents, Molec. Cancer Therapeut., 1 (2002) 365-369.
64. R. Burman, G.S. Stromstedt, M. Malmsten, U. Göransson, Cyclotide–membrane interactions: Defining factors of membrane binding, depletion and disruption, Biochimic. Biophysic. Acta, 1808 (2011) 2665-2673.
65. R. Burman, S. Gunasekera, A.A. Stromstedt, U. Goransson, Chemistry and biology of cyclotides: circular plant peptides outside the box, J. Nat. Prod., 77 (2014) 724-736.
66. R.J. Clark, M. Akcan, Q. Kaas, N.L. Daly, D.J. Craik, Cyclization of conotoxins to improve their biopharmaceutical properties, Toxicon., 59 (2012) 446-455.
67. D.J. Craik, J. Du, Cyclotides as drug design scaffolds, Curr. Opin. Chem. Biol., 38 (2017) 8-16.
68. C.K. Wang, D.J. Craik. Designing macrocyclic disulfide-rich peptides for biotechnological applications, Nat. Chem. Biol., 14 (2018) 417-427.
69. J.A. Camerero, M.J. Campbell, The potential of the cyclotide scaffold for drug development, Biomedicines, 7 (2019) E31.
70. P. G. Ojeda, M. H. Cardoso, O. H. Franco, Pharmaceutical applications of cyclotides, Drug Discover. Today, 24 (2019) 2152-2161.
71. R.J. Clark, J. Jensen, S.T. Nevin, B.P. Callaghan, D.J. Adams, Craik, The engineering of an orally active conotoxin for the treatment of neuropathic pain, Angew. Chem. Int. Ed., 49 (2010) 6545-6548.
72. L.Y. Chan, V.M. Zhang, Y.H. Huang, N.C. Waters, P.S. Bansal, D.J. Craik, N.L. Daly, Cyclization of the antimicrobial peptide gomesin with native chemical ligation: influences on stability and bioactivity, Chembiochem., 14 (2013) 617-624.
73. M. Akcan, R.J. Clark, N.L. Daly, A.C. Conibear, A. de Faoite, M.D. Heghinian, T. Sahil, D.J. Adams, F. Mari, D.J. Craik, Transforming conotoxins into cyclotides: Backbone cyclization of P-superfamily conotoxins, Biopolymers, 104 (2015) 682-692.
74. R.J. Clark, H. Fischer, L. Dempster, N.L. Daly, K.J. Rosengren, S.T. Nevin, F.A. Meunier, D.J. Adams, D.J. Craik, Engineering stable peptide toxins by means of backbone cyclization: stabilization of the alpha-conotoxin MII, Proc. Nat. Acad. Sc., 102 (2005) 13767-13772.
75. X. Chen, L. Zhang, Y. Wu, L. Wang, C. Ma, X. Xi, O.R. P. Bininda-Emonds, C. Shaw, T. Chen, M Zhou, Evaluation of the bioactivity of a mastoparan peptide from wasp venom and of its analogues designed through targeted engineering, Int. J. Biol. Sci., 14 (2018) 599-607.
76. N. Lawrence, A.S.M. Dennis, A.M. Lehane, A. Ehmann, P.J. Harvey, A.H. Benfield, O. Cheneval, S.T. Henriques, D.J. Craik, B.J. McMorran, Defense peptides engineered from human platelet factor 4 kill plasmodium by selective membrane disruption, Cell. Chem. Biol., 25 (2018) 1140-1150.
77. P. Quimbar, U. Malik, C.P. Sommerhoff, Q. Kaas, L.Y. Chan, Y.H. Huang, M. Grundhuber, K. Dunse, D.J. Craik, M.A. Anderson, N.L. Daly, High-affinity cyclic peptide matriptase inhibitors, J. Biol. Chem., 288 (2013) 13885-13896.
78. C.K. Wang, C.W. Gruber, M. Cemazar, C. Siatskas, P. Tagore, N. Payne, G. Sun, S. Wang, C.C. Bernard, D.J. Craik, Molecular grafting onto a stable framework yields novel cyclic peptides for the treatment of multiple sclerosis, ACS Chem. Biol., 9 (2014) 156-163.

79. C. D'Souza, S.T. Henriques, C.K. Wang, O. Cheneval, L.Y. Chan, N.J. Bokil, M.J. Sweet, D.J. Craik, Using the MCoTI-II cyclotide scaffold to design a stable cyclic peptide antagonist of set, a protein overexpressed in human cancer, Biochemistry, 55 (2016) 396-405.
80. C. Cobos Caceres, P.S. Bansal, S. Navarro, D. Wilson, L. Don, P. Giacomin, A. Loukas, N. L. Daly, An engineered cyclic peptide alleviates symptoms of inflammation in a murine model of inflammatory bowel disease, J. Biol. Chem., 292 (2017) 10288-10294.
81. L.Y. Chan, D.J. Craik, N.L. Daly, Cyclic thrombospondin-1 mimetics: grafting of a thrombospondin sequence into circular disulfide-rich frameworks to inhibit endothelial cell migration, Biosci. Rep., 35 (2015) e00270.
82. C.T.T. Wong, D.K. Rowlands, C.H. Wong, T.W.C. Lo, G.K.T. Nguyen, H.Y. Li, J.P. Tam, Orally active peptidic bradykinin B1 receptor antagonists engineered from a cyclotide scaffold for inflammatory pain treatment, Angew. Chem. Int. Ed., 51 (2012) 5620-5624.
83. Y. Qiu, M. Taichi, N. Wei, H. Yang, K.Q. Luo, J.P. Tam, An Orally active bradykinin B1 receptor antagonist engineered as a bifunctional chimera of sunflower trypsin inhibitor, J. Med. Chem., 60 (2017) 504-510.
84. F. Jia, J. Wang, J. Peng, P. Zhao, Z. Kong, K. Wang, W. Yan, R. Wang, D-amino acid substitution enhances the stability of antimicrobial peptide polybia-CP, Acta Biochim. Biophys. Sin. (Shanghai), 49 (2017) 916-925.
85. L. Sando, S.T. Henriques, F. Foley, S.M. Simonsen, N.L. Daly, K.N. Hall, K.R. Gustafson, M.I. Aguilar, D.J. Craik, A Synthetic mirror image of kalata B1 reveals that cyclotide activity is independent of a protein receptor, Chembiochem., 12 (2011) 2456-2462.
86. C.J. Armishaw, N.L. Daly, S.T. Nevin, D.J. Adams, D.J., Craik, P.F. Alewood, alpha-selenoconotoxins, a new class of potent alpha(7) neuronal nicotinic receptor antagonists, J. Biologi. Chem., 281 (2006) 14136-14143.
87. J. Kindrachuk, E. Scruten, S. Attah-Poku, K. Bell, A. Potter, L.A. Babiuk, P J. Griebel, S. Napper, Stability, toxicity, and biological activity of host defense peptide BMAP28 and its inversed and retro-inversed isomers, PeptideScience, 96 (2010) 14-24.
88. D.J. Craik, D.J. Adams, Chemical modification of conotoxins to improve stability and activity, Acs Chem. Biol., 2 (2007) 457-468.
89. N. Yin, Enhancing the oral bioavailability of peptide drugs by using chemical modification and other approaches, Medicin. Chem., 4 (2014) 763-769.

N. Akpınar Kocakulak et al. / Hacettepe J. Biol. & Chem., 2020, 48 (3), 231-238

Research Article

Hacettepe Journal of Biology and Chemistry

journal homepage: www.hjbc.hacettepe.edu.tr

The Effect of Exercise at High Altitude on Muscle Serum Enzymes and Some Biochemical Parameters

Yüksek İrtifada Yapılan Egzersizin Kas Serum Enzimleri ve Bazı Biyokimyasal Parametrelere Etkisi

Neşe Akpınar Kocakulak[1*], Meryem Şentürk[2], Hakan Gülmez[3], Meryem Eren[2], Zuhal Hamurcu[4]

[1]Faculty of Health Sciences, Department of Sport Science, İzmir Democracy University, İzmir, Türkiye.

[2]Faculty of Veterinary Medicine, Department of Basic Sciences, Erciyes University, Kayseri, Türkiye.

[3]Faculty of Medicine, Department of Family Medicine, Izmir Democracy University, İzmir, Türkiye.

[4]Medical Faculty, Department of Medical Biology, Betül Ziya Eren Genome and Stem Cell Center, Erciyes University, Kayseri, Türkiye.

ABSTRACT

High altitude conditions cause changes in organism functions. Low oxygen concentration, low heat and exposure to ultraviolet rays for a long time trigger these changes. In our study, the effects of exercise at 1055 m and 2500 m on: the levels or activities of malondialdehyde (MDA), creatinine, lactate dehydrogenase (LDH) and aspartate aminotransferase (AST), total protein, glucose, cholesterol were investigated. Twelve healthy individuals were included in the study. They exercised 3 hours a day for 5 days in both altitudes. Blood samples were taken and placed into the tubes with anticoagulants, both at the first day and on the fifth day, at 1055 m and 2500 m altitude before and after exercise, the samples were then centrifuged and separated from their plasma. The resuts indicate that glucose and AST (aspartate aminotransferase) increased at 2500 meters, while MDA (malondialdehyde) decreased. At 1500 meters, glucose and creatinine were found to be released, while AST (aspartate aminotransferase) was decreased. Considering the samples taken 10 days after the volunteers returned from 2500 m to 1055 m, the results were found to approach 2500 m pre-exercise values. When the results of 1055 m and 2500 m were compared to the 1st and 5th days, glucose and creatinine were found to be increased both at 1050 m and at 2500 m. It was observed that LDH (lactate dehydrogenase) increased significantly at 5th of 2500m compared to 1st day. Our results showed that both exercise and high altitude affect muscle serum enzymes and glucose MDA values, but these changes do not pose a risk of disease that would require medical intervention.

Key Words

Exercise, high altitude, hypoxia, biochemical parameter, muscle serum enzymes.

ÖZ

Yüksek irtifa şartları organizma fonksiyonlarında değişimlere neden olur. Solunan havadaki düşük oksijen konsantrasyonu, düşük ısı ve uzun sure ultraviyole ışınlarına maruz kalmak bu değişiklileri tetiklemektedir. Çalışmamız 1055m ve 2500 m'de yapılan egzersizin Malondialdehit (MDA), Kreatinin, LaktatDehidrojenaz (LDH) ve AspartatAminotransferaz (AST), Total Protein, Glucose, Kolestorol üzerine etkisi belirlenmeye çalışılmıştır. Çalışmaya 12 sağlıklı birey dahil edildi. Her iki yerde 5 gün boyunca günde 3 saat egzersiz yaptılar. Egzersizden önce ve egzersizden hemen sonra 1055 m ve 2500 m yükseklikte hem ilk gün hem de beşinci günde Antikoagülantlı tüplere alınan kan örnekleri santrifüj edilerek plazmalarına ayrılmıştır. 2500 metrede Glucose ve AST (aspartat aminotransferaz) artış gösterdiği bulundu. MDA (malondialdehid) ise azalmıştır. 1500 metrede ise yine Glucose, kreatinin arttığı bulunurken, AST (aspartataminotransferaz) azalmıştır. Gönüllüler 2500 m'den 1055 m'ye geri döndükten 10 gün sonra alınan örnekler değerlendirildiğinde sonuçların 2500 m egzersiz öncesi değerlerine yaklaştığı bulunmuştur. 1055 m ve 2500 m 1. ve 5. gün sonuçları karşılaştırıldığında Glucose ve kreatinin hem 1050 m de hem de 2500 m de arttığı bulunmuştur. LDH (laktatdehidrogenaz)'ın 2500 m de 1. Güne göre 5. gün büyük oranda artış gösterdiği görülmektedir. Sonuçlarımız hem egzersizin hem de yüksek irtifanın kas serum enzimleri, Glucose ve MDA değerlerini değiştirdiği fakat bu değişikliklerin tıbbi bir müdahale gerektirecek hastalık riski oluşturmadığını göstermiştir.

Anahtar Kelimeler

Egzersiz, yüksek irtifa, hipoksi, biyokimyasal parametre, kas serum enzimleri.

Article History: Received: Mar 16, 2020; Revised: Apr, 5 2020; Accepted: Apr 23, 2020; Available Online: Apr 23, 2020.

DOI: https://doi.org/10.15671/hjbc.704269

Correspondence to: Faculty of Health Sciences, Department of Sport Science, Izmir Democracy University, Izmir, Turkey.

E-Mail: nese.kocakulak@idu.edu.tr

INTRODUCTION

Body regulation mechanisms for survival in hypobaric hypoxic environments differ in each height environment. Height training is used by coaches and athletes both to acclimate for high-altitude competitions and to prepare for competitions at sea level [1]. There are researchers who argue that high-altitude training will increase aerobic performance, as well as authors who argue that it is no use to high-performance athletes. Exposure to low oxygen pressure is known to cause both metabolic and physiological changes [2,3]. Although oxygen demand will be limited due to hypoxia at high altitude, it is reported that exposure to high altitude (due to changes in ROS formation and antioxidant activity) can also cause oxidative damage, although production of reactive oxygen derivatives (ROS will be low [4]. ROSs contain one or more unpaired electrons with high energy. Normal cell metabolism converts 1–2% of oxygen molecules into ROSs. This ROS is potentially toxic. Although ROS has important contributions in regulating normal physical activities such as muscle contraction, significant increases in concentrations of ROSs can disrupt normal cell function, leading to oxidative damage of various biomolecules (protein, lipid) and cellular DNA [5,6]. Because of its role in organ, tissue damage and the etiopathogenesis of different diseases, ROS has been an increasingly popular field of medicine in recent years. High altitude conditions cause changes in organism functions. Low oxygen concentration, low heat and exposure to ultraviolet rays for a long time trigger these changes. Deep respiratory movements, increased heart rate, increased number of circulating erythrocytes and increased hemoglobin concentrations are the effects of acclimation to high altitude conditions. Because of these effects, camping in a hypoxic environment is used as a training program for professional athletes [7,8]. Malondialdehyde (MDA) levels have been measured in many studies as an indicator of oxidative stress [9]. Malondialdehyde (MDA) is one of the toxic end products produced by the breakdown of non-enzymatic oxidative lipid peroxides. Malondialdehyde (MDA) levels have been measured in many studies as an indicator of oxidative stress [9]. In clinical situations, Creatinine, Lactate Dehydrogenase (LDH) and Aspartate Aminotransferase (AST) are widely used in the diagnosis of skeletal muscle damage and tissue damage in skeletal muscles. At the same time, it is not yet fully understood how long-term excursion to high altitude affects glucose homeostasis. In addition, mild neuroglycopenia at high altitude can have serious side effects. Studies have emphasized that the effects of exogenous carbohydrate oxidation during exercise are not clear but can reflect differences in exercise intensity. In related studies, the effect of hypoxia on lipid peroxidation has been studied and studies on different examples of oxidative damage (such as blood, skeletal muscle, liver) have been limited and contradictory results have been obtained. [2]. In our study, we tried to determine the effect of height hypoxia in different climatic conditions when the exercise was performed under these conditions by examining the levels of Malondialdehyde (MDA), Creatinine, Lactate Dehydrogenase (LDH) and Aspartate Aminotransferase (AST), Total Protein, Glucose, Cholesterol.

MATERIALS and METHODS

Subjects: The study group consisted of 12 people with similar age and physical characteristics. The average age was 17.25±1.14 years, the average height was 165.92±2.61 cm. The average body mass and body mass index were 60.58±2.84 kg and 21.28±0.75 kg / m^2 (mean±SD), respectively. The people included in the study lived at an altitude of 1055 m above sea level and were not interested in skiing before. All subjects did not experience high altitude conditions for at least 6 months. Informed consent was obtained from all subjects before the study. The study protocol and the procedures were approved by the local ethical committee (No 09/54). The study was conducted in accordance with the Declaration of Helsinki or local laws depending on whichever afforded greater protection for the subjects.

Experimental protocols: Test protocols were performed on two locations: the studies at 1055 meters were performed at the Erciyes University campus which is located on the skirts of Erciyes Mountain (3917 m above sea level), Turkey/Kayseri. 2500 m high altitude studies were performed at the Erciyes ski- centre on the Erciyes Mountain

2500 meters studies; The subjects arrived after an hour by bus due to the fact that the centre is 25 km away from the town center of Erciyes Mountain. Experiments were started after two hours. They did basic interval ski exercises at 2500m. Their heart rhythm was kept between 140-160 beats/minute and they exercised on skis for 3 hours per day for 5 days. All subjects stayed at 2200 m altitude at Erciyes Mountain during the 5 days. Experiments were conductedon January 2 through6.

1055 meters studies; the subjects came back down to 1055 m from the mountain after two weeks (January 25-29) and began to work again. All the subjects performed the same exercises at 1055m as they did at 2500m. They performed exercise for 3 hours per day for 5 days. Their heart rhythms were kept between 140-160 beats/minute during exercise.

1st day and 5th day oxygen saturation, systolic and diastolic blood pressures, heart rate and Malondialdehyde (MDA), Creatine, Lactate Dehydrogenase (LDH) and Aspartate Aminotransferase (AST), Total Protein, Glucose, Colesterol levels or activities were measured before exercise and immediately after exercise at the two locations.

Collection of Samples: Five milliliters of heparinised peripheral blood samples were obtained before exercise and immediately after the exercise at 1055 m and 2500 m altitudes on both first day and fifth day. Also, the subjects came back down to 1055 m from the mountain, and the blood samples were taken after resting for ten days (January 17).

Performing Biochemical Analysis: Blood samples taken into anticoagulated tubes were centrifuged and separated into their plasma. Blood samples taken into anti-coagulant tubes were kept at room temperature for one hour, and then their serum was separated by centrifugation at 3000

Table 1. Comparison of biochemical parameters at 2500 m.

p value (Between Before-After)	Mean±SD	Tests (Mountain 2500m)	Mean±SD (10th day)	p value (Between 10th day)
0.01*	-0.21±2.04	AST Day 1 Before	0.36±0.19	0.35
	2.28±1.80	AST Day 1 After	0.36±0.19	0.003*
0.72	1.46±0.86	AST Day 5 Before	0.36±0.19	0.002*
	1.32±1.12	AST Day 5 After	0.36±0.19	0.02*
0.09*	6.16±0.23	Total Protein Day 1 Before	6.02±0.13	0.15
	6.04±0.05	Total Protein Day 1 After	6.02±0.13	0.66
0.66	6.19±0.15	Total Protein Day5 Before	6.02±0.13	0.009*
	6.16±0.13	Total Protein Day 5 After	6.02±0.13	0.07
0.001*	65.92±7.88	Glucose Day 1 Before	79.46±13.76	0.001*
	75.98±2.07	Glucose Day 1 After	79.46±13.76	0.40
0.22	71.40±22.09	Glucose Day 5 Before	79.46±13.76	0.33
	79.74±1.82	Glucose Day 5 After	79.46±13.76	0.94
0.28	181.83±14.60	Cholesterol Day 1Before	190.59±9.99	0.11
	188.15±19.05	Cholesterol Day 1 After	190.59±9.99	0.39
0.44	193.63±14.63	Cholesterol Day 5 Before	190.59±9.99	0.78
	187.08±23.11	Cholesterol Day 5 After	190.59±9.99	0.86
0.001*	3.37±0.76	MDA Day 1 Before	3.90±0.71	0.20
	1.63±0.36	MDA Day 1 After	3.90±0.71	0.000**
0.63	3.19±1.41	MDA Day 5 Before	3.90±0.71	0.08
	3.45±1.02	MDA Day 5 After	3.90±0.71	0.19
0.19	125.44±64.94	Creatinine Day 1 Before	98.77±31.25	0.20
	262.88±274.17	Creatinine Day 1 After	98.77±31.25	0.10
0.86	699.90±587.71	Creatinine Day 5 Before	98.77±31.25	0.01*
	744.70±715.70	Creatinine Day 5 After	98.77±31.25	0.02*
0.74	361.12±74.64	LDH Day 1 Before	589.66±146.31	0.68
	351.87±78.88	LDH Day 1 After	589.66±146.31	0.02*
0.11	717.00±184.02	LDH Day 5 Before	589.66±146.31	0.36
	822.10±162.28	LDH Day 5 After	589.66±146.31	0.83

*p<0.05; **p<0.001

rpm for 10 minutes. Serum and plasma samples were kept at -20 °C until analysis was performed. Serum biochemical parameter levels (AST, LDH, glucose, cholesterol, total protein, creatinine)were analyzed with commercial kits (Biolabo, France) and plasma MDA levels, Moreno et al. [10] were determined according to the method utilizing the spectrophotometer (UV/VIS Shimadzu 1208, Japan) .

Statistical analysis: The Statistical package for social sciences (SPSS) for Windows ver. 16.0 (SPSS Inc., Chicago, IL) was used for statistical analyzes. The paired samples t-tests were employed to do the comparison of measurable variables. A significant level was set at a *P- value of* < 0.05.

Results

The study was conducted with 12 people with similar age and physical properties and average age was 17.25±1.14 years, average height length was 165.92±2.61 cm, average body mass was 60.58±2.84 kg and body mass index 21.28±0.75 kg / m^2 (mean±SD).

At 2500 m (height of hypoxia), AST, total protein, and glucose increased on the first day before and immediately after the exercise, while a decrease in MDA was detected ($p < 0.05$; $p < 0.001$). It was found that the changed values returned to the reference ranges of the

Table 2. Comparison of biochemical parameters at 1055 m

p value (Between Before-After)	Mean±SD	Tests (1055m)	Mean±SD (10th day)	p value (Between 10th day)
0.04*	0.59±0.43	AST Day 1 Before	0.36±0.19	0.07
	0.32±0.15	AST Day 1 After	0.36±0.19	0.57
0.92	0.33±0.20	AST Day 5 Before	0.36±0.19	0.78
	0.34±0.25	AST Day 5 After	0.36±0.19	0.81
0.37	6.12±0.15	Total Protein Day 1 Before	6.02±0.13	0.08
	6.05±0.15	Total Protein Day 1 After	6.02±0.13	0.64
0.18	5.97±0.17	Total Protein Day 5 Before	6.02±0.13	0.43
	6.04±0.14	Total Protein Day 5 After	6.02±0.13	0.74
0.000**	87.02±10.87	Glucose Day 1 Before	79.46±13.76	0.12
	130.22±18.48	Glucose Day 1 After	79.46±13.76	0.000**
0.94	123.33±19.96	Glucose Day 5 Before	79.46±13.76	0.000**
	123.60±25.17	Glucose Day 5 After	79.46±13.76	0.000**
0.51	186.63±11.61	Cholesterol Day 1 Before	190.59±9.99	0.69
	191.05±13.88	Cholesterol Day 1 After	190.59±9.99	0.44
0.05	190.81±15.26	Cholesterol Day 5 Before	190.59±9.99	0.37
	179.66±17.44	Cholesterol Day 5 After	190.59±9.99	0.24
0.31	4.12±1.32	MDA Day 1 Before	3.90±0.71	0.93
	3.50±0.67	MDA Day 1 After	3.90±0.71	0.15
0.56	3.70±0.61	MDA Day 5 Before	3.90±0.71	0.14
	3.54±0.33	MDA Day 5 After	3.90±0.71	0.12
0.01	56.77±17.14	Creatinine Day 1 Before	98.77±31.25	0.003*
	77.00±22.24	Creatinine Day 1 After	98.77±31.25	0.02*
0.88	100.44±49.12	Creatinine Day 5 Before	98.77±31.25	0.76
	104.88±56.01	Creatinine Day 5 After	98.77±31.25	0.52
0.10	359.66±87.21	LDH Day 1 Before	589.66±146.31	0.42
	444.66±149.01	LDH Day 1 After	589.66±146.31	0.28
0.27	398.44±78.89	LDH Day 5 Before	589.66±146.31	0.90
	443.00±91.06	LDH Day 5 After	589.66±146.31	0.17

*p<0.05; **p<0.001

Table 3. Comparison of 2500m and 1055m 1st day and 5th day results.

Parameters	Mean	p value
AST_2500m_1_EO	-0.21±2.04	0.07
AST_2500m_5_ES	1.32±1.12	
AST_1055m_1_EO	0.59±0.43	0.06
AST_1055m_5_ES	0.34±0.25	
Total Protein _2500m_1_EO	6.16±0.23	0.97
Total Protein 2500m_5_ES	6.16±0.13	
Total Protein _1055m_1_O	6.12±0.15	0.33
Total Protein _1055m _5_S	6.04±0.14	
Glucose2500m_1_O	65.92±7.88	0.000**
Glucose2500m_5_S	79.74±1.82	
Glucose1055m_1_O	87.02±10.87	0.001*
Glucose_1055m_5_S	123.60±25.17	
Cholesterol _2500m_1_O	181.83±14.60	0.56
Cholesterol _2500m_5_S	187.08±23.11	
Cholesterol 1055m_1_O	186.63±11.61	0.30
Cholesterol _1055m_5_S	179.66±17.44	
MDA_2500m _1_O	3.37±0.76	0.97
MDA _2500m _5_S	3.45±1.02	
MDA_1055m _1_O	4.12±1.32	0.44
MDA_1055m _5_S	3.54±0.33	
Creatinine_2500m _1_O	125.44±64.94	0.03*
Creatinine_2500m _5_S	744.70±715.70	
Creatinine1055m _1_O	56.77±17.14	0.05
Creatinine1055m _5_S	104.88±56.01	
LDH_2500m _1_O	361.12±74.64	0.000**
LDH_2500m _5_S	822.10±162.28	
LDH_1055m _1_O	359.66±87.21	0.43
LDH_1055m _5_S	443.00±91.06	

*p<0.05**p<0.001

biochemical parameters after resting for 10 days following the time that the subjects returned to 1055m ($p < 0.05$; $p < 0.001$).

At 1055 m, increase in glucose, creatinine levels and decrease AST levels were observed immediately after the exercise on the first day ($p < 0.05$; $p < 0.001$). It was found that the biochemical parameters returned to the reference ranges as at 2500 m on the 10th day ($p < 0.05$; $p < 0.001$).

Discussion

For years, it has been thought that training should be done at high altitude to improve the performance of individuals at sea level. High altitude conditions cause changes in organism functions. Low oxygen concentration in the inhaled air, low heat, wind and exposure to ultraviolet rays for a long time trigger these changes [2,11]. Recent research suggests that high altitude-related hypoxia may be a model for long-term oxidative stress in healthy people. This study examined the effects of exposure to two independent inducers (exer-

cise and altitude) on the levels or activities of muscle serum enzymes (creatine, AST, LDH) and Glucose, Total protein, Cholesterol and MDA. In this study, we found that AST, Glucose, Creatine, LDH values increased after exercise at both 2500 m and 1055 m. In addition, AST, Creatine, LDH values were found to be higher than 2500 m altitude, except for glucose which was affected at an altitude of 2500 m. This shows that both exercise and height change the levels of muscle enzymes. The effects of exercise on muscle damage at high altitude are unknown. Studies emphasize that muscle enzyme levels should be interpreted cautiously. In particular, serum CK levels rise immediately after loading, and this height lasts for several days. The high serum CK level is attributed to increased muscular membrane permeability due to low oxygen delivery during contraction [12]. More recent research reports that this enzyme due to muscle fiber damage appears, reaches peak levels in the blood within 3-5 days, and this peak reflects the release of CK from the damaged muscle and its excretion in the reticuloendothelial system. In addition, serum CK levels are linked to many factors such as gender, age, ethnicity, basic muscle composition, and physical activity levels. Magrini at al. [13] conducted a study with 669 ultramaraton (161km) runners gathered at high altitude (2800 - 3840 m). 352 people of the runners who participated in the ultra marathon completed the race. Of these, only 36 people gave blood samples before and after, and the mean serum CK levels increased in these samples. It is also stated that this increase may be caused by high altitude environmental factors such as downhill and uphill strenuous eccentric contractions and low oxygen concentration, extreme low and high temperature, ultraviolet radiation and extreme wind changes. It is stated that in any damage to the skeletal muscles, as in the heart and liver, the AST value in the blood increases as in Creatine and LDH. Studies emphasize that LDH values increase especially in hypoxia. In our study, it is seen that it especially increased at 2500m. Physical exercise causes an increase in blood sugar levels, especially in high-intensity activity, mobilized from muscles and liver glycogenes to meet energy demands. Glucose for muscle activity is the fuel of choice by many cells [14]. Glucose is the most efficient fuel the body can use, consuming less oxygen than fat or protein per unit of energy produced [15]. Studies on humans and rodents show that acute exercise increases the transport of insulin-stimulated glucose to the muscles to meet physiologically relevant requirements [16]. Sufficient insulin is required for glucose and amino acids to enter the cells, thus providing fuel and essential elements for muscle activity. It is emphasized that plasma insulin increases during intense exercise to regulate glucose level and restore muscle glycogen [17]. There are contradictory results regarding the fasting glycemia increased, decreased and remained unchanged for healthy individuals exposed to high altitude. It is stated that these differences may be related to the high altitude exposure time [18]. It is stated that there is an increase in fasting glycemia in the first two days at high altitude. However, as the length of stay prolongs, acclimatization is provided and the resulting hyperglycemia is normalized and it is stated that it may fall below the pre-exposure values [19]. In our study, glucose levels increased at both heights. It is seen that this increase is more than 1055 meters. These results are important in that both high altitude and exercise cause an increase in muscle serum enzymes (AST, LDH, Creatine) and glucose. Studies in humans have reported conflicting results regarding the relationship between short-term (1–4 weeks) height hypoxia and oxidative stress. Some studies have found an increase in markers showing oxidative damage, such as lipid peroxidation [20], other studies have suggested that hypoxia is not associated with increased lipid peroxidation [21]. Several studies have reported that increased lipid peroxidation is associated with exercise [22,23]. Gonzalez at al. [24] studied 7 volunteers aged 19 to 23 years, who stayed for 3 days at an altitude of 3500 m above the sea level, and when they returned after 3 days, they investigated the effects of normal hypoxic conditions on these individuals. They took blood samples from the individuals in restful conditions and in both conditions they measured MDA, which is an indicator of oxidative damage in erythrocyte membrane lipids. When people returned to sea level again, they found that the MDA content increased significantly compared to the MDA content at altitude. Based on these results, they suggested that when people returning to work or having fun at 3500 m altitude back to sea level (reoxygenation), the risk of oxidative damage may occur in erythrocyte membrane lipids. At high altitude (2500m), there is a decrease in MDA value after exercise compared to Day 1 before exercise. In normoxia, it is estimated that approximately 2-3% of oxygen in the mitochondrial electron transport chain is reduced to water to form reactive oxygen derivatives (ROS) instead of ATP production [25]. In hypoxia, a decrease in the production of mitochondrial ROS has been reported due to the decrease in the amount of oxygen and the cessation of mitochondrial respiration

[26]. Maintaining homeostasis against adverse effects caused by stress depends on autonomic, hormonal, metabolic and immunological responses of the organism. As partial air expands, oxygen pressure decreases at altitude and affects the delivery of oxygen to working tissues, regardless of whether a person is moving uphill or downhill. It is reported that the altitudes can be divided into low altitude (<2,500 m), high altitude (2,500 m-3,500 m), very high altitude (3,500 m-5,800 m) and extreme altitude (> 5,800 m) [27]. In our study, we limited altitude to two altitude classes (1055 m and 2500 m). Volunteers returned from 2500 m to 1055 m after 5 days. Biochemical parameters were re-evaluated at the 10th day after the volunteers returned from 2500 m to 1055 m. We can say that at the end of 10 days, muscle serum enzymes, glucose and MDA returned to pre-exercise values or started to return. We think that it is important to consider the 10 day duration, which is sufficient forthe negative effects of high altitude to diminish. This information could be useful to determine the time periods to be restarted after descending from the elevation before programming the high-altitude training. As a result, both exercise and high altitude show that muscle serum enzymes, glucose and MDA values change but these changes do not pose any disease risk and do not require medical intervention.

References

1. Z. Ying, C. Ning, Autophagy Is a Promoter for aerobic exercise performance during high altitude training, Oxid. Med. Cell. Longev., 2018 (2018) 3617508-3617511.
2. P. Moller, L. Stefen, C. Lundby, N.V. Olsen Acute hypoxia and hypoxic exercise induce DNA strand breaks and oxidative DNA damage in humans, FASEB., 15 (2005) 1181-1186.
3. N.A. Kocakulak, The effect of high altitude exercise on oxidative stress Level, Nat. Appl. Sci. J., 1 (2018) 1-8.
4. J.A. Jefferson, J. Simoni, E. Escudero, M.E. Hurtado, E.R.Swenson, D.E.Wesson, G.F.Schreiner, R.B. Schoene, R.J. Johnson, A. Hurtado, Increased oxidative stress following acute and chronic high altitude exposure, High Altitude Med. Biol., 5 (2004) 61-69.
5. Z. Radak, J. Pucsuk, S. Boros, L. Josfai, AW. Taylor, Changes in urine 8 htdroxydeoxyguanozine levels of super marathon runners during a four-day race period, Life Sci., 66 (2000) 1763-1767.
6. H. Orhan, B. Van Holland, B. Krab, J. Moeken, N.P. Vermeulen, P. Hollander, J.H. Meerman, Evaluation of a multiparameter biomarker set for oxidative damage in man: Increased urinary excretion of lipid, protein and DNA oxidation products after one hour of exercise, Free Radic. Res., 38 (2004) 1269-1279.
7. R.J. Bloomer, A. H.Goldfarb, J.M. Mckenzie, Oxidative stress response to aerobic exercise: Comparison of antioxidant supplements, Med. Sci. Sports Exerc., 38 (2006) 1098-105.
8. A. Harman, S. Pfuhler, C. Dennog, D. Germadnik, A. Pılger, G. Speit, Exercise-induced DNA effects in human leukocytes are not accompanied by increased formation of 8-Hydroxy-2'-Deoxyguanosine or induction of micronuclei, Free Radic. Biol. Med., 24 (1997) 245-251.
9. M.L. Urso, P.M. Clarkson, Oxidative stress, exercise, and antioxidant supplementation, Toxicology, 189 (2003) 41-54.
10. I.M. Moreno, A. Mate, G. Repetto, C.M. Vázquez, A.M. Cameán, Influence of microcystin LR on the activity of membrane enzymes in rat intestinal mucosa, J. Physiol. Biochem., 59 (2003) 293-300.
11. Dosek, H.Ohno, Z. Acs, A.W. Taylor, Z. Radak, High altitude and oxidative stress, Respir. Physiol. Neurobiol., 158 (2007) 128-131.
12. M.F. Baird, S.M. Graham, J.S. Baker, G.F. Bickerstaff, Creatine-kinase- and exerciserelated muscle damage implications for muscle performance and recovery, J. Nutr. Metab., 2012 (2012) 960363- 960313.
13. D. Magrini, M. Khodaee, I. San-Millán, T. Hew-Butler, A.J. Provance, Serum creatine kinase elevations in ultramarathon runners at high altitude, Phys. Sportsmed., 45 (2017) 129-133.
14. J.M. Peake, S.J. Tan, J.F. Markworth, J.A. Broadbent, T.L. Skinner, D. Cameron-Smith, Metabolic and hormonal responses to isoenergetic high-intensity interval exercise and continuous moderate-intensity exercise, Am. J. Physiol. Endocrinol. Metab., 307 (2014) 539-552.
15. M.P. Schippers, O. Ramirez, M. Arana, P. Pinedo-Bernal, G.B. McClelland, Increase in carbohydrate utilization in high-altitude Andean mice, Curr. Biol., 22 (2012) 2350-2354.
16. G.D. Cartee, Mechanisms for greater insulin-stimulated glucose uptake in normal and insulin-resistant skeletal muscle after acute exercise, Am. J. Physiol. Endocrinol. Metab., 309 (2015) 949-959.
17. O.P. Adams, The impact of brief high-intensity exercise on blood glucose levels, Diabetes Metab. Syndr. Obes., 6 (2013) 113-122.
18. N.E. Hill, K. Deighton, J. Matu, S. Misra, N.S. Oliver, C. Newman, A. Mellor, J. O'Hara, D. Woods, Continuous glucose monitoring at high altitude-effects on glucose homeostasis, Med Sci Sports Exerc., 50 (2018) 1679-1686.
19. O.O. Woolcott, M. Ader, R.N. Bergman, Glucose homeostasis during short-term and prolonged exposure to high altitudes, Endoc. Rev., 36 (2015) 149-173.
20. S.L. Wing, E.W Askew, M.J. Luetkemeier, D.T. Ryujin, G.H. Kamimori , C.K. Grissom, Lack of effect of Rhodiola or oxygenated water supplementation on hypoxemia and oxidative stress, Wild Envir. Med., 14 (2003) 9-16.
21. N.A. Guzel, H. Sayan, D. Erbas , Effect of moderate altitude on exhaled nitric oxide, erythrocytes lipid peroxidation and superoxide dismutase levels, Jpn. J. Physiol., 50 (2000) 187-190.
22. Wozniak, G. Drewa, G. Chesy, A. Rakowsi, M. Rozwodowska, D. Olzewska, Effect of altitude training on the peroxidation and antioxidant enzymes in sportsment, Med. Sci. Sports Exerc., 33 (2001) 1109-1113.
23. M.C. Schmidt, E.W. Askew, D.E. Roberts, R.L. Prior, W.Y. Ensign, R.E. Hesslink, Oxidative stress in humans training to a cold, moderate altitude environment and their response to pytochemical antioxidant supplement, Wild Environ Med.,13 (2002) 94-105.
24. G. Gonzalez, G. Celedon, M. Escobar, C. Sotomayor, V. Ferre, D. Benitez, C. Behn, Red cellmembrane lipid changes at 3500 m and on return to sea level, High Alt. Med. Biol., 6 (2005) 320-326.

25. J.F. Turrens, Mitochondrial formation of reactive oxygen species, J. Physiol., 552 (2003) 335-344.
26. R.A. Papandreou,L. Cairns, A.L. Fontana, N.C. Lim, HIF-1 mediates adaptation to hypoxia by actively downregulating mitochondrial oxygen consumption, Cell Metab., 3 (2006) 187-97.
27. P. Møller, L. Risom, C. Lundby, L. Mikkelsen, S. Loft, Hypoxia and oxidation levels of DNA and lipids in humans and animal experimental models, IUBMB Life., 60 (2008) 707-23.

E. Aytaç / Hacettepe J. Biol. & Chem., 2020, 48 (3), 239-244

Research Article

Hacettepe Journal of Biology and Chemistry

journal homepage: www.hjbc.hacettepe.edu.tr

Comparison Essential Oil Contents *Origanum majorana* L. Obtained by Hydrodistillation and SFE

Hidrodistilasyon ve SFE Kullanarak Elde Edilen *Origanum majorana* L.'nin Uçucu Yağ Bileşiminin Karşılaştırılması

Ezgi Aytaç

Department of Plant Sciences, Faculty of Agriculture and Natural Sciences, Konya Food and Agriculture University, Konya, Turkey.

ABSTRACT

The volatile components of *Origanum majorana* L. essential oil obtained from both hydrodistillation and supercritical fluid extraction (SFE) were determined by GC–MS and GC-FID. Extraction of these biologically active compounds requires the usage of large amounts of environmentally unfriendly solvents and technologies operating with high costs. Supercritical fluid extraction is an environmentally friendly and efficient extraction technique for solid materials, being extensively studied for the separation of active compounds from herbs and other plants. The essential oil obtained by SFE contains mainly carvacrol (76.69% with GC-MS and 91.95% with GC-FID) which are responsible for the characteristic flavour and fragrance of marjoram oil. And also to compare with SFE, the essential oil obtained by hydrodistillation contains mainly carvacrol (70.47% with GC-MS and 89.00% with GC-FID). It can be concluded that almost all the biologically active compounds from marjoram herb can be efficiently extracted by SFE.

Key Words

Origanum majorana L., SFE, hydrodistillation, essential oil

ÖZ

Origanum majorana L'nin hem hidrodistilasyon hem de süperkritik akışkan ekstraksiyonu (SFE) ile elde edilen uçuğu yağ bileşimi GC-MS ve GC-FID ile belirlendi. Biyolojik aktif bileşenlerin ekstraksiyonu çevreye zarar veren çözücülerin aşırı kullanımını ve çok yüksek ücretli teknolojileri gerektirir. Süperkritik akışkan ekstraksiyonu şifalı bitkiler ve diğer bitkilerden aktif bileşenlerin ayrılması için yoğunlukla çalışılan katı materyaller için çevreye dost ve etkili bir ekstraksiyon tekniğidir. SFE'den elde edilen uçucu yağın yüksek oranda marjoram yağının tadından ve karakteristik kokusundan sorumlu olan karvakrolü (76.69% GC-MS ve 91.95% GC-FID) içerdiği tespit edildi. SFE ile karşılaştırıldığında hidrodistilasyon ile elde edilen uçucu yağlar da yüksek oranda karvakrol (70.47% GC-MS ve 89.00% GC-FID) içerir. Buradan çıkarılacak sonuç; marjoram bitkisinden elde edilen biyolojik aktif bileşenler SFE ile verimli bir şekilde ekstrakte edilebilir.

Anahtar Kelimeler

Origanum majorana L., SFE, hidrodistilasyon, uçucu yağ

Article History: Received: Jan 17, 2019; Revised Jun, 23 2019; Accepted: Jan 29, 2020; Available Online: May 3, 2020.

DOI: https://doi.org/10.15671/hjbc.514042

Correspondence to: E. Aytaç, Department of Plant Sciences, Konya Food and Agriculture University, Konya, Turkey.

E-Mail: ezgi.aytac@gidatarim.edu.tr

INTRODUCTION

Many medicinal plants are known to contain large amounts of antioxidants which can play an important role in scavenging free radicals and reactive oxygen species. Because of the drugs stresses, toxic substances, or diseases, the production of active oxygen species increases, which has the potential to cause oxidative damage [1]. Antioxidants have vital functions in avoiding oxidative mechanisms that cause to degenerative diseases [2]. Nowadays, free radicals show important functions in the etiology of cardiovascular diseases, such as cancer, Alzheimer, and Parkinson [3]. Evidence shows that the vegetable and fruit consumption decreases the risk of several pathological events, such as cancer and cardio- and cerebro vascular diseases [4]. Additionally, plants or their crude extracts have been used in the prevention and/or treatment of some diseases around the world [5].

Essential oils (EO) a group of plant derived secondary metabolites have well known antioxidant properties, which can be characterized directly via interaction with peroxyl radicals. Essential oils are aromatic oily liquids extracted from different parts of plants (leaves, seeds, roots, fruits, etc.) either by hydrodistillation or solvent extraction [6]. These natural products have got increasing attention in the chemical, food and pharmaceutical industries, because they can have a wide range of activities and good candidates to replace several synthetic compounds [7].

The volatile oils can be obtained by different processes, depending on the location of the plant, the amount and the characteristics required for the final product. These are the number of methods such as steam distillation (SD), hydrodistillation (HD), organic solvent extraction, microwave assisted distillation (MAD), microwave hydrodiffusion and gravity (MHG), high pressure solvent extraction (HPSE), supercritical fluid extraction (SFE), ultrasonic extraction (UE) and solvent free microwave extraction (SFME). However, the properties of the essential oils extracted through these methods have been found to vary depending on the method used [8]. The conventional techniques are pressing extraction with organic solvents (for delicate raw materials, as flowers petals), hydrodistillation (a common method, used for the extraction of volatile from aerial parts of plants) and extraction with supercritical fluids (interest in determined fraction of oil) and distillation (heat resistant substances) [9]. The alteration caused by hydrodistillation is remarkable as plant material in contact with steam undergoes many chemical changes. Hot steam will decompose many aldehydes and esters. Some water-soluble molecules may be lost by solution in the water, thus altering the chemical profile of the oil [9]. Supercritical fluid solvents such as SC-CO_2 are intermediates between liquid and gases and considered important in the separation processes based on the physicochemical characteristics including density, viscosity, diffusivity and dielectric constant which are easily manipulated by pressure and temperature. It also has a critical temperature (Tc = 304.1 K) that makes it suitable for the extraction of many natural products under mild conditions [9].

The mint family (Lamiaceae) includes aromatic plants widely used for culinary, medicinal, cosmetic and ornamental purposes, such as basil, rosemary, sage, oregano, lavender, thyme and mint [10]. ***Origanum*** spp. belongs to the Lamiaceae family, which consists of 49 taxa, subdivided to 10 sections, its species widely distributed in Eurasia and North Africa [11] being native to the mountainous areas of Mediterranean and Asia [12]. Species belonging to the genus ***Origanum*** are used since the ancient times as spices, medicinal, aromatic and ornamental plants [13]. In vitro pharmacological investigations showed their antibacterial, antifungal, antioxidant, antispasmodic, antimutagenic, antitumoral, analgesic, antithrombin and antihyperglycaemic activities [12].

Origanum majorana is a culinary herb and is called as "sweet marjoram" because of its citrus flavours. Additionally, Turkey has become a major supplier of ***Origanum*** herb and its oil to world markets due to its high quality. The fresh or dried highly aromatic leaves and flowering tops of sweet marjoram are widely used adding flavor to many foods. Its essential oil and alcoholic extracts have versatile applications in pharmaceuticals, perfumes and cosmetics. The essential oil of sweet marjoram from different origins was previously analyzed for the composition and biological activities [14]. Lamiaceae plants are collected from the wild or grown as commercial crops and used to prepare many commercial products, including herbal teas, spices, beverages, pharmaceutical products [15].Current data shows that the essential oils of origanum species are rich sources of active compounds with particular biological importance, known for its antibacterial and antifungal activities [16].

The objective of this work was to evaluate and compare the chemical profile of essential oils of marjoram (*Origanum majorana* L.) from the Mediterranean region of Turkey obtained by hydrodistillation (Clevenger apparatus) and supercritical CO_2. Because, the qualitative and quantitative changes in chemical compounds by using SFE compared with hydrodistillation are poorly studied.

MATERIALS and METHODS

Plant Material

Origanum majorana L. plants (about 1 kg) were collected from Akseki, Antalya which obtained from Alanya General Directorate of Forestry in June, 2017. Samples were allowed to dry in the shade. Seeds obtained from ripened fruits were separated from the plant material, and collected in a separate bag before storing at 6°C in a refrigerator until analysis. The seeds were ground in a using a mechanical mill. The dried, finely ground sweet marjoram sample was a greyish-brown fine powder with a characteristic scent. This powder was used for all the extractions.

Hydrodistillation Procedure (Clevenger Aparatus)

100g of *Origanum majorana* L. was used for hydrodistillation extracting system. The essential oil was extracted over a period of 90 min using a Clevenger apparatus and the yield of oil was recorded at every 5 min. After hydrodistillation, water was removed by decantation and the essential oil obtained was stored at 4°C in a dark-colored container to prevent light-sensitive decomposition.

Supercritical Fluid Extraction (SFE) Procedure

Supercritical CO_2 extraction is the best green extraction method to remove nonpolar components such as seed oils [17]. If supercritical fluid contains polar solvents such as methanol, ethanol or water more polar compounds can be extracted. Applied Separation supercritical extractor (Spe-ed SFE) equipped with a modifier pump (Applied Seperation Series 1500), pressure pump (Atlas Copco GX-4FF) and chiller (Applied Seperation Polyscience) was used for all the extractions. The system run for 30 min under following conditions:

Sample mass: 100 g
Temperature: 40°C
CO_2 flow rate: 7 kg/h
Pressure: 150 bar
Vessel volume: 0.50 L

Chemical Characterization (GC-MS and GC-FID Analyses)

The quantification of essential oil components was performed by gas chromatography (GC) in equipment Shimadzu GC-210. The analyses were carried out using a capillary column RESTEK, Rxi-5 Sil MS 30 Meter 0.25 mm ID 0.25 µm df, detector FID, following the temperature program: 40-180°C (3°C min^{-1}), 180-240°C (20°C min^{-1}), 240°C (20 min), temperature of injector 250°C, injection mode split, carrier gas He, injection volume of 0.4 µL (sample diluted in n-hexane 1:10).

The determination of chemical profile of essential oil components was carried out in a gas chromatography with mass spectrometer as detector (GC-MS), model Shimadzu GC 17A, ion source temp: 200°C, interface temp: 250°C, solvent cut time: 4 min. Chromatographic patterns as thymol, sabinene hydrate, α-terpinene and γ-terpinene (Fluka) and α-terpineol, camphene, 4-carvomenthenol, limonene, α-pinene, carvacrol, β-pinene, myrcene, p-cimene, limonene, 1,8-cineol, terpinolene and linalool (Sigma-Aldrich) were used to the chemical characterization of essential oils.

RESULTS and DISCUSSION

The mean yield of essential oils of marjoram obtained by Clevenger apparatus 4.2±0.23 g per 100 g of leaf. The values four times higher than that found by Busatta et al [18]. The mean yield obtained by the supercritical fluid extraction was 4.5±0.32 g per 100 g leaf and also it is 2.5 times higher than obtained by Busatta et al [18].

However, the quality and activity of extract is greatly dependent upon the process. Hydrodistillation (HD) with Clevenger aparatus and solvent extraction have been the major processes for a long time. During last decades, the use of supercritical fluids for extraction of plant volatile fraction has been increasingly preferred [19]. This is due to the advantages of the supercritical fluid extraction technique: rapid, selective, and convenient technique for extraction of natural compounds from aromatic and medicinal plants. Also, SFE extracts are considered as solvent free, which enhances their attractiveness for the consumer [20]. For instance, the color intensity of the extracts from both species was different, the Clevenger extracts were yellow, and the extracts by SFE exhibited a dark yellow color that can be attributed to the differences in chemical composition. This is probably due to the properties of SFE technique

including the low temperature and rapidity (40°C, 30 min), which minimize the high temperature exposure and consequently the lower thermal degradation than Clevenger (around 100°C, 90 min) [21].

Due to their structural relationship within the same chemical group, essential oil components are known to easily convert into each other by oxidation, isomerization, cyclization, or dehydrogenation reactions, triggered either enzymatically or chemically. Upon stability evaluation of essential oils, it needs to be kept in mind that the chemical composition may already vary in the starting material, being influenced by plant health, growth stage, habitat including climate, edaphic factors, as well as harvest time [22].

As terpenoids tend to be both volatile and thermolabile and may be easily oxidized or hydrolyzed depending on their respective structure [23], it is well accepted that the chemical composition of essential oils is moreover dependent on the conditions during processing and storage of the plant material, upon distillation as well as in the course of subsequent handling of the oil itself [24].

The results are in complete agreement with the literature [25,26], as both hydrodistillation and supercritical CO_2 extraction techniques produce almost the same main volatile compounds but with negligible monoterpene hydrocarbons for the second case. According to Temelli et al. [27] an attractive point of supercritical extraction is to obtain extracts rich in aroma compounds with the lowest possible monoterpene concentration, because they do not contribute much to the flavor of essential oils and also because they are very sensitive to heat and light and may decompose into undesirable substances [28].

In the literature, in the most cases, the comparison between hydrodistillation (HD) with Clevenger aparatus and SFE extraction showed a difference of yields but a few variations in chemical composition for the same major compounds in the extract. SFE extracts from marjoram were characterized by higher contents of heavier molecular weight compounds (retention time in the range 30 to 40 min) than in the case of the HD essential oils. In parallel, lighter components, for example, alpha-thujene, alpha-pinene, and gamma-terpinene, present in the HD essential oils, were weakly detected in the SFE extracts. This does not mean that such light compounds are not present in SFE extracts, but the presence of other compounds, especially heavy ones, will make these compounds in trace quantity. Indeed, it would be surprising that SFE does not extract such kind of lighter compounds, which are known for being soluble in CO_2 in these conditions.

The chromatographic analysis permitted the identification of carvacrol as the most prominent compounds present in the cultivated *Origanum majorana* L. with hydrodistillation and the SFE. Results (Table 1.) showed an important difference in monoterpene and sesquiterpenes (hydrocarbons and oxygenated) identified in each extract. Indeed, the sesquiterpenes were much better extracted by SFE than hydrodistillation. The opposite was noted for the monoterpenes: 11.49% (with GC-MS) in hydrodistillation compared to 3.84% (with GC-MS).

The extraction method influenced significantly the chemical composition of the extracts. The concentration of phenols increased from approximately 70 to 77 with GC-MS from hydrodistillation to SFE and also with GC-FID increased from approximately 89 to 92 with SFE in comparison to hydrodistillation. The major compound of marjoram essential oil obtained with SFE and hydrodistillation carvacrol, followed by δ-terpinene, myrcene and α-terpinene (Table 1.).

Some major compounds as α-terpinene, δ-terpinene and myrcene were found in the essential oils from hydrodistillation compared to those from SFE. A four times higher concentration of δ-terpinene and two times higher concentration of myrcene was obtained for both oils obtained by hydrodistillation with Clevenger apparatus.

So, the present works show the occurrence of qualitative differences on the essential oils, related to the extraction method (SFE and Hydrodistillation). A higher extraction capacity of phenols by SFE, allowing optimizing the extraction of compounds of interest by the choice of the most adequate extraction method was observed. According to these characteristic features *Origanum majorana* L. oil can be classified as valuable oil for human nutrition.

Table 1. Chemical composition of the essential oil from *Origanum majorana* L. obtained by hydrodistillation and SFE.

	Compound Name	Hydrodistillation		SFE	
		MS (%)	FID (%)	MS (%)	FID (%)
		Monoterpene Hydrocarbons			
1	α-Thujene	1.25	0.64	-	-
2	α-Pinene	0.96	0.51	0.37	0.19
3	Sabinene	-	-	-	-
4	β-Pinene	0.29	0.12	-	-
5	Myrcene	2.29	1.17	0.69	0.33
6	α-Phellandrene	0.31	0.12	0.16	0.05
7	α-Terpinene	1.48	0.63	1.10	0.48
8	Limonene	-	-	-	-
9	p-Cymene	-	-	-	-
10	γ-Terpinene	4.56	2.47	1.36	0.64
11	Terpinolene	0.35	0.08	0.16	0.06
	Total	11.49	5.74	3.84	1.75
		Oxygenated Monoterpenes			
12	1,8-Cineole	-	-	0.41	0.05
13	trans-Sabinene hydrate	0.60	0.22	-	-
14	cis-Sabinene hydrate	-	-	-	-
15	Linalool	0.33	0.01	0.37	0.14
16	trans-p-Menth-2-enol	-	-	-	-
17	cis-p-Menth-2-enol	-	-	-	-
18	Terpinen-4-ol	-	-	-	-
19	α-Terpineol	0.76	0.01	-	-
20	trans-Piperitol	-	-	-	-
21	cis –Piperitol	-	-	-	-
22	Geraniol	-	-	-	-
23	Linalyl acetate	-	-	-	-
	Total	1.69	0.24	0.78	0.19
		Phenols			
24	Thymol	-	-	-	-
25	Carvacrol	70.47	89.00	76.70	91.95
	Total	70.47	89.00	76.70	91.95
		Sesquiterpene Hydrocarbons			
26	β-Caryophyllene	1.34	0.43	1.35	0.47
27	Germacrene	-	-	-	-
	Total	1.34	0.43	1.35	0.47
		Oxygenated Sesquiterpenes			
28	Caryophyllene oxide	-	-	0.62	0.19
29	Spathulenol	-	-	-	-
	Total	-	-	0.62	0.19
	Total Identified Compounds	84.99	95.41	83.29	94.55

Acknowledgement
Thanks to Prof. Atalay Sokmen from Konya Food and Agriculture University for plant supply and identification.

References

1. B. Frei, Natural antioxidants in human health and disease, Free Rad. Biol. Medic., 20 (1996) 157-159.
2. A. Cardador-Martinez, G. Loacra-Pina, B.D. Oomah, Antioxidant activity in common beans (*Phaseolus vulgaris* L.), J. Agri. Food Chem., 50 (2002) 6975-6980.
3. V.N. Enujiugha, J.Y. Talabi, S.A. Malomo, A.L. Olagunju, DPPH radical scavenging capacity of phenolic extracts from african yam bean (*Sphenostylis stenocarpa*), Food Nutrit. Sci., 3 (2012) 7-13.
4. E.B. Rimm, A. Ascherio, E. Giovannucci, D. Spiegelman, M.J. Stampfer, W.C. Willett, Vegetable, fruit and cereal fiber intake and risk of coronary heart disease among men, J. Amer. Medic. Ass., 275 (1996) 447-451.
5. G. Semiz, A. Semiz, N. Mercan-Doğan, Essential oil composition, total phenolic content, antioxidant and antibiofilm activities of four Origanum species from southeastern Turkey, Int. J. Food Proper., 21 (2018) 194-204.
6. G.B. Salha, R.H. Diaz, J. Labidi, M. Abderrabba, Deterpenation of *Origanum majorana* L. essential oil by reduced pressure steam distillation, Indust. Crops Prod., 109 (2017) 116-122.
7. A. Cháfer, J. Torre, R. Muñoz, M.C. Burguet, Liquid-liquid equlibria of the mixture linalool + ethanol +water at different temperatures, Fluid Phase Equilibria, 238 (2005) 72-76.
8. O.O. Okoh, A.P. Sadimenko, A.J. Afolayan, Comparative evaluation of the antibacterial activities of the essential oils of *Rosmarinus officinalis* L. obtained by hydrodistillation and solvent free microwave extraction methods, Food Chem., 120 (2010) 308-312.
9. C. Busattaa, J. Barbosaa, R. I.Cardosoa, N. Paroula, M. Rodriguesb, D. Oliveirac, J.V. Oliveirac, R.L. Cansiana, Chemical profiles of essential oils of marjoram (*Origanum majorana*) and oregano (*Origanum vulgare*) obtained by hydrodistillation and supercritical CO_2, J. Essent. Oil Res., 29 (2017) 367-374.
10. R. Raja, Medicinally potential plants of Labiatae (Lamiaceae) family: An overview, J. Res. Plants Med. 6 (2012) 203-213.
11. J.H. Ietswaart, A taxonomic revision of the genus Origanum (Labiatae), Leiden Botanical series, Leiden University Press, 4 (1980)
12. S. Chishti, Z.A. Kaloo, P. Sultan, Medical importance of genus Origanum: A review, J. Pharmacognosy Phytother. 5 (2013) 170-177.
13. M. Meyers, Oregano and Marjoram, The Herb Society of America, Guide to the genus Origanum, The Herb Society of America, Kirtland, Ohio, 2005.
14. B. Teixeira, A. Maryues, C. Ramos, C. Serrano, O. Matos, N.R. Neng, J.M. Noqueira, J.A. Saraiva, M.L. Nunes, Chemical composition and bioactivity of different oregano (*Origanum vulgare*) extracts and essentail oil, J. Sci. Food Agric, 93 (2013) 2707-2714.
15. C.M. Asensio, N.R. Grosso, H.R. Juliani, Quality characters, chemical composition and biological activities of oregano (Origanum spp.) Essential oils from Central and Southern Argentina, Ind. Crop. Prod. 63 (2015) 203-221.
16. O. Baâtour, I. Tarchoun, N. Nasri, R. Kaddour, J. Harrathi, E. Drawi, M. Ben Nasri- Ayachi, B. Marzouk, M. Lachaâl, Effect of growth stages on phenolics content and antioxidant activities of shoots in sweet marjoram (*Origanum majorana* L.) varieties under salt stress, Afr. J. Biotechnol., 11 (2012) 16486-16493.
17. F. Chemat, M.A. Vian, G. Cravotto, Green extraction of natural products: concept and principles, Int. J. Molecul. Sci., 13 (2012) 8615-8627.
18. S.M. Pourmortazavi, S.S. Hajimirsadeghiİ Supercritical fluid extraction in plant essential and volatile oil analysis, J. Chromatogr. A, 1163 (2007) 2-24.
19. B. Berka-Zougali, M.A. Ferhat, A. Hassani, F. Chemat, K.S. Allaf, Comparative study of essential oils extracted from Algerian *Myrtus communis* L. leaves using microwaves and hydrodistillation. Int. J. Mol. Sci., 13 (2012) 4673-95.
20. Y. Yamini, F. Sefidkon, S.M. Pourmortazavi, Comparison of essential oil composition of Iranian fennel (*Foeniculum vulgare*) obtained by supercritical carbon dioxide extraction and hydrodistillation methods, Flav. Fragr. J., 17 (2002) 345-8.
21. A.C. Figueiredo, J.G. Barroso, L.G. Pedro, J.J.C. Scheffer, Factors affecting secondary metabolite production in plants: Volatile components and essential oils, Flav. Fragr. J., 23 (2008) 213-226.
22. C. Turek, F.C. Stintzing, Stability of Essential Oils: A review, Comprehensive Reviews in Food Science and Food Safety, Vol 12, 2013.
23. B. Simandi, M. Ozszagyan, E.A. Lemberkovics, A.A. Kery, J. Kaszacs, F. Thyrion, T. Matyas, Supercritical carbon dioxide extraction and fractionation of oregano oleoresin, Food Res. Int., 31 (1998) 723-728.
24. R.P.W. Scott, Essential oils, Encyclopedia of analytical science. 2nd ed. Amsterdam, London, New York: Elsevier (2005) 554-61.
25. M. Ordaza, A. Sanchez, Steam distillation and supercritical fluid extraction of some Mexican spices, Chromatographia, 30 (1990) 16-18.
26. F. Temelli, R.J. Braddock, C.S. Chen, Nagy, Supercritical carbon dioxide extraction of terpenes from orange essential oil In: Supercritical fluid extraction and chromatography: Techniques and applications; B.A. Charpentier, R. Sevenants, Eds.; ACS Symposium Series 366; American Chemical Society, Washington, DC, 1988; p 109.
27. M.R.A. Rodrigues, L.C. Krause, E.B. Caramoa, J.G. Santos, C. Dariva, J.V. Oliveira, Chemical composition and extraction yield of the extract of origanum vulgare obtained from sub- and supercritical CO_2, J. Agricult. Food Chem., 52 (2004) 3042-3047.
28. M. Sharifi-Rad, E.M. Varoni, M. Iriti, M. Martorell, W.N. Setzer, M.M. Contreras, B. Salehi, A.S. Nejad, S. Rajabi, M. Tajbakhsh, J. Sharifi-Rad, Carvacrol and human health: A comprehensive review, Phytother. Res., 32 (2018) 1675-1687.

F.E. Yiğit et al. / Hacettepe J. Biol. & Chem., 2020, 48 (3), 245-263

Review Article

Hacettepe Journal of Biology and Chemistry

journal homepage: www.hjbc.hacettepe.edu.tr

Microfluidic Devices: A New Paradigm in Toxicity Studies

Mikroakışkan Cihazlar: Toksisite Çalışmalarında Yeni Bir Yaklaşım

Fatma Esra Yiğit[1], Kutay İçöz[2,3], İffet İpek Boşgelmez[4*]

[1]Faculty of Pharmacy, Erciyes University, Kayseri, Turkey.

[2]Department of Bioengineering, Abdullah Gül University, Kayseri, Turkey.

[3]Department of Electrical and Electronics Engineering, Abdullah Gül University, Kayseri, Turkey.

[4]Department of Toxicology, Faculty of Pharmacy, Erciyes University, Kayseri, Turkey.

ABSTRACT

In recent years, great emphasis has been placed on non-animal toxicological methods (e.g. *in vitro* models, in silico or –omics data) as alternative strategies to reduce animal-testing, in line with the 3R (Replacement, Reduction, and Refinement) principle. These methods help in the rapid and accurate estimation of preclinical efficacy and safety associated with discovery of new drugs, and reduction of failure rates in clinical trials. Currently, the *in vitro* studies have been in a transformation or replacement from two-dimensional (2D) cell cultures to three-dimensional (3D) cell cultures that can mimic the physiology of tissues, organs, and organisms.

In this context, organ-on-a-chip systems have been developed by integration of 3D culture models with emerging microfluidic technologies. Since the organ-on-a-chip systems provide a good understanding of dose-response and toxicity mechanisms in drug research and development (R&D), the impact of xenobiotics on the human body can be predicted in a satisfactory level. Besides, these systems may support assessment of pharmacokinetic-pharmacodynamic parameters as well as detection of drug resistance. Models can be generated as "disease-models-on-a-chip" or with healthy cells to the evaluate response to xenobiotic under test.

In this review, we will focus on the microfluidic systems being used in organ-on-a-chip systems and emphasize their potential for toxicity studies in which micro-environments of examples including liver, kidney, brain, lung, heart, and intestines and their physiological properties as reflected to organ-on-a-chip models.

Key Words
Microfluidic devices, organ-on-a-chip, toxicity testing, drug R&D

ÖZ

Son yıllarda, 3R (yerine koyma, azaltma, iyileştirme) prensibi doğrultusunda deney hayvanı kullanımını azaltmak için alternatif toksikoloji metotlarına (örneğin, *in vitro* modeller, in silico veya –omics verilerine) büyük önem verilmektedir. Bu metotlar, yeni ilaçların keşfedilmesiyle ilişkili preklinik etkinlik ve güvenliğin hızlı ve doğru bir şekilde tahmin edilmesine ve klinik çalışmalarda başarısızlık oranlarının azaltılmasına yardımcı olmaktadır. Günümüzde *in vitro* çalışmalar; iki boyutlu (2D) hücre kültürlerinden, doku, organ ve hatta organizmanın fizyolojisini taklit edebilen üç boyutlu (3D) hücre kültürlerine dönüşüm veya değişim içindedir.

Bu bağlamda, 3D kültür modellerinin gelişmekte olan mikroakışkan teknolojilerine entegrasyonu ile çip-üstü-organ sistemleri geliştirilmiştir. Çip-üstü-organ sistemleri, ilaç araştırma ve geliştirme (Ar-Ge) sürecinde doz-yanıt ve toksisite mekanizmalarının iyi anlaşılmasını sağladığı için, ksenobiyotiklerin insan vücudu üzerindeki etkisinin tatmin edici düzeyde tahmin edilmesi mümkün olmaktadır. Ayrıca, bu sistemler farmakokinetik-farmakodinamik parametrelerin ve ilaç direncinin değerlendirilmesini destekleyebilir. Modeller, test edilen ksenobiyotiğe yanıtı incelemek için "çip-üstü-hastalık modelleri" şeklinde veya sağlıklı hücrelerle üretilebilir.

Bu derleme kapsamında; çip-üstü-organ sistemlerinde kullanılan mikroakışkan sistemleri ele alınmakta ve karaciğer, böbrek, beyin, akciğer, kalp ve bağırsaklar gibi çeşitli örneklerin mikro-ortamlarının ve fizyolojik özelliklerinin çip-üstü-organ modellerine yansıtıldığı toksisite çalışmaları için potansiyelleri vurgulanmaktadır.

Anahtar Kelimeler
Mikroakışkan cihazlar, çip-üstü-organ, toksisite testleri, ilaç Ar-Ge

Article History: Received: Aug 25, 2019; Revised: Dec, 11 2019; Accepted: Mar 13, 2020; Available Online: May 3, 2020.

DOI: https://doi.org/10.15671/hjbc.610448

Correspondence to: İ.İ. Boşgelmez, Dept of Toxicology, Faculty of Pharmacy, Erciyes University, Kayseri, Turkey.

E-Mail: ibosgelmez@erciyes.edu.tr

INTRODUCTION

The discovery of a potential drug, i.e. finding new molecules or modified-versions of existing ones, may become "finding a needle in a haystack". Moreover, drug development may be required to provide better routes of drug delivery to the target or to obtain superior pharmaceutical dosage forms. Last but not least, for application to the approval or licensure process, the potential new drug must pass many tests, which generally begin in the laboratory moving forward to *in vitro* and *in vivo* tests and if the candidate continues to show promise, it may proceed to the clinical studies. Therefore, drug discovery, development, and approval are not only complex and time-consuming but also, they require a perfectly harmonized system and teamwork. In this context, the preclinical step, as summarized in Figure 1, may comprise *in vitro* human cell cultures or experimental animal testing to obtain the efficacy and safety data of the drug candidate in terms of pharmacokinetics and pharmacodynamics, drug toxicity, and treatment method [1]. However, currently available *in vitro* human cell culture studies may not fully reflect the complexity of living systems and may not be capable of modeling the tissue-tissue or organ-organ communication. Also, they might have limited prediction capability in complex drug metabolism and the effect of metabolites on non-target tissues [2]. In addition, the animal tests are preferred because there are some difficulties in obtaining the primary cells homogeneously from the human tissue, as well as pitfalls including early aging of the cells, and the phenotypes or metabolic characteristics of the cells [3]. On the other hand, while currently accepted as the gold standard, the use of experimental animals is often costly, time-consuming, and an ethically debated process [4]. However, more critically, the findings related to drugs in experimental animals may not reflect the actual situation in humans, or may not be easily extrapolated from the test species [5].

Overall, the human body is composed of highly complex systems to perform various functions. Therefore, there is an urgent need to develop physiologically relevant, appropriate models similar to human tissues and organs for use in drug discovery and disease modeling. In this vein, recent advancements in microfluidic technologies have provided new and effective methods for providing drug research at the micro-level [6–9]. The technology resulting from these developments provides a practical solution to many of the problems associated with the

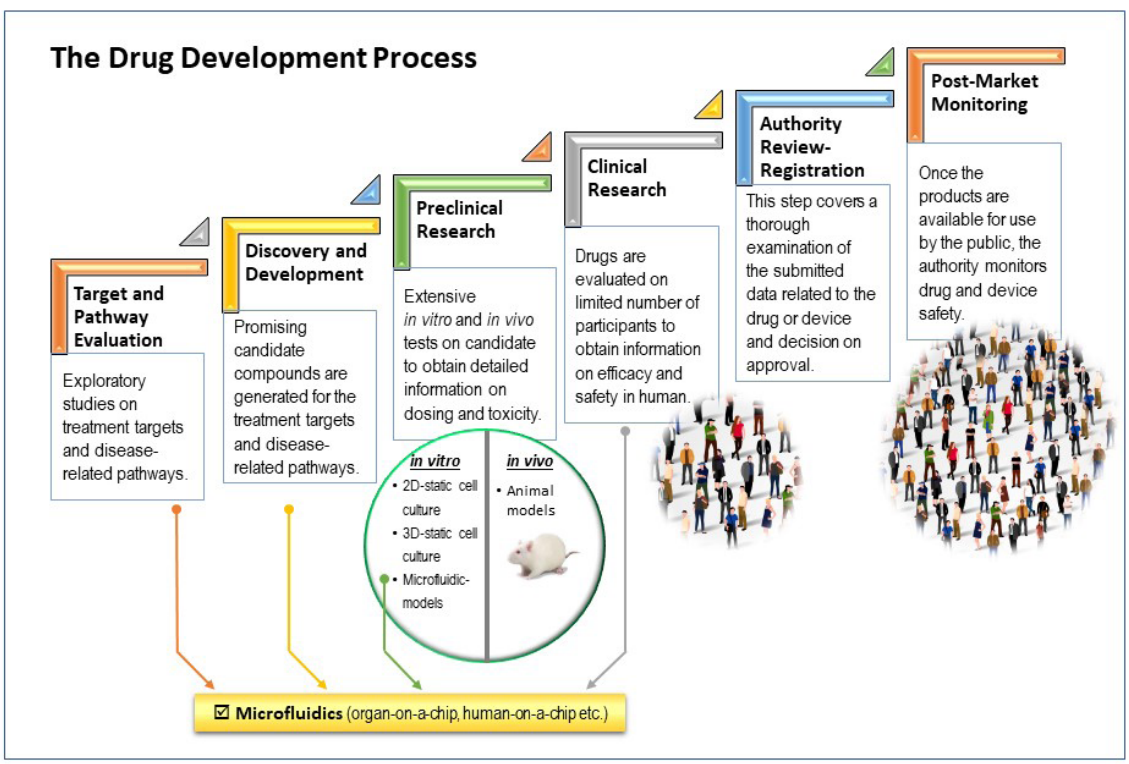

Figure 1. An overview of the drug research and development process and the role of "Microfluidics"

above-mentioned *in vitro* cell culture and experimental animal use. The organ-on-a-chip systems allow a wide-range of applications, including cell culture models [4]. Typical organ-on-a-chip systems are designed to perform activities and physiological responses of organs, which have controllable compartments and channels in the micrometer range, and enable the movement of small volumes of liquids or gases through these channels providing physiologically relevant conditions [3]. The main motives behind this technology is to replace current tools (e.g., animal testing, 2D cell culture studies) with more specific, accurate, and high-throughput tests which can help provide a faster research period so that the drugs can enter the market earlier; moreover, the number of researched drugs are expected to increase in these settings [4]. More complex devices may include multiple cell types separated by porous layers that mimic the basal membranes of barrier tissues [1]. These multichannel chips are the focus of research by providing modeling of tissue-tissue or tissue-blood interactions and barrier functions. Barrier tissues are important in understanding the integrity and function of the barrier, the communication between tissues or tissue-blood [3]. In the last few years, liver [10], kidney [11,12], lung [13], brain [14], heart [15,16], and multi-organ [17,18] and disease-models [19] have been used in drug research and toxicity assessments.

The scope of this review is to emphasize the importance of research on microfluidic devices in toxicity studies by 3-dimensional (3D) cell culture applications in tissue engineering, and to compile information on recent developments for potential applications of these technologies in various areas of toxicology, especially in drug research and development.

Microfluidics

Microfluidics is briefly defined as the emerging field of engineering and application of devices that apply a controlled fluid flow in micro-scale channels. It is the science and technology of systems that process very small amounts of fluids (e.g. 1 nL), using miniature-channels (tens to hundreds of micrometers) [20]. The main concept of microfluidics is to integrate the overall laboratory into a compact micro-dimensional system. A microfluidic chip is composed of micro-channels formed generally by molding or engraving. These micro-channel networks formed in the microfluidic chip are connected to the macro-environment using inlet and outlet ports with fluidic connectors of different sizes specially prepared on the chip.

A microfluidic platform serves as a consistent tool for miniaturization and parallelization of processes to be assayed [21]. Moreover, these systems provide the re-

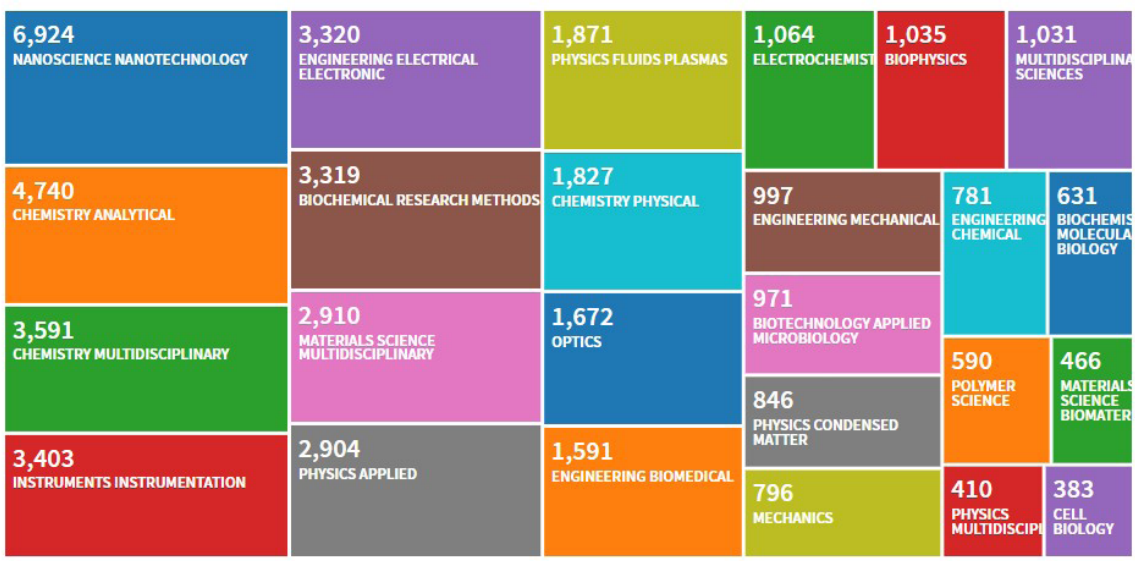

Figure 2. Distribution of top-25 "Web of Science Categories" within the published items on "Microfluidics" as of 15.01.2020. The top-5 topics are in the order of "Nanoscience-Nanotechnology", "Analytical Chemistry", "Multidisciplinary Chemistry", "Instruments-Instrumentation", and "Electrical-Electronic Engineering". The rank of "Pharmacology Pharmacy" field is 26th after "Cell Biology", with 353 items, while "Toxicology" is represented in the 76th rank with 41 items.

quired platform for the integration and automation of multiple assays, and also, they facilitate imaging and tracking of tests or conditions. The historical evolution and diverse aspects of microfluidic systems have been reviewed in detail elsewhere [20,21].

This technology may be applied to diverse areas including an increasing number of engineering fields, chemistry, life sciences, forensics, and more recently in health-related studies [22–25]. Microfluidic chips have found application areas such as drug R&D, disease modeling, and toxicity research. There are many examples realized with microfluidic chip platforms such as signal amplification [26], capturing targets using affinity and size-based separation via antibody-conjugated magnetic beads [27], and detection of rare mutations [28]. As shown in Figure 2, the distribution of "Web of Science Categories" within the published items on the topic "Microfluidics" reveals that the top-5 topics are in the order of "Nanoscience-Nanotechnology", "Analytical Chemistry", "Multidisciplinary Chemistry", "Instruments-Instrumentation", and "Electrical-Electronic Engineering". While the rank of "Pharmacology Pharmacy" field, with 353 items, is 26th after "Cell Biology"; currently "Toxicology" is represented in the 76th rank with 41 items. In this sense, an interesting review by Sackmann et al. [29] underlines the fact that the majority of publications related with microfluidics are published in engineering journals (85%), whereas the biology and medicine journals could take some publication share from interdisciplinary journals (9% and 6%, respectively).

Materials in Conventional Microfluidic Platforms

Since microfluidic technologies have found use in different applications with expanding demands that increase day by day, the selection of materials has a strong impact on the performance of the devices. Once chemicals or biological materials (e.g., proteins or cells) enter a microfluidic device, the characteristics of the material may impact the outcome [30]. As also shown in the historical timeline of developments in materials used in microfluidics [31], obviously, the synergistic innovation of materials and microfluidic platforms plays a critical role in the sophisticated and sustainable implementation of microfluidics-based technologies in various disciplines. Thus, on the one hand innovative materials serve for the emerging applications of microfluidics, on the other hand microfluidic systems provide robust and flexible platforms for the fabrication of materials with superior characteristics. Comprehensive studies which include reviews by Berthier et al. [32], Ahadian et al. [33], Zhang et al. [34], and Nielsen et al. [35] have summarized the materials used in microfluidics. Specifically, the comparative strengths and limitations of materials available for microfluidic cell-based device fabrication has also been covered in detail [32], in view of the ability to fabricate the microsystems, and to perform controllable cell-based experiments, as well as the potential for integrated micro-engineering applications.

The selection of microfluidic chip materials serves the aim to fabricate a micro-scale chip that is functional, low-cost, and portable. In other words, the main concerns in commercialization are ease of fabrication, reliability, ease of adoption by the end-user, and cost. In this sense, as briefly summarized in Table 1, there are different types of materials such as inorganics, elastomers, plastics, hydrogels, paper, hybrid and composite materials [36].

For microfluidic devices used in cellular analysis, there is often a need for a material in which the micro-channels are embedded to be porous (for exchange of nutrients, CO_2, O_2, etc.) to allow the cells to communicate with the external environment [37]. In general, hydrogels are considered suitable materials, since pores can be adjusted via thermal or electrical manipulations. Essentially, the choice of a suitable material for any type of microdevice depends on the microfluidic test applied. As a result of new microfluidic device applications and increasing demand for more flexible and advanced functionality, the range of materials applicable to microfluidic systems is continually expanding. The most commonly used substrates today include silicone, glass or quartz and polymers [37].

The microfluidic systems are generally produced from transparent polymeric materials, since this feature enables a user-friendly tracking or testing. In the late 1990s, with the concept of using polymer materials in microfluidics, the use of silicon and glass materials has shifted to polymers. Compared to silicon and glass, polymers are low-cost materials and feature a wide variety of properties to meet diverse application demands in disposable biomedical microfluidic devices, as well as various promising applications [38]. In general, elastomers (e.g. polydimethylsiloxane, PDMS) and plastics (e.g. polymethylmethacrylate, PMMA) are utilized (Figure 3).

Table 1. An overview of currently available materials used in microfluidic device fabrication [25,36,41].

Material	Technique for fabrication	Young's (Tensile) modulus (GPa)	Thermo-stability	Permeability to O_2 (mol/m x s x Pa)	Solvent-compatibility	Hydro-phobicity	Smallest channel dimension	Optical clarity
Silicon	photolithography	130-180	very high	<0.01	very high	hydrophilic	<100 nm	opaque
Glass	photolithography, 3D printing	50-90	very high	<0.01	very high	hydrophilic	<100 nm	high
Elastomers (PDMS)	casting	~0.0005	medium	~500	low	hydrophobic	<1 µm	high
Thermoset Poly-mers (SU-8, TPE)	casting, polymerization	2.0-2.7	high	0.03-1	high	hydrophobic	<100 nm	high
Thermoplastic polymers (PMMA, PS, PC, PU, PEGDA, COC)	thermomolding, laser cutting	1.4-4.1	medium to high	0.05-5	medium to high	hydrophobic	~100 nm	medium to high
Hydrogel	casting, polymerization	0.005-2	low	>1	low	hydrophilic	~10 µm	low to medium
Paper	photolithography, printing	0.0003-0.0025	medium	>1	medium	amphiphilic	~200 µm	low

PDMS: Poly-Di-Methyl Siloxane, TPE: Thermoset Polyester, PMMA: Poly-Methyl Methacrylate, PS: Polystyrene, PC: Polycarbonate, PU: Polyurethane, PEGDA: Poly-Ethylene Glycol Diacrylate, COC: Cyclic-Olefin Copolymer

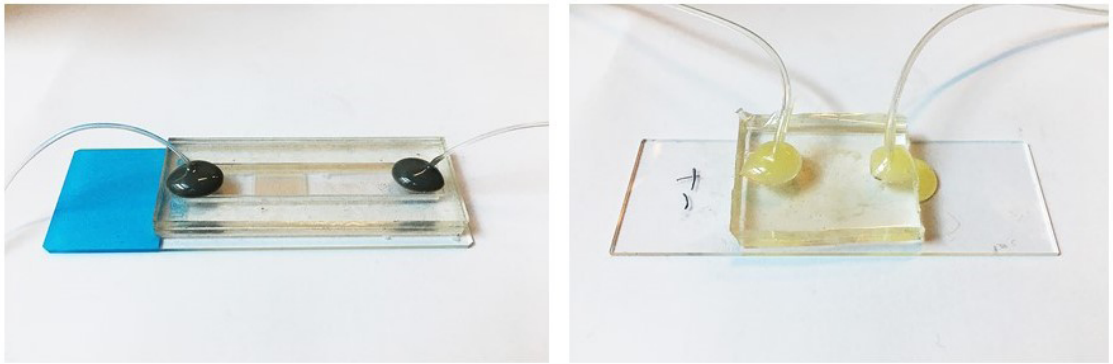

Figure 3. Two examples of microfluidic platforms. Left: A glass bottom and PMMA middle and top cover. In the channel, gold coated micro-arrays were designed for capturing cells and imaging. Right: A glass bottom and PDMS top layer, in the channel, micro posts were designed to filter out cells based on size.

Conventionally, microstructures can be manufactured by either casting, injection-molding or thermal-molding [39]. All of these methods are based on repeated use of a mold containing the prefabricated negative pattern of the final microstructure. A similar process is widely used for mass production of polymeric products, whereby the production costs of devices made of polymers are much affordable as compared to other materials. High aspect ratio and complex microstructures can be easily obtained from these materials [40]; however, the quality of the mold is critical.

The main limitations in the use of polymers are based on their relatively poor surface properties and compatibility problems with organic solvents. However, by understanding the concept of surface modification and unique surface properties (e.g. surface charge, hydrophobicity), functional surfaces can be obtained on different substrate materials by selecting suitable methods and reagents for modification [42]. A recent example is the application of a biodegradable-polymer as the base-material for the production of micro-devices with embedded microfluidic networks similar to microvascular systems, extending the application area to tissue engineering [43]. Similarly, Ogilvie et al. [44] have fabricated the channels using micro-milling and demonstrated that exposure of the polymers to an appropriate solvent vapor (chloroform for PMMA, cyclohexane for COC) reduced the surface roughness significantly. The re-flow of polymer when exposed to a solvent vapor has also been shown to reduce the surface roughness (from 200 nm to 15 nm). This novel surface treatment method may complement other rapid fabrication techniques for low-cost and high-quality microfluidic prototyping. In order to determine the best solvent mixture, Faghih and Sharp [45] have used solvent-based bonding with different solvent mixtures, curing times and temperatures. The results have shown that bonding strength and optical clarity have been improved when corona surface treatment was applied just before the solvent.

PDMS is probably the most preferred material in today's microfluidic devices due to several advantages. The first use of PDMS in microfluidic devices was described by Whitesides et al. (2001) [46]. PDMS has been shown to be a strikingly versatile material that enables a variety of new functions and applications in microfluidics. An interesting property of PDMS is its elasticity [37]. For example, multi-layer fluidic structures can be produced from PDMS; for this process, a small force that causes the deformation of a fluid channel is first applied for a short time, which can act as active valves or pumps [47]. Apparently, the most important issues in biological applications in microfluidic platforms are biocompatibility and cell viability. In this context, its low toxicity, high permeability to O_2 and CO_2, and excellent optical transparency, make PDMS a suitable material in the production of micro-channels for both proliferation and survival of the cells in optimum conditions and for technical observation [20]. In principle, PDMS is biocompatible (nontoxic to tissues and does not have harmful effects); it shows low autofluorescence and is inexpensive [48]. This material can be readily formed using PDMS molding; thus, there is no limit in the design of device [49]. On the other hand, PDMS can absorb small hydrophobic compounds [50]. Since

hydrophobic drugs and fluorescent molecules tend to spread to PDMS walls of microfluidic devices, the concentration decrease in solution may affect the accuracy and reliability of analyzes [51]. In other words, if PDMS absorbs and retains the active substance in test, it may not be possible to detect the potential toxicity due to the unexpected concentration decrease [49]. In a study in which four cardiac drugs were tested on the PDMS-based chip, and drug absorption of the PDMS material was measured by HPLC, the absorption was shown to be variable and time-dependent and not as determined by hydrophobicity as previously claimed. The presence of two commercially available lipophilic coatings and cells appeared to affect absorption [52]. However, the investigation of the adhesive properties of the cells on a chip showed that it had no negative effect on cellular conditions and cellular behavior. PDMS-based microfluidic systems have been shown to maintain the normal cell viability for several weeks. The biocompatibility of microfluidic systems based on PDMS, and other materials such as silicon oxide and glass, was investigated and showed good cell viability [53].

Some alternative thermoplastics including polystyrene, polycarbonate, and PMMA are also available, and these materials are both optically transparent and less absorbent than PDMS [54]. Besides obtaining the desired specifications with sufficient quality to ensure the functionality, a major key factor is the selection of appropriate fabrication method, considering the overall cost of the method, including equipment, operational, and production costs, as discussed by Guckenberger et al. [55]. In an effort to make microfluidic research more accessible and cost-effective, thermoplastic materials have gained interest as an alternative to conventional materials, particularly for commercial applications. Thermoplastic materials offer a number of advantages with respect to PDMS molding for rapid, low-cost microfluidics due to their better mechanical properties, hydrophilicity and versatility in design and fabrication [56]. Being composed of linear and branched molecules, the thermoplastic materials are durable against temperature and pressure changes and they resist structural breakdown. These materials have good physical and chemical characteristics (e.g., low electrical conductivity and high chemical stability), and they are cost effective for mass production. Thermoplastics can be softened and made to flow by applying heat and pressure. During cooling, the polymer hardens and without any chemical alteration it takes the shape of the container or mold. Low cost fabrication methods for high-throughput production of microfluidic systems can be successfully achieved using thermoplastics [57]. In addition, the laser cutting method is available for polystyrene and PMMA to create layers of microfluidic devices [58]. In a recent study, Day et al. presented injection molded open microfluidic inserts fabricated from polystyrene, to use with standard cell culture well plates that allow control of evaporation and enable high resolution imaging for cell cultures. These microfluidic inserts developed for cultures suitable for mass production and have been tested with samples including culture of primary testis cells from surgical patients [59].

Recent improvements in microfluidics, with advancements of soft-lithographic and micromachining techniques in the last couple of decades, have allowed the development of versatile platform technologies providing cost-, labor-, and time-efficient operation with small volumes of reagents and samples [60]. In a microfluidic platform integrated with micro-gas exchanger capable of imposing various physiological conditions, such as flow and hypoxia, in a closed system, an approach minimizing the cost of materials and complexity in design and manufacturing of microfluidic channels with precise oxygen tension control has been presented [61]. To benefit the advantages of different materials and fabrication methods, microfluidics systems are composed of hybrid materials [62]. A viable option especially for small hydrophobic systems is the use of glass-based systems that limit the absorption in cell-based assays [63]. The paper is generally highly preferred for commercial disposable biological assays, while it may be incorporated into a hybrid chip to take advantage of the above-mentioned materials. Thus, combinations can be created based on the desired functions [36].

Manufacturing techniques for microfluidics can be divided into three categories: subtractive (etching), additive (also known as 3D printing), and molding (also known as formative). Photolithography can be defined as the process of transferring specified geometric shapes on a mask to the surface of a silicon wafer. Digital manufacturing (additive or subtractive) is a very good case study for improving fabrication processes [64]. The state-of-the-art three-dimensional (3D) printing technology can offer a good alternative to the production of biochips [65], especially in conjunction with computer-aided designs. Since printing takes place layer-by-layer, sensors and mechanical parts can be inserted into the chip

at any point or position. Because of the low material cost, it is considered suitable for routine and practical use in drug R&D studies [49]. However, this technology is in its infancy and there are many aspects that need to be developed [66]. For instance, a 3D hollow micro glass structure is difficult to produce with 3D printing, because the materials used during production block the hollow parts. Kotz et al. (2019), developed a new technique to prevent clogging of hollow parts and with this new technique, they produced the glass chip using three-dimensional printers [67]. In the microfluidic device fabrication, it was suggested that the emerging use of advanced additive manufacturing technologies, including 3D-printing, may provide better opportunities in many applications. For example, Alapan et al. [62] have presented a novel hybrid manufacturing technique that combines 3D printing and laser micromachined lamination for complex 3D microfluidic device fabrication. In this hybrid technique, the assembly of 3D printed parts together with laser micromachined layers via lamination approach has been shown to offer a cost- and labor-efficient fabrication of standardized microfluidic discrete elements and modules. As an alternative to lithography, lamination-based fabrication approaches are becoming prevalent, in which a laser micromachined layer is sandwiched between a 3D printed layer and a glass surface, forming channels in micrometer scale (50–500 µm). Lamination method offers numerous advantages over lithography, including simple manual assembly, use of off-the-shelf materials, cost-efficient fabrication, disposable usage, and operation by minimally trained personnel.

For more details, we refer to several comprehensive reviews on specific topics including the state-of-the-art in micro and nanoscale devices with highlight to major platform technologies, namely microcantilevers, micro/nanopillars, and microfluidics [68], hydrogels [69], paper-based systems [70], and emerging terms such as "Pharm-Lab on a Chip" [71]. In addition, several fields including forensic sciences have adopted use of microfluidic devices, such as in the tests of controlled substances (e.g., methamphetamine, amphetamine, cocaine, and oxycodone) [72], in the estimation of the post-mortem interval using paper-based analytical devices at crime scenes [73], and as presumptive tests in fast, simple and simultaneous screening of four biological fluids at crime scenes [74].

Organ-on-a-Chip Systems and a Brief Overview on Applications in Toxicology

An "organ-on-a-chip" is a microfluidic device designed to obtain a functional unit in which the selected cells of the organ are cultured in a continuously-perfused, small-sized (micro or nano) chamber-system to simulate the physiological conditions [1]. An example of an organ-on-a-chip system is depicted in Figure 4. This system includes interconnected four compartments to model the four human tissues: intestine, liver, skin and kidney.

One of the major challenges for the pharmaceutical industry appears as the safety issues that become evident during the post-market phase. In recent years, the main safety concerns regarding drugs seems to be related with- but not limited to- cardiac, renal, and hepatic toxicities which can lead to serious adverse reactions, even to life-threatening consequences and death. Such an alarm may end up with the withdrawal of the drug. Therefore, it is extremely critical to identify the toxic effects in an early phase in order to prevent long-term consequences. For this purpose, the development of rapid and highly accurate toxicology assays and models has become a strategic issue for the pharmaceutical industry [75]. As depicted in Figure 1, prior to clinical trials, there are preliminary studies to establish a safe dose. In drug toxicity studies, the availability of microfluidic devices may provide a great advantage in these steps [76].

As described earlier, experimental animals have long been in use to provide a systemic view since they offer strictly-controlled models similar to human physiology; however, they have some limitations. Besides ethical concerns, several real-life examples, including drug safety issues, have shown that these models may not accurately reflect or predict the actual consequences in human, due to species differences. In need of a standardized platform that mimic the "human" within an "*in vitro*" environment, the researchers started to develop models with high-throughput characteristics, that are less time-consuming, more feasible, and also controllable.

In this context, the earlier applications adopted conventional cell culture models that are typically performed in two dimensions (2D) using flat cell culture plates; thus, 2D cell culture applications, although consisting of human cell lines, still could not completely simulate

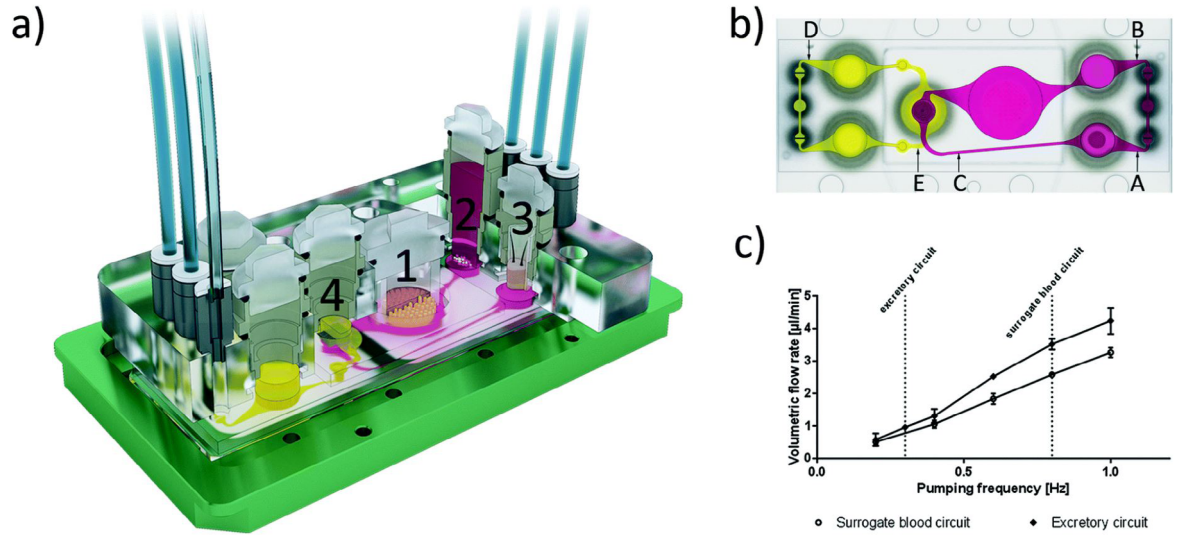

Figure 4. A multi-organ-on-a-chip device comprising four organs [17].
a) The 3D view of the device comprises two polycarbonate cover-plates, the PDMS-glass chip (footprint: 76 mm × 25 mm; height: 3 mm) accommodating a surrogate blood flow circuit (pink) and an excretory flow circuit (yellow). The culture compartments are numbered as (1)intestine, (2)liver, (3)skin, and (4)kidney. A central cross-section of each tissue culture compartment aligned along the interconnecting microchannel is depicted.
b) The fluid dynamics in device: Top view of the four-organ-chip layout illustrating the positions of three measuring spots (A, B and C) in the surrogate blood circuit and two spots (D, E) in the excretory circuit.
c) Average volumetric flow rate plotted against pumping frequency of the surrogate blood flow circuit and the excretory circuit.
Reprinted with permission from Ref[17] Copyright© 2015 The Royal Society of Chemistry.

the required complex nature of model tissue and disease processes [77]. This can be briefly explained by the fact that the 2D cell cultures lack the components which are available "*in vivo*", including the complex and information-rich environment with extracellular matrix components, mixed cell populations, diverse interactions, and cell-secreted factors [78].

In order to overcome this limitation, 3D culture systems that allow better reflection of the properties specific to complex tissues have been developed by means of tissue engineering [79]. In the last decade, the use of 3D culture models has been in rise, especially to increase the similarity to *in vivo*. Briefly, the 3D cell culture is created in an artificial environment where cells are allowed to grow and interact with their environment in three dimensions. The organization within 3D culture systems provides a more realistic and physiologically relevant micro-environment, allowing various cellular interactions [49,80]. In addition, creating 3D-printed *in vitro* tissue models is advantageous for well-preserved tissue functions and long-term culture; however, this option also comes with its own challenges, including the insurance to sustain regular liver cell functions for more than 30 days [81], high variability in the size of the organoids as well as the difficulty of retaining the cells in consistent positions in these structures for required durations [1].

To this end, 3D cell culture applications are of interest, since they help to produce more realistic models of organ-on-a-chip [82]. The environment in microfabricated systems mimics those found *in vivo*. Most importantly, the microfluidic devices can be designed to resemble the cellular structures and traffic inside the human body, chemical environment can be organized to mimic the complex and dynamic 3D network, the materials used for fabrication of microfluidic devices are often compatible with the required conditions and processes such as O_2 and CO_2 gas exchange, nutrition, moisture, removal of metabolites, thus enable better growth and proliferation of cells in 3D culture, the devices offer a multifaceted technology handling various processes such as culture, replenishment of medium, cell detachment, sampling, mixing, capture, and detection; moreover, the use of nanoliter volumes of samples and reagents makes the system very cost effective [83]. Kwak et al. developed microfluidic platforms using 2D

and 3D cancer cell cultures, and reported that while 2D models are easy to use and reproduce, 3D models have been preferred to eliminate the cellular difference in drug resistance resulting from differences in tumor microenvironment [84]. In an approach to investigate the efficacy of photodynamic therapy, Zuchowska and colleagues have used microfluidic culture models based on spheroids consisting of a co-culture of cancer and non-malignant breast cells [85], and also in 3D lung spheroid cultures [86].

In general, monitoring organ-on-a-chip systems appears to be a typical challenge. Zhang et al. have developed an automated modular physical, biochemical, and optical sensing platform, interfaced with a multi–organ-on-a-chip system. In an uninterrupted and automated manner, this platform monitors microenvironmental parameters (e.g., pH, O_2, temperature), measures soluble biomarkers via electrochemical immunobiosensors, and observes morphology using miniature microscopes. The system has been used to monitor acetaminophen-

Table 2. A brief overview of some microfluidics-related studies on toxicity/drug testing

Organs	Details	References
Liver	The decellularized liver matrix-based liver tumor-on-a-chip and its application for drug toxicity testing	Lu et al., 2018 [10]
	Investigation of drug interactions in encapsulated hepatocytes in 3D micro tissues	Li et al., 2014 [93]
	Characterization of toxicity of various compounds using liver co-culture and smart-scale analysis	Shintu et al., 2012 [94]
	Testing the effects of ethanol-induced toxicity on liver sections	Hattersley et al., 2011 [95]
	Investigation of drug metabolism using liver and intestinal sections	van Midwoud et al., 2010 [96]
	3D HepaTox Chip preparation for hepatotoxicity testing	Toh et al., 2009 [97]
Kidney	Screening drug-transporter interactions and toxicity in 3D microfluidic proximal tubule epithelial cells model	Vriend et al., 2018 [11]
	Exposure to nephrotoxic cisplatin in a microfluidic system of renal proximal tubular epithelial cells	Vormann et al., 2018 [12]
	Exposure to fluid flow to investigate nephrotoxicity and establish its function	Jang et al., 2013 [98]
	Testing the effects of drugs on a dynamic kidney microfluidic chip	Baudoin et al., 2007 [99]
Brain	Drug permeability test through blood-brain barrier	Yeon et al., 2012 [100]
	Permeability of atenolol, caffeine, cimetidine, hydroxyzine, prazosin, propranolol, trazodone tested in a model of the blood-brain barrier	Shayan et al., 2011 [101]
Heart	The *in vitro* effect of isoproterenol on electrically-stimulated cardiac microtissues (within heart-on-a-chip) was tested.	Agarwal et al., 2013 [102]
	A drug dose-response experiment was performed by applying epinephrine in a heart-on-a-chip design developed for *in vitro* cardiac contraction and pharmacological studies.	Grosberg et al., 2011 [15]
Lung	Modeling of the nasal epithelium for formaldehyde toxicity testing	Wang et al., 2014 [13]
	Modeling of disease functions by means of a chip undergoing cyclic mechanical stress	Huh et al., 2012 [19]
	The cellular response and resistance to anticancer drug were tested.	Siyan et al., 2009 [103]
Intestine	Creation of a microfluidic chip model to examine the gastrointestinal tract and estimate drug toxicity	Mahler et al., 2009 [90]
	Testing the permeability of the drug in the intestinal epithelial cell membrane by micro-hole trap	Yeon et al., 2009 [104]

induced organ toxicity in a liver-and-heart-on-a-chip platform and also liver-cancer-and-heart-on-a-chip platform challenged with doxorubicin [87].

The organ-on-a-chip systems developed for drug screening and development purposes and their main advantages over the conventional methods were summarized, and it has been emphasized that these platforms provide more accurate models closer to native tissues [88]. As shown in Table 2, we listed some organ-on-a-chip systems that display the expected outcomes, with promising results. The liver is the main organ where drugs are metabolized and is therefore a common target for drug-induced toxicity, presenting a hot-topic in this field. Since the liver is susceptible to a wide range of diseases, relevant systems to test the potential hepatotoxic xenobiotics are of highest interest [89]. Hepatic phenotypes and functionality are lost due to the rapid differentiation of 2D liver cell cultures, and 3D cell culture systems more accurately reflect physiology; therefore, various 3D culture strategies are still under development and in optimization phases. In many of these models, hepatocytes retain their phenotype for a long time. It also provides an opportunity to investigate the potential of newly developed chemicals to cause chronic hepatotoxicity. Mahler et al. (2009) have utilized a model of gastrointestinal tract organ-on-a-chip system to test the impact of oral acetaminophen overdose. As the concentration of acetaminophen increased, the levels of glutathione and liver cell viability were reduced, which indicate the organ-specific effects caused by the hepatotoxic metabolite of acetaminophen [90]. Another point is the complex interaction between hepatocytes and immune cells: In the future, the development of more integrated culture models to investigate immunotoxicity may also be possible [91].

Antibiotics can lead to several side effects, including nephrotoxicity and hepatotoxicity. Since the effects of antimicrobials on mammalian cells require extensive studies, as well as the urgent need for inexpensive, fast and accurate tools and techniques that can help in the discovery and development of new antimicrobial drugs, a viable tool is required. In this sense, microfluidic devices are considered to be an excellent option to facilitate the evaluation of antibiotic activity and focus on recent developments of microfluidic devices for rapid antibiotic susceptibility testing. Two microfluidic systems have been developed in order to facilitate the evaluation of the side effects of antibiotics and the toxicity of the drug on human tissues in the treatment of infections. The first one is a cell-on-a-chip system that provides cytotoxicity information in the testing of drug candidates (e.g., mechanism of action, dose-response). The other is an organ-on-a-chip system that provides pharmacokinetic and toxicological information required in drug development [92].

Another representative example is the respiratory system. The upper respiratory tract acts as the first line of defense against many air pollutants. Finger-like protrusions called cilia located on the mucous membrane are moved back and forth when irritated, and this coordinated movement is critical to help detoxify xenobiotics in exposure via inhalation. A model which simulates this specific protective mechanism, in which human nasal epithelial cells are integrated, has been used to evaluate the toxicity of formaldehyde in gas phase transmitted by air [13]. A lung-on-a-chip system was described in [105] is a microphysiological system that replicates the functional unit of the living human lung. The microdevice includes a poly(dimethysiloxane) membrane so that mechanical stretching can be applied to adherent cell layers mimicking human breathing. In this context, Hiemstra et al. have reviewed the current literature and suggested that in view of the rapid developments in 3D culture of primary epithelial cells, generation of lung epithelial cells from induced pluripotent stem cells and organ-on-a-chip technology, these state-of-the-art models designed for evaluation of inhaled toxicants is expected to offer an alternative or complementary to animal exposure studies [106].

Since organs function within an orchestration in the body, encompassing a vast complex of networks, the generated microfluidic systems are expected to simulate the physiological conditions. Organs in the human body are often interconnected by complex biological mechanisms. There is a strict communication between different organs and tissues by networks. Mimicking the biological mechanisms of the human body requires the development of a model that mimics multiorgan interactions. How multiple organs respond to drugs is an extremely critical issue that can affect the efficacy and toxicity of drugs. Multiple organ models allow the examination of the linkage between different organs to better evaluate the safety and efficacy of a compound [107]. A number of organ-specific toxicity models are available; however, drugs may interact with multiple tissues/organs in the body, causing a complex overall response [108].

In Table 3, we summarized some multiple-organ-on-a-chip examples that provide a snapshot of microfluidic platforms with promising results.

Similar to these examples, Oleaga et al. (2016) used a chip system comprising four organ systems (liver, heart, nerve and muscle) in which a continuous flow of a serum-free environment was achieved in order to evaluate multi-organ toxicity. The effects of electrical and mechanical responses to five drugs (doxorubicin, valproic acid, acetaminophen, 3-acetamidophenol and atorvastatin calcium) were observed in each compartment. It was concluded that the findings were consistent with the toxicity data in humans and animals. For example, doxorubicin has been shown to lead to a decrease in the frequency of cardiomyocytes. This is due to the toxicity caused by the metabolite of doxorubicin. When acetaminophen was applied to the system, there was a decrease in hepatocyte viability. This

Table 3. A snapshot of studies about multi-organ-on-a-chip systems.

Multi-Organ Applications	Drugs and Applications	References
Liver Heart (incl. a heart-only system)	- The cardiotoxic response to terfenadine has been shown in the system. - Another previously discovered proprietary small drug molecule that is transformed into a cardiotoxic metabolite has also been tested in the heart:liver system.	McAleer et al., 2019 [109]
Liver Intestine	The model describes the characterization of pharmacokinetic properties of acetaminophen.	Marin et al., 2019 [18]
Kidney Intestine	This intestine-kidney chip, containing co-culture of the intestinal and glomerular endothelial cells, provided an integrated, cost-effective platform for assessment of drug absorption-related nephrotoxicity *in vitro*. Consistent with clinical evidence, the nephrotoxicity of a selected drug (digoxin) has been shown to be altered via absorption by other drugs.	Li et al., 2017 [110]
Liver Intestine Skin Kidney	The four-organ-chip system has been reported to provide near-to- physiological fluid-to-tissue ratios. This is the first approach in a microfluidic system, to generate an absorption-distribution-metabolism-excretion (ADME) profile and repeated-dose systemic toxicity testing of drug candidates.	Maschmeyer et al., 2015 [17]
Liver Skin	The system supports two different culture modes: - tissue exposed to the fluid flow, - tissue shielded from underlying fluid flow by standard Transwell® cultures. Liver micro-tissues has been shown to exert sensitivity at different molecular levels to troglitazone.	Wagner et al., 2013 [111]
Liver Intestine (tumor)	The system correctly assays the overall digestive properties of oral anticancer agents (e.g., cyclophosphamide and tegafur). Anticancer activity and drug metabolism were tested.	Imura et al., 2012 [112]
Liver Brain (tumor)	The cytotoxicity of anticancer drugs, including temozolomide and ifosfamide, was tested.	Ma et al., 2012 [113]
Liver Bone marrow (tumor)	Anticancer drug (e.g., 5-FU) was tested in a microfluidic device based on a pharmacokinetics-pharmacodynamics model connected by fluid channels to test drug toxicity.	Sung et al., 2010 [114]
Liver Colon cancer Bone marrow cell line	Anticancer effects of 5-FU and tegafur were tested.	Sung and Shuler, 2009 [115]

system appears as the first pump-free organ-on-a-chip that can reflect the body's response to drugs for 14-days [116]. The critical importance of bioactivation was illustrated in a study. Li et al. (2018) developed a liver-kidney chip capable of effectively evaluating drug metabolism in the liver and conducted a nephrotoxicity study on this device. The active substances used in the experiment were identified as nephrotoxic, leading to changes in cell viability, LDH leakage and permeability of kidney cells to large protein molecules after biotransformation in the liver. Nephrotoxic responses after hepatic metabolism observed in the liver-kidney chip were similar to physiological responses in the clinic [117].

In a different perspective, a multi-organ microfluidic platform was established to recapitulate the entire brain metastasis (BM) process, and it was applied to the BM pathology research, especially blood-brain barrier (BBB) extravasation [118]. With synergistic use of the chip and traditional models, the researchers demonstrated that Aldo-keto reductase family 1 B10 (AKR1B10) was significantly elevated in lung cancer BM; in addition, the value of AKR1B10 as a diagnostic serum biomarker for lung cancer patients suffering from BM could be demonstrated. The role and mechanisms of AKR1B10 in BM that it promotes the extravasation of cancer cells through the BBB were also evaluated.

Besides their potential use in drug R&D, the microfluidic devices have been applied to detection or evaluation of other analytes including environmental pollutants, pesticides, and some toxins. Bovard et al. (2018) designed an acute and chronic toxicity study on a chip composed of lung and liver cells. The capacity of liver cells to metabolize and regulate their toxicity was assessed using aflatoxin B1 [107]. In a study by Jellali et al. (2018), the effects of two pesticides, namely DDT and permethrin on hepatocytes grown in biochips were investigated. Although their toxicity has been extensively studied, the molecular mechanisms, including the impact on liver where their detoxification occurs, and their metabolic effects are not clear. This study showed deterioration of time-dependent sugar/lipid homeostasis with DDT and permethrin. In addition, high doses of DDT have been shown to cause cell death, inflammatory response, and oxidative stress [119]. A recent application is a microfluidic paper-based analytical device with benzoquinone-mediated ***E. coli*** respiration method, that is suitable for practical use due to its simple operation, low cost and portability. Similarly, the pesticide residues in vegetable juices have been detected [120]. An *in vitro* analytical platform has been developed to investigate neurotoxic snake venom proteins rapidly with microfluidic high-resolution screening. In this device, 47 snake venoms were profiled using the acetylcholine binding protein to mimic the target of neurotoxic proteins, in particular nicotinic acetylcholine receptors [121].

As the development of nanomaterials increases, the nanotoxicologists face a major challenge in developing a model that can accurately mimic human physiology. In general, extrapolation of results from animal tests of nanomaterials is often a misrepresentation of clinical effects. ***In vitro*** experiments fail to control the exposure levels of nanomaterials and cannot take into account some physicochemical aspects, such as particle aggregation. Ashammakhi et al. (2020) have proposed that microphysiological systems, especially multiorgan-on-a-chip systems, which can be specifically designed to test the systemic toxicity, can be of use to evaluate the toxicity of nanomaterials [122]. The potential of microfluidic systems is evaluated for nanotoxicity research in various experiments. For example, in neuron-like-PC12 cells cultured in microfluidic devices, cytotoxic effects of surface-modified quantum dots have been demonstrated [123].

As described earlier, specific challenges, such as the demand to restrict the absorption of small hydrophobic molecules on the PDMS platform, also can lead to production of systems that meet the criteria. For example, Hirama et al. (2019) have recently produced a glass-based organ-on-a-chip and obtained a more stable flow compared to PDMS platforms, limiting the absorption of small hydrophobic molecules, and increasing cell adhesion. It was concluded that this glass chip could be used in cell-based assays to test small hydrophobic molecules [63].

However, organ-on-a-chip systems have not yet been utilized to validate toxicity profiles for approval of drugs, as well as in the assessment of carcinogenicity and reproductive toxicity. Thus, the comprehensive validation of the chips for chronic toxicity testing will be necessary to use this technology. Further information on innovative designs on the main technologies (self-organized spherical 3D human organoids, microfabricated 3D human organ chips, and 3D bio-printed human organ constructs) to mimic key properties of human organs are reviewed in detail [124].

Last but not least, especially in the last decade, the number of studies that apply commercial organ-on-a-chip platforms have increased along with the establishment of dedicated companies such as Emulate, CN Bio, TissUse, Mimetas, Insphero, Ascendance Bio, Kirkstall, Hurel, Synvivo, Axosim, and Nortis. The non-redundant list of microfluidic companies is available at https://ufluidix.com/circle/microfluidic-companies/ and https://www.fluidicmems.org/microfluidic-companies. As an example, for the evaluation of renal drug interactions with efflux transporters, Vriend et al. (2018) have used a platform suitable for medium to high-throughput screenings, consisting of 96 chips containing the most important renal drug transporters in an OrganoPlate® from Mimetas [11].

DISCUSSION

The rapid increase in the number of publications on microfluidic devices reflects the increasing interest of the scientific community. In this review, we provided a snapshot of the current applications in organ-on-a-chip systems combining 3D microstructures, multiple cells, and microfluidic connections, which were developed to mimic the desired organs as functional models in physiological micro-environments as a current application and highlighted for use in pharmacy, especially regarding examples in toxicology research.

The studies on this subject show that it can be possible to evaluate all organs of a human body, on-a-chip for toxicological and disease-related issues. The toxicological studies of multi-organ-on-a-chip systems will probably open a window to reveal some particular tissue-tissue interactions that can lead to particular mechanisms of toxicity. Regardless of the organ being imitated, the properties of tissue mainly depend on the source of the cells; thus, particular attention is crucial in the selection of the cell type according to the desired endpoint. These models are expected to provide in-depth understanding of the interactions between drugs and metabolites in organs in terms of efficacy and/or safety. Moreover, the multi-organ-on-a-chip systems can be more effectively used in ADME studies and provide an opportunity to improve the estimation of some properties of compounds in patients. The multi-organ-on-a-chip systems are expected to create a new paradigm for drug development by contributing to a better understanding of the dose-response relationships, the treatment failures in some patients or the detection of adverse reactions, supporting potential side effects and promoting the evaluation of pharmacokinetic/pharmacodynamic parameters.

Depending on the interactions between microfluidics, biosensors and tissue engineering; biomedical devices become more comprehensive and mimic the complex functions of diseased or damaged tissues and organs. Despite relatively limited biomedical applications of microfluidics *in vitro* or *ex vivo*, we may propose that in the near future microfluidic platforms will probably be more widely used in diagnostic and clinical settings such as the capturing of tumor cells in circulation.

Developing microfluidics from simple systems to complex systems, being part of groundbreaking and futuristic ideas, it is likely that studies on the chip will play a role in improving body on a chip development approaches [125]. The multidisciplinary feature of microfluidics requires continued coordination between engineering, physical, and biological sciences to achieve good efficiency [41]. As a result of the development of new production processes, organ-on-a-chip and multi-organ-on-a-chip, which are associated with a potential future reduction in manufacturing costs, will probably become efficient and provide standardized platforms for toxicity studies [49].

FUTURE PROSPECTS

The ultimate aim of the researchers is to switch from an organ-on-a-chip to a human-on-a-chip system. Human-on-a-chip system can combine the relationships of organs, blood distribution, and blood flow according to human physiology. These systems can simulate human metabolism, including the biotransformation of a drug, its therapeutic and toxic effects [126]. In future approaches; progress is expected to be made in areas such as developing new designs for micro systems, increasing research on organ systems on-chip, and identifying new cell resources and materials to support adaptation to medical needs in humans [127]. When combined with cells or biopsies collected from patients, these models can also be used as a tool for personalized-drug screening [125].

Considering the social impact of organ-on-a-chip technology is crucial for its future development. While existing technologies are still too expensive for widespread use, new steps are being taken. Downward price pres-

sure will lead to lower prices. Conventional *in vitro* and *in vivo* models will be replaced by these new preclinical technologies. The commercial interest in organ-on-a-chip technology is growing, and the market for this technology is estimated to reach six billion dollars in about 5 years [128].

The development of an efficient production process for the commercialization of chips is a situation that must be overcome. It is emphasized that wide-ranging cooperation between pharmaceutical companies can be effective in this issue [129]. Apparently, there is a need for standardization of models for each of the organs to be imitated for extensive organ-on-a-chip and multi-organ-on-a-chip applications. As microfluidic systems become readily available, researchers will not need to develop a specially crafted laboratory for each application. This will increase the industrial development of microfluidics [53].

In the coming years, we will probably discuss the use of microfluidic systems in many fields, such as the context of precision medicine; indeed, the "personalized organs-on-chips", designed to reflect the individual's physiology, may provide an integral solution to personalized treatment and prevention strategies [130].

References

1. S.N. Bhatia, D.E. Ingber, Microfluidic organs-on-chips, Nat. Biotechnol. 32 (2014) 760–772.
2. M.B. Esch, A.S.T. Smith, J.M. Prot, C. Oleaga, J.J. Hickman, M.L. Shuler, How multi-organ microdevices can help foster drug development, Adv. Drug Deliv. Rev. 69–70 (2014) 158–169.
3. C.M. Sakolish, M.B. Esch, J.J. Hickman, M.L. Shuler, G.J. Mahler, Modeling barrier tissues *in vitro*: Methods, achievements, and challenges, EBioMedicine. 5 (2016) 30–39.
4. J.D. Caplin, N.G. Granados, M.R. James, R. Montazami, N. Hashemi, Microfluidic organ-on-a-chip technology for advancement of drug development and toxicology, Adv. Healthc. Mater. 4 (2015) 1426–1450.
5. R. Greek, A. Menache, Systematic reviews of animal models: Methodology versus epistemology, Int. J. Med. Sci. 10 (2013) 206–221.
6. A. Skardal, T. Shupe, A. Atala, Organoid-on-a-chip and body-on-a-chip systems for drug screening and disease modeling, Drug Discov. Today. 21 (2016) 1399–1411.
7. L. Ewart, K. Fabre, A. Chakilam, Y. Dragan, D.B. Duignan, J. Eswaraka, J. Gan, P. Guzzie-Peck, M. Otieno, C.G. Jeong, D.A. Keller, S.M. de Morais, J.A. Phillips, W. Proctor, R. Sura, T. Van Vleet, D. Watson, Y. Will, D. Tagle, B. Berridge, Navigating tissue chips from development to dissemination: A pharmaceutical industry perspective, Exp. Biol. Med. 242 (2017) 1579–1585.
8. S. Ishida, Organs-on-a-chip: Current applications and consideration points for *in vitro* ADME-Tox studies, Drug Metab. Pharmacokinet. 33 (2018) 49–54.
9. H. Kimura, Y. Sakai, T. Fujii, Organ/body-on-a-chip based on microfluidic technology for drug discovery, Drug Metab. Pharmacokinet. 33 (2018) 43–48.
10. S. Lu, F. Cuzzucoli, J. Jiang, L.G. Liang, Y. Wang, M. Kong, X. Zhao, W. Cui, J. Li, S. Wang, Development of a biomimetic liver tumor-on-a-chip model based on decellularized liver matrix for toxicity testing, Lab Chip. 18 (2018) 3379–3392.
11. J. Vriend, T.T.G. Nieskens, M.K. Vormann, B.T. van den Berge, A. van den Heuvel, F.G.M. Russel, L. Suter-Dick, H.L. Lanz, P. Vulto, R. Masereeuw, M.J. Wilmer, Screening of drug-transporter interactions in a 3D microfluidic renal proximal tubule on a chip, AAPS J. 20 (2018) 87.
12. M.K. Vormann, L. Gijzen, S. Hutter, L. Boot, A. Nicolas, A. van den Heuvel, J. Vriend, C.P. Ng, T.T.G. Nieskens, V. van Duinen, B. de Wagenaar, R. Masereeuw, L. Suter-Dick, S.J. Trietsch, M. Wilmer, J. Joore, P. Vulto, H.L. Lanz, Nephrotoxicity and kidney transport assessment on 3D perfused proximal tubules, AAPS J. 20 (2018) 90.
13. W. Wang, Y. Yan, C.W. Li, H.M. Xia, S.S. Chao, D.Y. Wang, Z.P. Wang, Live human nasal epithelial cells (hNECs) on chip for *in vitro* testing of gaseous formaldehyde toxicity via airway delivery, Lab Chip. 14 (2014) 677–680.
14. L.M. Griep, F. Wolbers, B. de Wagenaar, P.M. ter Braak, B.B. Weksler, I.A. Romero, P.O. Couraud, I. Vermes, A.D. van der Meer, A. van den Berg, BBB on chip: microfluidic platform to mechanically and biochemically modulate blood-brain barrier function, Biomed. Microdevices. 15 (2013) 145–150.
15. A. Grosberg, P.W. Alford, M.L. McCain, K.K. Parker, Ensembles of engineered cardiac tissues for physiological and pharmacological study: Heart on a chip, Lab Chip. 11 (2011) 4165–4173.
16. G. Khanal, K. Chung, X. Solis-Wever, B. Johnson, D. Pappas, Ischemia/reperfusion injury of primary porcine cardiomyocytes in a low-shear microfluidic culture and analysis device, Analyst. 136 (2011) 3519–3526.
17. I. Maschmeyer, A.K. Lorenz, K. Schimek, T. Hasenberg, A.P. Ramme, J. Hübner, M. Lindner, C. Drewell, S. Bauer, A. Thomas, N.S. Sambo, F. Sonntag, R. Lauster, U. Marx, A four-organ-chip for interconnected long-term co-culture of human intestine, liver, skin and kidney equivalents, Lab Chip. 15 (2015) 2688–2699.
18. T.M. Marin, N. de Carvalho Indolfo, S.A. Rocco, F.L. Basei, M. de Carvalho, K. de Almeida Gonçalves, E. Pagani, Acetaminophen absorption and metabolism in an intestine/liver microphysiological system, Chem. Biol. Interact. 299 (2019) 59–76.
19. D. Huh, D.C. Leslie, B.D. Matthews, J.P. Fraser, S. Jurek, G.A. Hamilton, K.S. Thorneloe, M.A. McAlexander, D.E. Ingber, A human disease model of drug toxicity–induced pulmonary edema in a lung-on-a-chip microdevice, Sci. Transl. Med. 4 (2012) 159ra-147.
20. G.M. Whitesides, The origins and the future of microfluidics, Nature. 442 (2006) 368–373.
21. D. Mark, S. Haeberle, G. Roth, F. Von Stetten, R. Zengerle, Microfluidic lab-on-a-chip platforms: Requirements, characteristics and applications, Chem. Soc. Rev. 39 (2010) 1153–1182.
22. Y. Li, S. Wang, R. Huang, Z. Huang, B. Hu, W. Zheng, G. Yang, X. Jiang, Evaluation of the effect of the structure of bacterial cellulose on full thickness skin wound repair on a microfluidic chip, Biomacromolecules. 16 (2015) 780–789.

23. R.R.G. Soares, D. Ramadas, V. Chu, M.R. Aires-Barros, J.P. Conde, A.S. Viana, A.C. Cascalheira, An ultrarapid and regenerable microfluidic immunoassay coupled with integrated photosensors for point-of-use detection of ochratoxin A, Sensors Actuators B Chem. 235 (2016) 554–562.
24. F.E. Yigit, İ.İ. Bosgelmez, Emerging potential of microfluidic chips in the field of forensics. 3rd Reg. TIAFT Meet. Turkey, 18-20 Oct. 2018, 175-176.
25. W. Zhou, J. Le, Y. Chen, Y. Cai, Z. Hong, Y. Chai, Recent advances in microfluidic devices for bacteria and fungus research, TrAC Trends Anal. Chem. 112 (2019) 175–195.
26. K. İçöz, O. Mzava, Detection of proteins using nano magnetic particle accumulation-based signal amplification, Appl. Sci. 6 (2016) 394.
27. W. Huang, C.L. Chang, N.D. Brault, O. Gur, Z. Wang, S.I. Jalal, P.S. Low, T.L. Ratliff, R. Pili, C.A. Savran, Separation and dual detection of prostate cancer cells and protein biomarkers using a microchip device, Lab Chip. 17 (2017) 415–428.
28. D. Pekin, Y. Skhiri, J.C. Baret, D. Le Corre, L. Mazutis, C. Ben Salem, F. Millot, A. El Harrak, J.B. Hutchison, J.W. Larson, D.R. Link, P. Laurent-Puig, A.D. Griffiths, V. Taly, Quantitative and sensitive detection of rare mutations using droplet-based microfluidics, Lab Chip. 11 (2011) 2156-2166.
29. E.K. Sackmann, A.L. Fulton, D.J. Beebe, The present and future role of microfluidics in biomedical research, Nature. 507 (2014) 181–189.
30. X. Zhang, S.J. Haswell, Materials matter in microfluidic devices, MRS Bull. 31 (2006) 95–99.
31. X. Hou, Y.S. Zhang, G.T. Santiago, M.M. Alvarez, J. Ribas, S.J. Jonas, P.S. Weiss, A.M. Andrews, J. Aizenberg, A. Khademhosseini, Interplay between materials and microfluidics, Nat. Rev. Mater. 2 (2017) 17016.
32. E. Berthier, E.W.K. Young, D. Beebe, Engineers are from PDMS-land, Biologists are from Polystyrenia, Lab Chip. 12 (2012) 1224–1237.
33. S. Ahadian, R. Civitarese, D. Bannerman, M.H. Mohammadi, R. Lu, E. Wang, L. Davenport-Huyer, B. Lai, B. Zhang, Y. Zhao, S. Mandla, A. Korolj, M. Radisic, Organ-on-a-chip platforms: A convergence of advanced materials, cells, and microscale technologies, Adv. Healthc. Mater. 7 (2018) 1700506.
34. B. Zhang, A. Korolj, B.F.L. Lai, M. Radisic, Advances in organ-on-a-chip engineering, Nat. Rev. Mater. 3 (2018) 257–278.
35. J.B. Nielsen, R.L. Hanson, H.M. Almughamsi, C. Pang, T.R. Fish, A.T. Woolley, Microfluidics: Innovations in materials and their fabrication and functionalization, Anal. Chem. 92 (2020) 150–168.
36. K. Ren, J. Zhou, H. Wu, Materials for microfluidic chip fabrication, Acc. Chem. Res. 46 (2013) 2396–2406.
37. X. Liu, B. Lin, Materials Used in Microfluidic Devices, in: Encycl. Microfluid. Nanofluidics, Springer US, Boston, MA, 2014: pp. 1–5.
38. C.W. Tsao, Polymer Microfluidics: Simple, low-cost fabrication process bridging academic lab research to commercialized production, Micromachines. 7 (2016) 225.
39. H. Becker, L.E. Locascio, Polymer microfluidic devices, Talanta. 56 (2002) 267–287.
40. S.A. Soper, A.C. Henry, B. Vaidya, M. Galloway, M. Wabuyele, R.L. McCarley, Surface modification of polymer-based microfluidic devices, Anal. Chim. Acta. 470 (2002) 87–99.
41. P.N. Nge, C.I. Rogers, A.T. Woolley, Advances in microfluidic materials, functions, integration, and applications, Chem. Rev. 113 (2013) 2550–2583.
42. I. Wong, C.M. Ho, Surface molecular property modifications for poly(dimethylsiloxane) (PDMS) based microfluidic devices, Microfluid. Nanofluidics. 7 (2009) 291–306.
43. K.R. King, C.C.J. Wang, M.R. Kaazempur-Mofrad, J.P. Vacanti, J.T. Borenstein, Biodegradable microfluidics., Adv. Mater. 16 (2004) 2007–2012.
44. I.R.G. Ogilvie, V.J. Sieben, C.F.A. Floquet, R. Zmijan, M.C. Mowlem, H. Morgan, Reduction of surface roughness for optical quality microfluidic devices in PMMA and COC, J. Micromechanics Microengineering. 20 (2010) 065016.
45. M.M. Faghih, M.K. Sharp, Solvent-based bonding of PMMA–PMMA for microfluidic applications, Microsyst. Technol. 25 (2019) 3547–3558.
46. G.M. Whitesides, E. Ostuni, S. Takayama, X. Jiang, D.E. Ingber, Soft lithography in biology and biochemistry, Annu. Rev. Biomed. Eng. 3 (2001) 335–373.
47. T. Thorsen, S. Maerkl, S. Quake, Microfluidic large-scale integration, Science 298 (2002) 580–584.
48. M.C. Bélanger, Y. Marois, Hemocompatibility, biocompatibility, inflammatory and *in vivo* studies of primary reference materials low-density polyethylene and polydimethylsiloxane: A review, J. Biomed. Mater. Res. 58 (2001) 467–477.
49. D. Bovard, A. Iskandar, K. Luettich, J. Hoeng, M.C. Peitsch, Organs-on-a-chip: A new paradigm for toxicological assessment and preclinical drug development, Toxicol. Res. Appl. 1 (2017) 1–16.
50. M.W. Toepke, D.J. Beebe, PDMS absorption of small molecules and consequences in microfluidic applications, Lab Chip. 6 (2006) 1484–1486.
51. J.D. Wang, N.J. Douville, S. Takayama, M. ElSayed, Quantitative analysis of molecular absorption into PDMS microfluidic channels, Ann. Biomed. Eng. 40 (2012) 1862–1873.
52. B.J. van Meer, H. de Vries, K.S.A. Firth, J. van Weerd, L.G.J. Tertoolen, H.B.J. Karperien, P. Jonkheijm, C. Denning, A.P. IJzerman, C.L. Mummery, Small molecule absorption by PDMS in the context of drug response bioassays, Biochem. Biophys. Res. Commun. 482 (2017) 323–328.
53. A. Alrifaiy, O.A. Lindahl, K. Ramser, Polymer-based microfluidic devices for pharmacy, biology and tissue engineering, Polymers (Basel). 4 (2012) 1349–1398.
54. S. Halldorsson, E. Lucumi, R. Gómez-Sjöberg, R.M.T. Fleming, Advantages and challenges of microfluidic cell culture in polydimethylsiloxane devices, Biosens. Bioelectron. 63 (2015) 218–231.
55. D.J. Guckenberger, T.E. de Groot, A.M.D. Wan, D.J. Beebe, Micromilling: a method for ultra-rapid prototyping of plastic microfluidic devices, Lab Chip. 15 (2015) 2364–2378.
56. C. Matellan, A.E. del Río Hernández, Cost-effective rapid prototyping and assembly of poly(methyl methacrylate) microfluidic devices, Sci. Rep. 8 (2018) 6971.
57. E. Gencturk, S. Mutlu, K.O. Ulgen, Advances in microfluidic devices made from thermoplastics used in cell biology and analyses, Biomicrofluidics. 11 (2017) 051502.
58. S. Moon, U.A. Gurkan, J. Blander, W.W. Fawzi, S. Aboud, F. Mugusi, D.R. Kuritzkes, U. Demirci, Enumeration of CD4+ T-cells using a portable microchip count platform in tanzanian hiv-infected patients, PLoS One. 6 (2011) e21409.
59. J.H. Day, T.M. Nicholson, X. Su, T.L. van Neel, I. Clinton, A. Kothandapani, J. Lee, M.H. Greenberg, J.K. Amory, T.J. Walsh, C.H. Muller, O.E. Franco, C.R. Jefcoate, S.E. Crawford, J.S. Jorgensen, A.B. Theberge, Injection molded open microfluidic well plate inserts for user-friendly coculture and microscopy, Lab Chip. 20 (2020) 107–119.

60. J.C. Krebs, Y. Alapan, B.A. Dennstedt, G.D. Wera, U.A. Gurkan, Microfluidic processing of synovial fluid for cytological analysis, Biomed. Microdevices. 19 (2017) 20.
61. M. Kim, Y. Alapan, A. Adhikari, J.A. Little, U.A. Gurkan, Hypoxia-enhanced adhesion of red blood cells in microscale flow, Microcirculation 24 (2017) e12374.
62. Y. Alapan, M.N. Hasan, R. Shen, U.A. Gurkan, Three-dimensional printing based hybrid manufacturing of microfluidic devices, J. Nanotechnol. Eng. Med. 6(2) (2015) 021007.
63. H. Hirama, T. Satoh, S. Sugiura, K. Shin, R. Onuki-Nagasaki, T. Kanamori, T. Inoue, Glass-based organ-on-a-chip device for restricting small molecular absorption, J. Biosci. Bioeng. 127 (2019) 641–646.
64. A. Naderi, N. Bhattacharjee, A. Folch, Digital manufacturing for microfluidics, Annu. Rev. Biomed. Eng. 21 (2019) 325–364.
65. J.U. Lind, T.A. Busbee, A.D. Valentine, F.S. Pasqualini, H. Yuan, M. Yadid, S.J. Park, A. Kotikian, A.P. Nesmith, P.H. Campbell, J.J. Vlassak, J.A. Lewis, K.K. Parker, Instrumented cardiac microphysiological devices via multimaterial three-dimensional printing, Nat. Mater. 16 (2017) 303–308.
66. H.G. Yi, H. Lee, D.W. Cho, 3D Printing of organs-on-chips, Bioengineering. 4 (2017) 10.
67. F. Kotz, P. Risch, K. Arnold, S. Sevim, J. Puigmartí-Luis, A. Quick, M. Thiel, A. Hrynevich, P.D. Dalton, D. Helmer, B.E. Rapp, Fabrication of arbitrary three-dimensional suspended hollow microstructures in transparent fused silica glass, Nat. Commun. 10 (2019) 1439.
68. Y. Alapan, K. Icoz, U.A. Gurkan, Micro- and nanodevices integrated with biomolecular probes, Biotechnol. Adv. 33 (2015) 1727–1743.
69. H. Liu, Y. Wang, K. Cui, Y. Guo, X. Zhang, J. Qin, Advances in hydrogels in organoids and organs-on-a-chip, Adv. Mater. (2019) e1902042.
70. M. Kaljurand, Paper microzones as a route to greener analytical chemistry, Curr. Opin. Green Sustain. Chem. 19 (2019) 15–18.
71. Y. Ai, F. Zhang, C. Wang, R. Xie, Q. Liang, Recent progress in lab-on-a-chip for pharmaceutical analysis and pharmacological/toxicological test, TrAC Trends Anal. Chem. 117 (2019) 215–230.
72. S.C. Bell, R.D. Hanes, A microfluidic device for presumptive testing of controlled substances, J. Forensic Sci. 52 (2007) 884–888.
73. P.T. Garcia, E.F.M. Gabriel, G.S. Pessôa, J.C. Santos Júnior, P.C. Mollo Filho, R.B.F. Guidugli, N.F. Höehr, M.A.Z. Arruda, W.K.T. Coltro, Paper-based microfluidic devices on the crime scene: A simple tool for rapid estimation of post-mortem interval using vitreous humour, Anal. Chim. Acta. 974 (2017) 69–74.
74. R.L. Cromartie, A. Wardlow, G. Duncan, B.R. McCord, Development of a microfluidic device (µPADs) for forensic serological analysis, Anal. Methods. 11 (2019) 587–595.
75. S. Loiodice, A. Nogueira da Costa, F. Atienzar, Current trends in in silico, *in vitro* toxicology, and safety biomarkers in early drug development, Drug Chem. Toxicol. 42 (2019) 113–121.
76. A. Balijepalli, V. Sivaramakrishan, Organs-on-chips: research and commercial perspectives, Drug Discov. Today. 22 (2017) 397–403.
77. K.A. Fitzgerald, M. Malhotra, C.M. Curtin, F.J. O' Brien, C.M. O' Driscoll, Life in 3D is never flat: 3D models to optimise drug delivery, J. Control. Release. 215 (2015) 39–54.
78. B.M. Baker, C.S. Chen, Deconstructing the third dimension – how 3D culture microenvironments alter cellular cues, J. Cell Sci. 125 (2012) 3015–3024.
79. D. Loessner, C. Meinert, E. Kaemmerer, L.C. Martine, K. Yue, P.A. Levett, T.J. Klein, F.P.W. Melchels, A. Khademhosseini, D.W. Hutmacher, Functionalization, preparation and use of cell-laden gelatin methacryloyl–based hydrogels as modular tissue culture platforms, Nat. Protoc. 11 (2016) 727–746.
80. D. Antoni, H. Burckel, E. Josset, G. Noel, Three-dimensional cell culture: A breakthrough *in vivo*, Int. J. Mol. Sci. 16 (2015) 5517–5527.
81. X. Ma, J. Liu, W. Zhu, M. Tang, N. Lawrence, C. Yu, M. Gou, S. Chen, 3D bioprinting of functional tissue models for personalized drug screening and *in vitro* disease modeling, Adv. Drug Deliv. Rev. 132 (2018) 235–251.
82. H.J. Kim, D.E. Ingber, Gut-on-a-Chip microenvironment induces human intestinal cells to undergo villus differentiation, Integr. Biol. 5 (2013) 1130-1140.
83. N. Gupta, J.R. Liu, B. Patel, D.E. Solomon, B. Vaidya, V. Gupta, Microfluidics-based 3D cell culture models: Utility in novel drug discovery and delivery research, Bioeng. Transl. Med. 1 (2016) 63–81.
84. B. Kwak, A. Ozcelikkale, C.S. Shin, K. Park, B. Han, Simulation of complex transport of nanoparticles around a tumor using tumor-microenvironment-on-chip, J. Control. Release. 194 (2014) 157–167.
85. A. Zuchowska, K. Marciniak, U. Bazylinska, E. Jastrzebska, K.A. Wilk, Z. Brzozka, Different action of nanoencapsulated meso-tetraphenylporphyrin in breast spheroid co-culture and mono-culture under microfluidic conditions, Sensors Actuators B Chem. 275 (2018) 69–77.
86. A. Zuchowska, E. Jastrzebska, M. Chudy, A. Dybko, Z. Brzozka, 3D lung spheroid cultures for evaluation of photodynamic therapy (PDT) procedures in microfluidic Lab-on-a-Chip system, Anal. Chim. Acta. 990 (2017) 110–120.
87. Y.S. Zhang, J. Aleman, S.R. Shin, T. Kilic, D. Kim, S.A. Mousavi Shaegh, S. Massa, R. Riahi, S. Chae, N. Hu, H. Avci, W. Zhang, A. Silvestri, A. Sanati Nezhad, A. Manbohi, F. De Ferrari, A. Polini, G. Calzone, N. Shaikh, P. Alerasool, E. Budina, J. Kang, N. Bhise, J. Ribas, A. Pourmand, A. Skardal, T. Shupe, C.E. Bishop, M.R. Dokmeci, A. Atala, A. Khademhosseini, Multisensor-integrated organs-on-chips platform for automated and continual in situ monitoring of organoid behaviors, Proc. Natl. Acad. Sci. 114 (2017) E2293–E2302.
88. Y.A. Jodat, M.G. Kang, K. Kiaee, G.J. Kim, A.F.H. Martinez, A. Rosenkranz, H. Bae, S.R. Shin, Human-derived organ-on-a-chip for personalized drug development, Curr. Pharm. Des. 24 (2019) 5471–5486.
89. C.H. Beckwitt, A.M. Clark, S. Wheeler, D.L. Taylor, D.B. Stolz, L. Griffith, A. Wells, Liver 'organ on a chip,' Exp. Cell Res. 363 (2018) 15–25.
90. G.J. Mahler, M.B. Esch, R.P. Glahn, M.L. Shuler, Characterization of a gastrointestinal tract microscale cell culture analog used to predict drug toxicity, Biotechnol. Bioeng. 104 (2009) 193–205.
91. V.M. Lauschke, D.F.G. Hendriks, C.C. Bell, T.B. Andersson, M. Ingelman-Sundberg, Novel 3D culture systems for studies of human liver function and assessments of the hepatotoxicity of drugs and drug candidates, Chem. Res. Toxicol. 29 (2016) 1936–1955.
92. J. Dai, M. Hamon, S. Jambovane, Microfluidics for antibiotic susceptibility and toxicity testing, Bioengineering. 3 (2016) 25.
93. C.Y. Li, K.R. Stevens, R.E. Schwartz, B.S. Alejandro, J.H. Huang, S.N. Bhatia, Micropatterned cell–cell interactions enable functional encapsulation of primary hepatocytes in hydrogel microtissues, Tissue Eng. Part A. 20 (2014) 2200–2212.

94. L. Shintu, R. Baudoin, V. Navratil, J.M. Prot, C. Pontoizeau, M. Defernez, B.J. Blaise, C. Domange, A.R. Péry, P. Toulhoat, C. Legallais, C. Brochot, E. Leclerc, M.E. Dumas, Metabolomics-on-a-chip and predictive systems toxicology in microfluidic bioartificial organs, Anal. Chem. 84 (2012) 1840–1848.
95. S.M. Hattersley, J. Greenman, S.J. Haswell, Study of ethanol induced toxicity in liver explants using microfluidic devices, Biomed. Microdevices. 13 (2011) 1005–1014.
96. P.M. van Midwoud, M.T. Merema, E. Verpoorte, G.M.M. Groothuis, A microfluidic approach for *in vitro* assessment of interorgan interactions in drug metabolism using intestinal and liver slices, Lab Chip. 10 (2010) 2778–2786.
97. Y.C. Toh, T.C. Lim, D. Tai, G. Xiao, D. van Noort, H. Yu, A microfluidic 3D hepatocyte chip for drug toxicity testing, Lab Chip. 9 (2009) 2026–2035.
98. K.J. Jang, A.P. Mehr, G.A. Hamilton, L.A. McPartlin, S. Chung, K.Y. Suh, D.E. Ingber, Human kidney proximal tubule-on-a-chip for drug transport and nephrotoxicity assessment, Integr. Biol. 5 (2013) 1119–1129.
99. R. Baudoin, L. Griscom, M. Monge, C. Legallais, E. Leclerc, Development of a renal microchip for *in vitro* distal tubule models, Biotechnol. Prog. 23 (2007) 1245–1253.
100. J.H. Yeon, D. Na, K. Choi, S.W. Ryu, C. Choi, J.K. Park, Reliable permeability assay system in a microfluidic device mimicking cerebral vasculatures, Biomed. Microdevices. 14 (2012) 1141–1148.
101. G. Shayan, Y.S. Choi, E. V. Shusta, M.L. Shuler, K.H. Lee, Murine *in vitro* model of the blood–brain barrier for evaluating drug transport, Eur. J. Pharm. Sci. 42 (2011) 148–155.
102. A. Agarwal, J.A. Goss, A. Cho, M.L. McCain, K.K. Parker, Microfluidic heart on a chip for higher throughput pharmacological studies, Lab Chip. 13 (2013) 3599–3608.
103. W. Siyan, Y. Feng, Z. Lichuan, W. Jiarui, W. Yingyan, J. Li, L. Bingcheng, W. Qi, Application of microfluidic gradient chip in the analysis of lung cancer chemotherapy resistance, J. Pharm. Biomed. Anal. 49 (2009) 806–810.
104. J.H. Yeon, J.K. Park, Drug permeability assay using microhole-trapped cells in a microfluidic device, Anal. Chem. 81 (2009) 1944–1951.
105. D. Huh, A human breathing lung-on-a-chip, Ann. Am. Thorac. Soc. 12 (2015) S42–S44.
106. P.S. Hiemstra, G. Grootaers, A.M. van der Does, C.A.M. Krul, I.M. Kooter, Human lung epithelial cell cultures for analysis of inhaled toxicants: Lessons learned and future directions, Toxicol. Vitr. 47 (2018) 137–146.
107. D. Bovard, A. Sandoz, K. Luettich, S. Frentzel, A. Iskandar, D. Marescotti, K. Trivedi, E. Guedj, Q. Dutertre, M.C. Peitsch, J. Hoeng, A lung/liver-on-a-chip platform for acute and chronic toxicity studies, Lab Chip. 18 (2018) 3814–3829.
108. J.H. Sung, Y.I. Wang, N. Narasimhan Sriram, M. Jackson, C. Long, J.J. Hickman, M.L. Shuler, Recent advances in body-on-a-chip systems, Anal. Chem. 91 (2019) 330–351.
109. C.W. McAleer, A. Pointon, C.J. Long, R.L. Brighton, B.D. Wilkin, L.R. Bridges, N. Narasimhan Sriram, K. Fabre, R. McDougall, V.P. Muse, J.T. Mettetal, A. Srivastava, D. Williams, M.T. Schnepper, J.L. Roles, M.L. Shuler, J.J. Hickman, L. Ewart, On the potential of *in vitro* organ-chip models to define temporal pharmacokinetic-pharmacodynamic relationships, Sci. Rep. 9 (2019) 9619.
110. Z. Li, W. Su, Y. Zhu, T. Tao, D. Li, X. Peng, J. Qin, Drug absorption related nephrotoxicity assessment on an intestine-kidney chip, Biomicrofluidics. 11 (2017) 034114.
111. I. Wagner, E.M. Materne, S. Brincker, U. Süßbier, C. Frädrich, M. Busek, F. Sonntag, D.A. Sakharov, E. V. Trushkin, A.G. Tonevitsky, R. Lauster, U. Marx, A dynamic multi-organ-chip for long-term cultivation and substance testing proven by 3D human liver and skin tissue co-culture, Lab Chip. 13 (2013) 3538–3547.
112. Y. Imura, E. Yoshimura, K. Sato, Micro total bioassay system for oral drugs: Evaluation of gastrointestinal degradation, intestinal absorption, hepatic metabolism, and bioactivity, Anal. Sci. 28 (2012) 197–199.
113. L. Ma, J. Barker, C. Zhou, W. Li, J. Zhang, B. Lin, G. Foltz, J. Küblbeck, P. Honkakoski, Towards personalized medicine with a three-dimensional micro-scale perfusion-based two-chamber tissue model system, Biomaterials. 33 (2012) 4353–4361.
114. J.H. Sung, C. Kam, M.L. Shuler, A microfluidic device for a pharmacokinetic–pharmacodynamic (PK–PD) model on a chip, Lab Chip. 10 (2010) 446–455.
115. J.H. Sung, M.L. Shuler, A micro cell culture analog (μCCA) with 3-D hydrogel culture of multiple cell lines to assess metabolism-dependent cytotoxicity of anti-cancer drugs, Lab Chip. 9 (2009) 1385–1394.
116. C. Oleaga, C. Bernabini, A.S.T. Smith, B. Srinivasan, M. Jackson, W. McLamb, V. Platt, R. Bridges, Y. Cai, N. Santhanam, B. Berry, S. Najjar, N. Akanda, X. Guo, C. Martin, G. Ekman, M.B. Esch, J. Langer, G. Ouedraogo, J. Cotovio, L. Breton, M.L. Shuler, J.J. Hickman, Multi-Organ toxicity demonstration in a functional human *in vitro* system composed of four organs, Sci. Rep. 6 (2016) 20030.
117. Z. Li, L. Jiang, Y. Zhu, W. Su, C. Xu, T. Tao, Y. Shi, J. Qin, Assessment of hepatic metabolism-dependent nephrotoxicity on an organs-on-a-chip microdevice, Toxicol. Vitr. 46 (2018) 1–8.
118. W. Liu, J. Song, X. Du, Y. Zhou, Y. Li, R. Li, L. Lyu, Y. He, J. Hao, J. Ben, W. Wang, H. Shi, Q. Wang, AKR1B10 (Aldo-keto reductase family 1 B10) promotes brain metastasis of lung cancer cells in a multi-organ microfluidic chip model, Acta Biomater. 91 (2019) 195–208.
119. R. Jellali, P. Zeller, F. Gilard, A. Legendre, M.J. Fleury, S. Jacques, G. Tcherkez, E. Leclerc, Effects of DDT and permethrin on rat hepatocytes cultivated in microfluidic biochips: Metabolomics and gene expression study, Environ. Toxicol. Pharmacol. 59 (2018) 1–12.
120. J. Zhang, Z. Yang, Q. Liu, H. Liang, Electrochemical biotoxicity detection on a microfluidic paper-based analytical device via cellular respiratory inhibition, Talanta. 202 (2019) 384–391.
121. J. Slagboom, R.A. Otvos, F.C. Cardoso, J. Iyer, J.C. Visser, B.R. van Doodewaerd, R.J.R. McCleary, W.M.A. Niessen, G.W. Somsen, R.J. Lewis, R.M. Kini, A.B. Smit, N.R. Casewell, J. Kool, Neurotoxicity fingerprinting of venoms using on-line microfluidic AChBP profiling, Toxicon. 148 (2018) 213–222.
122. N. Ashammakhi, M.A. Darabi, B. Çelebi-Saltik, R. Tutar, M.C. Hartel, J. Lee, S.M. Hussein, M.J. Goudie, M.B. Cornelius, M.R. Dokmeci, A. Khademhosseini, Microphysiological systems: Next generation systems for assessing toxicity and therapeutic effects of nanomaterials, Small Methods. 4 (2020) 1900589.
123. S.K. Mahto, T.H. Yoon, S.W. Rhee, Cytotoxic effects of surface-modified quantum dots on neuron-like PC12 cells cultured inside microfluidic devices, BioChip J. 4 (2010) 82–88.
124. J. Park, I. Wetzel, D. Dréau, H. Cho, 3D Miniaturization of human organs for drug discovery, Adv. Healthc. Mater. 7 (2018) 1700551.

125. A. Perestrelo, A. Águas, A. Rainer, G. Forte, Microfluidic organ/body-on-a-chip devices at the convergence of biology and microengineering, Sensors. 15 (2015) 31142–31170.
126. G.J. Mahler, M.B. Esch, T. Stokol, J.J. Hickman, M.L. Shuler, Body-on-a-chip systems for animal-free toxicity testing, Altern. Lab. Anim. 44 (2016) 469–478.
127. F. Zheng, F. Fu, Y. Cheng, C. Wang, Y. Zhao, Z. Gu, Organ-on-a-chip systems: Microengineering to biomimic living systems, Small. 12 (2016) 2253–2282.
128. L.H.M. van de Burgwal, P. van Dorst, H. Viëtor, R. Luttge, E. Claassen, Hybrid business models for 'Organ-on-a-Chip' technology: The best of both worlds, PharmaNutrition. 6 (2018) 55–63.
129. T. Kanamori, S. Sugiura, Y. Sakai, Technical aspects of microphysiological systems (MPS) as a promising wet human- in-vivo simulator, Drug Metab. Pharmacokinet. 33 (2018) 40–42.
130. A. van den Berg, C.L. Mummery, R. Passier, A.D. van der Meer, Personalised organs-on-chips: functional testing for precision medicine, Lab Chip. 19 (2019) 198–205.

N. İdil et al. / Hacettepe J. Biol. & Chem., 2020, 48 (3), 265-274

Research Article

Hacettepe Journal of Biology and Chemistry

journal homepage: www.hjbc.hacettepe.edu.tr

A Retrospective Study on Urinary Tract Infection Agents Isolated from Children and Their Antibiotic Susceptibility

Çocuklardan İzole Edilen İdrar Yolu Enfeksiyonu Etkenlerinin ve Antibiyotik Duyarlılıklarının Retrospektif Değerlendirilmesi

Neslihan Idil[1*], Esra Deniz Candan[2], Abbas Yousefi Rad[3]

[1]Department of Biology, Faculty of Sciences, Hacettepe University, Ankara, Turkey.

[2]Vocational School of Health Services, Giresun University, Giresun, Turkey.

[3]Clinical Microbiology, Koru Hospitals, Yüksek İhtisas University, Ankara, Turkey.

ABSTRACT

Antibiotics are important agents in the treatment of urinary tract infection (UTI). However, the use of antibiotics is an important risk factor causing antibiotic resistance. Antibiotic inappropriate resistance is one of the most important problems of increased uropathogenic resistance, especially in pediatric urology. Deficiencies in empirical prescription practices can make this problem even worse. In this study, the demographic characteristics of pediatric patients, UTI agents, and antibiotic resistance of these agents were retrospectively evaluated by an automated system. The data from 719 UTI agents isolated from children were separately analyzed for four different age groups (0-2, 2-6, 6-12, and 12-17). The most commonly isolated infection agents were *Escherichia coli* (68.01%), *Klebsiella pneumoniae* (19.75%), *Klebsiella oxytoca* (3.34%), *Enterobacter cloacae* (2.23%), and *Pseudomonas aeruginosa* (1.95%). Among the age groups, 0-2 age group was quite diverse in terms of infection agents and antibiotic resistance values of these agents were significantly high in this group ($p<0.05$). Regarding the antibiotic resistance, the most noteworthy ones were the resistance against ampicillin (70.2%), amoxicillin-clavulanate (49.0%), cefixime (38.2%), and trimethoprim/sulfamethoxazole (37.1%). Our study indicated that children in 0-2 age group were under higher risk in terms of UTI agents and their antibiotic resistance but this risk was reduced with increasing age. Moreover, the ratio of girls with UTI was greater than that of boys within 0-2 age group. There was high resistance against cephalosporin, ampicillin, amoxicillin-clavulanate, and trimethoprim/sulfamethoxazole, whereas the resistance against carbapenem (imipenem, ertapenem and meropenem) was found to be low and there was no significant increase.

Key Words

Antibiotic resistance, *Escherichia coli*, pediatric urology, urinary tract infection.

ÖZ

Antibiyotikler idrar yolu enfeksiyonlarının tedavisinde önemli bir dayanak noktası olmasına rağmen, bilinçsiz kullanımları antibiyotik direncinin gelişimi için önemli bir risk faktörüdür. Antibiyotik direnci, özellikle çocuk ürolojisinde, artan üropatojen direncinin en önemli sorunlarından bir olarak karşımıza çıkmaktadır. Ampirik reçete uygulamalarındaki eksiklikler bu sorunu daha da kötüleştirmektedir. Bu çalışmada; pediatrik hastaların demografik özellikleri, idrar yolu enfeksiyonu etkenleri ve bu etkenlerin antibiyotik direnç durumları otomatize sistem ile retrospektif olarak değerlendirilmiştir. Çocuklardan izole edilen 719 idrar yolu enfeksiyonu etkeninden elde edilen veriler dört pediatrik yaş grubu (0-2 yaş, 2-6 yaş, 6-12 yaş ve 12-17 yaş) için ayrı ayrı analiz edildi. En sık izole edilen enfeksiyon etkenleri sırasıyla; *Escherichia coli* (%68.01), *Klebsiella pneumoniae* (%19.75), *Klebsiella oxytoca* (%3.34), *Enterobacter cloacae* (%2.23) ve *Pseudomonas aeruginosa* (%1,95) şeklindedir. Yaş grupları içerisinde; 0-2 yaş grubu enfeksiyon etkenleri açısından oldukça çeşitlilik göstermektedir. Aynı zamanda; bu grup içerisinde bu etkenlerin sahip olduğu antibiyotik dirençlerinin anlamlı bir şekilde yüksek olduğu saptanmıştır ($p<0.05$). Antibiyotik direnç durumları incelendiğinde; en dikkat çekici olanlar ampisilin (%70.2), amoksisilin-kluvanat (%49.0), cefixime (%38.2) ve trimetoprim/sülfametoksazol (%37.1)'e olan dirençlerdir. Çalışmamızda, 0-2 yaş grubu çocukların idrar yolu enfeksiyonu etkenleri ve bu etkenlerin sahip olduğu antibiyotik direnç açısından daha fazla risk altında oldukları, yaşın artışı ile bu riskin azaldığı ve grup içerisinde idrar yolu enfeksiyonu olan kız çocuklarının oranının daha fazla olması önemli bulunmuştur. Çalışmamızda; sefalosporinlere, ampisilin, amoksisilin-klavulanat ve trimetoprim/sülfametoksazol'e karşı yüksek direnç bulunurken karbapenem (imipenem, ertapenem, meropenem) direnci düşük düzeyde saptanmış olup anlamlı olabilecek bir artış olmadığı görülmüştür.

Anahtar Kelimeler

Antibiotik direnci, *Escherichia coli*, pediatrik üroloji, idrar yolu enfeksiyonu.

Article History: Received: Aug 25, 2019; Revised: Dec, 11 2019; Accepted: Mar 13, 2020; Available Online: May 3, 2020.

DOI: https://doi.org/10.15671/hjbc.639411

Correspondence to: N. Idil, Department of Biology, Faculty of Sciences, Hacettepe University, Ankara, Turkey.

E-Mail: nsurucu@hacettepe.edu.tr

INTRODUCTION

Urinary tract infection (UTI) is the infection of the kidneys, ureters, bladder, and urethra [1]. UTI is the second most common infection in childhood after respiratory tract infections [2,3]. UTI, one of the main bacterial infections causing acute morbidity, affects up to 180.000 children in the age of 6 (3-7% girls and 1-2% boys) according to a cumulative incidence of studies in the USA. In addition 12-30% of these children were also infected with recurrent fever infections [3]. Flora alterations, urinary tract anomalies, and immature immune system are among the causes of frequent infections in this age group [3, 4]. Renal damage induced by recurrent fever infection causes long-term complications including hypertension, renal dysfunction and chronic renal failure in later period [5, 6].Thus, detection of risk factors, development of appropriate diagnostic methods, and therefore a rapid and reliable treatment of UTI are of great importance to reduce the morbidity rate and related complications. The epidemiology of UTI varies depending on age and gender. Approximately 5% of girls and 2% of boys are infected with an UTI at least once [7]. The global prevalence in children under two is 7% [8]. In Infants, it is very difficult to identify the UTI symptoms. Clinicans should diagnose early to initiate appropriate treatment and prevent complications including hypertension and chronic kidney disease [9]. UTI frequently occurs in the adolescence period following the toilet training period after the infancy period [10]. Approximately, 60-90% of UTIs appear as pyelonephritis in the pre-school period. There is a risk of severe problems in patients who are not regularly treated or monitored for these infections [5,8].

Majority of UTI agents are *Escherichia coli*, *Klebsiella* species, and *Proteus* species, although these agents differ depending on age and gender as well as the catheterization and hospitalization. Moreover, *Enterococcus faecalis* and *Pseudomonas* species showing high antibiotic resistance are also found in patients who were hospitalized or have anatomic anomalies [11]. Antibiotic resistance of these microorganisms varies depending on their location. In recent years, antibiotic resistance has been an increasingly important problem worldwide in the first stage of treatment [12]. Antibiotics used for the treatment include trimethoprim/sulfamethoxazole (TMP/SMX), cephalosporins, and amoxicillin [13]. Regarding the childhood UTI, *E. coli*, which is a common infection agent, indicates increasing resistance against beta-lactam antibiotics and TMP/SMX. Widespread antibiotic use increases the antibiotic resistance and therefore, triggers the invention of new antibiotics to be used in the treatment of infections. This situation increases the economic burden in the healthcare sector and leads to an additional increase in antibiotic resistance.

Studies on the local epidemiology of common uropathogens and their antimicrobial resistance in UTI increase the treatment success and encourage a more efficient antibiotic use. Correspondingly, this study aims to retrospectively assess the demographic characteristics, infection agents, and antibiotic resistance in pediatric patients diagnosed between 2016 and 2018.

MATERIALS and METHODS

Demographic characteristics

719 UTI agent samples were included isolated from children in a private research hospital in Ankara, Turkey between January 2016 and September 2018. The isolated samples were classified according to their age, sex, microorganisms and antibiotic susceptibility. Patients were divided into different age groups which are 0-2, 2-6, 6-12 and 12-17.

Antimicrobial resistance

In this study, resistances of 719 UTI agent samples against 19 different antimicrobial agents were examined. These antimicrobial agents were, namely, ertapenem, imipenem, meropenem, amikacin, gentamicin, ampicillin, amoxicillin/clavulanate, piperacillin/tazobactam, ciprofloxacin, norfloxacin, cefixime, ceftazidime, ceftriaxone, cefepime, nitrofurantoin, TMP/SMX, fosfomycin, colistin, and aztreonam.

Identification of the microorganisms and determination of resistance against antimicrobial agents were carried out using an automated identification and susceptibility testing system (BD Phoenix TM, BD diagnostic systems Sparks, MD, USA). The obtained results from antimicrobial resistance testing were evaluated according to the European Committee on Antimicrobial Susceptibility Testing (EUCAST) criteria (EUCAST, version 1.3, 2011.) Infection agents and their resistance states were retrospectively evaluated.

Statistical Analysis

Data analysis was carried out using SPSS software (version 18.0, SPSS Inc. Chicago, IL). Descriptive values were

specified as number (n), percentage (%), and median. The normal distribution of variables was evaluated using visual (histogram and probability graphs) and analytical methods (Kolmogorov-Smirnov/Shapiro-Wilk tests). Pearson Chi-square test was used to compare the categorical variables. Continuous variables were compared using the Mann-Whitney U test because they did not match the normal distribution. Homogeneity of the groups was evaluated by the Levene's test and Tamhane's posthoc test. In this study, p values below 0.05 were considered as statistically significant.

RESULTS and DISCUSSION

Clinical results

A total of 719 UTI agent samples obtained from children in the age groups of 0-2 (n= 428), 2-6 (n= 153), 6-12 (n= 116), and 12-17 (n= 22) were examined. In total, 16 different UTI agents have been identified from these urine specimens (Table 1).

The most frequently isolated microorganism in UTI agent samples was *Escherichia coli* (68.01%); followed by *Klebsiella, Enterobacter, Pseudomonas*, and *Proteus* species. Particularly in recent years, the incidence of high resistant gram-negative bacteria in complicated urinary tract infections has increased. In accordance with our study, the most common UTI agents isolated from children in previous years were reported as *Escherichia coli*, followed by *Klebsiella*, *Proteus* species, *Enterococcus faecalis* and *Pseudomonas* species [11][14] *E. coli* is known as the most common bacteria (80%) in children with UTI [14]. *Klebsiella* spp., *Proteus* spp., *Enterobacter* spp., *Serratia* spp., *Pseudomonas* spp. and *Proteus mirabilis* are among the other most common infection agents [15].

UTI Risk Factors

The incidence of UTI varies according to age and gender. In childhood, UTI is one of the most common infectious diseases, especially in children under two years. The incidence of UTI in girls increases after the first age and the onset of toilet training. According to national and international studies, the majority of children with UTI are girls. The distribution of UTI agents according to age groups and gender status is presented in Table 2. Regarding age groups of patients, 428 (59.5%) patients are in 0-2 age, 153 (21.3%) in 2-6, 116 (16.1%) in 6-12, 22 (3.1%) in 12-17 age. In a similar study, 1021 (23.1%) patients were under one year of age, 1547 (34.9%) were 1-5, 1018 (22.9%) were 6-10, and 835 (19.1%) were over 10 years old [16]. Moreover, another similar study found that 0-2 age group patients constitute a percentage of 56.6% (n= 125), followed by 3-7 (26.2%, n=58) and 8-15 age groups (17.2%, n= 38) [17]. Therefore, UTI is observed more often in 0-2 age group compared to other age groups as supported by this study and several other studies.

Table 1. Descriptive information about the bacterial strains isolated from UTI agent samples in this study.

Infection agents	Number	Percentage (%)
Escherichia coli	489	68.01
Klebsiella pneumoniae	142	19.75
Klebsiella oxytoca	24	3.34
Enterobacter cloacae	16	2.23
Pseudomonas aeruginosa	14	1.95
Proteus vulgaris	7	0.97
Providencia rettgeri	7	0.97
Enterobacter aerogenes	5	0.70
Proteus mirabilis	5	0.70
Morganella morganii	3	0.42
Citrobacter freundii	2	0.28
Cedecea lapagei	1	0.14
Citrobacter koseri	1	0.14
Citrobacter werkmanii	1	0.14
Serratia fonticola	1	0.14
Serratia marcescens	1	0.14

Table 2. Distribution of UTI agents according to age and gender groups in children.

	Age (years)				Gender	
	0-2	2-6	6-12	12-17	Female	Male
E. coli	259	120	98	12	408	81
Klebsiella spp.	130	13	16	7	104	62
Enterobacter spp.	18	2	0	1	9	12
P. aeruginosa	7	4	2	1	9	5
Proteus spp.	5	7	0	0	9	3
M. morganii	3	0	0	0	1	2
Citrobacter spp.	2	1	0	1	3	1
P. rettgeri	2	5	0	0	6	1
Serratia spp.	2	0	0	0	1	1
C. lapagei	0	1	0	0	1	0
Total cases	428	153	116	22	551	168

In accordance with other studies in the literature, this study found that 76.6% of the patients were girls, whereas only 23.4% were boys. In similar studies, 61.5% and 51% of patients were girls in 0-17 and 0-15 age groups, respectively [16,17]. Thus, the ratio of girls with UTI was found to be higher than that of boys. Similarly, 77.7% of patients (n= 525) were girls and 59.1% (n= 399) were under the age of two [18]. Therefore, the findings of this study are consistent with previous studies regarding both age and gender groups in children.

In our study, the most common observed agent was *E. coli* (56.8%) across all age groups. However, the reproductive frequency in *E. coli* decreased as the age advanced in children. The situation was similar for not only in *Klebsiella,* but *Enterobacter* sp. and *P. aeroginosa.* However, contrary to our study, Topal (2018) found that the reproductive frequency in *E. coli* increased as the age advanced [17].

Antizbiotic resistance

UTI in childhood causes important problems that affect their life standard. Therefore, quick and appropriate diagnosis and suitable empirical therapy are crucial for children with UTI. The antimicrobial resistance of causative agents varies depending on many factors. In any empirical therapy, the causative agents and the lowest antimicrobial resistance for this microorganism should be considered. Low-spectrum antibiotics should be used as a priority in the treatment of UTI due to the reliability, cost-effectiveness, and development of antibiotic resistance. In children with a risk of increased antibiotic resistance, broad-spectrum antibiotics are used. Although amoxicillin, amoxicillin-clavulanate, cephalosporins, nitrofurantoin, and TMP-SMX are the most frequently prescribed drugs in the UTI treatment in Turkey, ampicillin and TMP-SMX are frequently used in empirical therapies [17].

In this study, among 19 different antimicrobial agents, the highest resistance rates were against ampicillin, amoxicillin/clavulanate, cephalosporin group, TMP/SMX, and aztreonam, respectively. The lowest resistance rates were observed against imipenem, amikacin, and meropenem, respectively (Figure 1). Resistance against these antibiotics was found to be mainly in *E. coli* and

Klebsiella strains (Table 3). Low resistance against amikacin and imipenem antibiotics was also reported and amikacin resistance was found to be quite low in *E. coli* and *Klebsiella* strains, in accordance with our study [17]. Aminoglycoside group antibiotics are one of the preferable antibiotics owing to low resistance in the treatment of UTI as supported by the findings of literature. Moreover, imipenem is noted as a broad-spectrum antibiotic that is less frequently used and it can be preferred in cases with resistance against other antibiotics.

Our study indicated that ampicillin (62.1%), amoxicillin-clavulanate (45.5%), and TMX/SMX (37.4%) resistance were quite high in *E. coli* strains. Also, there was a resistance development for TMP/SMX (37.1%) and therefore, this antibiotic could not be used in the first stage treatment. Similarly, it is also reported that resistance values against ampicillin and TMP-SMX were high [19]. In Turkey, resistance values of *E. coli* against TMP-SMX and ceftriaxone were reported to be 34.7%, 17%, respectively [20]. In another study, resistance rates of ampicillin and TMP-SMX in *E. coli* were 81.5% and 67%, respectively [21]. Kömürlüoğlu et al. (2017) reported that ampicillin and TMP-SMX resistance values were found to be 68.9% and 46.7% in *E. coli*, whereas the values were 100% and 38.6% in *Klebsiella* spp., respectively. Moreover, in a previous study in Turkey, ampicillin resistance values were 56.4%, 78.3%, and 42.3% in *E. coli*, *Klebsiella* species and *Proteus* species, respectively [21]. Consequently, a high rate of ampicillin resistance detected in our study was consistent with findings of previous literature.

The resistances against ampicillin (96.9%) and nitrofurantoin (76.4%) were also found to be relatively high in *Klebsiella* species which is the second most common agent isolated in this study (Table 3). A possible reason behind these high values is that these agents are frequently used in the empirical treatment of UTI in Turkey. However, dissimilar to other agents, the resistance against nitrofurantoin in *Klebsiella* species was quite noteworthy in our study. In addition, aztreonam resistance values were found to be 27.8% and 44.2% in *E. coli* and *Klebsiella* species, respectively.

There is also a high degree of resistance against cephalosporins, which are frequently used in the treatment of UTI. Our study found that there were resistances against cefixime, ceftriaxone and ceftazidime antibiotics which are among the 3rd generation cephalosporins, whereas there was resistance development against cefepime that is among the 4th generation cephalosporins (Table 3). The development of resistance against cefixime (38.2%), ceftriaxone (34.2%), ceftazidime (32.3%), and cefepime (29.6%) antibiotics over time can also be associated with the frequent use of these antibiotics. A previous study reported that resistance values of *E. coli* and *Klebsiella* spp. against cefixime, a common oral antibiotic, were 31.3% and 38.2%, respectively. The highest levels of cefepime resistance were in *Acinetobacter* (53.3%), *Klebsiella* spp. (36.9%), and *E. coli* (26.8%). Ceftazidime resistance values were 30.2% in *E. coli*, 39.4% in *Klebsiella* spp., 15.1% in *Pseudomonas*, 40.5% in *Enterobacter*, and 47.8% in *Acinetobacter*. The highest rates of ceftriaxone resistance were found in Enterobacter (47.1%), *Klebsiella* spp. (41.6%) and *E. coli* (31.5%) [14]. In

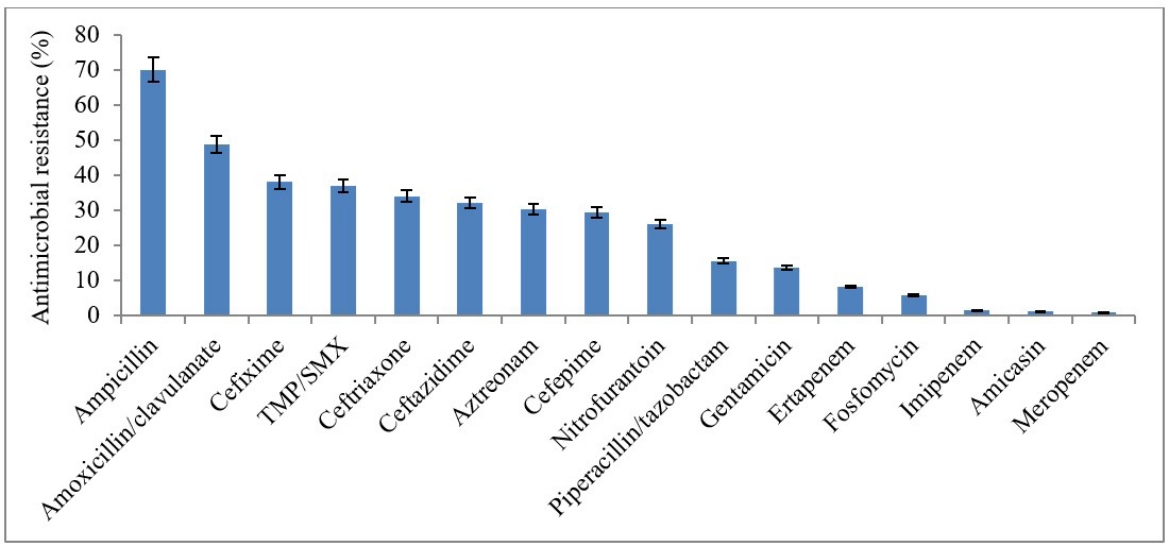

Figure 1. Antimicrobial resistance distribution of urinary tract infection agents isolated from children.

Table 3. Antimicrobial resistance distributions according to urinary tract infection factors isolated from children.

Antibiotic agents	*E. coli* (n= 486)	*Klebsiella* spp. (n=165)	*Enterobacter* spp. (n= 21)	*P. aeruginosa* (n= 14)	*Proteus* spp. (n= 12)	*M. morganii* (n= 3)	*Citrobacter* spp. (n= 4)	*P. rettgeri* (n= 7)	*Serratia* spp. (n= 2)	*C. lapagei* (n= 1)	Total
Ampicillin	302	160	15	13	8	3	1	2	1	0	505 (70.2)
Amoxicillin/clavulanate	221	85	18	13	2	3	3	6	1	0	352 (49)
Trimethoprim/sulfamethoxazole	182	72	0	10	2	1	0	0	0	0	267 (37.1)
Cefixime	158	81	11	14	4	2	1	2	1	1	275 (38.2)
Ceftazidime	147	78	5	0	0	0	0	0	1	1	232 (32.3)
Ceftriaxone	140	75	8	14	5	1	0	1	1	1	246 (34.2)
Cefepime	135	71	4	0	1	0	0	0	1	1	213 (29.6)
Aztreonam	135	73	6	2	0	0	0	0	1	1	218 (30.3)
Norfloxacin	102	43	0	9	0	1	0	0	0	1	156 (21.7)
Ciprofloxacin	72	21	0	0	0	1	0	0	0	1	95 (13.2)

Antibiotic agents	*E. coli* (n= 486)	*Klebsiella* spp. (n= 165)	*Enterobacter* spp. (n= 21)	*P. aeruginosa* (n= 14)	*Proteus spp.* (n= 12)	*M. morganii* *(n= 3)*	*Citrobacter* spp. (n= 4)	*P. rettgeri* (n= 7)	*Serratia* spp. (n= 2)	*C. lapagei* (n= 1)	Total
Gentamicin	43	50	1	0	4	0	0	0	1	0	99 (13.8)
Piperacillin/tazobac-tam	43	64	5	1	0	0	0	0	0	0	113 (15.7)
Ertapenem	12	23	6	14	1	0	0	2	1	1	60 (8.3)
Meropenem	4	3	0	1	0	0	0	0	0	0	8 (1.1)
Nitrofurantoin	4	126	17	14	12	3	2	7	2	1	188 (26.1)
Imipenem	2	4	0	1	4	0	0	0	0	0	11 (11.5)
Amicasin	2	5	0	0	0	0	0	0	1	1	9 (1.3)
Fosfomycin	2	17	3	13	2	3	0	2	1	0	43 (6)
Colistin	0	1	0	0	12	3	0	7	2	1	26 (2.6)

a study in Greece, the sensitivity to the 3rd generation cephalosporins (cefotaxime, ceftriaxone, and ceftazidime) in *E. coli* was found to be between 95.6% and 97.4%. In our study, the cephalosporin resistance was found to be slightly higher compared with the literature. It is thought that the expansion in the usage area of cephalosporin group antibiotics which are used as the first choice and the use of prophylactic antibiotics play an important role in the development of resistance against these antibiotics. Given the presence of increasing resistance, especially the 3rd generation cephalosporins should be used more selectively.

Carbapenems are the most preferred group for parenteral treatment of UTI caused by microorganisms which are resistant to many antibiotics. It was reported that carbapenem resistance was the highest in *E. coli* strains (18.5%) [21], whereas the carbapenem resistance was reported as 1.2% in a different study [22]. In the studyof Konca et al. [23], imipenem and ertapenem resistance values were found to be 4.1% and 4.6% in all gram-negative bacteria, respectively. In another study, meropenem resistance was 1.3%, imipenem resistance was 1.5%, and ertapenem resistance was 1.7% in *E. coli* [19]. In our study, the low rate of resistance against carbapenem group antibiotics was identified in *E. coli* and *Klebsiella* species. Carbapenem resistance was found to be quite low in accordance with other studies in the literature and there has been no significant increase in the resistance compared to previous studies.

In 0-2 age group, there were high levels of resistance against all of the tested antibiotics in this study (Figure 2). The highest resistance was against gentamicin (78.8%), whereas the lowest resistance was against imipenem (45.5%). Among the age groups, the lowest antibiotic resistance levels were found in 12-17 age group. In this group, the highest resistance was against meropenem (12.5%), whereas the lowest resistance was against ertapenem (1.7%). Antibiotic resistance values in the four different age groups (0-2, 2-6, 6-12, and 12-17) indicated a normal distribution except for 12-17 age group ($p=0.44$) but it was also evaluated as in a normal distribution. According to statistical analysis results, antibiotic resistance was significantly higher in 0-2 age group (Group 1), whereas in 12-17 age group (Group 4), the resistance was significantly lower than other age groups ($p<0.05$) (Table 4). UTI agents and antibiotic resistance were evaluated in children under two years old in a joint study comprising 18 pediatric nephrology centers from 10 European countries [24] Springer-Verlag Berlin Heidelberg. Knowledge of the distribution spectrum of causative organisms and their resistance patterns has become a core requirement for the rational and effective management of urinary tract infections. In the context of a prospective trial on the use of antibiotic prophylaxis in infants with underling kidney malformations, we conducted an online survey among paediatric nephrologists on positive urine cultures (July 2010–June 2012, which predominantly isolated *E. coli* strains and found that the highest antibiotic resistance values were against ampicillin, trimethoprim, cephalosporins and co-amoxiclav derivative antibiotics, in accordance with our study. Therefore, these resistance levels create a severe threat particularly for children not only in Turkey but also in the world.

In conclusion, ampicillin, cephalosporins, amoxicillin-clavulanate, and TMP/SMX should not be empirically commenced. In order to avert a rapid resistance development that is closely associated with widespread and inappropriate antibiotic use, the use of random antibiotics should be avoided and particularly the 3rd generation cephalosporins should be used more selectively. Although our data reflect only the results of patients admitted to a single hospital, classification of pathogens and determination of resistance rates against oral and parenteral antibiotics make our study valuable as it assesses the resistance patterns in patients.

References

1. R. Quigley, Diagnosis of urinary tract infections in children, Curr. Opin. Pediatr., 21 (2009) 194-198.
2. İ. Şahin, Ş. Öksüz, D. Kaya, İ. Şencan, A. Gülcan, Antibiotic susceptibility of uropathogenic gram negative rods isolated from inpatient and outpatient children, ANKEM Derg. 18 (2004) 101-104.
3. B. Becknell, M. Schober, L. Korbel, J.D. Spencer, The diagnosis, evaluation and treatment of acute and recurrent pediatric urinary tract infections, Expert Rev. Anti. Infect. Ther., 13 (2015) 81-90.
4. S. Swerkersson, U. Jodal, C. Åhrén, S. Hansson, Urinary tract infection in small outpatient children: The influence of age and gender on resistance to oral antimicrobials, Eur. J. Pediatr., 173 (2014) 1075-1081.
5. P. H.Conway, A.Cnaan, T. Zaoutis, B. V. Henry, R. W. Grundmeier, R. Keren, Recurrent urinary tract infections in children: Risk factors and association with prophylactic antimicrobials, J. Am. Med. Assoc., 298 (2007) 179-186.
6. N. Taneja, S. S. Chatterjee, M. Singh, S. Singh, M. Sharma, Pediatric urinary tract infections in a tertiary care center from north India, Indian J. Med. Res. 131 (2010) 101-105.

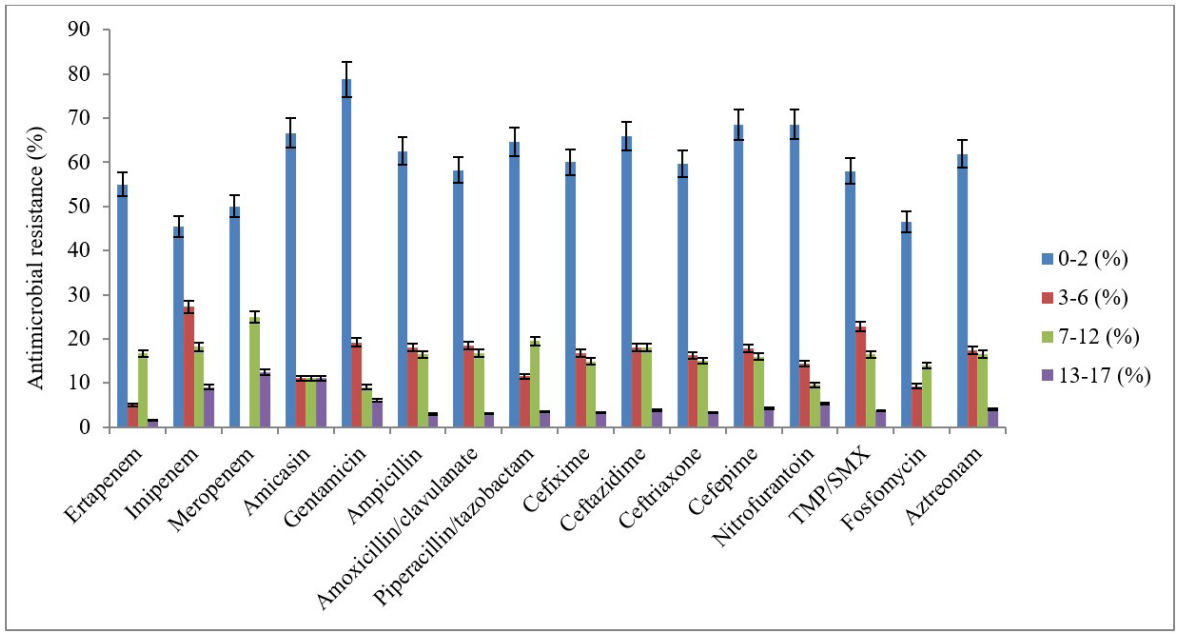

Figure 2. Comparison of antimicrobial resistance of urinary tract infection agents isolated from children with age groups.

Table 4. Statistical analysis of antibiotic resistance levels in four different age groups (Group 1: 0-2, Group 2: 2-6, Group 3: 6-12, and Group 4: 12-17).

(I) VAR00001		Mean Difference (I-J)	Std. Error	Significance	95% Confidence Interval	
					Lower Bound	Upper Bound
1.00	2.00	70.52632*	19.90999	.011	12.7880	128.2646
	3.00	73.31579*	19.75320	.008	15.8618	130.7698
	4.00	93.84211*	19.10285	.001	37.4724	150.2118
2.00	1.00	-70.52632*	19.90999	.011	-128.2646	-12.7880
	3.00	2.78947	7.67403	1.000	-18.5854	24.1644
	4.00	23.31579*	5.79835	.004	6.3200	40.3116
3.00	1.00	-73.31579*	19.75320	.008	-130.7698	-15.8618
	2.00	-2.78947	7.67403	1.000	-24.1644	18.5854
	4.00	20.52632*	5.23472	.005	5.2072	35.8454
4.00	1.00	-93.84211*	19.10285	.001	-150.2118	-37.4724
	2.00	-23.31579*	5.79835	.004	-40.3116	-6.3200
	3.00	-20.52632*	5.23472	.005	-35.8454	-5.2072

Note: * symbol indicates that the mean difference is significant at 0.05 level.

7. S. Habib, Highlights for management of a child with a urinary tract infection. Int. J. Pediatr., (2012).
8. N. Shaikh, N. E. Morone, J. E. Bost, M. H. Farrell, Prevalence of urinary tract infection in childhood: A meta-analysis, Pediatr. Infect. Dis. J., 27 (2008) 302-308.
9. M. Wennerström, S. Hansson, U. Jodal, E. Stokland, Primary and acquired renal scarring in boys and girls with urinary tract infection, J. Pediatr., 136 (2000) 30-34.
10. S. Hellerstein, J. S.Linebarger, Voiding dysfunction in pediatric patients, Clin. Pediatr. (Phila)., 42 (2003) 43-49.
11. A. M. Sefton, The impact of resistance on the management of urinary tract infections. Int. J. Antimicrob. Agents., 16 (2000) 489-491.
12. J.S. Stultz, C.D. Doern, E. Godbout, Antibiotic resistance in pediatric urinary tract infections. Curr. Infect. Dis. Rep., 18 (2016) 1-9.
13. Urinary tract infection: Clinical practice guideline for the diagnosis and management of the initial UTI in febrile infants and children 2 to 24 months- Amer. Acad. Pediat., 128 (2011) 595-610.
14. R.J. Gaspari, E. Dickson, J. Karlowsky, G. Doern, Antibiotic resistance trends in paediatric uropathogens, Int. J. Antimicrob. Agents, 26 (2005) 267-271.
15. F.A. Orrett, P.J. Brooks, E.G Richardson, S. Mohammed, Paediatric nosocomial urinary tract infection at a regional hospital, Int. Urol. Nephrol.,31 (1999) 173-179.
16. A. Kömürlüoğlu, K. Aykaç, Y. Özsürekçi, S. Tanir Başaranoğlu, A. Biçakçigil, Ü. Liste, B. Altun, B. Sancak, A. B. Cengiz, A. Kara, M. Ceyhan, Antibiotic resistance distribution of gram-negative urinary tract infectious agents: single center experience, Turkish J. Pediatr. Dis. (2017) 10-17.
17. Y. Topal, Çocuklarda idrar yolu enfeksiyonu: güncel veriler eşliğinde bir değerlendirme, Ortadoğu Tıp Derg., 10 (2018) 26-33.
18. R.H. Hanna-Wakim, S.T. Ghanem, M.W. El Helou, S.A. Khafaja, R.A. Shaker et al., Epidemiology and characteristics of urinary tract infections in children and adolescents, Front. Cell. Infect. Microbiol., 26 (2015) 5-45.
19. H.F. Shao, W.P. Wang, X.W. Zhang, Z.D. Li., Distribution and resistance trends of pathogens from urinary tract infections and impact on management, ZhonghuaNan Ke Xue 9 (2003) 690-696.
20. B. Çoban, N. Ülkü, H. Kaplan, B. Topal, H. Erdoğan, E. Baskin, Çocuklarda idrar yolu enfeksiyonu etkenleri ve antibiyotik dirençlerinin beş yillik değerlendirmesi, Turk Pediatr. Ars.49 (2014) 124-129.
21. R. Yılmaz, E. Karaaslan, M. Özçetin, B. Arslan, M. Kilinç, N. Ö. K. Çocuklarda idrar yolları enfeksiyonu etkenleri ve antibiyotik duyarlılıkları Agents of urinary tract infections in children and their antibiotic susceptibility, J. Contempor. Med., 2 (2012) 17-21.
22. C. Konca, M. Tekin, F. Uckardes, S. Akgun, H. Almis, I. H. Bucak, Y. Genc, M.Turgut, Antibacterial resistance patterns of pediatric community-acquired urinary infection: Overview. Pediatr. Int., 59 (2017) 309-315.
23. E. Mantadakis, E.K. Vouloumanou, M. Panopoulou, E. Tsouvala, A. Tsalkidis, A. Chatzimichael, M. E. Falagas, Susceptibility patterns of uropathogens identified in hospitalised children with community-acquired urinary tract infections in Thrace, Greece. J. Glob. Antimicrob. Resist., 3 (2015) 85-90.
24. I. Alberici, A. K. Bayazit, D. Drozdz, S. Emre, M. Fischbach, J. Harambat, A. Jankauskiene et al., Pathogens causing urinary tract infections in infants: a European overview by the ESCAPE study group, Eur. J. Pediatr., 174 (2015)783-90.

N.A. Kocakulak et al. / Hacettepe J. Biol. & Chem., 2020, 48 (3), 275-282

Research Article

Hacettepe Journal of Biology and Chemistry

journal homepage: www.hjbc.hacettepe.edu.tr

The Effects of Match Conditions on the Shaped Elements of Blood And Iron Level of Football Players

Futbolcularda Müsabaka Şartlarının Kanın Şekilli Elemanları ve Demir Düzeyine Etkisi

Neşe Akpınar Kocakulak[1*], Yahya Polat[2], Musa Karakükcü[3], Serdar Sucan[2], Çağrı Çelenk[2]

[1]Department of Sport Sciences, Faculty of Health Sciences, Izmir Democracy University, İzmir, Turkey.

[2]Faculty of Sports Science, Erciyes University, Kayseri, Turkey.

[3]Department of Pediatrics Hematology and Oncology, Faculty of Medicine, Erciyes University, Kayseri, Turkey.

ABSTRACT

The conditions of football match and intensive exercise changes the hematological parameters. It is also known that, endurance training causes "sports anemia" which is an athlete specific anemia type. The purpose of our study is to research the effects of pre-match and post-match on the shaped elements of blood and iron level of football players. The study group consisted of 12 volunteer male athletes who are playing football in Turkish A2 League for 'Erciyes Spor Kulübü'. The pulsations, systolic/diastolic blood pressures, vertical/long jumps and elasticity of participating football players are measured and their blood samples were taken before and after the football match. There were statistically significant differences between the values of erythrocyte, leukocyte, thrombocyte, iron and iron binding ($p<0.05$) whereas there weren't any significant differences between PCT (procalcitonin), RBC (red blood cell) and MCH (mean cell hemoglobin) levels ($p>0.05$) in football players before and after the match. According to our results, match conditions and intensive exercise cause serious changes in iron levels and shaped elements of blood. The blood samples which will be taken at the pre-season, mid-season and late-season periods in accordance with the frequencies specified in the current literature can be important to follow the individual blood profile standards of each football players.

Key Words
Hematology, endurance training, iron, performance.

ÖZ

Futbol maçı ve yoğun egzersiz koşulları hematolojik parametreleri değiştirebilmektedir. Dayanıklılık antrenmanlarının sporcuya özgü bir anemi türü olan "spor anemisine" neden olduğu da bilinmektedir. Çalışmamızın amacı, futbolcularda müsabaka şartlarının kanın şekilli elemanları ve demir seviyesi üzerindeki etkilerini araştırmaktır.Çalışma grubu Türkiye A2 Liginde ' Erciyes Spor Kulübü' futbol oynayan 12 gönüllü erkek sporcudan oluşturuldu. Katılan futbolcuların nabızları, sistolik/diyastolik kan basınçları, dikey/uzun sıçramaları ve esnekliği ölçülmüş ve kan örnekleri futbol maçından önce ve sonra alınmıştır. Eritrosit, lökosit, trombosit, demir ve demir bağlanması ($p <0.05$) değerleri arasında istatistiksel olarak anlamlı fark bulunurken, PCT (prokalsitonin), RBC (kırmızı kan hücresi) ve MCH (ortalama hücre hemoglobini) seviyeleri arasında müsabaka öncesi ve sonra anlamlı bir fark yoktu ($p> 0.05$). Sonuçlarımıza göre, maç koşulları ve yoğun egzersiz demir seviyelerinde ve kanın şekilli elemanlarında ciddi değişikliklere neden olmaktadır. Sezon öncesi, sezon ortası ve sezon sonu dönemlerinde mevcut literatürde belirtilen sıklıklara göre alınacak kan örnekleri, her futbolcunun bireysel kan profili standartlarının takibi için önemli olabilir.

Anahtar Kelimeler
Hematoloji, dayanıklılık eğitimi, demir, performans.

Article History: Received: Dec 25, 2019; Revised: Jan 20 2020; Accepted: Apr 23, 2020; Available Online: May 11, 2020.

DOI: https://doi.org/10.15671/hjbc.664347

Correspondence to: N.A. Kocakulak; Department of Sport Science ,Faculty of Health Sciences, İzmir Democracy University, İzmir, Turkey.

E-Mail: nese.kocakulak@idu.edu.tr

INTRODUCTION

Football (a.k.a. Soccer) is an intermittent and multidisciplinary team sport which involves intensively high and low exercises as well as requires a significant level of endurance. A football player usually wants to show his/her optimal performance during the football match via 150 to 200 powerful movements such as running, dribbling, jumping and tackling in a short span of time [1]. Football player optimal performance depends on many physical and physiological components at the same time the physical demands are also very significant in modern football. Besides technical skills, football also requires strength, agility and endurance. The aerobic capacity of football players cannot be compared with the aerobic capacity of endurance athletes such as long-distance runners, cross-country skiers and professional cyclists. Among the athletes who are playing ball games, football players show the highest maximum oxygen consumption per kilogram of their body weight [2] . Physical activity is an integral function of living systems. It affects many systems including the hematological parameters. Physical activity plays an important role in humans; people can regulate their physical and physiological balance as well as other body factors including hematological levels by adapting exercise habit or in other words cardiovascular activity. Despite being considered as physically normal and healthy, football players could face with homeostatic, biochemical and hematological changes in their results due to intense training, competitions and match-related psycho-physiological stress [3]. Exercising generally has positive effects on body functions, on the other hand, some adverse effects such as increase in hematocrit, blood flow velocity and plasma viscosity have been reported during post-exercise period [4]. In athletes, although the hematological changes derived from endurance training are usually not found clinically relevant and these changes fall within the defined reference range for general population, some difference can be observed. In addition to this, there are significant individual differences in pre-exercise period as well as in responses to the same physical stress. Knowing the reference range of football player's pre-match blood parameters could provide information regarding to the deviations in post-match or post-exercise [4]. For that reason, monitoring the hematological parameters is significant for the determination of imbalances that may potentially affect health status and performance of the football players during training and the season [5]. Hematological parameters are widely used and extremely cheap method for monitoring the athletes performance. In particular, RBC (Red Blood Cell) is an important parameter for evaluating the training efficiency [6]. Although there are several factors that affect aerobic capacity, the most important ones are oxygen transport for the skeletal muscles via cardiovascular system and the body oxygen consumption. These factors are frequently used as an index for evaluating the physical performance of football players. On the other hand, the efficient oxygen transport to the body tissues also related to the size of heart, blood volume and the amount of hemoglobin in the circulatory system [5]. In some of the studies, it is found that the erythrocyte counts, hemoglobin concentrations, mean corpuscular volume (MCV) and mean corpuscular hemoglobin concentration (MCHC) of athletes are lower than sedentary (non-athletes) whereas in some other studies it is found that there is slight increase or no difference between athletes and non-athletes [7-9]. These differences in the studies arise from variety of conditions such as intensity of the training, types of training, body mass index (BMI) and anthropometric characteristics of the athletes and different sport disciplines [3-7]. In recent years, the effects of training and physical exercise on the erythrocyte system have been a hot topic and most of the sport anemia studies are primarily centered on endurance training [3]. Decrease in the hematocrit, hemoglobin concentration and erythrocyte count due to endurance training is called sports anemia which is a special medical case seen in sportsmen and explained by plasma volume expansion frequently occurred during and after physical exercise [6-10]. It has been reported that many things can contribute to sports anemia such as plasma volume increase, exercise-induced oxidative stress, increased body temperature, acidosis, gastrointestinal bleeding, acute and chronic inflammation, and damage in red blood cells [11]. It has also been suggested that various exercise types cause changes in circulating numbers thrombocytes and leukocytes. It has been reported that the increase in leukocytes with exercise is similar to that seen during a bacterial infection [12-14].

The aim of this study is to investigate the changes in football players' blood parameters such as erythrocyte counts, hemoglobin, hematocrit, MCV and MCHV values, WBC, PLT, PCT, leukocytes, iron levels and iron binding capacity, before and after the football match.

MATERIALS and METHODS

Individuals and Exercise Protocol: The study group consisted of 12 volunteer male athletes who are playing football in Turkish A2 League for 'Erciyes Spor Kulübü' which is trying to be promoted to the upper league. The volunteers have average age of 19.08±0.36 years old, average height of 1.80±0.02 cm and average weight of 70.16±1.74kg. The study was approved by Erciyes University, Medical Faculty, Ethics Committee. Furthermore, all volunteers who participated in the study were provided with the informed consent form and the research study started after receiving the necessary permits from the relevant university.

Exercise Program: From the male athletes who are playing football in Turkish A2 League for 'Erciyes Spor Kulübü' which is trying to be promoted to the upper league were taken before and immediately after the match pulse, systolic diastolic blood pressure, flexibility, vertical park, long jump measurements and blood samples.

Peripheral Blood Sampling and Analysis: Participating football players' blood samples were taken before and immediately after the match and mixed with 2 ml EDTA in tubes. The samples were sent to the analysis by barcoding within 30 minutes after being taken to ensure that they were not hemolyzed and clotted.These samples (Cell-DYN 3500R (Abbott)) and total iron binding capacity values (Beckman Coulter Unicel DXC 800) were examined in Erciyes University, Central Laboratories.

Statistical Analysis: After the normal distribution compliance of the data was tested the statistical evaluation was done by paired t-test. Significance level was determined as '0.05'. Data were presented with mean±standard deviation.

RESULTS

The characteristics of participating football players and their pulsation, systolic/diastolic blood pressure, vertical/long jump and elasticity values are given in Table I.

DISCUSSION

Match conditions can lead both physiological and metabolic changes in the athletes body. Therefore, the relationship between athletic performance, heavy exercise, physiological and hematological changes must be well known [15]. Football players best performance which they try to show during the football match, depends on many physiological factors and among them the blood parameters have importance. The type and intensity of exercise as well as match conditions, trauma, and stress affect hematological parameters [16,17]. Acute changes in various blood parameters can be seen a few hours of after training. Hemoconcentration which occurred due to sweat loss and fluid shifts in interstitial spaces, is considered to be an important mechanism of changes arise from exercising [18]. Some studies have shown that regular exercise training increases total hemoglobin, red blood cell count and oxygen carrying capacity whereas

Table 1. Physical and Physiological Characteristics of Football Players.

Variables	Group	n	X±Sx	t	P
Pulsation (pulse/min)	Pre-test	12	75.83±3.86	-4.356	0.001**
	Post-test	12	93.75±3.36		
Systolic blood pressure (mmHg)	Pre-test	12	116.25±2.43	2.014	0.069
	Post-test	12	102.42±5.22		
Diastolic blood pressure (mmHg)	Pre-test	12	70.25±3.43	0.227	0.825**
	Post-test	12	68.50±7.00		
Elasticity (cm)	Pre-test	12	15.83±2.00	-3.932	0.002
	Post-test	12	24.25±1.20		
Vertical jump (cm)	Pre-test	12	36.58±1.53	-5.501	0.000***
	Post-test	12	43.42±1.20		
Long jump (cm)	Pre-test	12	222.00±5.40	-0.319	0.755
	Post-test	12	223.83±6.34		

*p<0.05, **p<0.01, ***p<001

Table 2. Comparison of Erythrocyte Values Before and After the Football Match.

Variables	Group	n	X±Sx	t	P
HGB (Hemoglobin)	Pre-test	12	14.925±1.1917	4.094	.002**
	Post-test	12	14.5250±1.15532		
RBC (Erythrocyte)	Pre-test	12	5.1100±.27736	1.795	0.100
	Post-test	12	5.0058±.33069		
HCT (Hematocrit)	Pre-test	12	47.192±3.1303	4.977	0.000***
	Post-test	12	45.0333±3.15719		
MCV (Mean Corpuscular Volume)	Pre-test	12	91.658±5.5049	13.001	0.000***
	Post-test	12	89.5083±5.51815		
MCH (Mean Corpuscular Hemoglobin)	Pre-test	12	29.017±2.2898	1.246	0.239
	Post-test	12	28.9000±2.25630		
MCHC (Mean Corpuscular Hemoglobin Concentration)	Pre-test	12	31.625±.7362	-4.759	0.001**
	Post-test	12	32.2417±.73045		
RDW (Red Cell Distribution Width)	Pre-test	12	14.108±1.0596	9.916	0.000***
	Post-test	12	13.6833±.95806		
HDW (Hemoglobin Concentration Distribution Width)	Pre-test	12	2.6825±.13903	-2.778	0.018*
	Post-test	12	2.7308±.15774		

*p<0.05, **p<0.01, ***p<001

In Erythrocytes; when the pre-match and post-match values are compared, it is observed that there was a decrease in HGB, HCT, MCV and RDW values whereas there was an increase in MCHC and HDW values (p<0.05). On the other hand, there wasn't any difference in RBC and MCH values (p>0.05).

some studies have shown that endurance exercises are useful for blood volume when performed with stretching exercises [5-19].

On the other hand, there are also some studies that indicate heavy endurance exercises are also responsible for the formation of the sports anemia [18]. A potential problem is highlighted in the literature by emphasizing that 12% of the selected footballers have iron depletion, 10% of them have iron deficiency and 6% of them have iron depletion anemia [20]. In our study, when the pre-match and post-match measurement of the football players are compared, it is found out that there was a decrease in their iron levels because of the heavy match conditions (p <0.05). While the absorption of Fe in the body is made in the intestines, the non-absorbed part is excreted through the feces, urine and sweat, in addition to this small amount of Fe is lost via hair and nail growth. Insufficient iron uptake, weak iron absorption, increase in body temperature, gastrointestinal bleeding and red blood cell destruction in other words intravenous hemolysis triggers iron deficiency in athletes [18,19]. It is stated that, hemolysis is increased by the use of athletic shoes which do not have running and shock absorbing functions, on hard grounds that increase soil reaction power, incorrect running techniques and the old erythrocytes in the circulation [11]. The resulting iron deficiency is thought to be caused by defective thermoregulation, intravenous hemolysis, hematuria, sweating, low iron intake or weak intestinal absorption which are developed because of the match conditions. Malcovati et al. [21] observed seasonal hematological parameters and iron levels of elite football players in their study. Although football players' iron levels are showed a different course during the season, they were peaked in the middle of the season and fall with high stress towards the end of the season. This situation shows similarity with our study. On the other hand, the study of Banfi et al. about elite rugby athletes indicated that the iron levels of the athletes remained constant during the season [14]. This situation does not resemble our study. In our study, when we compare pre-match and post-match measurements of the participating football players, we found out that their total iron binding capacity (TIBC) increased after the match (p <0.05) and we think that this increase occurred due to the decrease of iron level throughout the exercise.

Erythrocytes plays an important role in meeting the increased oxygen demand during the exercise [21].

Table 3. Comparison of Thrombocyte Values Before and After the Football Match.

Variables	Group	n	X±Sx	t	P
PLT	Pre-test	12	239.91±11.81	-2.977	0.013
	Post-test	12	265.33±14.41		
MPV	Pre-test	12	7.16±0.14	6.535	0.000***
	Post-test	12	7.58±0.15		
PCT	Pre-test	12	0.18±0.01	-1.086	0.301
	Post-test	12	0.19±0.01		
PDW	Pre-test	12	41.64±1.06	3.365	0.006
	Post-test	12	39.47±1.15		

*p<0.05, **p<0.01, ***p<001

In Thrombocytes; when the pre-match and post-match values are compared, it is observed that there was an increase in PLT and MPV (respectively 239,91±265,33 and 7,16±7,58) whereas there was a decrease in PDW (41,64± 39,47) (p<0.05). On the other hand, there wasn't any difference in PCT values (p>0.05).

Our study showed that HCT (hematocrit), MCV (mean hemoglobin volume), MCH (mean erythrocyte hemoglobin), CH (erythrocyte hemoglobin) and RDW (erythrocyte distribution width) values are decreased compared to pre-match (p <0.05). Hemoglobin is the protein which carries oxygen from respiratory organs to tissues and carries carbon dioxide and protons from tissues to respiratory organs. Because of the critical role of hemoglobin in oxygen transport, sports hematology has been rapidly advancing in recent years and has been identified as a subgroup in athletic health. Hematocrit is significant for the measurement of hemoglobin and erythrocytes in the blood. It is indicated that, decreased hemoglobin and hematocrit values during intense exercise or competitive periods are a well-defined adaptation (characteristics) of sportsmen and professional football players [2] . Hematocrit, MCV, MCH values decrease in intensive anemias but some of the studies indicate that if the body loses water especially in submaximal exercises, the hematocrit value increases due to increased plasma volume with decreased fluid [21]. In some of the studies, hematologic findings of the athletes were examined for 3 years and it is found out that decrease of the erythrocyte, hemoglobin and hematocrit values are maximizing at the end of competition [22]. In addition, Halson et al. [23] prepared a training program for the participating athletes, in which athletes did normal workout for 2 weeks followed by intensive workout for 4 weeks; after the examination of the findings, it is observed that the erythrocyte and hemoglobin parameters showed rhythmic and insignificant declines in the first, second and third weeks whereas they showed regular and meaningful increases in fourth, fifth and sixth weeks. It has been reported that acute swimming exercise decreases ratios of erythrocytes, Hb and Hct in rats compared to pre-swimming values. Banfi et al. [14] have examined the hematological parameters of elite rugby players during a season and stated that hemoglobin and hematocrit values are increased in the first half of the season whereas they decreased towards the end of season; to sum up they recorded two different outcomes for the first and second half of the season. Fallon et al. [24] stated that intensive sportive competition and severe efforts are the sign of hemoglobin and hematocrit reduction. Similar statements made by Rietjens and et al. for cyclists, Schumacher et al. for triathlon and Malcovati et al. for football [20,25,26,]. Therefore, data obtained from the academic literature supports our study and it is thought that decrease of hemoglobin and hematocrit values in erythrocyte parameters are caused by the increased concentration due to maximal exercise, stress, changing metabolic activity and iron deficiency caused by exercise. Also, in our study, we found that there was a decrease in erythrocyte values immediately after the match compared to pre-match values but it was not found to be significant according to p value. Some studies stated that regular and moderate exercises reduce risk of infection compared to sedentary life (non-sportive life) whereas some other studies indicate that prolonged and heavy exercises increases the risk of infection. It is significant to know that how density, duration and type of exercise affect the immune function of body. The changes in the immune function which trigged by exercise can occur both acutely and in the long term [5]. Acute immune response to the exercise is temporary and it can fade away if the person stops or decreases the exercise. Exercises also increase the catecholamine concentration and growth hormo-

Table 4. Comparison of Leukocyte Values Before and After the Football Match.

Variables	Group	n	X±Sx	t	P
WBC (White Blood Cell) (μ/L)	Pre-test	12	6.15±0.33	-5.675	0.000***
	Post-test	12	13.18±1.19		
NE% (Neutrophil)	Pre-test	12	52.10±2.21	-10.211	0.000***
	Post-test	12	80.58±1.70		
EO% (Eosinophil)	Pre-test	12	1.93±0.24	6.241	0.000***
	Post-test	12	0.40±0.05		
LY% (Lymphocyte)	Pre-test	12	35.92±1.86	9.366	0.000***
	Post-test	12	13.56±1.49		
BA% (Basophil)	Pre-test	12	0.49±0.06	4.442	0.000***
	Post-test	12	0.22±0.03		
MO% (Monocyte)	Pre-test	12	7.22±0.43	4.906	0.000**
	Post-test	12	4.44±0.36		

*p<0.05, **p<0.01, ***p<001

According to Table VI, there are statistically significant difference between the pre-match and post-match WBC, NE%, EO%, LY%, BA% and MO% levels of the leukocyte values (p<0.05). When the pre-match and post-match values are compared, it is observed that there was an increase in WBC (6,15±13,18) and NE% (52,10±80,58) whereas there was a decrease in EO%, LY%, BA% and MO% levels (respectively 1,93±0,40, 35,92±13,56, 0,49±0,22 and 7,22±4,44).

ne. These hormones increase the neutrophil in blood due to exercise-induced stress. Some studies show that high cortisol levels are observed after intensive exercise [7]. In our study, Leukocyte (WBC) and Neutrophil values increased immediately after the match compared to the pre-match values but there was a decrease in Eosinophil, Basophil, Lymphocyte and Monocyte values (p<0.005) compared to pre-match values. Neutrophils, Eosinophils, Basophils, Lymphocytes and Monocytes are important leukocytes which are responsible for the defense of the organism. It is stated that, after the strenuous exercise, granulocytes in other words the total WBC percentages increase. It is indicated that, some of the changes in blood parameters (such as hematocrit and RBC counts) returned to resting levels short after the exercise is over, on the other hand some of them lasted for almost 12 hours. Lymphocytes have receptors that sense various stress hormones [21]. It has been reported that leukocyte and lymphocyte amounts in long-term training are not different from resting sedentary people, but maximal exercises lead to leukocytosis and lymphocytosis in both trained and sedentary people, while submaximal exercises cause leukocytosis and lymphocytosis in sedentary without any change in trained people [27]. Moreover, it is stated that WBC activation is closely related to type and level of exercise as well as the athletes' athletic capacity [27]. Neutrophils, Eosinophils, Basophils, Lymphocytes, Monocytes are important leukocytes responsible for the organism defense. Heavy metal overload and stress cause excessive release of the adrenal gland hormones such as adrenaline and cortisone. These hormones negatively affect the production and functions of leukocytes as well as suppress the thymus. Stress stimulates the sympathetic nervous system and stimulated sympathetic nervous system suppresses the immune system. Parasympathetic nervous system controls activities such as resting, relaxing, sleeping, regenerating and curing (regulation) that support the immune system. If this body balance fails in favor of the sympathetic system, the immune system may become worn out due to a constant drive and alarm condition and may suffer from malfunction [28]. Neutrophils are particularly interesting as they increase susceptibility to the infections. In aerobic exercises, the risk of bacterial infection is higher than the anaerobic exercises. In their studies, Heisterberg et al. [29] particularly emphasized the significance of two periods in the performance optimization of professional football players. The first one is the pre-season preparation period. This period usually involves high-intensity endurance training and heavy-resistance exercise training that increases certain immune parameters. The second period is the end of the season. At this period, it has been emphasized that physical constraints are more evident because as the time pass critical indicators such as MCH, MCHC, MCV and hematocrit have been deviated compared to their pre-season values and adverse changes in immune defenses. For that reason,

Table 5. Comparison of Total Iron Binding Capacity Values Before and After the Football Match.

Variables	Group	n	X±Sx	t	P
Fe (Iron)	Pre-test	12	119.92±47.927	3.087	0.010*
	Post-test	12	86.0833±24.32155		
TIBC (Total Iron Binding Capacity)	Pre-test	12	373.75±29.453	-3.273	0.007**
	Post-test	12	383.0000±28.46050		

*p<0.05, **p<0.01, ***p<001

When the pre-match and post-match iron levels and iron binding capacities are compared, it is found out that the iron levels were decreasing (119,92±86,0833) whereas the free iron binding capacity was increasing (373,75±383,0000) compared to the pre-match values (p <0.05).

the coaches and the physical staff must be extra cautious when programming the training schedule for the season [30]. Differences in blood parameters can occur as a result of changes in intensity and type of competition and training.

In conclusion, in our study, it is found out that, at the end of the season, blood samples taken from professional football players who were playing in promotion group, immediately after the match showed significant changes in the shaped element of blood and iron levels compared to the pre-match values. The blood samples which will be taken at the pre-season, mid-season and late-season periods in accordance with the frequencies specified in the current literature can be important to follow the individual blood profile standards of each football players. At the same time, we believe that the blood samples can contribute to the monitoring of elite soccer players' high physical strain and overload as well as following their performance, and ensure early intervention to the deviations.

References

1. D. Draganidis, A. Chatzinikolaou, A.Z. Jamurtas, J. Carlos Barbero, D. Tsoukas, A.S. Theodorou, K. Margonis, Y. Michailidis, A. Avloniti, A. Theodorou, A. Kambas, I. Fatouros, The time-frame of acute resistance exercise effects on football skill performance: The impact of exercise intensity, J. Spor. Sci., 31(2013) 714-722.
2. M.F. Heisterberg, J. Fahrenkrug, P. Krustrup, A. Storskov, Kjaer, J. L. Andersen, Extensive monitoring through multiple blood samples ın professional soccer players, J. Strength. Cond. Res., 27 (2013) 1260-1271.
3. G. Banfi, P.Morelli, Relation between values of haemoglobin, erythrocytes and reticulocytes and bady mass index in elite athletes of different sports disciplines, Int. Jnl. Lab. Hem., 29 (2007) 484-485.
4. R.S. Ajmani, J.L.Fleg, A.A. Demehin, J.G. Wright, F. O'Connor, J.M. Heim, E.Tarien, J.M.Rifkind, Oxidative stress and hemorheological changes induced by acute treadmill exercise, Clin. Hemorheol. Microcirc., 28 (2003) 29-40.
5. E. Varamenti, Z. Nikolovski, M.I. Elgingo, A.Z. Jamurtas, M. Cardinale, Training-ınduced variations in haematological and biochemical variables in adolescent athletes of arab origin throughout an entire athletic season, J. Hum. Kinet., 64 (2018) 123-135.
6. J. Malczewska-Lenczowska, D. Sitkowski, J. Orysiak, A. Pokrywka, Z. Szygula,Total haemoglobin mass, blood volume and morphological indices among athletes from different sport disciplines, Arch. Med. Sci., 9 (2013) 780-787.
7. A.S.R.Silva, V. Santhiago, M. Papoti, C.A. Gobatto, Hematological parameters and anaerobic threshold in Brazillian soccer players throught a training program, Int. Jnl. Lab. Hem., 30 (2008) 158-166.
8. T. Mashiko, T. Umeda, S. Nakaji, K. Sugawara, Effects of exercise on the physical condition of college rugb players during summer training camp, Br J Sport Med, 38 (2004) 186-190.
9. G. Lippi, F. Schena, G.L. Salvagno, R. Aloe, G.Banfi, G.C. Guidi, Foot-strike haemolysis after a 60-km ultramarathon, Blood Transfus, 10 (2012) 377-383.
10. M. Gleeson, A.K. Blannin, D.A. Sewell, R. Cave, Short-term changes in the blood leukocyte and platelet count following different durations of high-intensity treadmill running, J. Spor. Sci. 13 (1995) 115-123.
11. G.G. Wardyna, S.I. Rennarda, S.K. Brusnahanb, T.R. McGuirec, M. L. Carlsona, L. M. Smithd, S. McGranaghana, J. G. Sharpb, Effects of exercise on hematological parameters, circulating side population cells, and cytokines, Experimen. Hematology, 36 (2008) 216-223.
12. V.Cinar, R.Mogulkoç, A.K. Baltaci, Calcium supplementation and 4-week exercise on blood parameters of athletes at rest and exhaustion, Biol. Trace Elem. Res., 134 (2010) 130-135.
13. M.N. Sawka, V.A. Convertino, E.R. Eichner, S.M. Schnieder, A.J. Young, Blood volume: importance and adaptations to exercise training, environmental stresses, and trauma/ sickness, Med. Sci. Spor. Exerc., 32 (2000) 332-348.
14. G. Banfi, M. Del Fabbro, C. Mauri, M.M. Corsi, G. Melegati, Haematological parameters in elite rugby players during a competitive season, Clin. Lab. Haem., 28 (2006) 183-188.
15. S. Meister, K. Aus der Fünten, T. Meyer, Repeated monitoring of blood parameters for evaluating strain and overload in elite football players: is it justified?, J. Spor. Sci., 32 (2014) 1328-1331.

16. M. Hu, W. Lin, Effects of exercise training on red blood cell production: ımplications for anemia, Acta Haematol., 127 (2012) 156-164.
17. S.M Ostojic, Z. Ahmetovic, Weekly training volume and hematological status in female top-level athletes of different sports, J. Spor. Med. Phys. Fitness, 48 (2008) 398-403.
18. S.F. Clark, Iron deficiency anemia, Nutr. Clin. Pract., 23 (2008) 128-141.
19. S.M. Ostojic, Z. Ahmetovic, Indicators of iron status in elite soccer players during the sports season. International J. Labor. Hematol., 31 (2009) 447-52.
20. L. Malcovati, C. Pascutto, M. Cazzola, Hematologic passport for athletes competing in endurance sports: a feasibility study, Haematologica, 88 (2003) 570-581.
21. D.J. Shaskey, G.A. Gren, Sports haematology, Sports Med, 29(2000) 27-38.
22. Y.O. Schumacher, D. Grathwohl, J.M. Barturen, M. Wollenweber, L. Heinrich, A. Schmid, G. Huber, J. Keul, Haemoglobin, haematocrit and red blood cell indices in elite cyclists. Are the control values for blood testing valid?, Int. J. Spor. Med., 21 (2000) 380-385.
23. S.L Halson, G.I. Lnacaster, A.E. Jeukendrup, M. Gleeson, İmmunological responses to overreaching in cyclists, Med. Sci. Spor. Exerc., 35 (2003) 854-86.
24. K.E Fallon, G. Sivyer, K. Sivyer, A. Dare, Changes in haematological parameters and iron metabolism associated with a 1600 kilometre ultramarathon, Br. J. Spor. Med., 33 (1999) 27-32.
25. G.J. Rietjens, H. Kuipers, F. Hartgens, H.A. Keizer, Red blood cell profile of elite olympic distance triathletes. A three-year follow-up, Int. J. Spor. Med., 23 (2002) 391-396.
26. Y.O. Schumacher, R. Jankovits, D. Bültermann, A. Schmid, A. Berg, Hematological indices in elite cyclists, Scand. J. Med Sci Sports, 12 (2002) 301-308.
27. M. Gleeson, C. Williams, Intense exercise training and immune function, Nestle Nutr. Inst. Workshop Ser., 76 (2013) 39-50.
28. S. Meister, O. Faude, T. Ammann, R. Schnittker, T. Meyer, Indicators for high physical strain and overload in elite football players, Scand. J. Med. Sci. Spor., 23 (2013) 156-163.
29. M.F. Heisterberg, J. Fahrenkrug, J.L. Andersen, Multiple blood samples in elite soccer players. Is it worthwhile?, J. Spor. Sci., 13 (2014) 1324-1327.
30. S. Reinke, T. Karhause, W. Doehner, W. Taylor, K. Hottenrott, G.N. Duda, P. Reinke, H.D. Volk, S.D. Anker , The ınfluence of recovery and training phases on body composition, peripheral vascular function and ımmune system of professional soccer, Players. PLoS One, 4 (2019) e4910.

D. Gök / Hacettepe J. Biol. & Chem., 2020, 48 (3), 283-290

Research Article

Hacettepe Journal of Biology and Chemistry

journal homepage: www.hjbc.hacettepe.edu.tr

One-pot Three-component Synthesis of Novel Quinazoline-4-carboxylic Acid and Derivatives

Aynı Ortamda Üç Bileşenli Yeni Kinazolin-4-karboksilik Asit ve Türevlerinin Sentezi

Derviş Gök

Depart. of Chemistry and Chemical Processing Technologies, Kutahya Technical Sciences Vocational School, Dumlupinar University, Kutahya, Turkey.

ABSTRACT

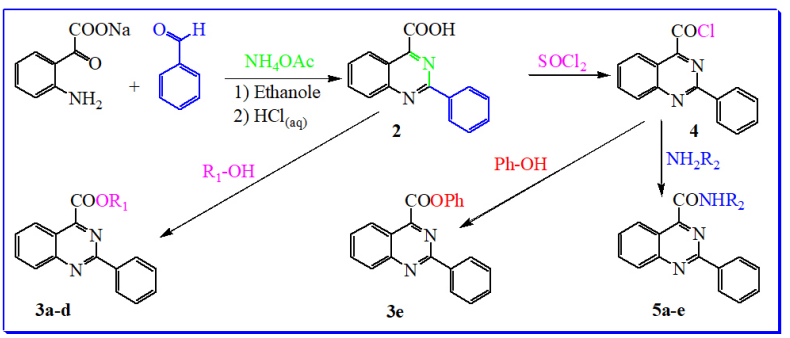

2-Phenyl-quinazoline-4-carboxylic acid (2) was synthesized from the one-pot three-component reaction of (2-amino-phenyl)-oxo-acetic acid sodium salt obtained from the hydrolysis of isatin with ammonium acetate and benzaldehyde. Some novel quinazoline-ester derivatives (3a-d) were then obtained by the reaction between 2 and various alcohols. Finally, quinazoline-amide derivatives (5a-e) were synthesized from the reaction of various amines and 2-phenyl-quinazoline-4-carbonyl chloride (4), obtained by the reaction of compound 2 with $SOCl_2$. The structures of synthesized compounds were clarified by ^{1}H NMR, ^{13}C NMR, IR, mass spectrometry analysis methods.

Key Words

Quinazoline-4-carboxylic acid, isatin, ester, amide.

ÖZ

Amonyum asetat ve benzaldehit ile isatinin hidrolizinden elde edilen (2-amino-fenil)-okso-asetik asit sodyum tuzunun aynı ortamda üç bileşenli reaksiyonundan 2-fenil-kinazolin-4-karboksilik asit (2) sentezlendi. Daha sonra 2 ve çeşitli alkoller arasındaki reaksiyonlarından bazı yeni kinazolin-ester türevleri (3a-d) elde edildi. Son olarak 2 bileşiği ile $SOCl_2$'nin reaksiyonundan elde edilen 2-fenil-kinazolin-4-karbonil klorür ve çeşitli aminlerin reaksiyonundan kinazolin-amit türevleri (5a-e) sentezlendi. Sentezlenen bileşiklerin yapıları ^{1}H NMR, ^{13}C NMR, IR, kütle spektrometri analiz metotları tarafından doğrulandı.

Anahtar Kelimeler

Kinazolin-4-karboksilik asit, isatin, ester, amit.

Article History: Nov 18, 2018; Revised Dec, 23 2019; Accepted: Jan 29, 2020; Available Online: May 3, 2020.

DOI: https://doi.org/10.15671/hjbc.736847

Correspondence to: D. Gök, Department of Chemistry and Chemical Processing Technologies, Kutahya Technical Sciences Vocational School, Dumlupinar University, Kutahya, Turkey.

E-Mail: dervis.gok@dpu.edu.tr

INTRODUCTION

Quinazoline and its derivatives are among the most important N-heterocyclic structures. The compounds containing the quinazoline ring both form the core structure of many natural products and exhibit useful biological activities such as anticancer [1], antimicrobial [2], anti-oxidant [3], antimalarial [4], anti-inflammatory [5], antiplasmodial [6], antiviral [7], anti-HIV [8], anticonvulsant [9], and anti-diabetic [10]. Bicyclic quinazoline ring constitutes the core structure of some drug molecules such as icotinib [11], lapatinib [12], and prazosin [13]. In addition, some compounds based on quinazoline are used as anticancer drugs such as erlotinib [14] and gefitinib [15].

Studies have shown that some quinazoline derivatives are a novel chiral fluorescent tubulin binding agent with highly potent antiproliferative properties against human cancer cells [16]. Furthermore, quinazoline derivatives are known to exhibit aurora a kinase inhibitor effect [17] and cytotoxic activity against human cancer cell [18]. Some of them also exhibit the inhibitory effect of epidermal growth factor receptor tyrosine kinase [19] and act as anti-cancer DNA binding alkaloids [20]. In the study of Seo et al., 3,4-dihydroquinazoline derivatives have been found to perform excellent T-type calcium channel blocking activity [21].

The above studies clearly demonstrate the importance of quinazoline derivatives. Their increasing importance has led to the development of different methods for their synthesis. Some reactions for their synthesis are aerobic oxidative coupling reactions of N-arylamidines with benzyl alcohol or aromatic aldehydes in air [22], cyclization and aromatization reactions of amidine hydrochlorides with methyl 2-halobenzoate, 2-halophenylketone, or 2-halobenzaldehyde derivatives [23], and cyclization reactions benzamidines and 2-bromobenzylbromides [24].

Different procedures have been developed for the synthesis of quinazolines such as photochemical methods [25], copper-catalyzed syntheses [26], reactions of urea maltose and ammonium chloride mixture [27], the use of microwave irradiation [28], and tandem reactions from benzylic amines and 2-aminobenzophenones [29].

The isatin compound was used as the starting compound in many reactions. It was also the starting compound of our reactions. It was hydrolyzed in alkaline medium to form (2-amino-phenyl)-oxo-acetic acid sodium salt. Quinazoline-4-carboxylic acid derivative was synthesized from one-pot three-component reaction of (2-amino-phenyl)-oxo-acetic acid sodium salt with ammonium acetate and benzaldehyde compounds. The literature review showed that the carboxyl group bound to the quinazoline ring was absent and that it was synthesized for the first time in our study. This paper reports the synthesis and characterization of some new quinazoline-4-carboxylic acid derivatives.

Firstly, quinazoline-4-carboxylic acid sodium salt was synthesized via reactions between readily available benzaldehyde (2-amino-phenyl)-oxo-acetic acid sodium salt and ammonium acetate in ethanol under mild conditions without catalyst. Two mechanisms are proposed for this reaction where the quinazoline ring is formed [30]. The proposed mechanisms are shown in scheme 1.

In the first reaction mechanism (path a), the condensation reaction of the aldehyde and 2-aminobenzophenone gives aldimine compound. The condensation reaction of ammonium acetate with this intermediate then gives diimine compound. The diimine compound is converted to the quinazoline compound by the cyclization reaction followed by aromatization reactions. In the other mechanism (path b), the condensation reaction of the aldehyde and ammonium acetate gives aldimine compound. Subsequent cyclization and aromatization reactions of 2-aminobenzophenone with this intermediate aldimine are converted to the quinazoline compound. The quinazoline compound formed in these two reaction mechanisms is obtained by air oxidation of the 1,2-dihydroquinazoline compound.

As seen from the reaction mechanism, one of the two nitrogen atoms found in the quinazoline ring comes from the amine group of the hydrolysis isatin compound and the other is the reactant ammonium acetate. Since we used the sodium salt of the hydrolysis isatin compound in the quinazoline reaction, we obtained the quinazoline compound as the carboxylic acid salt (**1**). Then, when we acidified this carboxylic acid salt with $HCl_{(aq)}$, we converted to 2-phenyl-quinazoline-4-carboxylic acid (**2**). The presence of the carboxyl group bound to the quinazoline ring then allowed the synthe-

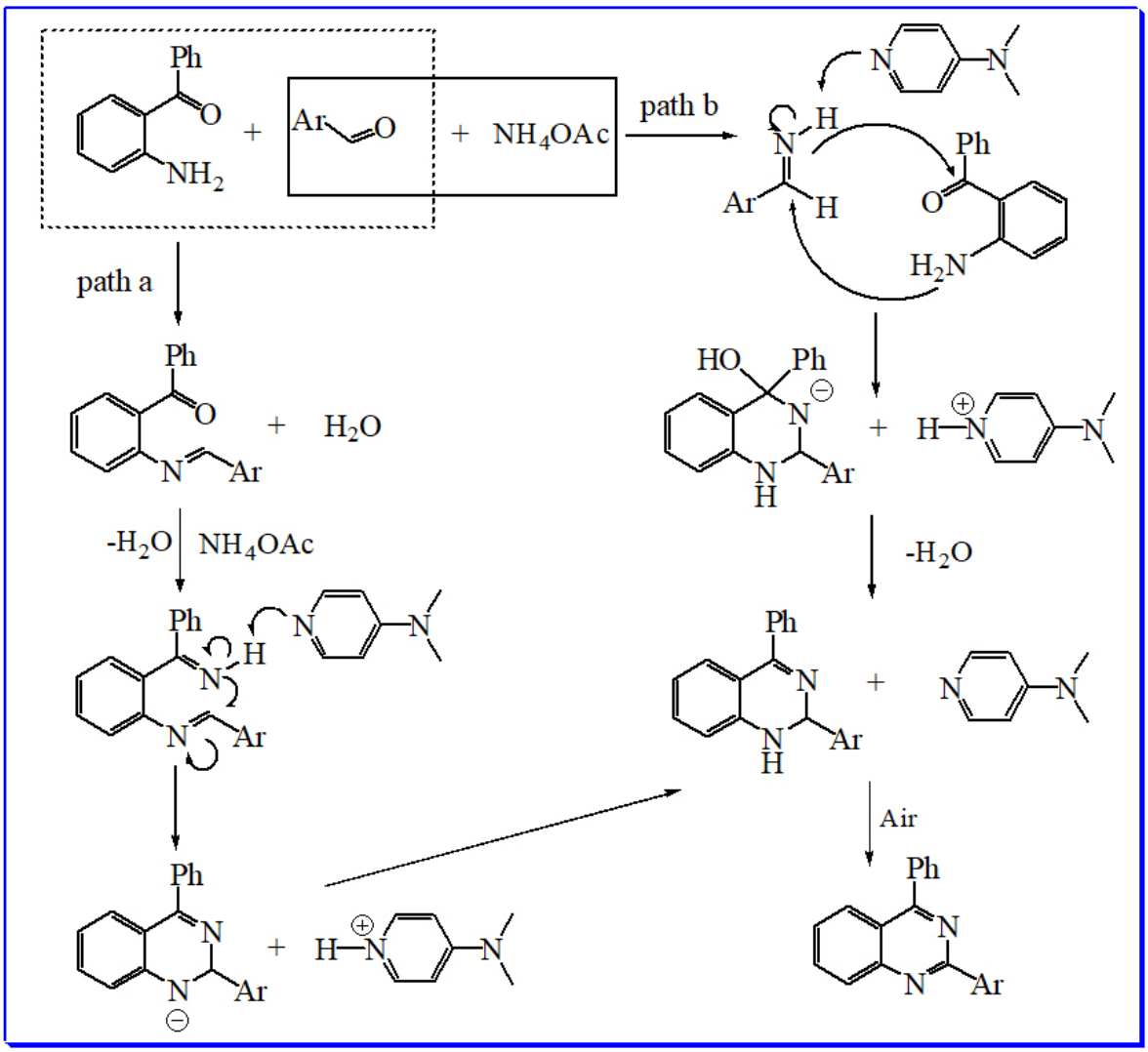

Scheme 1. Proposed mechanisms for the synthesis of 1,2-dihydroquinazolines and quinazolines with DMAP-catalyzed [30].

sis of carboxylic acid derivatives. The carboxyl group in the quinazoline ring was easily converted to the ester (**3a-e**) acid chloride (**4**) and amide (**5a-e**) derivatives. The synthesis of compounds is shown in scheme 2.

MATERIALS and METHODS

Chemicals and Instruments

The chemicals used in the synthesis of all new compounds were purchased from Merck and Aldrich Chemical Company. All chemicals and solvents were of spectroscopic reagent grade. The reactions were monitored by thin-layer chromatography (TLC) using aluminum sheets coated with silica gel 60_{F254} (Merck) Purity of the synthesized compounds was confirmed by TLC in the same way. Spots were detected by their absorption under UV light (λ = 254 nm). Melting points were measured on a Stuart SMP30 apparatus. The IR data (Agilent Technologies Inc., Santa Clara, CA) were recorded on a Bruker Vertex 70 Sample compartment spectrometer using potassium bromide pellets. ^{1}H NMR and ^{13}C NMR spectra were recorded on a Bruker AVANS 300 MHz spectrometer operating at 300 MHz and 75 MHz for ^{1}H and ^{13}C nuclei, respectively, in deuterochloroform and dimethyl sulphoxide-d_6 with tetramethylsilane as internal standard. Shifts were given in ppm, coupling constant (J) values were presented in hertz (Hz), and the abbreviations were as follows: s (singlet), d (doublet), t (triplet), and m (multiplet). The mass analyses were performed on an Agilent Technologies 6530 Accurate-Mass Q-TOF LC/MS at the advanced technology research center of Dumlupinar University (ILTEM).

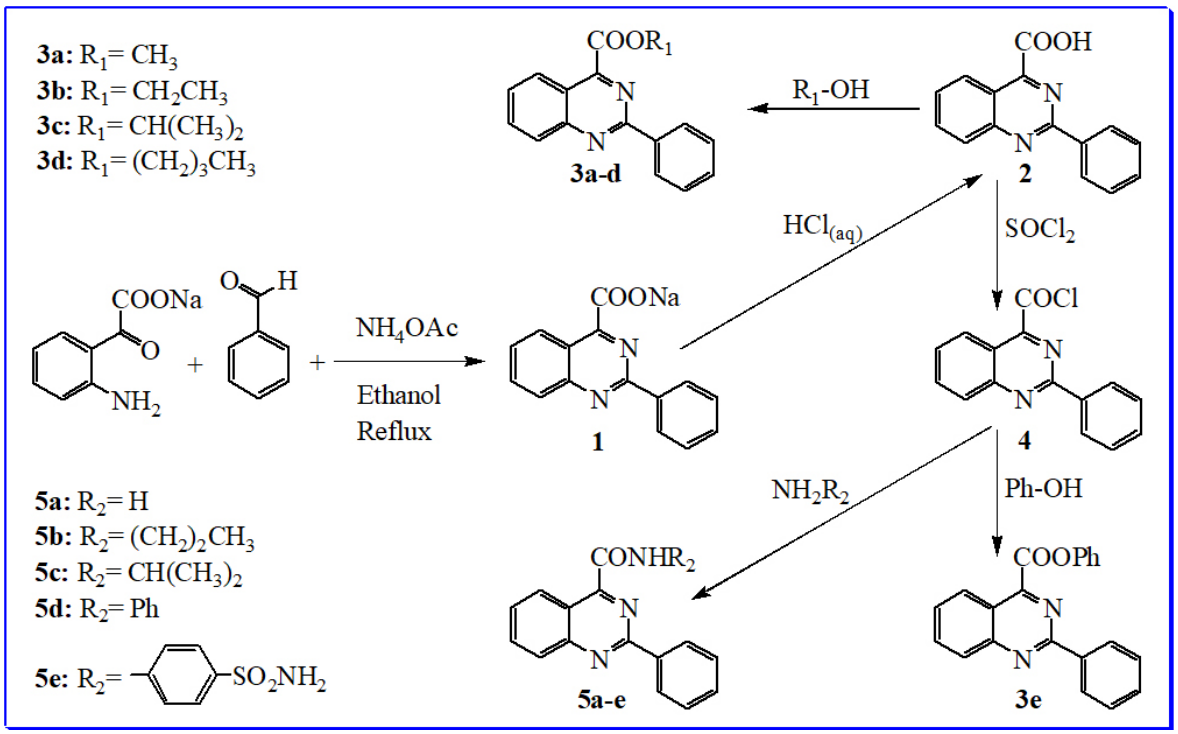

Scheme 2. Synthesis of novel quinazoline-4-carboxylic acid derivatives.

Synthesis

1. 2-Phenyl-quinazoline-4-carboxylic acid sodium salt (1). A mixture of ammonium acetate (0.154 g, 2 mmol) and benzaldehyde (0.106 g, 1 mmol) were added to a solution of (2-amino-phenyl)-oxo-acetic acid sodium salt (0.187 g, 1 mmol) in ethanol (10 mL) at room temperature. The mixture was stirred and heated to reflux for 24 h. The formed precipitate was filtered while it was still hot. The product was crystallized from water and dried in vacuo at 70°C. Yield: 0.08 g (29%); mp above 350°C; IR (*ν*, cm^{-1}): 3061 (Ar CH), 1650 (C=O), 1587-1459 (C=C and C=N); ^{1}H NMR (300 MHz, DMSO-d_6) δ (ppm): 8.55-8.52 (m, 2H, Ar-H), 8.13 (d, J=8.25 Hz, 1H, Ar-H), 7.97-7.87 (m, 2H, Ar-H), 7.63-7.53 (m, 4H, other Ar-H); ^{13}C NMR (75 MHz, DMSO-d_6) δ (ppm): 170.54 (COONa), 169.49, 159.82, 150.88, 138.42, 134.27, 130.93, 129.02, 128.54, 128.35, 128.23, 127.23, 119.62; HRMS (QTOF-ESI): *m/z* calcd for $C_{15}H_9N_2NaO_2$: 272.0562; found: 273.0637 $[M+1]^+$.

2. 2-Phenyl-quinazoline-4-carboxylic acid (2). Compound **1** (0.272 g, 1 mmol) was added to distilled water (10 mL). The obtained solution was heated to 90°C and slowly acidified with 2N $HCl_{(aq)}$ till reaching pH 1. The resulting mixture was kept at 5°C overnight. Then, the precipitate was filtered off and washed with water (3 x 15 mL). The product was crystallized from toluene and dried in vacuo at 70°C. Yield: 0.21 g (84%); mp 153°C; IR (*ν*, cm^{-1}): 3500-2500 (COOH), 3056 (Ar CH), 1713 (C=O, acid), 1614-1442 (C=C and C=N); ^{1}H NMR (300 MHz, DMSO-d_6) δ (ppm): 14.42 (br, s, 1H, COOH), 8.60-8.57 (m, 2H, Ar-H), 8.42 (d, J=8.32 Hz, 1H, Ar-H), 8.19-8.09 (m, 2H, Ar-H), 7.82 (t, J=7.60, 1H, Ar-H), 7.62-7.59 (m, 3H, other Ar-H); ^{13}C NMR (75 MHz, DMSO-d_6) δ (ppm): 166.79 (C=O, acid), 159.88, 159.47, 151.85, 137.18, 135.67, 131.60, 129.26, 129.18, 129.09, 128.66, 126.42, 119.77; HRMS (QTOF-ESI): *m/z* calcd for $C_{15}H_{10}N_2O_2$: 250.0742; found: 251.0816 $[M+1]^+$.

3. 2-Phenyl-quinazoline-4-carboxylic acid methyl ester (3a). H_2SO_4 (95-97%, 0.5 mL) was added to a solution of **2** (0.25 g, 1 mmol) in methanol (20 mL) at room temperature, and the mixture was stirred and heated to reflux for 6 h. The resulting mixture was filtered while it was still hot. The solvents were removed on a rotary evaporator at 40°C. The residue was washed with water (3 x 15 mL). The product was crystallized from methanol-water mixture and dried in vacuo at 40°C. Yield: 0.19 g (72%); mp 109°C; IR (*ν*, cm^{-1}): 3093 (Ar CH), 2951 (aliphatic CH), 1726 (C=O, ester), 1617-1457 (C=C and C=N); ^{1}H NMR (300 MHz, $CDCl_3$) δ (ppm): 8.66-8.63 (m, 2H, Ar-H), 8.52 (d, J= 8.51 Hz, 1H, Ar-H), 8.18 (d, J=8.58 Hz,

1H, Ar-H), 7.96 (t, J=8.36, 1H, Ar-H), 7.68 (t, J=8.22, 1H, Ar-H), 7.57-7.53 (m, 3H, other Ar-H), 4.16 (s, 3H, OC$\underline{H}_3$); ^{13}C NMR (75 MHz, $CDCl_3$) δ (ppm): 165.59 (C=O, ester), 160.18, 157.08, 152.38, 137.23, 134.50, 130.98, 129.15, 128.73, 128.70, 128.33, 125.90, 120.46, 53.27 (OCH_3); HRMS (QTOF-ESI): ***m/z*** calcd for $C_{16}H_{12}N_2O_2$: 264.0899; found: 265.0976 $[M+1]^+$.

4. 2-Phenyl-quinazoline-4-carboxylic acid ethyl ester (3b). H_2SO_4 (95-97%, 0.5 mL) was added to a solution of **2** (0.25 g, 1 mmol) in ethanol (25 mL) at room temperature, and the mixture was stirred and heated to reflux for 5 h. The resulting mixture was filtered while it was still hot. The solvents were removed on a rotary evaporator at 40°C. The residue was washed with water (3 x 15 mL). The obtained oily product was dried in vacuo at 40°C. Yield: 0.17 g (61%); mp oily; IR (***v***, cm^{-1}): 3064 (Ar CH), 2981 (aliphatic CH), 1727 (C=O, ester), 1616-1458 (C=C and C=N); ^{1}H NMR (300 MHz, $CDCl_3$) δ (ppm): 8.67-8.63 (m, 2H, Ar-H), 8.46 (d, J= 8.47 Hz, 1H, Ar-H), 8.15 (d, J=8.52 Hz, 1H, Ar-H), 7.94 (t, J=7.70, 1H, Ar-H), 7.65 (t, J=7.77, 1H, Ar-H), 7.57-7.52 (m, 3H, other Ar-H), 4.63 (q, J=7.14 Hz, 2H, OC$\underline{H}_2$), 1.54 (t, J=7.10 Hz, 3H, C$\underline{H}_3$); ^{13}C NMR (75 MHz, $CDCl_3$) δ (ppm): 164.34 (C=O, ester), 159.24, 156.76, 151.44, 136.46, 133.48, 130.04, 128.27, 127.84, 127.75, 127.28, 124.91, 119.44, 61.68 (OCH_2), 13.44 (CH_3); HRMS (QTOF-ESI): ***m/z*** calcd for $C_{17}H_{14}N_2O_2$: 278.1055; found: 278.1664 $[M]^+$.

5. 2-Phenyl-quinazoline-4-carboxylic acid isopropyl ester (3c). H_2SO_4 (95-97%, 0.5 mL) was added to a solution of **2** (0.25 g, 1 mmol) in isopropanol (20 mL) at room temperature, and the mixture was stirred and heated to reflux for 5 h. The resulting mixture was filtered while it was still hot. The solvents were removed on a rotary evaporator at 40°C. The residue was washed with water (3 x 15 mL). The obtained oily product was dried in vacuo at 40°C. Yield: 0.17 g (58%); mp oily; IR (***v***, cm^{-1}): 3064 (Ar CH), 2981 (aliphatic CH), 1723 (C=O, ester), 1616-1457 (C=C and C=N); ^{1}H NMR (300 MHz, $CDCl_3$) δ (ppm): 8.66-8.64 (m, 2H, Ar-H), 8.39 (d, J= 8.44 Hz, 1H, Ar-H), 8.14 (d, J=8.49 Hz, 1H, Ar-H), 7.93 (t, J=8.33, 1H, Ar-H), 7.65 (t, J=7.35, 1H, Ar-H), 7.57-7.51 (m, 3H, other Ar-H), 6.28 (heptet, J=6.28 Hz, 1H, OC$\underline{H}$), 1.53 (d, J=6.25 Hz, 6H, 2C$\underline{H}_3$); ^{13}C NMR (75 MHz, $CDCl_3$) δ (ppm): 164.89 (C=O, ester), 160.18, 158.32, 152.27, 137.39, 134.33, 130.91, 129.19, 128.75, 128.62, 128.09, 125.72, 120.23, 70.65 (OCH), 21.94 (CH_3); HRMS (QTOF-ESI): ***m/z*** calcd for $C_{18}H_{16}N_2O_2$: 292.1212; found: 292.2651 $[M]^+$.

6. 2-Phenyl-quinazoline-4-carboxylic acid butyl ester (3d). H_2SO_4 (95-97%, 0.5 mL) was added to a solution of **2** (0.25 g, 1 mmol) in ***n***-butanol (30 mL) at room temperature, and the mixture was stirred and heated to reflux for 5 h. The resulting mixture was filtered while it was still hot. The solvents were removed on a rotary evaporator at 40°C. The residue was washed with water (3 x 15 mL). The obtained oily product was dried in vacuo at 40°C. Yield: 0.16 g (52%); mp oily; IR (***v***, cm^{-1}): 3064 (Ar CH), 2960 (aliphatic CH), 1726 (C=O, ester), 1616-1458 (C=C and C=N); ^{1}H NMR (300 MHz, $CDCl_3$) δ (ppm): 8.65-8.62 (m, 2H, Ar-H), 8.44 (d, J= 8.47 Hz, 1H, Ar-H), 8.15 (d, J=8.55 Hz, 1H, Ar-H), 7.94 (t, J=7.72, 1H, Ar-H), 7.65 (t, J=7.76, 1H, Ar-H), 7.57-7.51 (m, 3H, other Ar-H), 4.57 (t, J=6.72 Hz, 2H, OC$\underline{H}_2$), 1.89 (pentet, J=7.88 Hz, 2H, $OCH_2C\underline{H}_2$), 1.56 (hextet, J=7.54 Hz, 2H, C$\underline{H}_2CH_3$), 1.03 (t, J=7.33 Hz, 3H, C$\underline{H}_3$); ^{13}C NMR (75 MHz, $CDCl_3$) δ (ppm): 165.34 (C=O, ester), 160.13, 157.72, 152.34, 137.38, 134.33, 130.92, 129.18, 128.73, 128.64, 128.14, 125.80, 120.36, 66.35 (OCH_2), 30.67 ($OCH_2\underline{C}H_2$), 19.25 ($\underline{C}H_2CH_3$), 13.80 (CH_3); HRMS (QTOF-ESI): ***m/z*** calcd for $C_{19}H_{18}N_2O_2$: 306.1368; found: 307.1469 $[M+1]^+$.

7. 2-Phenyl-quinazoline-4-carbonyl chloride (4). A mixture of **2** (0.25 g, 1 mmol) and $SOCl_2$ (%95; 5 mL) were heated in an oil bath (80°C) for 6 h. The solvents were removed on a rotary evaporator at 50°C. The residue was washed with ether (3 x 15 mL). The product was crystallized from toluene-hexane mixture and dried in vacuo at 70°C. Yield: 0.20 g (75%); mp 149°C; IR (***v***, cm^{-1}): 3065 (Ar CH), 1711 (C=O, carbonyl), 1624-1457 (C=C and C=N); ^{1}H NMR (300 MHz, $CDCl_3$) δ (ppm): 9.37 (d, J=8.63 Hz, 1H, Ar-H), 8.64-8.60 (m, 2H, Ar-H), 8.39 (d, J=8.42 Hz, 1H, Ar-H), 8.07 (t, J=7.83, 1H, Ar-H), 7.80 (t, J=8.29, 1H, Ar-H), 7.61-7.59 (m, 3H, other Ar-H); ^{13}C NMR (75 MHz, DMSO-d_6) δ (ppm): 166.70 (C=O, carbonyl), 160.04, 159.46, 151.79, 137.16, 135.75, 131.63, 129.29, 129.24, 129.07, 128.65, 126.40, 119.72; HRMS (QTOF-ESI): ***m/z*** calcd for $C_{15}H_9ClN_2O$: 268.0403; found: 269.0955 $[M+1]^+$.

8. 2-Phenyl-quinazoline-4-carboxylic acid phenyl ester (3e). A mixture of phenol (0.094 g, 1 mmol) and triethylamine (0.10 g, 1 mmol) were added to a solution of **4** (0.268 g, 1 mmol) in toluene (30 mL) at room temperature. The mixture was stirred and heated to reflux for 5 h. The reaction mixture was filtered while it was still hot. The solvents were removed on a rotary evaporator at 40°C. The residue was washed with ether (3 x 15 mL). The product was crystallized from toluene and dried in

vacuo at 40°C. Yield: 0.14 g (43%); mp 121°C; IR (***v***, cm^{-1}): 3095 (Ar CH), 1749 (C=O, ester), 1615-1455 (C=C and C=N); ^{1}H NMR (300 MHz, $CDCl_3$) δ (ppm): 8.73-8.69 (m, 2H, Ar-H), 8.64 (d, J= 8.51 Hz, 1H, Ar-H), 8.20 (d, J=8.53 Hz, 1H, Ar-H), 7.98 (t, J=7.75, 1H, Ar-H), 7.70 (t, J=7.64, 1H, Ar-H), 7.60-7.33 (m, 8H, other Ar-H); ^{13}C NMR (75 MHz, $CDCl_3$) δ (ppm): 163.67 (C=O, ester), 160.23, 156.22, 152.69, 150.73, 137.25, 134.57, 131.09, 129.76, 129.38, 128.80, 128.75, 128.56, 126.57, 125.74, 121.62, 120.74; HRMS (QTOF-ESI): ***m/z*** calcd for $C_{21}H_{14}N_2O_2$: 326.1055; found: 327.1138 $[M+1]^+$.

9. 2-Phenyl-quinazoline-4-carboxylic acid amide (5a). A mixture of **4** (0.268 g, 1 mmol) and THF (30 mL) were cooled to 0°C. The obtained solution was slowly added to ammonium hydroxide solution (0.15 mL, 2 mmol) at 0°C, stirred, and kept at this temperature for 2 h. The reaction mixture was continued and stirred at room temperature for an additional 2 h. The obtained solution was filtered. The solvents were removed on a rotary evaporator at 40°C. The residue was washed with ether (3 x 15 mL). The product was crystallized from toluene-THF mixture and dried in vacuo at 70°C. Yield: 0.19 g (76%); mp 198°C; IR (***v***, cm^{-1}): 3178 (NH), 3069 (Ar CH), 1710 (C=O, amide), 1615-1488 (C=C and C=N); ^{1}H NMR (300 MHz, $CDCl_3$) δ (ppm): 9.40 (d, J=7.94 Hz, 1H, Ar-H), 8.61-8.58 (m, 2H, Ar-H), 8.15 (d, J=8.49 Hz, 1H, Ar-H), 7.95 (t, J=7.73, 1H, Ar-H), 7.69 (t, J=7.68, 1H, Ar-H), 7.59-7.55 (m, 3H, other Ar-H), 5.83 (br, s, 2H, NH_2); ^{13}C NMR (75 MHz, $CDCl_3$) δ (ppm): 167.24 (C=O, amide), 154.90, 153.37, 137.16, 134.53, 130.96, 128.93, 128.74, 128.61, 128.40, 127.50, 121.09; HRMS (QTOF-ESI): ***m/z*** calcd for $C_{15}H_{11}N_3O$: 249.0902; found: 250.0962 $[M+1]^+$.

10. 2-Phenyl-quinazoline-4-carboxylic acid propylamide (5b). *n*-Propylamine (0.118 g, 2 mmol) was added to a solution of **4** (0.268 g, 1 mmol) in toluene (30 mL) at room temperature. The mixture was stirred and heated to reflux for 5 h. The reaction mixture was filtered while it was still hot. The solvents were removed on a rotary evaporator at 40°C. The residue was washed with ether (3 x 15 mL). The product was crystallized from toluene and dried in vacuo at 70°C. Yield: 0.18 g (62%); mp 147°C; IR (***v***, cm^{-1}): 3314 (NH), 3068 (Ar CH), 2934 (aliphatic CH), 1649 (C=O, amide), 1614-1486 (C=C and C=N); ^{1}H NMR (300 MHz, $CDCl_3$) δ (ppm): 9.47 (d, J=8.62 Hz, 1H, Ar-H), 8.60-8.57 (m, 2H, Ar-H), 8.34 (br, s, 1H, NH), 8.12 (d, J=8.53 Hz, 1H, Ar-H), 7.94 (t, J=7.71, 1H, Ar-H), 7.67 (t, J=7.55, 1H, Ar-H), 7.60-7.53 (m, 3H, other Ar-H), 3.55 (q, J=7.11, 2H, $NHC\underline{H}_2$), 1.77 (hextet, J=7.22 Hz, 2H, $C\underline{H}_2CH_3$), 1.08 (t, J=7.35 Hz, 3H, $C\underline{H}_3$); ^{13}C NMR (75 MHz, $CDCl_3$) δ (ppm): 164.87 (C=O, amide), 158.79, 155.75, 153.21, 137.25, 134.38, 130.85, 128.78, 128.69, 128.35, 127.77, 121.11, 41.33 ($NHCH_2$), 22.91 ($\underline{C}H_2CH_3$), 11.56 ($CH_2\underline{C}H_3$); HRMS (QTOF-ESI): ***m/z*** calcd for $C_{18}H_{17}N_3O$: 291.1372; found: 292.1435 $[M+1]^+$.

11. 2-Phenyl-quinazoline-4-carboxylic acid isopropylamide (5c). İsopropylamine (0.118 g, 2 mmol) was added to a solution of **4** (0.268 g, 1 mmol) in toluene (30 mL) at room temperature. The mixture was stirred and heated to reflux for 5 h. The reaction mixture was filtered while it was still hot. The solvents were removed on a rotary evaporator at 40°C. The residue was washed with ether (3 x 15 mL). The product was crystallized from toluene-hexane mixture and dried in vacuo at 70°C. Yield: 0.17 g (58%); mp 143°C; IR (***v***, cm^{-1}): 3300 (NH), 3067 (Ar CH), 2936 (aliphatic CH), 1642 (C=O, amide), 1613-1486 (C=C and C=N); ^{1}H NMR (300 MHz, $CDCl_3$) δ (ppm): 9.47 (d, J=8.30 Hz, 1H, Ar-H), 8.60-8.55 (m, 2H, Ar-H), 8.13-8.08 (m, 2H, NH and Ar-H), 7.93 (t, J=7.67, 1H, Ar-H), 7.67 (t, J=7.86, 1H, Ar-H), 7.61-7.52 (m, 3H, other Ar-H), 4.37 (octet, J=5.10, 1H, NHC$\underline{H}$), 1.39 (d, J=6.57 Hz, 6H, $2C\underline{H}_3$); ^{13}C NMR (75 MHz, $CDCl_3$) δ (ppm): 165.54 (C=O, amide), 160.37, 155.83, 153.17, 137.24, 134.35, 130.85, 128.77, 128.69, 128.36, 128.30, 127.75, 121.11, 41.72 (CH), 22.72 (CH_3); HRMS (QTOF-ESI): ***m/z*** calcd for $C_{18}H_{17}N_3O$: 291.1372; found: 292.1447 $[M+1]^+$.

12. 2-Phenyl-quinazoline-4-carboxylic acid phenylamide (5d). Aniline (0.186 g, 2 mmol) was added to a solution of **4** (0.268 g, 1 mmol) in THF (30 mL) at room temperature. The mixture was stirred and heated to reflux for 6 h. The reaction mixture was filtered while it was still hot. The solvents were removed on a rotary evaporator at 40°C. The residue was washed with ether (3 x 15 mL). The product was crystallized from THF-hexane mixture and dried in vacuo at 40°C. Yield: 0.17 g (52%); mp 117°C; IR (***v***, cm^{-1}): 3315 (NH), 3063 (Ar CH), 1663 (C=O, amide), 1614-1486 (C=C and C=N); ^{1}H NMR (300 MHz, $CDCl_3$) δ (ppm): 10.31 (br, s, 1H, NH), 9.57 (d, J=8.64 Hz, 1H, Ar-H), 9.42 (d, J=8.61 Hz, 1H, Ar-H), 8.64-8.56 (m, 3H, Ar-H), 8.22-8.16 (m, 2H, Ar-H), 7.86 (d, J=7.53 Hz, 2H, Ar-H), 7.60-7.57 (m, 4H, Ar-H), 7.49 (t, J=7.53 Hz, 1H, Ar-H); ^{13}C NMR (75 MHz, $CDCl_3$) δ (ppm): 164.17 (C=O, amide), 162.46, 158.57, 153.46, 152.43, 137.30, 134.63, 131.02, 129.22, 129.00, 128.93, 128.66, 128.35, 127.61, 124.98, 120.13, 116.23; HRMS (QTOF-ESI): ***m/z*** calcd for $C_{21}H_{15}N_3O$: 325.1215; found: 325.1454 $[M]^+$.

13. 2-Phenyl-quinazoline-4-carboxylic acid (4-sulfamoyl-phenyl)-amide (5e). 4-aminobenzenesulfonamide (0.344 g, 2 mmol) was added to a solution of **4** (0.268 g, 1 mmol) in THF (30 mL) at room temperature. The mixture was stirred and heated to reflux for 6 h. The reaction mixture was filtered while it was still hot. The solvents were removed on a rotary evaporator at 40°C. The residue was washed with ether (3 x 15 mL). The product was crystallized from THF-toluene mixture and dried in vacuo at 70°C. Yield: 0.18 g (44%); mp 285°C; IR (***v***, cm^{-1}): 3331 (NH), 3105 (Ar CH), 1681 (C=O, amide), 1615-1485 (C=C and C=N), 1342 (SO_2 asym.), 1155 (SO_2 sym.); ^{1}H NMR (300 MHz, DMSO-d_6) δ (ppm): 11.35 (s, 1H, NH), 8.70-8.61 (m, 3H, Ar-H), 8.22-8.05 (m, 4H, Ar-H), 7.91-7.80 (m, 3H, Ar-H), 7.63-7.61 (m, 3H, other Ar-H), 7.36 (s, 2H, $SO_2N\underline{H}_2$); ^{13}C NMR (75 MHz, DMSO-d_6) δ (ppm): 164.30 (C=O, amide), 160.28, 159.29, 152.12, 141.55, 140.13, 137.13, 135.85, 131.74, 129.30, 129.13, 128.95, 128.23, 127.23, 126.76, 120.65, 120.12; HRMS (QTOF-ESI): ***m/z*** calcd for $C_{21}H_{16}N_4O_3S$: 404.0943; found: 405.1014 $[M+1]^+$.

RESULTS and DISCUSSION

When we look at the literature, it is seen in our study that we synthesize the carboxylic acid derivative which is directly bound to the quinazoline ring for the first time. Because the quinazoline derivatives show a wide range of biological activities, we hope that the compounds we synthesized in this study will contribute to medical chemistry.

When we look at the reaction mechanism, an aromatic amine compound (DMAP) is used as a catalyst in the synthesis of quinazoline. Since we do not use a catalyst in our reaction, it is believed that the catalytic function is the hydrolysis isatin compound containing the aromatic amine group. That is, the hydrolysis isatin compound acts as both a catalyst and a component of the reaction. At the same time, while the hydrolysis isatin compound is insoluble in hot ethanol, it completely dissolves in warm ethanol together with ammonium acetate and benzaldehyde. The quinazoline derivative carboxyl acid salt formed in the hot ethanol during the reaction forms a precipitate. This allowed the reaction to be separated from the other reaction components and by-products by hot filtration. In the one-pot three-component reaction in the quinazoline synthesis, the reaction time was very long (24 h) and the yield (29%) was very low, but we could easily distinguish it from the reaction medium. Carboxylic acid ester derivatives were readily obtained in the presence of sulfuric acid by the reaction of alkyl alcohols and the quinazoline carboxylic acid compound. However, the phenol ester can be obtained by reacting the phenol with the carboxylic acid chloride which is more active than the carboxylic acid compound. Similarly, quinazoline amide derivatives were also obtained from the simple reaction of the carboxylic acid chloride compound with various amines.

As a result, we successfully synthesized ester and amide derivatives of the quinazoline-4-carboxylic acid compound we synthesized by one-pot three-component reaction. Since the quinazoline compounds exhibit versatile biological activity, we think that the compounds we synthesize will contribute to medicinal chemistry.

Acknowledgements

We are grateful to the Dumlupinar University Technology Research Fund for the financial support of this study through project number of 2015/24.

References

1. H.M. Shallal, W.A. Russu, Discovery, synthesis, and investigation of the antitumor activity of novel piperazinylpyrimidine derivatives, Eur. J. Med. Chem., 46 (2011) 2043-2057.
2. G. Grover, S.G. Kini, Synthesis and evaluation of new quinazolone derivatives of nalidixic acid as potential antibacterial and antifungal agents, Eur. J. Med. Chem., 41 (2006) 256-262.
3. A.B.A. El-Gazzar, M.M. Youssef, A.M.S. Youssef, A.A. Abu-Hashem, F.A. Badria, Design and synthesis of azolopyrimidoquinolines, pyrimidoquinazolines as antioxidant, anti-inflammatory and analgesic activities, Eur. J. Med. Chem., 44 (2009) 609-624.
4. P. Verhaeghe, N. Azas, M. Gasquet, S. Hutter, C. Ducros, M. Laget, S. Rault, P. Rathelot, P. Vanelle, Synthesis and antiplasmodial activity of new 4-aryl-2-trichloromethylquinazolines, Bioorg. Med. Chem. Lett., 18 (2008) 396-401.
5. R.A. Smits, M. Adami, E.P. Istyastono, O.P. Zuiderveld, C.M.E. van Dam, F.J.J. de Kanter, A. Jongejan, G. Coruzzi, R. Leurs, I.J.P. de Esch, Synthesis and QSAR of quinazoline sulfonamides as highly potent human histamine h-4 receptor inverse agonists, J. Med. Chem., 53 (2010) 2390-2400.
6. C. Mendoza-Martinez, J. Correa-Basurto, R. Nieto-Meneses, A. Marquez-Navarro, R. Aguilar-Suarez, M.D. Montero-Cortes, B. Nogueda-Torres, E. Suarez-Contreras, N. Galindo-Sevilla, A. Rojas-Rojas, A. Rodriguez-Lezama, F. Hernandez-Luis, Design, synthesis and biological evaluation of quinazoline derivatives as anti-trypanosomatid and antiplasmodial agents, Eur. J. Med. Chem., 96 (2015) 296-307.

7. T. Herget, M. Freitag, M. Morbitzer, R. Kupfer, T. Stamminger, M. Marschall, Novel chemical class of pUL97 protein kinase-specific inhibitors with strong anticytomegaloviral activity, Antimicrob. Agents. Ch., 48 (2004) 4154-4162.
8. T.P. Selvam, P.V. Kumar, A.S. Kumar, I.A. Emerson, Study of inhibitory mechanism and binding mode of the thiazolo quinazoline compounds to HIV-1 integrase by docking, J. Pharm. Res., 3 (2010) 1637–1647.
9. S.K. Kashaw, V. Kashaw, P. Mishra, N.K. Jain, J.P. Stables, Synthesis, anticonvulsant and CNS depressant activity of some new bioactive 1-(4-substituted-phenyl)-3-(4-oxo-2-phenyl/ethyl-4H-quinazolin-3-yl)-urea, Eur. J. Med. Chem., 44 (2009) 4335-4343.
10. M.S. Malamas, J. Millen, Quinazolineacetic acids and related analogs as aldose reductase inhibitors, J. Med. Chem., 34 (1991) 1492-1503.
11. J.P. Xu, X.Y. Liu, S. Yang, C.G. Zhang, L. Wang, Y.K. Shi, Icotinib as initial treatment in lung adenocarcinoma patients with brain metastases, Thorac. Cancer, 7 (2016) 437-441.
12. D. Cameron, M. Casey, M. Press, D. Lindquist, T. Pienkowski, C.G. Romieu, S. Chan, A. Jagiello-Gruszfeld, B. Kaufman, J. Crown, A. Chan, M. Campone, P. Viens, N. Davidson, V. Gorbounova, J.I. Raats, D. Skarlos, B. Newstat, D. Roychowdhury, P. Paoletti, C. Oliva, S. Rubin, S. Stein, C.E. Geyer, A phase III randomized comparison of lapatinib plus capecitabine versus capecitabine alone in women with advanced breast cancer that has progressed on trastuzumab: updated efficacy and biomarker analyses, Breast Cancer Res. Treat., 112 (2008) 533-543.
13. R.N. Brogden, R.C. Heel, T.M. Speight, G.S. Avery, Prazosin: a review of its pharmacological properties and therapeutic efficacy in hypertension, Drugs, 14 (1977) 163-197.
14. R.S. Herbst, Erlotinib (Tarceva): an update on the clinical trial program, Semin. Oncol., 30 (2003) 34-46.
15. M. Murphy, B. Stordal, Erlotinib or gefitinib for the treatment of relapsed platinum pretreated non-small cell lung cancer and ovarian cancer: a systematic review, Drug Resist. Updat., 14 (2011) 177-190.
16. G.M. Chinigo, M. Paige, S. Grindrod, E. Hamel, S. Dakshanamurthy, M. Chruszcz, W. Minor, M.L. Brown, Asymmetric synthesis of 2,3-dihydro-2-arylquinazolin-4-ones: methodology and application to a potent fluorescent tubulin inhibitor with anticancer activity, J. Med. Chem., 51 (2008) 4620-4631.
17. T. Sardon, T. Cottin, J. Xu, A. Giannis, I. Vernos, Development and biological evaluation of a novel aurora A kinase inhibitor, Chembiochem., 10 (2009) 464-478.
18. S.L. Cao, Y. Wang, L. Zhu, J. Liao, Y.W. Guo, L.L. Chen, H.Q. Liu, X. Xu, Synthesis and cytotoxic activity of N-((2-methyl-4(3H)-quinazolinon-6-yl)methyl)dithiocarbamates, Eur. J. Med. Chem., 45 (2010) 3850-3857.
19. D.W. Fry, A.J. Kraker, A. McMichael, L.A. Ambroso, J.M. Nelson, W.R. Leopold, R.W. Connors, A.J. Bridges, A specific inhibitor of the epidermal growth factor receptor tyrosine kinase, Science, 265 (1994) 1093-1095.
20. N. Malecki, P. Carato, B. Rigo, J.F. Goossens, R. Houssin, C. Bailly, J.P. Henichart, Synthesis of condensed quinolines and quinazolines as DNA ligands, Bioorgan. Med. Chem., 12 (2004) 641-647.
21. H.N. Seo, J.Y. Choi, Y.J. Choe, Y. Kim, H. Rhim, S.H. Lee, J. Kim, D.J. Joo, J.Y. Lee, Discovery of potent T-type calcium channel blocker, Bioorg. Med. Chem. Lett., 17 (2007) 5740-5743.
22. W. Zhang, F. Guo, F. Wang, N. Zhao, L. Liu, J. Li, Z.H. Wang, Synthesis of quinazolines via CuO nanoparticles catalyzed aerobic oxidative coupling of aromatic alcohols and amidines, Org. Biomol. Chem., 12 (2014) 5752-5756.
23. C. Huang, Y. Fu, H. Fu, Y.Y. Jiang, Y.F. Zhao, Highly efficient copper-catalyzed cascade synthesis of quinazoline and quinazolinone derivatives, Chem. Commun., (2008) 6333-6335.
24. C.C. Malakar, A. Baskakova, J. Conrad, U. Beifuss, Copper-Catalyzed Synthesis of Quinazolines in Water Starting from o-Bromobenzylbromides and Benzamidines, Chem. Eur. J., 18 (2012) 8882-8885.
25. R. Alonso, A. Caballero, P.J. Campos, D. Sampedro, M.A. Rodriguez, An efficient synthesis of quinazolines: a theoretical and experimental study on the photochemistry of oxime derivatives, Tetrahedron, 66 (2010) 4469-4473.
26. Y. Ohta, Y. Tokimizu, S. Oishi, N. Fujii, H. Ohno, Direct Synthesis of Quinazolines through Copper-Catalyzed Reaction of Aniline-Derived Benzamidines, Org. Lett., 12 (2010) 3963-3965.
27. Z.H. Zhang, X.N. Zhang, L.P. Mo, Y.X. Li, F.P. Ma, Catalyst-free synthesis of quinazoline derivatives using low melting sugar-urea-salt mixture as a solvent, Green Chem., 14 (2012) 1502-1506.
28. F. Portela-Cubillo, J.S. Scott, J.C. Walton, Microwave-Promoted syntheses of quinazolines and dihydroquinazolines from 2-aminoarylalkanone o-phenyl oximes, J. Org. Chem., 74 (2009) 4934-4942.
29. J.T. Zhang, D.P. Zhu, C.M. Yu, C.F. Wan, Z.Y. Wang, A simple and efficient approach to the synthesis of 2-phenylquinazolines via sp(3) C-H functionalization, Org. Lett., 12 (2010) 2841-2843.
30. C. Derabli, R. Boulcina, G. Kirsch, B. Carboni, A. Debache, A DMAP-catalyzed mild and efficient synthesis of 1,2-dihydroquinazolines via a one-pot three-component protocol, Tetrahedron Lett., 55 (2014) 200-204.

A. Çetin et al. / Hacettepe J. Biol. & Chem., 2020, 48 (3), 291-299

Research Article

Hacettepe Journal of Biology and Chemistry

journal homepage: www.hjbc.hacettepe.edu.tr

Investigation of The Synergistic Effects of Trastuzumab And Gambogic Acid in Her-2 Positive Breast Cancer Cell Line

Her-2 Pozitif Meme Kanseri Hücre Hattında Trastuzumab ve Gambojik Asit Sinerjik Etkilerinin İncelenmesi

Ahmet Çetin[1], Aykut Özgür[2], Mehmet Kuzucu[3], Murat Çankaya[3]*

[1]Erzincan Binali Yıldırım University, Graduate School of Natural and Applied Sciences, Department of Biology, Erzincan, Turkey.

[2]Tokat Gaziosmanpaşa University, Artova Vocational Sch., Depart. of Veterinary Medicine, Laboratory and Veterinary Health Program, Tokat, Turkey.

[3]Erzincan Binali Yıldırım University, Faculty of Arts and Sciences, Department of Biology, Erzincan, Turkey.

ABSTRACT

HER2 positive breast cancer is one of the biggest health problems in the world, causing millions of deaths every year. Drug combination modeling studies are extensively evaluated in treating many diseases. Pharmacological studies over the last half-century have shown that gambogic acid has potent anti-tumor activity against many types of cancer, including breast cancer. In this study, we examined the synergistic anticancer effect of gambogic acid and trastuzumab in HER2 positive breast cancer cell line (MDA-MB-453). In-vitro synergistic and antiproliferative effects of trastuzumab plus gambogic acid studies were determined with XTT method and the combination index (CI) values of the trastuzumab and gambogic acid combination were calculated by CompuSyn software. To determine molecular mechanisms of the trastuzumab and gambogic acid combination in MDA-MB-453 cells, the differences of gene and protein expression levels of HER2, caspase-9 and Bax were analyzed with using RT-qPCR and ELISA techniques. The combination of 50 µg/ml trastuzumab and 5 µM gambogic acid showed the best synergistic effect at 24 h incubation in MDA-MB-453 cells according to the in-vitro cell proliferation, RT-qPCR and ELISA test. Gambogic acid effects on HER2 positive breast cancer cell line shows its potential as natural compound to inhibit breast cancer cell proliferation in combination with trastuzumab.

Key Words
Trastuzumab, gambogic acid, breast cancer, HER-2.

ÖZ

HER2 pozitif meme kanseri, her yıl milyonlarca ölüme neden olan dünyanın en büyük sağlık sorunlarından biridir. İlaç kombinasyonu modelleme çalışmaları birçok hastalığın tedavisinde kapsamlı bir şekilde değerlendirilmektedir. Son yarım yüzyıl boyunca yapılan farmakolojik çalışmalar, gambojik asidin meme kanseri de dahil olmak üzere birçok kanser türüne karşı güçlü bir anti-tümör aktiviteye sahip olduğunu göstermiştir. Bu çalışmada HER2 pozitif meme kanseri hücre hattında (MDA-MB-453) gambojik asit ve trastuzumabın sinerjistik antikanser etkisini inceledik. Trastuzumab artı gambojik asit çalışmalarının in vitro sinerjistik ve antiproliferatif etkileri XTT yöntemi ile belirlenmiş ve trastuzumab ve gambojik asit kombinasyonunun kombinasyon indeksi (CI) değerleri CompuSyn yazılımı ile hesaplanmıştır. MDA-MB-453 hücrelerinde, trastuzumab ve gambojik asit kombinasyonlarının moleküler mekanizmalarını belirlemek ve HER2, kaspaz-9 ve Bax'ın protein ve gen ekspresyonu seviyelerindeki farklılıklar RT-PCR (qRT-PCR) ve ELISA teknikleri kullanılarak analiz edildi. RT-qPCR ve ELISA testine göre; 50 µg / ml trastuzumab ve 5 µM gambojik asit kombinasyonu, MDA-MB-453 hücre hattında 24 saatlik inkübasyonda en iyi sinerjistik etkiyi gösterdi. Gambojik asitin HER2 pozitif meme kanseri hücre hattı üzerine etkisi, , trastuzumab ile kombinasyonunun meme kanseri hücre proliferasyonunu inhibe eden doğal bileşik potansiyeline sahip olduğunu gösterir.

Anahtar Kelimeler
Trastuzumab, gambojik asit, meme kanseri, HER-2.

Article History: Received: Jan 13, 2020; Revised: Mar 15, 2020; Accepted: Mar 15, 2020; Available Online: Apr 27, 2020.

DOI: https://doi.org/10.15671/hjbc.672695

Correspondence to: M. Çankaya, Erzincan Binali Yıldırım University, Faculty of Arts and Sciences, Department of Biology, Erzincan, Turkey.

E-Mail: cankayamuratt@gmail.com

INTRODUCTION

Breast cancer is the most diagnosed cancer type in women worldwide, with approximately 2 million new cases diagnosed and 627,000 patients died in 2018 [1]. Breast cancer is mainly categorized into three types: hormone receptor-positive (estrogen receptor and progesterone receptor), human epidermal growth factor receptor-2 positive (HER2-positive, HER2+) and triple-negative breast cancer. Amplification of HER2 gene or overexpression of HER2 protein is called HER2-positive and these processes cause occurrence and progression of tumorigenesis in normal breast cells. HER2 is a transmembrane tyrosine kinase receptor which is over-expressed in about 10-20 percent of breast cancers. There are several treatment strategies available for HER2-positive breast cancer, depending on the type and stage [2,3].

Chemotherapy is one of the most important steps in treatment of HER2-positive breast cancer and especially, development of HER2 targeted drugs has been significant therapeutic strategy in breast cancer. Trastuzumab (Herceptin®) is a recombinant DNA-derived humanized monoclonal antibody which selectively inhibits HER2-positive breast cancer tumorigenesis alone or in combination with other chemotherapeutics and natural products. HER-2 receptor consists of three conserved domains: extracellular ligand-binding domain, a transmembrane region, and an intracellular (cytoplasmic tyrosine kinase) domain. Trastuzumab binds to the extracellular domain of HER2 receptor with high affinity and prevents cleavage of this domain, resulting in interruption of cancer cell survival [4,5]. In order to increase therapeutic efficiency, administration of trastuzumab in combination with FDA approved drugs and natural products have been investigated in pre-clinical and clinical studies in cancer. In early and advanced HER2-positive breast cancer patients, trastuzumab is used in combination with paclitaxel, docetaxel, carboplatin [6-8]. Overexpression of HER2 is associated with resistance to hormonal therapy (particularly tamoxifen) in breast cancer. Therefore, combining hormonal agents, tamoxifen and aromatase inhibitors, with trastuzumab may be potential therapeutic aspect as hormonal therapy in breast cancer [9].

Gambogic acid is a natural product which is originally isolated from ***Garcinia hanburyi*** tree grown in Southeast Asia. Traditionally, gambogic acid has been used in treatment of many different diseases for a long time. Numerous studies reported that, gambogic acid possesses diverse biological properties such as anti-cancer, anti-microbial, anti-oxidant and anti-inflammatory [10,11]. In recent decades, biological activities of gambogic acid have been investigated in almost all steps of tumourigenesis, and it inhibits the proliferation of various human cancer cells. According to ***in-vitro*** and ***in-vivo*** studies, gambogic acid induces apoptosis, inhibits angiogenesis and overcomes drug resistance in human cancer cells via different signaling pathways [10-13]. Gambogic acid has been approved for phase II clinical trial for solid tumor therapy by the Chinese Food and Drug Administration [14]. However, the anticancer mechanisms of the gambogic acid are not fully understood yet. Therefore, further molecular studies are needed to understand the biological effect of the gambogic acid in cancer.

In this study, we examined the combined effect of trastuzumab and gambogic acid as well as its mechanism of action was determined by using RT-PCR and ELISA techniques on HER2-positive human breast cancer cell line, MDA-MB-453. Obtained results indicated that gambogic acid plus trastuzumab directly decreased cell proliferation and induced inhibition of HER-2 signaling pathway. Moreover, this combination affects apoptosis via caspase-9 and Bax pathways. Combined therapy of trastuzumab and gambogic acid may be promising medicinal compound to treat HER-2 positive breast cancer.

MATERIALS and METHODS

Materials

MDA-MB-453 cell line was from ATCC (American Type Culture Collection, USA). Dulbecco's modified Eagle's medium (DMEM), heat-inactivated fetal bovine serum, trypsin–EDTA, phosphate buffer saline (PBS), L-glutamine, penicillin-streptomycin and XTT ((2,3-bis-(2-methoxy-4-nitro-5-sulfophenyl)-2H-tetrazolium-5-carboxanilide) cell proliferation kit was obtained from Biological Industries Ltd. Gambogic acid was purchased from Abcam. Trastuzumab was supplied from Roche. RNA isolation and cDNA synthesis kits were purchased from Thermo Scientific. Human Bax, HER-2 and caspase-9 ELISA kits were from Sinogeneclon Co., Ltd. All other chemical reagents were purchased from Merck and Sigma Aldrich.

Table 1. Definition of CI index values.

CI>1	Antagonism	CI=1.1-1.2	Slight antagonism
		CI=1.2-1.45	Moderate antagonism
		CI=1.45-1.33	Antagonism
		CI=3.3-10	Strong antagonism
		CI>10	Very strong antagonism
CI=1	Additive	CI=1	Additive
CI<1	Synergism	CI=0.85-0.9	Slight synergism
		CI=0.7-0.85	Moderate synergism
		CI=0.3-0.7	Synergism
		CI=0.1-0.3	Strong synergism
		CI<0.1	Very strong synergism

Cell line and culture

For *in-vitro* experiments, MDA-MB-453 (HER2-positive human breast cancer) cell line was cultured in DMEM (high glucose) medium with 10% fetal bovine serum, 1% l-glutamine, 100 IU/mL penicillin and 10 mg/mL streptomycin. Cells were cultivated in a humidified incubator at 37°C within an atmosphere containing 5% CO_2.

Cell proliferation assay

The XTT test was used to quantify the number of viable cells in each of the well in different concentrations [15,16]. Initially, the cancer cells were seeded in sterile 96-well culture plate ($10x10^4$ cells in each well), and the different concentrations of gambogic acid (10-5-2.5-1.25-0.625-0.3125 µM), trastuzumab (100-50-25-12.5-6.25-3.125 µg/ml) and gambogic acid+trastuzumab were incubated with cells for 12-72 hours at 37 °C in a humidified incubator within an atmosphere containing 5% CO_2. At the end of the incubation times, 50 µl XTT reagents were added to each well for determination of living cells. After 4h, the absorbance was measured using micro plate reader at 450 nm, and then the percentage of cell viability was calculated.

Combined effect analysis

The interactions of the gambogic acid and trastuzumab were determined with using the combination index (CI) method (median-effect principle). CI values of gambogic acid and trastuzumab were calculated using CompuSyn free software. To enhance therapeutic efficiency and minimize resistance of drugs, combination chemotherapy is widely used in treatment of various diseases such as cancer. The Chou-Talalay method based on the median-effect equation was developed for analyzing drug combinations quantitatively. Further, this method encompasses the Michaelis-Menten, Henderson-Hasselbalch, Scatchard, and Hill equations. In this context, CompuSyn software (ComboSyn, Inc., Paramus, NJ, USA) is analyzed drug combinations using median-effect principle, and calculated CI values to determine combination types (CI<1, CI=1 and CI>1 was accepted as synergism, addition and antagonism, respectively (Table-1) [17].

RT-qPCR Analysis

To determine the alteration of HER2, Bax, caspase-9 and GAPDH gene expressions with gambogic acid (5 µM), trastuzumab (50 µg/ml) and gambogic acid+trastuzumab (5 µM+50 µg/ml) at the end of the 24h incubation, qPCR experiments were carried out on MDA-MB-453 cells. Total RNA was extracted and first strand cDNA synthesis made according to the manufacturer's protocols. Primers were designed using Primer 3.0 program and synthesized by Macrogen Inc., with the following sequences (5′ to 3′) and qPCR conditions: HER-2 forward: TTGTGGCCTTCTTTGAGTTCGGTG and reverse: GGTGCCGGTTCAGGTACTCAGTCA at 95°C (10 min) followed by 45 cycles of 95°C (30 sec), 59°C (30 sec) and 72°C (45 sec), caspase-9 forward: CGAACTAACAGGCAAGCAGC and reverse: ACCTCACCAAATCCTCCAGAAC at 95°C (10 min) followed by 45 cycles of 95°C (15 sec), 60°C (1 min) and 72°C (45 sec), Bax forward: CCTGTGCACCAAGGTGCCGGAACT and reverse: CCACCCTGGTCTTGGATCCAGCCC at 95°C (10 min) followed by 45 cycles of 95°C (30 sec), 59°C (30 sec) and 72°C (30 sec), GAPDH forward: CGAACTAACAGGCAAGCAGC and reverse: TCGCCCCACTTGATTTTGG at 95°C (10 min) followed by 45 cycles of 95°C (15 sec), 64°C (30 sec) and 72°C (15 sec). qPCR was carried out using a SYBR Green Master Mix (Qiagen-330500) with a reacti-

on mixture containing 1 µl cDNA, 2 µl each primer and 12,5 µl SYBR Green Master Mix (total volume 25 µl). All assays were run in triplicate (Qiagen Rotor Gene). C_T values were assessed and relative expression of target genes was determined using the $2^{-\Delta\Delta Ct}$ method.

ELISA Tests

To investigate protein expression levels of the HER2, Bax and caspase-9 with gambogic acid (5 µM), trastuzumab (50 µg/ml) and gambogic acid+trastuzumab (5 µM+50 µg/ml) at the end of the 24h incubation, commercial sandwich ELISA kits were used on MDA-MB-453 cells according to the manufacturers' instructions. Expression levels of the proteins were measured spectrophotometrically.

Statistical Analysis

Differences in the mean values of measured activities were evaluated statistically using the SPSS 17.0 program (Univariate Variance Analyses and Pearson Correlation). Probability values of $p < 0.05$ were considered to be significant.

RESULTS AND DISCUSSION

Cell Proliferation Assay

The cytotoxic activities of trastuzumab and gambogic acid were evaluated on MDA-MB-453 cell line by XTT assay individually and in combination. CI values of trastuzumab-gambogic acid combination were determined with CompuSyn software and Table-2 shows mean CI values of combinations at different incubation times. Gambogic acid was dissolved in DMSO and diluted in DMEM before cell proliferation assay. The control cells were treated with DMEM containing 0.1% DMSO to determine cytotoxicity of the gambogic acid. We treated MDA-MB-453 cells with different concentrations of trastuzumab 100-50-25-12.5-6.25-3.125 µg/ml, 10-5-2.5-1.25-0.625-0.3125 µM gambogic acid and the combination of trastuzumab and gambogic acid during 12, 24 and 48h.

Significant anti-proliferative activity did not observe when the treatment was applied for 12h. Treatment with gambogic acid alone as well as the combination of trastuzumab significantly inhibited cell proliferation after 24h and 48h. trastuzumab did not serve essential anti-proliferative activity from 12h to 48h in 100-3.125 µg/ml concentrations range. However, trastuzumab inhibited cell proliferation in combination with gambogic acid for certain concentrations for 24 and 48h (Figure-1-3). Trastuzumab is routinely used in the first-line treatment of patients with advanced breast cancers that express HER2. Nevertheless, initial and eventual resistance to HER2-based therapy with trastuzumab is frequently observed in significant number of patients with HER2-positive breast cancer. To overcome trastuzumab-induced resistance mechanisms in HER-2 positive breast cancer, incorporation of new compounds in combinational therapy with trastuzumab are being extensively studied in pre-clinical and clinical studies [18,19].

100 µg/ml trastuzumab +10 µM gambogic acid, 50 µg/ml trastuzumab +5 µM gambogic acid, and 25 µg/ml trastuzumab +2,5 µM gambogic acid significantly reduced cell viability when the treatment was applied for 48h, and 50% reduction in cell viability was achieved with these combinations. Moreover, 50 µg/ml trastuzumab+5 µM gambogic acid and 25 µg/ml trastuzumab+2,5 µM gambogic acid exhibited anti-proliferative activity during 24h against MDA-MB-453 cells. Briefly, 50 µg/ml trastuzumab+5 µM gambogic acid, and 25 µg/ml trastuzumab+2,5 µM gambogic acid showed similar combinational effect to inhibit survival of MDA-MB-453 cells in 24 and 48h. According to the CI values of the trastuzumab-gambogic acid combinations (Table-2), 50 µg/ml trastuzumab+5 µM gambogic acid exhibited the lowest CI values for 24h and therefore this combination was accepted as optimum for HER-2 positive breast cancer cells.

Table 2. CI values of the trastuzumab-gambogic acid combinations.

	12 HOURS	24 HOURS	48 HOURS
		CI	
100 µg/ml trastuzumab + 10 µM gambogic acid	0.98 ± 0.01	0.91 ± 0.02	1.64 ± 0.04
50 µg/ml trastuzumab + 5 µM gambogic acid	0.62 ± 0.02	0.50 ± 0.03	0.86 ± 0.05
25 µg/ml trastuzumab + 2.5 µM gambogic acid	0.78 ± 0.04	0.59 ± 0.03	0.78 ± 0.02

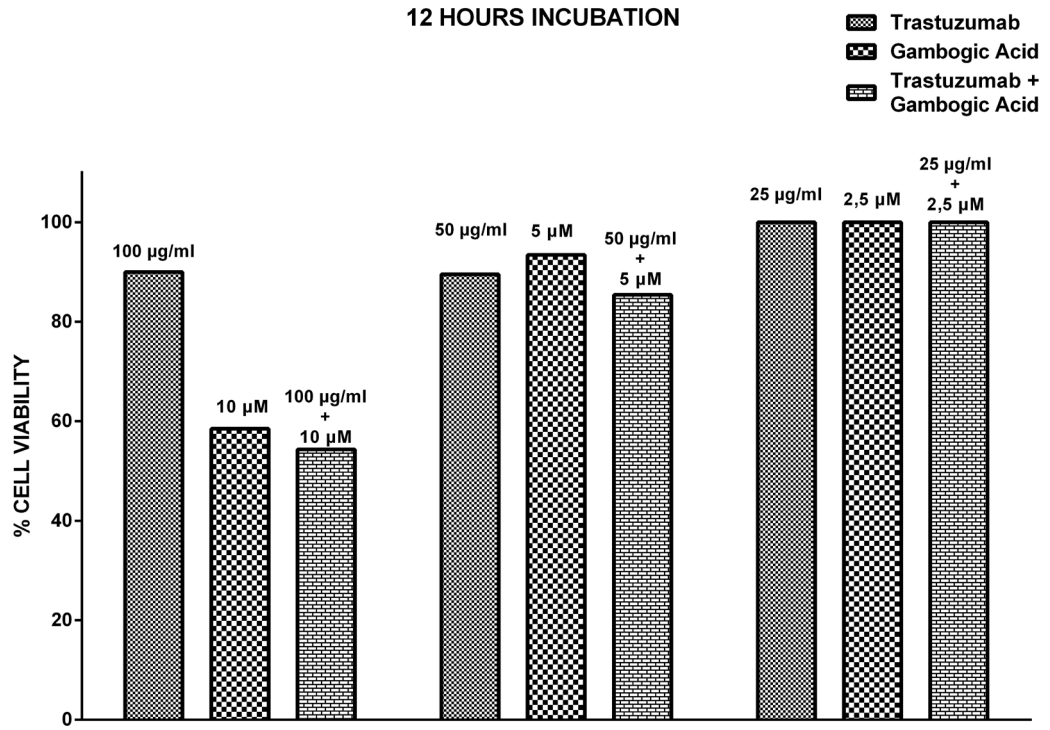

Figure 1. Antitumor activity of trastuzumab, gambogic acid and trastuzumab+gambogic acid for MDA-MB-453 cell line at 12h.

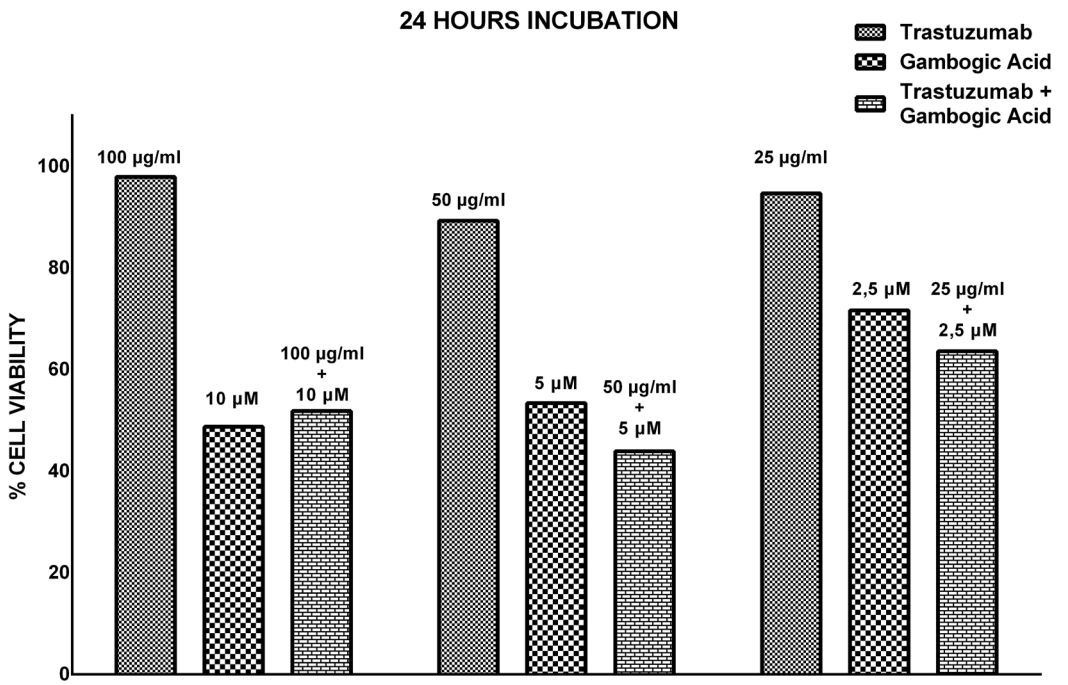

Figure 2. Antitumor activity of trastuzumab, gambogic acid and trastuzumab+gambogic acid for MDA-MB-453 cell line at 24h.

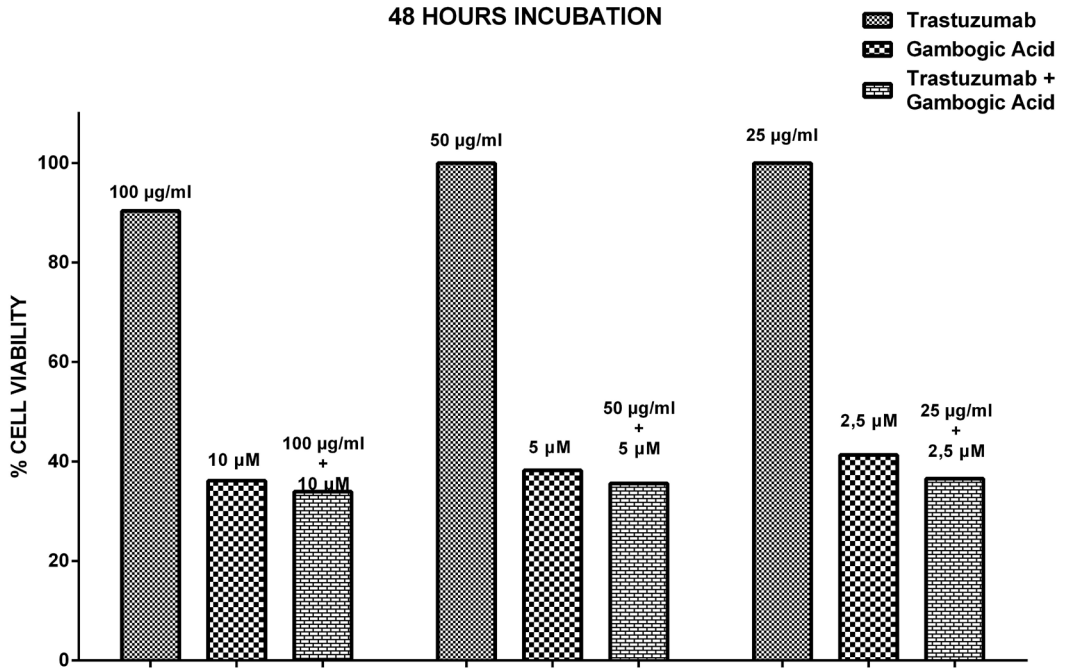

Figure 3. Antitumor activity of trastuzumab, gambogic acid and trastuzumab+gambogic acid for MDA-MB-453 cell line at 48h.

RT-qPCR Analysis and ELISA Tests

Gene expression analysis was performed 50 µg/ml TRS and 5 µM gambogic acid combinations at 24h with the best agonistic effect calculated as CI 0.50 ± 0.03. Almost all cancer patients, upregulation of HER2 expression at the gene and protein level have been correlated with poor prognosis in breast cancer [20]. In this study, it was shown that treatment with combination of trastuzumab and gambogic acid suppressed HER2 expression levels better than individual treatment (Figure-4). In cells treated with a combination of 50 µg/ml trastuzumab and 5 µM gambogic acid, the ELISA findings of HER2 protein decreased by 60.17% (36.4 IU/L) compared to control, correlating with decreased gene expression levels (Table-3). Gambogic acid increasing anti-proliferative activity of trastuzumab, suggests that the use of gambogic acid with trastuzumab as an adjunct therapy in the treatment of HER2 positive breast cancer may be more effective.

The intrinsic apoptotic pathway begins with the release of cytochrome-C (Cyt-C) into the cytosol, causing a change on the permeability of mitochondrial membrane by Bax (B-cell lymphoma-2-associated X) protein. Apoptotic Protease Activating Factor-1 (Apaf-1) after release of Cyt-C, polymerizes in an dATP or ATP dependent mechanism [21,22]. Apaf-1 enabling the assembly of the apoptosome, activates caspase-9 (cas-9) and in this manner initiating the caspase cascade [20]. According to the findings trastuzumab and gambogic acid induced to intrinsic apoptotic pathway individually. The gene expression level of cas-9 was found to increase approximately 6 and 5 times (Figure-5) in trastuzumab and gambogic acid treatment, respectively. On the other hand, in cells treated with a combination of 50 µg / ml trastuzumab and 5 µM gambogic acid, ELISA results of cas-9 protein level was determined as lowest (21 ng/ml) and correlating with gene expression levels (Table-3). This maybe suggests that treated with a combination of trastuzumab and gambogic acid induces cell death by a pathway other than intrinsic apoptosis. In order to explain this situation to be precise, it is necessary to investigate gene expression levels of some genes such as Bcl2, Apaf-1 and protein levels by western-blot in addition to flow-cytometry. According to the results of gene expression analysis, when trastuzumab and gambogic acid were applied separately, it was found to down-regulate Bax gene (0.5 and 1.5 fold change, respectively). When ELISA results are examined, it is seen that there is a similar change in the amount of protein supporting these results (Table-3). Conversely, trastuzumab-gambogic acid combination treatment (50 µg/ml trastuzumab and 5 µM gambogic acid) increased Bax gene expression (Figure-6) and amount of protein. In this case it may be considered an indication of the formation of trastuzumab resistance.

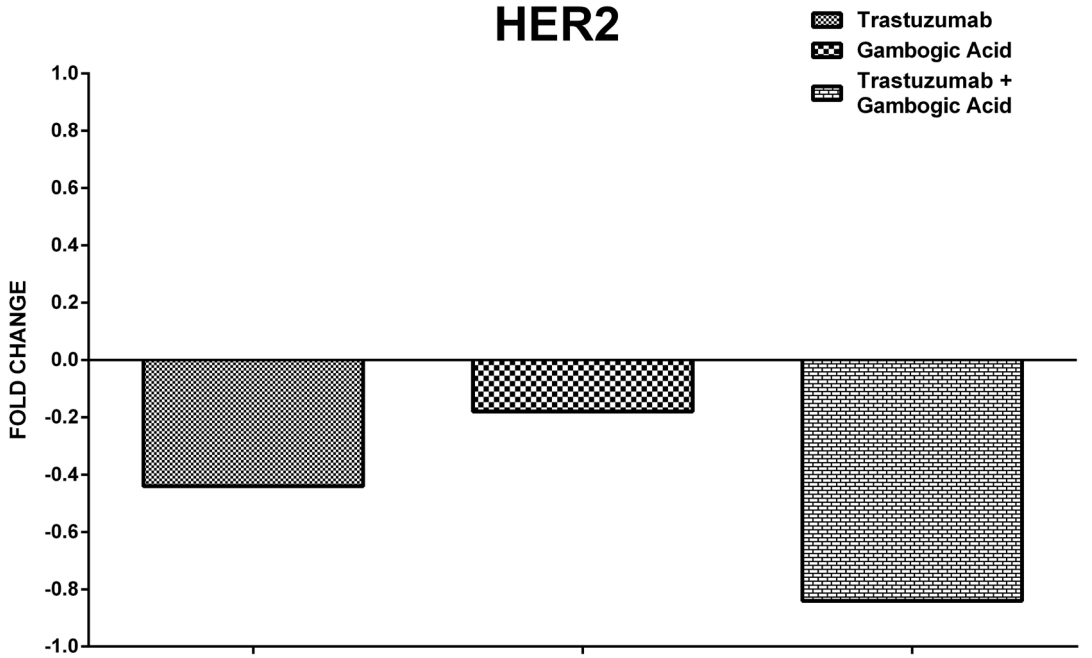

Figure 4. Relative fold change for HER2 gene in trastuzumab, gambogic acid and trastuzumab+gambogic acid by RT-qPCR.

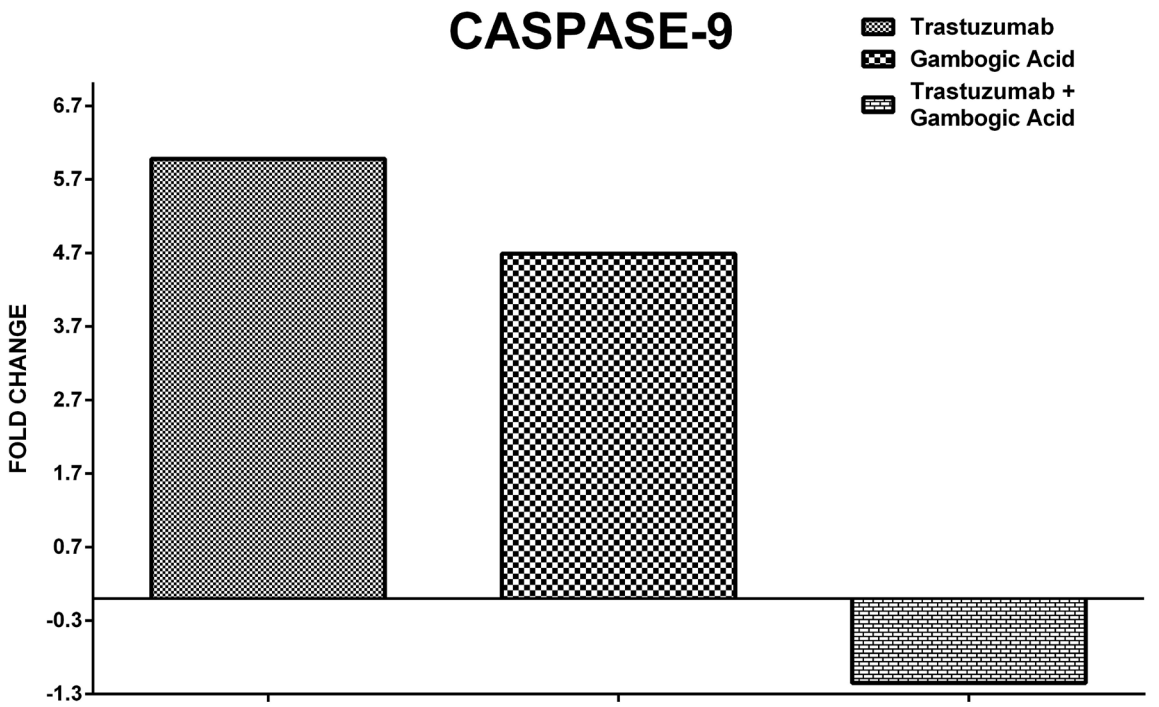

Figure 5. Relative fold change for caspase-9 gene in trastuzumab, gambogic acid and trastuzumab+gambogic acid by RT-qPCR.

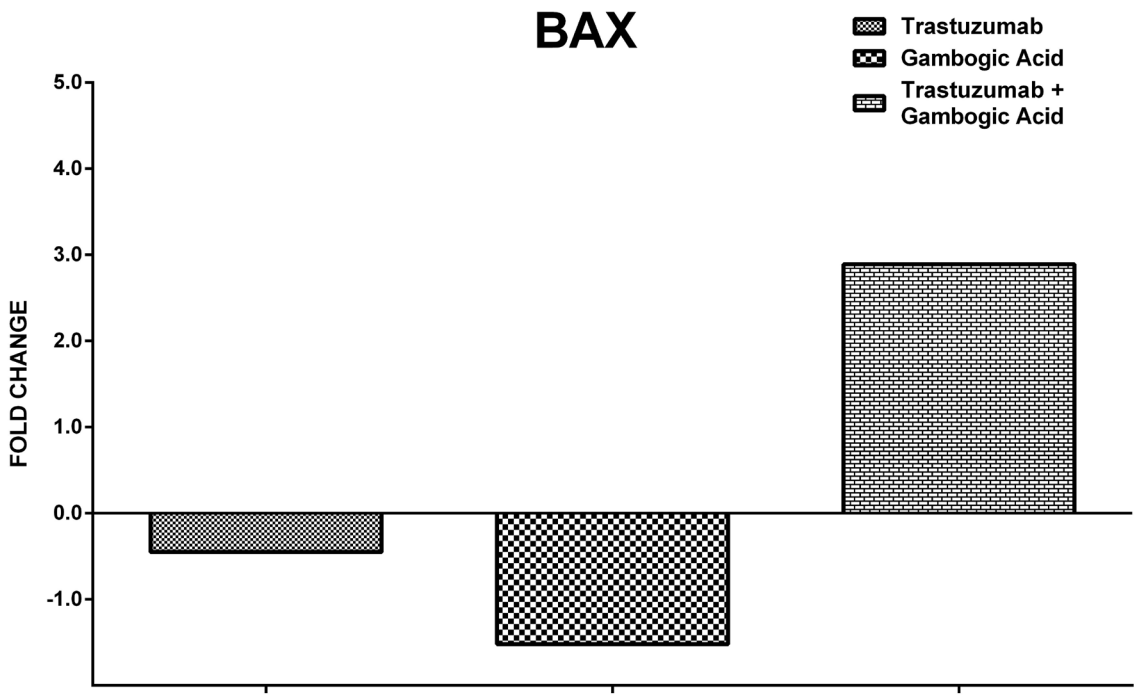

Figure 6. Antitumor activity of trastuzumab, gambogic acid and trastuzumab+gambogic acid for MDA-MB-453 cell line at 48h.

Table 3.ELISA Tests results of trastuzumab, gambogic acid and trastuzumab+gambogic acid.

	Bax (ng/ml)	Caspase 9 (ng/ml)	HER2 (IU/L)
Control	10.27	28.50	91.40
Trastuzumab (50µg/ml)	9.90	46.50	80.30
Gambogic Acid (5µM)	9.59	37.08	51.33
Trastuzumab (50µg/ml) + Gambogic Acid (5µM)	12.05	21.00	36.40

Trastuzumab is the standard treatment for HER2 positive breast cancer and significantly improved clinical outcomes. Nevertheless, approximately 50% of HER2 positive breast cancer patients can not heal with this drug [23]. Compared to monotherapy, agonistic growth inhibition and anti-proliferative effect was achieved by the combination treatment of gambogic acid and trastuzumab. Findings showed significant agonistic cytotoxic effect in MDA-MB-453 cells at 24th hour 50 µg / ml trastuzumab and 5 µM gambogic acid according to the cell proliferation, RT-qPCR and ELISA studies.

Conclusion

Trastuzumab is clinically used target specific drug to treat either early-stage or advanced-stage/metastatic HER-2 positive breast cancer. Nevertheless, resistance to trastuzumab is often observed in significant number of patients with HER-2 positive breast cancer. To increase therapeutic efficiency and minimize drug resistance of trastuzumab is important research topics in HER2-positive breast cancer. Therefore, many natural and synthetic compounds have been utilized in combinational therapy with trastuzumab. In this study, gambogic acid has increased anti-proliferative activity of the trastuzumab according to the cytotoxicity, RT-qPCR and ELISA tests. Especially, gambogic acid+trastuzumab was dramatically decreased expression level of the HER-2 at gene and protein level. Further, this combination may stimulate cell death by a pathway other than intrinsic apoptosis according to the expression of Bax and caspase-9 in MDA-MB-453 cells. In conclusion, gambogic acid-trastuzumab combination can be suggested as a potent candidate for treatment of HER-2 positive breast cancer.

Conflict of Interest
Authors declare that he has no conflict of interest.

Acknowledgments - This study was supported by Erzincan Binali Yıldırım University Scientific Research Projects Coordinatorship, project no. FDK-2018-565.

References

1. F. Bray, J. Ferlay, I. Soerjomataram, R.L. Siegel, L.A. Torre, A. Jemal, Global cancer statistics 2018: GLOBOCAN estimates of incidence and mortality worldwide for 36 cancers in 185 countries, CA Cancer J. Clin., 68 (2018) 394-424.
2. H.M. Asif, S. Sultana, S. Ahmed, N. Akhtar, M. Tariq, HER-2 Positive Breast Cancer - a Mini-Review, Asian Pac. J. Cancer Prev., 17 (2016) 1609-1615.
3. S. Pernas, S.M. Tolaney, HER2-positive breast cancer: new therapeutic frontiers and overcoming resistance, Ther. Adv. Med. Oncol., (2019) 11.
4. W. Dean-Colomb, F.J. Esteva, Her2-positive breast cancer: herceptin and beyond, Eur. J. Cancer., 44 (2008) 2806-2812.
5. S. Shak, Overview of the trastuzumab (Herceptin) anti-HER2 monoclonal antibody clinical program in HER2-overexpressing metastatic breast cancer. Herceptin Multinational Investigator Study Group, Semin. Oncol., 26 (1999) 71-77.
6. Y. Okawa, K. Sugiyama, K. Aiba, A. Hirano, S. Uno, T. Hagino, K. Kawase, H. Shioya, K. Yoshida, N. Usui, M. Kobayashi, T. Kobayashi, Successful combination therapy with trastuzumab and Paclitaxel for adriamycin- and docetaxel-resistant inflammatory breast cancer, Breast Cancer., 11 (2004) 309-312.
7. E.A. Perez, Carboplatin in combination therapy for metastatic breast cancer, Oncologist., 9 (2004) 518-527.
8. M.S. van Ramshorst, E. van Werkhoven, I.A.M. Mandjes, M. Schot, J. Wesseling, M.T.F.D. Vrancken Peeters, J.M. Meerum Terwogt, M.E.M. Bos, H.M. Oosterkamp, S. Rodenhuis, S.C. Linn, G.S. Sonke, Trastuzumab in combination with weekly paclitaxel and carboplatin as neo-adjuvant treatment for HER2-positive breast cancer: The TRAIN-study, Eur. J. Cancer., 74 (2017) 47-54.
9. N. Hayashi, N. Niikura, H. Yamauchi, S. Nakamura, N.T. Ueno, Adding hormonal therapy to chemotherapy and trastuzumab improves prognosis in patients with hormone receptor-positive and human epidermal growth factor receptor 2-positive primary breast cancer, Breast Cancer Res. Treat., 137 (2013) 523-531.
10. D. Kashyap, R. Mondal, H.S. Tuli, G. Kumar, A.K. Sharma, Molecular targets of gambogic acid in cancer: recent trends and advancements, Tumour Biol., 37 (2016) 12915-12925.
11. K. Banik, C. Harsha, D. Bordoloi, B. Lalduhsaki Sailo, G. Sethi, H.C. Leong, F. Arfuso, S. Mishra, L. Wang, A.P. Kumar, A.B. Kunnumakkara, Therapeutic potential of gambogic acid, a caged xanthone, to target cancer, Cancer Lett., 416 (2018) 75-86.
12. G.M. Huang, Y. Sun, X. Ge, X. Wan, C.B. Li, Gambogic acid induces apoptosis and inhibits colorectal tumor growth via mitochondrial pathways, World J Gastroenterol., 21 (2015) 6194-6205.
13. X. Wang, W. Chen, Gambogic acid is a novel anti-cancer agent that inhibits cell proliferation, angiogenesis and metastasis, Anticancer Agents Med. Chem., 12 (2012) 994-1000.
14. Y.I. Chi, X.K. Zhan, H. Yu, G.R. Xie, Z.Z. Wang, W. Xiao, Y.G. Wang, F.X. Xiong, J.F. Hu, L. Yang, C.X. Cui, J.W. Wang, An open-labeled, randomized, multicenter phase IIa study of gambogic acid injection for advanced malignant tumors, Chin Med J (Engl)., 126 (2013) 1642-1646.
15. M. Gümus, A. Ozgur, L. Tutar, A. Disli, I. Koca, Y.Tutar, Design, Synthesis, and evaluation of heat shock protein 90 inhibitors in human breast cancer and its metastasi, Curr. Pharm. Biotechnol., 17 (2016) 1231-1245.
16. İ. Koca, A. Özgür, M. Er, M. Gümüş, K. Açikalin Coşkun, Y. Tutar, Design and synthesis of pyrimidinyl acyl thioureas as novel Hsp90 inhibitors in invasive ductal breast cancer and its bone metastasis, Eur. J. Med. Chem., 122 (2016) 280-290.
17. I.V. Bijnsdorp, E. Giovannetti, G.J. Peters, Analysis of drug interactions, Methods Mol. Biol., 731 (2011) 421-434.
18. M. Luque-Cabal, P. García-Teijido, Y. Fernández-Pérez, L. Sánchez-Lorenzo, I Palacio-Vázquez, Mechanisms behind the resistance to trastuzumab in HER2-amplified breast cancer and strategies to overcome it, Clinç Medç Insights Oncol., 10 (2016) 21-30.
19. G. Li, J. Guo, B.Q. Shen, D.B. Yadav, M.X. Sliwkowski, L.M. Crocker, J.A. Lacap, G.D.L. Phillips, mechanisms of acquired resistance to trastuzumab emtansine in breast cancer cells, Mol. Cancer Ther., 17 (2018) 1441-1453.
20. S.J. Riedl, W. Li, Y. Chao, R. Schwarzenbacher, Y. Shi, Structure of the apoptotic protease-activating factor 1 bound to ADP, Nature, 434 (2005) 926-933.
21. S.J. Riedl, G.S. Salvesen, The apoptosome: signalling platform of cell death, Nat. Rev. Mol. Cell Biol., 8 (2007) 405-413.
22. H. Zou, W.J. Henzel, X. Liu, A. Lutschg, X. Wang, Apaf-1, a human protein homologous to C. elegans CED-4, participates in cytochrome c-dependent activation of caspase-3, Cell 90 (1997) 405-413.
23. E.A. Perez, J. Cortés, A.M. Gonzalez-Angulo, J.M. Bartlett, HER2 testing: current status and future directions, Cancer Treatç Rev., 40 (2014) 276-284.